Reliability Assessment of Structural Concrete with Special Reference to Stirrup Design

by
Kenneth Kwesi Mensah

Dissertation presented for the degree of Doctor of Philosophy in Civil Engineering at Stellenbosch University

Promoters: Dr. C. Viljoen & Prof. J.V. Retief

Faculty of Engineering

March 2015

DECLARATION

By submitting this dissertation electronically, I declare that the entirety of the work contained therein is my own, original work, that I am the sole author thereof (save to the extent explicitly otherwise stated), that reproduction and publication thereof by Stellenbosch University will not infringe any third party rights and that I have not previously in its entirety or in part submitted it for obtaining any qualification.

December 2014

Abstract

Structural design standards based on the principles of structural reliability are gaining worldwide acceptance and are fast becoming the new basis for structural safety verification. The application of these principles to establish a standardised basis for structural design using partial factor limit states design procedures is done in the European Standard for the *Basis of Structural Design* EN 1990 from which it is adapted to the South African Standard *Basis of Design for Building and Industrial Structures* SANS 10160-1. South Africa (SA) is on the advent of adopting the European Concrete Design Standard EN 1992-1-1 (EC2) as the equivalent standard for local use. This investigation seeks to provide a transparent quantitative reliability basis for the SA's adoption of EC2, as well as provide for its subsequent implementation under local conditions and practice.

The investigation kicks-off with a critical review of the reliability framework for structural resistance. The review establishes the relationships between the key elements of the framework, shedding light on issues SA needs to consider as it adopts EC2. Important issues for SA to consider include (1) target levels of structural performance (β_T-values), (2) partial factors, (3) model uncertainties, and (4) quality control.

Design for shear resistance was investigated in greater detail by comparison of EC2's Variable Strut Inclination Method (VSIM) for stirrup design against alternative approaches, namely, (1) South Africa's currently operational SANS 10100-1 procedure, and (2) the *fib* Model Code 2010 first Level of Approximation (LoA I) and *fib* LoA III, which are based on the Modified Compression Field Theory (MCFT). Unbiased capacity predictions from the MCFT-based sectional analysis Program Response-2000 (R2k) served as LoA IV best-estimate results during this assessment. Results of this investigation showed that EC2 offers higher capacity predictions in excess of 1 MPa of stirrup reinforcement, with significantly higher predictions in the range of 1 to 2 MPa. A reliability performance assessment was therefore commissioned to assess safety regimes in terms of achieved reliability across a parametric range of the amount of stirrup reinforcement (from 0.45 to 2.0 MPa).

The First Order Reliability Method (FORM) was implemented as part of the reliability performance assessment of the EC2's VSIM design procedure. The model uncertainty for shear

resistance (stirrup failures) was characterised according to a database of published stirrup-reinforced concrete beam shear tests. Three cases of the Model Factor for shear resistance were derived from the experimental database for alternative shear resistance prediction models; two of which formed part of basic investigations conducted using the conventionally formulated performance function, and the other was integrated as part of an independent validation procedure using R2k predictions to obtain the reliability model.

Results obtained from the basic reliability model (β_{VSIM}-values) generally indicated lower levels of reliability with an increase in stirrup reinforcement and concrete strength, compared to those estimated from the R2k-based reliability model (β_{R2k}-values). The disparity between β_{VSIM} and β_{R2k}-values revealed that systematic effects affect each model's ability to predict the expected value of true shear resistance V_{true}. There is reasonable evidence to suggest that the predictions of V_{true} can be improved by accounting for each model's peculiar sensitivity to concrete strength, consequently providing more representative estimates of β. However, in the interim, β_{VSIM} and β_{R2k}-values, respectively, represent reasonable lower and upper bound estimates of the performance of EC2's VSIM design procedure.

Opsomming

Die beginsels van struktuur betroubaarheid word wêreldwyd aanvaar as basis vir struktuur ontwerp standaarde en die versekering van voldoende struktuur veiligheid. Hierdie beginsels word in die Europese Standaard *Basis of Structural Design* EN 1990 toegepas om gestandaardiseerde partiële faktor gebaseerde limietstaat ontwerp prosedures daar te stel, van waar dit aangepas is vir die Suid-Afrikaanse Standaard *Basis of Design for Building and Industrial Structures* SANS 10160-1. Suid-Afrika (SA) staan op die punt om die Europese beton ontwerp standaard EN 1992-1-1 (EC2) aan te neem as die ekwivalente standaard vir plaaslike gebruik. Hierdie ondersoek het as doel om ‘n deursigtige kwantitatiewe betroubaarheidsbasis daar te stel vir die aanneming van EC2 as SA standaard en om voorsiening te maak vir die implementering daarvan onder plaaslike toestande en –praktyk.

Die ondersoek begin met ‘n kritiese oorsig van die betroubaarheidsraamwerk vir strukturele weerstand. Die oorsig stel die verhouding vas tussen sleutel elemente van die raamwerk en werp lig op aspekte wat SA moet oorweeg in die aanneming van EC2. Belangrike aspekte vir oorweging sluit (1) teiken betroubaarheidsvlakke vir struktuur gedrag (β_T-waardes), (2) partiele faktore, (3) model onsekerhede en (4) kwaliteitsbeheer in.

Skuif weerstandsontwerp is in groter detail ondersoek deur die EC2 se Veranderbare Stut Hoek Metode (VSHM) vir skuifbeuel ontwerp te vergelyk met alternatiewe benaderings, naamlik, (1) Suid Afrika se huidig operasionele SANS 10100-1 prosedure, (2) *fib* Model Code 2010 se sogenaamde eerste Vlak van Benadering (VvB I) en *fib* VvB III, gebaseer op die Aangepaste Drukveld Teorie (ADT). Onbevooroordeelde kapasiteit voorspellings van die ADT-gebaseerde snit analise program “Response-2000 (R2k)” is in die evaluering gebruik as VvB IV bes benaderde resultate. Die ondersoek toon dat EC2 hoër kapasiteit voorspel vir skuifbeuel bewapening tot 1 MPa en beduidend hoër kapasiteite voorspel vir skuifbeuel bewapening tussen 1 en 2 MPa. ‘n Betroubaarheidsprestasie studie is vervolgens geloots om die veiligheid in terme van behaalde betroubaarheid te bepaal oor ‘n parametriese bereik van 0.45 tot 2.0 MPa skuifbeuel bewapening.

Die Eerste Orde Betroubaarheids Metode (EOBM) is implementeer as deel van die betroubaarheidsprestasie beoordeling van die EC2 VSHM ontwerp prosedure. ‘n Databasis van

gepubliseerde skuifbeuel-bewapende betonbalk skuiftoetse is gebruik om die model onsekerheid vir die verskillende skuifweerstandsmodelle statisties te beskryf. Drie Model Faktore is uit die eksperimentele databasis afgelei, twee waarvan gebruik is in basiese ondersoeke met die konvensioneel geformuleerde prestasie funksie en die derde as deel van 'n onafhanklike bevestigingsprosedure gebaseer op R2k voorspellings.

Resultate wat verkry is uit die basiese betroubaarheidsmodel (β_{VSHM}-waardes) was laer (meer konserwatief), en het ook vinniger afgeneem met 'n toename in skuifbeuel bewapening as die waardes wat uit die R2k-gebaseerde betroubaarheidsmodel (β_{R2k}-waardes) verkry is. Die verskil tussen β_{VSIM} en β_{R2k}-waardes toon dat sistematiese effekte die vermoë van elk van die modelle beïnvloed om die verwagte waarde van die werklike skuifweerstand V_{werklik} te voorspel. Daar is redelike bewyse om aan te voer dat die voorspellings van V_{werklik} verbeter sal kan word deur elke model se unieke sensitiwiteit teenoor betonsterkte in ag te neem, om sodoende meer verteenwoordigende β waardes te verkry. Intussen verteenwoodig die β_{VSIM} en β_{R2k}-waardes onderskeidelik redelike onder- en bogrens skattings vir die prestasie van EC2 se VSHM ontwerp prosedure.

Acknowledgements

I would like to extend a vote of thanks and appreciation to my supervisors, Prof. Retief and Dr. Viljoen, for their excellent guidance and mentorship over the past five years. Furthermore, I must express gratitude towards the various opportunities I enjoyed along the way, from which I gained some very enlightening and invaluable exposure.

A special thanks to my family for their love, constant supply of all sorts of support, and for keeping me rooted at all times and through all situations. You truly are the spectacle through which I view the earth.

The Stellenbosch Institute of Structural Engineering (ISI) and the Water Research Commission (WRC) provided sufficient financial support to bring this project from point of inception through to completion. The support has been greatly appreciated, particularly since it allowed the opportunity for me to grow not only as an engineer, but very much as an individual as well.

Lastly, but certainly not least, I would like to thank the good Lord who placed all things, people, and situations encountered in life to bring me to this point. For this, I am truly grateful.

Table of Contents

List of Figures

CHAPTER 4

CHAPTER 5

CHAPTER 6

CHAPTER 7

CHAPTER 8

CHAPTER 9

List of Tables

CHAPTER 7

CHAPTER 8

CHAPTER 9

CHAPTER 10

List of Symbols

a	Shear span
a	Half-diameter of longitudinal reinforcement
a_d	Design value of geometrical data
A_{sw}	Area of the 2-legs of a stirrup or shear reinforcement
b_w	Beam width
C	Concrete cover
d	Effective depth of member
e	Diameter of stirrup or link
f_1	Principal tensile stress in cracked reinforced concrete
f_2	Principal compressive stress in cracked reinforced concrete
f_c	Compressive cylinder strength of concrete
f_{ck}	Characteristic compressive cylinder strength of concrete
f_{cm}	Mean compressive cylinder strength of concrete
f_{cr}	Principal tensile stress in reinforced concrete at cracking
f_{yw}	Yield strength of stirrups
f_{ywm}	Mean yield strength of stirrups
f_{ywk}	Characteristic yield strength of stirrups
h	Height or depth of a member
K_{FI}	Multiplication factor for actions, used as differentiation measure
n_l	Number of layers of longitudinal reinforcement provided in design
p	Probability or fractile estimate required from a distribution
$P(\cdot)$	Probability argument or statement
P_f	Probability of failure
R	Function of resistance determined on the basis of design values of individual material properties and geometrical data
R_d	Function of design resistance determined as for R (above), but divided by γ_{Rd}
s	Spacing of stirrups
u'_N	Modified transformed variable of the three-parameter log-normal distribution
u_p	Standardised p-fractile of a distribution

$u_{norm,p}$	Fractile of a standardised random variable with a normal distribution
U	Standardised variable
$V_{Rd,max}$	Upper limit of shear resistance due to crushing of concrete compressive struts
$V_{Rd,s}$	Design ultimate shear resistance of member due, solely, to stirrup resistance
x_i^*	Checking point value of basic variable X at the i^{th} iteration of FORM analysis
x_p	$p-$fractile estimate of the distribution
X_i	Material strengths and/or product properties
$X_{k,i}, X_k$	Characteristic values of material strengths and/or product properties
$X_{d,i}, X_d$	Design value of material strengths and/or product properties
z	Internal lever arm
α_{cc}	Coefficient accounting of scale effects of concrete
α_X	Direction cosine of sensitivity factor of specified variable X
β	Reliability index
β_T	Target level of reliability
$\beta_{T,R}$	Target level of reliability for resistance
γ_C	Partial safety factor for concrete
$\gamma_{m,i}$	Partial safety factor for material strength or product property
γ_{Rd}	Partial safety factor that covers model uncertainties of resistance and geometrical data variations
γ_S	Partial safety factor for steel
γ_m	Partial safety factor for material or product properties catering for uncertainty in their representative values
γ_M	Operational partial factor for material property, assumed as taking some account of model and geometrical uncertainty
γ^*	Partial factor due to increased quality control of material strength
ε_1	Principal tensile strain in cracked reinforced concrete
ε_2	Principal compressive strain in cracked reinforced concrete
ε_x	Longitudinal strain in the web of a beam
ε_y	Transverse strain in the web of a beam
η	General representation of conversion factor taking scale effects into account
θ	Angle of inclination of concrete compressive struts relative to horizontal axis
μ_X	Mean value of the random variable X

ρ_l	Longitudinal reinforcement ratio
ρ_w	Web or shear reinforcement ratio
σ_X	Standard deviation of basic variable X
$\mu_X^N;\ \sigma_X^N$	Transformed normal mean and standard deviation, respectively, of variable X
φ	Probability density
Φ	Probability distribution
$\varphi(\boldsymbol{X})$	Probability density distribution of the vector of basic variables X
ω_l	Longitudinal tension reinforcement index
ω_t	Shear reinforcement index

Chapter 1

INTRODUCTION TO THE RELIABILITY BASIS OF STRUCTURAL DESIGN

1.1 THE CONCEPT OF BASIS OF DESIGN AND CODIFICATION

The structural engineering fraternity has the social responsibility to ensure that all structures designed and constructed are safe and, further, perform as expected during service. To be able to achieve safe and durable structures, design and construction professionals require a system of verifying adequate structural performance of buildings and structures by applying rational and safe procedures through the different stages of a project: planning, design, analysis, detailing, construction, and maintenance of structures. This is typically done through a code of practice with a well-established design basis specifying procedures and guidelines that enable assessments of structural performance and safety. Guidelines are therein also given to achieve certain levels of performance through detailing rules and quality management provisions for design and construction.

A design code, or design provisions in general, should represent sound and well-established methods of engineering practice that have been thoroughly researched and validated by relevant experience (Ellingwood, 1994). In deriving code provisions, they should be calibrated extensively to validate their use across the field of application in practice. Provisions should however not be too complex to use by design engineers in practice who do not always have time to study innovative trends in research, and are often under time demands of projects. A code is therefore a platform of disseminating efficient and current methods of design and construction between research and practice.

Principles of structural reliability form the basis for the performance assessment and calibration of design provisions for structural design. This research is primarily concerned with implementing reliability techniques to assess the performance of the Variable Strut Inclination Method (VSIM) for shear design as suggested by the European design standard for concrete structures EN 1992-1-1 (EN 1992-1-1, 2004). Some general background of the structural reliability theory and structural design standards is given Sections 1.2 to 1.4, before the specific aims and objectives of the study are established in Section 1.5.

1.2 UNCERTAINTIES IN STRUCTURAL DESIGN, PARTIAL FACTOR LIMIT STATES DESIGN, AND THE CONCEPT OF STRUCTURAL RELIABILITY

Problems of structural design must generally be solved in the face of various uncertainties. Uncertainties arise not only in the assessment of actions which the structure has to sustain, and from the occasional lack of control during the production processes of the materials and components required, but also from incomplete knowledge about the mechanical formulations describing the response of the structure and its capacity to sustain those actions. Structural reliability techniques, compared to other basis of design formats, are aimed at rationally quantifying and assessing the effects of uncertainties associated with all aspects of structural design.

The uncertainties in the design and construction process are represented by way of mathematical statistics and the assessment of structural performance is conducted through probabilistic concepts and analyses. Such treatment of uncertainties gives a rational scientific (decision tool) approach to the calibration of structural design provisions.

Modern and technologically advanced design codes adopt the Partial Factor Limit States Design Method as their basis for design. This method applies partial factors, the vector $\{\boldsymbol{\gamma}\}$, to increase action values as well as reduce material property and resistance values to generate their design values for use in a limit state assessment. Characteristic values, the vector $\{\boldsymbol{X_k}\}$, are also introduced into limit state functions where partial factors are applied to make an economically but safe assessment of structural performance.

The governing condition of a limit state assessment is that the action effects, E, should be less than the available resistance, R, i.e. $E < R$. In this method, dimensions are generally implemented at nominal values, but in some cases (second-order effects, geometrical imperfections, buckling) can assume design values by applying some tolerance limit. This method can account for the variability of materials by applying partial safety factors to the material properties. Further, it can also be used for safety verification of cross-sections and members as well, since the action effects and resistance force of cross-sections are calculated for use in the limit state verification.

Until recently, partial safety factors used in limit state design verifications were derived mainly by expert judgement and by reference to sound traditional designs, thereby lacking the

appropriate rational and scientific treatment they require. Structural reliability techniques arise as an attempt or method to represent variability and performance of physical models of structural systems, by taking account of the distributions of the basic variables in mechanical formulations used for limit state verifications. Basic variables are the most fundamental quantities the designer has to consider in mechanical formulations. For structural concrete resistance, these typically include concrete strength (f_c), steel strength (f_y), member geometry (b_w, h), etc.

Structural reliability techniques are consistent with the Partial Factor Limit States Design format in the sense that partial factors can be derived from reliability analyses and calibration exercises (Level II or III safety assessment) and then applied in limit state verifications (Level I safety assessment). The application of structural reliability as the theoretical basis for limit states design ensures that improved economic performance is achieved together with improved safety performance across a wide range of practical design situations. The design provisions of the suite of structural Eurocodes are formulated on reliability principles.

1.2.1 Aleatoric and epistemic uncertainties

Other uncertainties, apart from those associated with the prediction of action effects and resistance, affect structural performance. Aleatoric uncertainties arise due to the natural or inherent variability in a physical process which may never be determined with accuracy. It is simply a *random* uncertainty we may have to deal with but try to control through efficient design practice. Epistemic uncertainties are more *systematic*. They are due to one of two reasons:

1. Either due to insufficient knowledge or lack of understanding that leaves some unknown aspect unaccounted for,
2. Or due to intentional conservative assumptions and simplifications made, which are implemented to achieve operational design

Regardless of any of the sources of epistemic uncertainties listed above, they can be quantified and subsequently calibrated against to build sufficient conservatism into design procedures. Model uncertainties, which describe the inherent bias of prediction models,

caused mainly by intentional simplifications incorporated to achieve operational models for design, are epistemic uncertainties.

1.2.2 Quality control

Structural failures are not only caused by the unfavourable uncertainties that affect a limit state assessment. Gross errors are, in fact, found to be the major cause of structural failures. Table 1.1 shows the origins and causes of structural failures.

Table 1.1. Origin and causes of structural failures (ISO workshop, 2011)

Origin	*Design* 20%	*Execution* 50%	*Use* 15%	*Others* 15%
Causes	*Gross errors* 80%		*Adv. cond.* 20%	

Gross errors can be limited by quality control during design and construction, as well as through routine maintenance. An important part of assuring reliability is to give guidelines on quality management that aim primarily to reduce gross errors in design and increase the quality and integrity of constructed facilities (ISO workshop, 2011).

1.3 CURRENT STATE OF RELIABILITY IMPLEMENTATION IN DESIGN CODES

The probabilistic basis of structural design is developed extensively and continuously updated in the Joint Committee on Structural Safety (JCSS) Probabilistic Model Code (JCSS, 2001). The current collaborators whose efforts support the JCSS are renowned structural engineering bodies; International Association of Bridge and Structural Engineering (IABSE), Conseil International du Bâtiment (CIB), Fédération International du Béton (*fib*), European Convention for Constructional Steelwork (ECCS), Réunion Internationale des Laboratories et

Experts des Matériaux (RILEM). Each of these constitutive bodies of the JCSS specialises in an aspect that is key to structural engineering. The Probabilistic Model Code thus contains a wealth of comprehensive information and proposals on various issues in structural design across different materials that require reliability treatment. The systematically presented structural reliability principles in the JCSS Probabilistic Model Code are laid down in a standardised manner in the International Standard ISO 2394 *General Principles on Reliability for Structures* (ISO, 1998). The application of these principles to establish a standardised basis for structural design using partial factor limit states design procedures is done in the European Standard for the *Basis of Structural Design* EN 1990 (EN 1990, 2002) from which it is adapted to the South African *Basis of Design Standard for Building and Industrial Structures* SANS 10160-1 (SANS 10160-1, 2011).

The basis of design requirements stipulated in EN 1990 and SANS 10160-1 apply to all aspects of structural design: This includes reliability levels of structural performance and their differentiation and management; identification of various limit states and design situations; the specification of all the basic variables; separate treatment of actions and material-based resistance. In the process of converting the principles of structural reliability into deterministic design rules through a method of calibration, the emphasis is placed to a large extent on actions whilst the provision for structural concrete is then left to the materials based design standards. Although a reliability framework is developed also for structural resistance in the form of generic partial factors, model and resistance factors for respective classes of failure modes, systematic calibration of the materials standards is limited (Holický, Retief & Dunaiski, 2007).

Parametric studies of representative cases of structural resistance are used to derive guidelines for structural resistance performance that could be used as basis-of-structural-design requirements to be considered in the formulation of the materials standards (Holický et al., 2007). Ideally, all aspects of the basis of design requirements should be considered. Such explicit reliability guidelines for the specification of structural resistance should improve the unification between the standards for the basis of structural design, actions and structural materials.

1.3.1 Appraisal of the *fib* 2010 Model Code

The *fib* 2010 Model Code, initially established as the CEB-FIP Model Code**,** is an advanced state of the art technical document aimed at synthesising research findings and technical information with a view of translating them into practice. The Model Codes have served as fundamental reference and background documents during the entire building process of the structural Eurocodes, since their inception in the mid-seventies to on-going Eurocode writing activities at current, and will surely still be used in future (Walraven, 2005).

The *fib* 2010 Model Code represents a substantial improvement in terms of the implementation of the reliability framework in the preparation of its stipulations, mainly introduced and partially developed in the 1978 CEB-FIP Model Code (CEB-FIP, 1978a & b). After introducing the general reliability framework, the 1978 Model Code then only proceeded to give detail on the implementation for actions but with no specific guidance for resistance. Its successor, the CEB-FIP 1990 Model Code (CEB-FIP, 1993), showed no extensions of the reliability framework in its provisions, giving reference to the 1978 Model Code for guidance on reliability with its focus delving more towards the establishment of more general and advanced material characteristics and design models.

The first complete draft of the 2010 Model Code (*fib*, 2010a & b) has shown significant improvements from its predecessor (the CEB-FIP 1990 Model Code) in terms of implementation of the reliability framework, with visible trends of reliability aspects considered through different methods and cases of the entire design process. The nature of reliability implementation would depend on what aspect of construction practice is being considered, from design through to construction and maintenance. More explicit treatment of reliability is made visible from the on-set of the basis of design verification procedures, allowing for full probabilistic safety formats, usually preferred in evaluating the residual life of existing structures, as well as reliability or probability based partial factor limit states verifications which are more commonly adopted for newer designs. Furthermore, the newly introduced Levels of Approximation (LoAs) for shear design are attractive features that cater for different levels of assessment of structural performance, and therefore reliability, as detailed below.

Levels of Approximation (LoAs) for shear design in the 2010 Model Code

Section 2.2 in EN 1990 on Reliability Management declares that levels of reliability relating to structural resistance and serviceability can be achieved by, amongst a combination of other issues, the accuracy of the design models used. Therefore some differentiation of the design of structures is possible through the type of design models used in design i.e. simple models routine design versus complex and advanced analyses where accuracy is essential. Generally, more accurate design models are computationally more involving and require more effort to execute.

Ties to reliability (provision for different levels of structural performance) in this regard are visible in the 2010 *fib* Draft Model Code where Levels of Approximation, I through IV, are suggested for use. The levels differ in the complexity, effort and level of detail as the LoA increases i.e. from LoA I to IV. As alluded to earlier, different LoAs are best-suited for different applications, depending on the accuracy of assessment required e.g. LoA I quick to use for simple assessments, whereas LoA IV more elaborate and time-consuming for more accurate results.

1.4 RESEARCH MOTIVATION AND SIGNIFICANCE

The European Commission's initiative to harmonise technical barriers between EU member states to allow exchange of information and intensify trade relations has caused each member states' national structural design standards to be replaced by a unified set of Eurocodes. In this transformation, The British Standard *The Structural Use of Concrete* BS 8110-1 (BS 8110-1, 1997) on which the currently operational South African standard *The Structural Use of Concrete* SANS 10100-1 (SANS 10100-1, 2000) is based, is being withdrawn and replaced by a new operational Eurocode Standard for *Design of Concrete Structures* EN 1992-1-1 (EN 1992-1-1, 2004). For the on-going revision of South Africa's standard for the design of concrete structures, which will be newly referred to as SANS 51992-1-1 (Draft), the South African Concrete Code Committee has chosen to adopt EN 1992-1-1.

The Eurocodes can be viewed as a general set of reference standards which need to be made operational as national standards through the selection of Nationally Determined Parameters in National Annexes. A key parameter for which national choice is allowed and has grave effect on matters concerning reliability is the selection of the target level of reliability β (EN 1990, 2002). The structural Eurocodes are based on a default value of $\beta = 3.8$ for the Reference Class of RC2 structures and SA utilises a justifiably lower value of $\beta = 3.0$ for minimum reliability for the same class of structures. Differentiated Reliability Classes (RCs) are possible, based on a scheme of socio-economic principles of risk. SANS 10160-1 offers four Reliability classes (RC1 – RC4), of which RC 2 ($\beta_{RC2} = 3.0$) and RC 3 ($\beta_{RC3} = 3.5$) mostly apply to the design of conventional buildings and routine structures. These two reliability classes correspond to RC 2 for Eurocode.

Retief and Dunaiski (2009) propose that the reliability assessment of a future South African concrete standard could therefore consist firstly of reviewing the degree to which EN 1992-1-1 complies with and applies reliability principles as set out in EN 1990; and secondly to calibrate it in accordance with SANS 10160-1 requirements, including required levels and classes of reliability for the restricted scope of building structures.

Using EN 1990 and EN 1992-1-1 and their relation as base, this report describes a systematic assessment of the degree to which the application of the reliability framework presented in the basis of design requirements has been achieved in the present generation of structural concrete design standards. More importantly, attempts are made to identify ways in which the process can be advanced. Special attention is drawn to issues that are specific to South African conditions and practice in structural concrete.

1.5 AIMS AND OBJECTIVES OF THE STUDY

The basic premise of the present investigation is that the principles of structural reliability provide the basis for the implementation of structural design standards which are optimally adapted to local conditions. The two challenges in considering the transfer of Eurocode EN 1992-1-1 to South Africa are vast differences in conditions between European and South

African structural practice and the fact that reliability is implicitly imbedded in codified procedures. The investigation therefore seeks to provide a transparent quantitative reliability basis for the SANS 51992-1-1 and its subsequent implementation under local conditions. Figure 1.1 provides a flowchart which systematically describes the aims of this study, with the specific objectives of the dissertation given in 1.5.1 below.

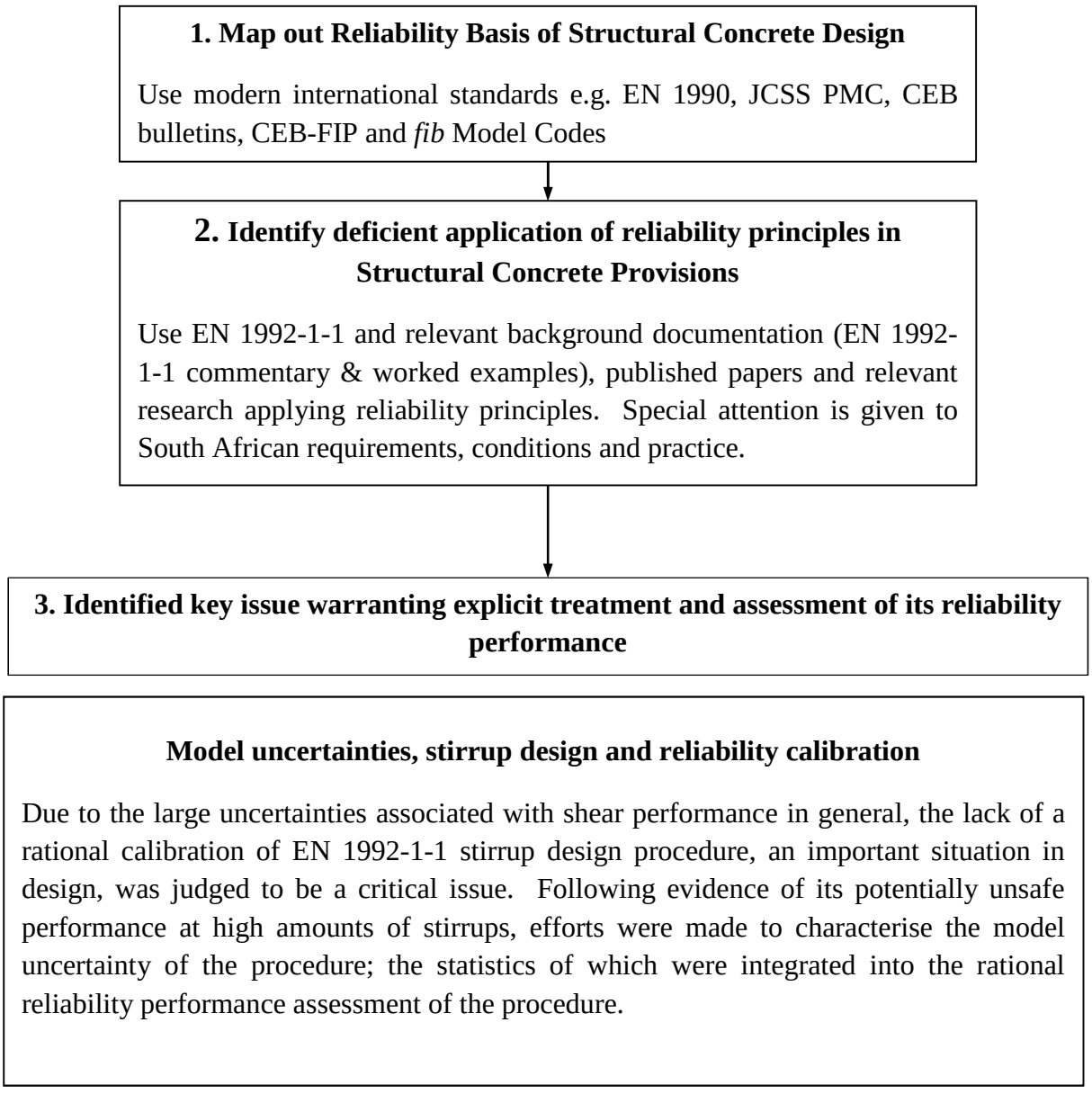

Figure 1.1. General aims of the study

1.5.1 Specific objectives of the study

Following from the general aims of the study presented in Figure 1.1, the specific objectives of the dissertation are:

1. To present a critical review of the reliability basis for structural resistance, elaborating on specific issues that South Africa needs to account for as it adopts EN 1992-1-1.

2. To compare the performance of the EC2 stirrup design procedure to available alternative methods from the *fib* 2010 Model Code and SANS 10100-1

3. To derive Model Factor statistics for the reliability assessment of the EC2 stirrup design procedure.

4. To incorporate derived Model Factor statistics, together with adequate representation of other basic variables, as part of a basic but rational reliability performance assessment of EC2's stirrup design procedure.

5. To implement an alternative and more advanced General Probabilistic Model (GPM) for shear resistance in a separate reliability performance assessment of EC2's stirrup design procedure. The purpose of this separate assessment was to validate the results from (3) above.

6. To give general guidance about the reliability performance management of EC2's stirrup design procedure according to SANS 10160-1 and EN 1990 requirements for resistance; some concepts of which can be applied to other modes of resistance.

1.6 STRUCTURE OF THE DISSERTATION

This dissertation details the body of research undertaken as part of the assessment of the reliability performance of the various procedures used for the design of concrete structures. The level of implementation of reliability principles in establishing current provisions for structural concrete are also critically reviewed, with a view of providing progressive guidelines where deficiencies are identified. Emphasis is placed on procedures for stirrup design, following from a broad survey of the basis of design for concrete structures which also considered aspects such as (1) partial factors and their interplay with local conditions and practice, and (2) model uncertainties amongst others. The research is presented over ten (10) Chapters, from 2 to 11, which are briefly described below.

Chapter 2 first takes a general view at the reliability framework for structural resistance, and then delves to focus on issues that are central to South Africa's adoption of EN 1992-1-1. Model uncertainties for reliability analysis and the reliability performance of the EN 1992-1-1 model for stirrup design are identified as critical issues requiring further investigation.

Chapter 3 gives the background to the various analogies and philosophies that have historically been applied when providing stirrups to reinforced concrete members. The different mechanisms causing actual failures in RC members both with and without stirrup reinforcement are discussed. The Chapter closes off by giving the detailed theoretical background of the analogy that EC2 recommends for the provision of stirrups to RC members. EC2 applies the Variable Strut Inclination Method (VSIM) as the analogy for stirrup design.

Chapter 4 serves to conveniently give the background to an alternative analogy that can be used in the analysis and design of RC members subjected to shear stresses, namely the Modified Compression Field Theory (MCFT). The MCFT serves as background to (1) fib LoA I and III approaches to shear design, and (2) sectional analysis program Response 2000, all of which were applied as part of the performance assessment of VSIM.

Chapter 5 compares the performance of the EN 1992-1-1 VSIM against the SANS 10100-1, *fib* LoA I, and *fib* LoA III stirrup design approaches. The unbiased shear capacity predictions of Sectional Analysis program Respose-2000, which can be considered as a LoA IV approximation according to the *fib* classification system, were applied in the parameter study as best-estimate results.

Chapter 6 presents the general background of the approach taken to the reliability performance assessment of the EN 1992-1-1 stirrup design procedure. It establishes concepts of the First Order Reliability Method (FORM) used for the performance assessment, as well as detailing some the statistical models that were employed in developing relevant probability models.

Chapter 7 elaborates on the correlation, regression, and parameter studies that were conducted to establish the statistics and probability models for the three cases of Model Factors used in this study. The Model Factors were integrated, and gave guidance, to the reliability performance assessments conducted in Chapters 8 and 9.

Chapter 8 presents the basic performance assessments, conducted using the FORM approach to reliability analysis, that were undertaken using the conventionally derived General Probabilistic Model (GPM) for shear resistance.

Chapter 9 presents performance assessments that were done using an alternative, more advanced, General Probabilistic Model (GPM) for shear resistance. The GPM was generated based on unbiased capacity predictions from R2k. These sets of analyses were commissioned to validate results from the basic investigations reported in Chapter 8.

Chapter 10 tasks itself with the important duty of providing a critical appraisal of the various topics presented in Chapters 2 to 9. Key outcomes from the various Sections are employed as part of a general discussion on the management of reliability performance for stirrup design.

Chapter 11 takes a brief, but systematic view, at all presented topics then concludes the investigation. Lastly, recommendations for future work are shared.

1.7 NOTE ON REFERENCE TO STANDARDS

Repeated reference is made throughout the dissertation to EN 1992-1-1, EN 1990, the JCSS Probabilistic Model Code, and the first draft of the *fib* 2010 Model Code. For ease of reference and for convenience, the terms EC2, EC0, JCSS PMC, and *fib* MC 2010 are adopted to refer to aforementioned standards, respectively.

Chapter 2

REVIEW OF THE RELIABILITY BASIS FOR STRUCTURAL CONCRETE RESISTANCE

The basic premise of this investigation derives from the view that reliability principles are the rational means of providing a substantive basis to adopt general design provisions to suit local conditions and practice. As already established in Chapter 1, South Africa's adoption of EC2 should consist of:

1. A review of the principles of structural reliability according to relevant literature; with a specific focus on requirements for resistance (i.e. to map out the reliability framework for structural concrete resistance).
2. An inspection of the level to which the reliability framework for structural resistance is applied in deriving provisions for EC2; done with the intention to bring to light generic investigations to be adapted to reflect SA conditions and practice.
3. To extend the framework for structural resistance in areas historically suffering from deficient application of reliability principles in establishing design guidelines. An issue further investigated in this report is the reliability performance of the Variable Strut Inclination Method (VSIM). The VSIM is the design analogy that EC2 recommends for use when providing stirrups to reinforced concrete members. Both (i) model uncertainties related to the prediction of shear resistance of stirrup-reinforced concrete members, and (ii) their inclusion as part of a rational reliability performance assessment of VSIM procedures formed the main thrust of subsequent Chapters of this report.

This Chapter therefore aims to draw focus to pertinent issues affecting the reliability performance of structural concrete resistance that should be accounted for as SA adopts EC2. Important reliability elements to consider include an appraisal of prescribed levels of structural performance (target β-values), partial factors, model uncertainties and quality control. These factors are concisely reviewed with a specific view on their interaction with local SA conditions and practice.

2.1 MANAGEMENT OF STRUCTURAL RELIABILITY FROM EUROCODE

Reliability can be reflected and managed throughout the process of structural analysis, design and construction. In general, any procedure, measure or action affecting structural performance or affecting the quality of constructed works, whether or not they can be quantified, can be viewed as having implications on reliability performance.

It is therefore advised that as South Africa reviews EC2 as reference for on-going revisions of the concrete code, the various champions in charge of various aspects of codified design as Materials, Structural Mechanics, and Detailing, should be responsible to verify the correctness, rationality, and applicability of the provisions in each of the respective sections. Table 2.1 presents a concise summary of the Sections and issues in EC2 to be reviewed by the various champions of the South African concrete code review committee responsible for Materials, Structural Mechanics, and Detailing.

Table 2.1. Roles for verification of EC2 by the South African review committee

Limit State	**Failure Mode**	**Materials**	**Structural Mechanics**		**Detailing**	
			Analysis	**Resistance**	**General**	**Elements**
Ultimate	Flexure	**SECTION 3:** Characteristic values. Rheological models **SECTION 10, 11, 12** Material classes	**SECTION 5** Modelling uncertainty for action effects; behaviour	**SECTION 6, 7** Valid SM models for resistance; serviceability behaviour	**SECTION 8** Validity of assumptions for resistance. Constructability	**SECTION 9** Ditto for elements. (Importance for seismic resistance – Robustness)
	Shear					
	Torsion					
	Punching					
	Fatigue					
	Durability					
Service	Stress					
	Cracking					
	Detailing					

2.2 THE BASIS OF DESIGN FOR STRUCTURAL RESISTANCE

All the structural Eurocodes rely on EC0 for the basis of structural design. The provisions of EC0 are material-independent, establishing general requirements for the different structural materials (concrete, steel, composite, timber, etc.). The design philosophy for safety verification is based on the limit state concept used in conjunction with the partial factor method. In the case of partial factor limit states design, performance requirements are expressed in terms of design situations to be considered, limit state principles and associated reliability levels. A significant part of the basis-of-design procedures stipulates action combination schemes for the various design situations and limit states. Provision for structural resistance is then left to materials-based design standards; with guidance given for the implementation of the principles of structural reliability in the standardisation process provided in annexes and referenced material.

Parametric studies of representative cases of structural resistance should be used to derive guidelines for structural resistance performance that could be used as basis-of-structural-design requirements to be considered in the formulation of materials standards (Holický et al., 2007). Holický et al. (2007) suggest that in the calibration of materials standards in accordance with the reliability framework, parameters to be taken into account include the specification of characteristic material properties, partial material, model and resistance factors, and the nature of failure consequences for the various failure modes. However, the general procedures for concrete design entail the way in which provision is made for sufficient reliability of structural resistance. This is typically done through schemes of partial factors and specification of characteristic values for basic variables applicable to design procedures.

2.2.1 The Limit States Design inequality and structural performance

The Eurocodes adopt the partial factor method, or limit states semi-probabilistic method, as the method for verification of structural safety (European Concrete Platform, 2008a). A limit state can be defined as a condition beyond which the structure no longer fills the relevant

design criteria. The governing condition of a limit state assessment is that the action effects should be less than the available resistance. This can be generally characterised by the inequality $E_d < R_d$, where the subscript 'd' refers to design values, E refers to actions and action effects and R to resistance. The design value method is a very important step from probabilistic design methods toward operational partial factors method (Holický & Retief, 2010). This is the practical way to ensure that the reliability index β is equal to or larger than the target value (EN 1990, 2002).

2.2.2 Ultimate and Serviceability Limit States

Two categories are defined by the consequences associated with the attainment of a limit state: Ultimate Limit State (ULS) and Serviceability Limit State (ULS). Ultimate limit states are associated with loss of equilibrium of the whole structure, or failure or excessive deformation of a structural member and they generally concern the safety of people. Table 2.2 shows the ultimate limit state classification for structures according to EC0.

Table 2.2. Classification of the Ultimate Limit Sates

Notation	Definition
EQU	Loss of static equilibrium of the structure or any part of it considered as a rigid body, where: - minor variations in the value or the spatial distribution of actions from a single source are significant (e.g. self-weight variations) -the strengths of construction materials or ground are generally not governing
STR	Internal failure or excessive deformation of the structure or structural members, including footings, piles, basement walls, etc., where the strength of construction materials of the structure governs.
GEO	Failure or excessive deformation of the ground where the strengths of soil or rock are significant in providing resistance
FAT	Fatigue failure of the structure or structural members

Serviceability limit states correspond to conditions beyond which specified service requirements for a structure or structural member are no longer met. Exceeding these limits causes limited damage but means that the structures do not meet design requirements: functional requirements (not only of the structure, but also of machines and services), comfort of users, appearance, damage to finishes and non-structural members (European Concrete Platform, 2008a). EC0 identifies three different types of combinations for serviceability limit states verifications:

1. Characteristic combination applicable to the more severe irreversible limit states,
2. Frequent combination applicable to reversible limit states, and
3. Quasi-permanent combination applicable to reversible limit states.

2.2.3 Basic variables, design values, and design situations

Basic variables, the vector $\{\boldsymbol{X}\}$, are used in structural resistance R and load E models that are implemented in limit state verifications at their design values (i.e. $E_d < R_d$). Design values of the basic variables, the vector $\{\boldsymbol{X_d}\}$, are achieved by the use of partial safety factors, the vector $\{\boldsymbol{\gamma}\}$, applied to characteristic values, the vector $\{\boldsymbol{X_k}\}$, of the basic variables adopted in design calculations. The basic variables relevant to structural resistance are material or product properties and geometrical data. Verifications of the limit state inequality are to be carried out for all relevant design situations and load cases. Design situations refer to sets of physical conditions representing the real conditions occurring during a certain time interval for which the design will demonstrate that relevant limit states are not exceeded. In common cases, deign situations are classified as:

1. *Persistent design situations*, referring to conditions of normal use,
2. *Transient situations*, referring to temporary conditions of the structure e.g. during construction or repair,
3. *Accidental situations*, involving exceptional conditions of the structure or its exposure, including fire, explosion, impact etc., and
4. *Seismic situations*, where the structure is subjected to a seismic event.

Each design situation is characterised by the presence of several actions on the structure. As such, much focus in EC0 is directed towards the treatment of combinations of actions and associated partial factors for each design situation relevant to each limit state. Stipulation of the resistance basis of design requirements, on the other hand, are presented at a high level of abstraction, providing for the diverse characteristics of structural material, ranging from structural steel, through concrete, to geotechnical design.

2.2.4 Specification of design resistance R_d by the partial factor method

For the design resistance, R_d is symbolically expressed in terms of the design values of the material properties (X_d), geometry (a_d) and model uncertainty (θ_d):

$$R_d = R\{X_{d1}, X_{d2}, \dots\ a_{d1}, a_{d2}, \dots\ \theta_{d1}, \theta_{d2}, \dots\} \qquad [2.1]$$

Design values of the material properties X_d are not introduced directly into the design models used for limit state verifications. Characteristic or some other suitable representative value of the material property is rather used in combination with the appropriate partial factor to describe the design value of the basic variable in the limit state model. EC0 defines the characteristic value of a property of a material as the 5 % fractile of its statistical distribution where a minimum value of the property is the minimal failure limit and as the 95 % fractile where a maximum value is the limiting value. The minimal failure limit is usually applicable to material or product properties in problems of structural design. Table 2.3 below, reproduced from the Eurocode 2 Commentary (European Concrete Platform, 2008a) details the steps to obtain design resistance R_d from individual resistance parameters X_i, mostly at the Ultimate Limit State.

Table 2.3. Procedure to determine the design values of resistances from component parameters (European Concrete Platform, 2008a)

Expression	Comment
X_i	Material strengths and product resistances involved in the verifications are identified.
$X_{k,i}$	Characteristic values of material strengths and product resistances are introduced.
$X_{d,i} = \eta \frac{X_{k,i}}{\gamma_{m,i}}$	The design value of a material property is determined on the basis of its characteristic value, through the two following operations: a) divide b a partial factor γ_m, to take into account unfavourable uncertainties on the characteristic of this property, as well as any local defaults; b) multiply, if applicable, by a conversion factor η mainly aimed at taking into account scale effects.
$R\left(\eta \frac{X_{k,i}}{\gamma_{m,i}}; \mathrm{a}_d\right)$	Determine the structural resistance on the basis of design values of individual material properties and of geometrical data.
$R_d = \frac{1}{\gamma_{Rd}} R\left(\eta \frac{X_{k,i}}{\gamma_{m,i}}; \mathrm{a}_d\right)$	The design value of structural resistance is determined on the basis of the individual material properties and of geometrical data divided by a partial factor γ_{Rd} that covers the model uncertainties of resistance and the geometrical data variations, if these are not explicitly taken into account in the model.
$R_d = R\left(\eta \frac{X_{k,i}}{\gamma_{M,i}}; \mathrm{a}_d\right)$	Factor γ_{Rd} is often integrated in the global safety factor $\gamma_{M,i}$, by which the characteristic material strength is divided: $\gamma_{M,i} = f(\gamma_{Rd}, \gamma_{m,i})$

2.2.5 Model uncertainties and the systematic calibration of partial factors for resistance

It is clear from Table 2.3 that the provision for model uncertainties as part of resistance safety factors is an important development in terms of implications for materials standards that will be based the limit states design concept. However, to date, calibration and performance assessment studies for structural mechanics models usually represent model uncertainties based on expert guidance. The proper way to account for model uncertainties is to determine

its characteristics from a fitting of the prediction model under investigation to a database of tests representative of the mode of resistance under investigation.

Holický et al. (2007) considered specific examples of modelling uncertainty in order to demonstrate their importance in the design process. The study considered cases in research where the model factors are determined statistically from data sets describing flexural and shear behaviour of reinforced concrete elements. Model uncertainty (θ) was therein shown not only to vary across the different modes of structural concrete resistance (mean and standard deviation $\mu_\theta = 1.08,\ \sigma_\theta = 0.10$ for flexure; $\mu_\theta = 1.23, \sigma_\theta = 0.38$ for EC2 shear with no links) but also varies along the parametric range of a single mode of resistance (showing sensitivity to design parameters).

Partial factors used for structural design should be appropriately derived to cater for the various model uncertainty sensitivities described above, taking into account uncertainties associated with other variables as well (strength, geometry etc.). Model uncertainties for other failure modes should be studied and quantified for derivation of adequate safety elements in this regard. Figure 2.1, reproduced from Annex C in EC0, gives a schematic representation of the factors necessary in calibrating partial factors for action effects, γ_F, and for resistance, γ_M.

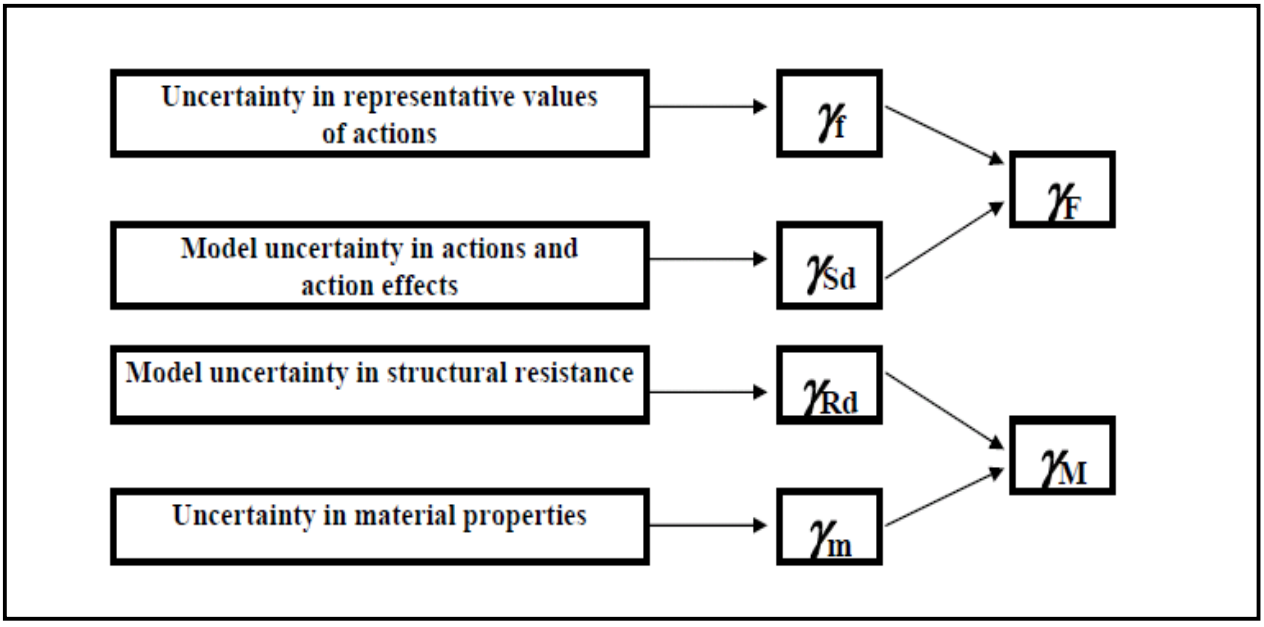

Figure 2.1. Relation between individual partial factors (EN 1990, 2002)

Partial factors for different modes of failure should be derived from representative parametric studies. The First Order Reliability Method (FORM), which is described in detail in Chapter 5, is prescribed for use in assessing the design values of resistance. This method allows reliability analyses and calibration to be separated for actions E and resistances R. Partial factors γ are determined as the ratio between characteristic values of resistance X_k (determined by use of characteristic values of basic variables) and design values of resistance X_d (determined from FORM analyses) i.e. $\gamma_i = \frac{X_{k,i}}{X_{d,i}}$.

The target reliability index, β_T, is an integral part of the FORM procedure and therefore influences the magnitudes of partial factors derived from the process. Partial factors can be considered as direct measures of reliability that are tied to limit state verifications for different failure modes. The reliability index β for members and structures is left open for national choice and selecting a different target value implies that relevant parametric studies should be conducted to derive values for partial factors for resistance as well as action effects. The target values of reliability β as recommended by the Eurocodes that are applicable to each of the limit states for specified periods are given in Table 2.4 for structural class RC2 members. It is essential to note that preceding descriptions for partial factor determination are applicable at ULS.

Table 2.4. Target reliability index β for Class RC2 structural members

Limit state	**Target reliability levels**	
	1 year	50 years
Ultimate	4.7	3.8
Fatigue		1.5 to 3.8
Serviceability (irreversible)	2.9	1.5

For SLS the partial factors for the properties of materials, γ_M, should be taken as unity (1.0) except if differently specified in EN 1992 to EN 1999. This implies that for serviceability limit state verifications, resistance is determined at its characteristic value R_k.

2.2.6 Quality management and reliability differentiation

Quality management is an essential component in achieving prescribed levels of structural reliability. It has a controlling effect on the practically achieved values and variability of the basic variables that affect structural resistance e.g. concrete strength (f_c), steel strength (f_y), geometry etc. The provisions of the Eurocodes are subject to the basic assumptions that design and execution will be carried out by qualified and experienced personnel, as well as adequate supervision and quality control being provided during the execution of work. The design provisions in the Eurocodes are deemed, if complied with, to lead to a class of structures of Reliability Class RC2. Different levels of reliability (β), distinguished through Reliability Classes (RCs), are achievable due to differently applied levels of design and execution inspection that aim mainly to reduce gross errors.

An independent alternative measure of achieving reliability differentiation, though not normally used, is to adjust the action partial factors upward or downward by 10 % depending on the reliability class. Adjustment of resistance partial factors due to increased control is allowed, but with no relationship to reliability differentiation.

2.2.7 Application of the reliability framework to structural concrete

Although a reliability framework is developed also for structural resistance in the form of partial factors, model and resistance factors for respective classes of failure modes, systematic calibration of the materials standards is limited (Holický, Retief & Dunaiski, 2007). EN 1990 and SANS 10160-1 both present an elaborate scheme of action partial safety factors to be applied to various design situations and the associated limit states. For structural concrete resistance, on the other hand, a simple scheme of partial factors is employed to cover a very broad scope of design procedures for concrete resistance.

For conventional reinforced concrete, the partial material factors $\gamma_C = 1.5$ for concrete and $\gamma_S = 1.15$ for steel can be seen to prevail during ultimate limit state verifications across all modes of resistance (at the ultimate limit state) and design situations. Numerous reliability analyses and calibration studies (Holický et al., 2007; Holický et al., 2010) have however

shown that partial factors are in fact applicable to all basic random variables affecting structural performance.

The use of γ_C and γ_S in determining the design resistance for conventional reinforced concrete can therefore be considered as a simplified and approximate treatment of all the unfavourable uncertainties affecting resistance performance. Model uncertainties (θ), which reflect the accuracy of prediction of uncalibrated resistance models, have also been shown (Holický et al., 2007; Holický & Markova, 2007; Holický et al., 2010) to have a significant influence on resistance reliability performance.

2.3 APPLICATION OF THE RELIABILITY FRAMEWORK TO STRUCTURAL CONCRETE IN SOUTH AFRICA

EN 1992-1-1 would have to be calibrated in accordance with the basis of design requirements as set by SANS 10160-1 to enable its use as a local South African design standard. Due to the adoption process, South Africa is bound to implement the full text of EN 1992-1-1, as published by CEN, together with a National Annex (NA) containing the verdict on the NDPs suitable for local use. The Eurocodes cater for a comprehensive range of structures across Europe that goes beyond the scope of standard South African practice. The level of competence thus required to apply the future SANS 51992-1-1 can broadly be described as normal practice and specialist applications (SANS 51992-1-1, Draft).

In addition to the general NA, a South African specific NA will also be published to provide local guidance and warning about specialist applications requiring additional proof of sufficient competence and skills by the designer. The differently applied reference levels of reliability (β) as exercised by EN 1990 and SANS 10160-1 will most certainly play a key role in specifying some of the NDPs to be enforced in SA.

Strictly speaking, the differently adopted β-values should have an effect on the operational partial factors adopted in design; with larger values of the partial factors derived for EN 1990

reliability requirements ($\beta = 3.8$ for RC2) as compared to those derived according to SANS 10160-1 requirements ($\beta = 3.0$ for RC2). The effect that β has on operational partial resistance factors is showcased in the following Sections, thereby highlighting the relationship between partial factors and achieved reliability.

The differences in quality regimes experienced between SA and European levels of standard construction practice are expected to have an effect on levels of achieved reliability. However, the lack of South African data reflecting the influence of local practice and production quality on the distributions of common basic variables impedes a rational comparison. Instead, South African quality levels of standard practice are generally perceived as lower than those of equivalent European practice. This judgement based assumption usually leads to some degree of conservatism being exercised when reviewing the results of South African calibration studies, to cater for the effect of increased quality due to the use of European models in the various analyses.

Following from the general basis of design requirements explored in Section 2.2 above, this Section takes a closer look at pertinent reliability performance to consider as SA adopts EC2. Important reliability elements to consider include an appraisal of prescribed levels of structural performance (target β-values), partial factors, model uncertainties and quality control. These factors are concisely reviewed with a specific view on their interaction with local SA conditions and practice.

2.3.1 Discussion of the SANS 10160-1 prescribed levels of performance

Member states of the European community and other countries using the Eurocodes as base for their standards development are required to set reference reliability levels, commonly referred to as target reliability levels β_T, based on structural risk acceptance criteria suitable for national practice. For South African standards, the different levels of risk acceptance criteria correspond to a minimum reliability. Table 2.5 presents the classification of Reliability Classes as described by SANS 10160-1 with some examples of design situations in which each class may be applicable.

Table 2.5. Classification of SANS 10160-1 Reliability Classes

Class	$\boldsymbol{\beta_T}$	**Accidental Consequence Class**	**Seismic Class (Public safety)**	**Geotechnical Category**
RC1	2.5	Single occupancy ≤ 3 storeys	Minor (agriculture)	Small structure; no stability or movement
RC2	3.0	Residential, office etc; ≤ 4 storeys	Ordinary	Conventional structure / foundation
RC3	3.5	Residential, office etc; 5 - 15 storeys	Important (schools; assembly)	Ground / structure require geotechnical input
RC4	4.0	Public in large #; stadia > 5000	Vital (hospital; fire; power)	Large; unusual; complex; risky;

In a rational analysis the target reliability β_T is considered as a control parameter subject to optimisation (JCSS, 2001). However, to date, national reliability levels are set by calibration to a long experience of building tradition. For South African structural design standards, a reference level of reliability of $\beta = 3.0$ of class RC2 is prescribed for use by the national basis of design standard SANS 10160-1. This value of reference reliability was set from extensive calibration of structures designed in accordance with the now outdated national loading and basis of design code SABS 0160-1989 (Milford, 1988). Furthermore, the reference level of reliability set for use in South Africa is also defendable from recommended values suggested for use by the JCSS PMC and the international standard ISO 2394.

Table 2.6 shows the relation between the SANS 10160-1 and EC0 Reliability Classes together with their associated consequences of failure. It is clear from the Table that in addition to adopting different reference levels of reliability β from Eurocode, SANS 10160-1 also specifies four Reliability Classes, RC1 to RC4, as classifiable for structures. It should be noted that although RC2 serves as reference, with $\beta = 3.0$, RC2 and RC3 in fact represent a division of the Eurocode RC2, differentiated generally at buildings of four and five storeys (Retief & Dunaiski, 2009) as shown in Table 2.6.

Table 2.6. Reliability classes and associated consequences of failure for SANS 10160-1 and EC0

Class	**Function of facility, probability or consequence of failure**		**Class**
	SANS 10160-1	***EN 1990***	
RC1 $\beta = 2.5$	Low loss of life, economic, social ; small environmental	Low for loss of human life, and economic, social or environmental small or negligible	RC1 $\beta = 3.3$
RC2 $\beta = 3.0$	Moderate loss of life, economic, social; Considerable environmental	Medium for loss of human life, economic, social or environmental considerable	RC2 $\beta = 3.8$
RC3 $\beta = 3.5$	High loss of human life, very great economic, social, environmental		
RC4 $\beta = 4.0$	Post-disaster function / beyond the boundaries	High for loss of human life, or economic, social or environmental very great	RC3 $\beta = 4.3$

Table 2.7 presents the more fundamental schemes of recommended levels of reliability, differentiated by risk criteria, suggested for use by ISO 2394 and the JCSS Probabilistic Model Code (PMC). South Africa's reference class RC2 structures ($\beta_T = 3.0$) reflects the scope of the standard SANS 10160-1; applying to buildings and common industrial structures. Such general constructions can be viewed to attract a moderate (according to ISO) or normal (according to JCSS) cost of implementing safety measures. Hence, the SANS 10160-1 minimum level of performance of $\beta_T = 3.0$ for RC2 structures is comparable (for moderate consequences of failure, see Table 2.6) to the ISO and JCSS suggested values of 3.1 and 3.2, respectively, as shown shaded in Table 2.7.

Table 2.7. Schemes of recommended levels of reliability by ISO 2394 and JCSS PMC based risk principles

Relative cost of safety measures	ISO 2394			
	Consequences of failure			
	Small	Some	Moderate	Great
High	0	1.5	2.3	3.1
Moderate	1.3	2.3	3.1	3.8
Low	2.3	3.1	3.8	4.3
Relative cost of safety measures	JCSS Probabilistic Model Code			
	Consequences of failure			
	Minor	Moderate		Large
Large	1.7	2.0		2.6
Normal	2.6	3.2		3.5
Small	3.2	3.5		3.8

The β-values and associated consequences of failure from Tables 2.6 and 2.7 are presented in Figure 2.2 to depict the levels of performance for (1) the four Reliability Classes (RC1 – RC4) from SANS 10160-1, versus (2) RC1 – RC3 from Eurocode, versus (3) ISO performance at moderate cost of safety measures, versus (4) JCSS performance at normal cost of safety measures.

The Figure clearly indicates that SANS levels of performance are closely related to those of ISO and JCSS, with EN performance levels shown clearly to have been selected on a conservative basis. It can therefore be reasonably deduced/postulated that the SANS levels of performance are fully acceptable (from viewpoint of ISO 2394 & JCSS PMC) but economical (compared to EN values).

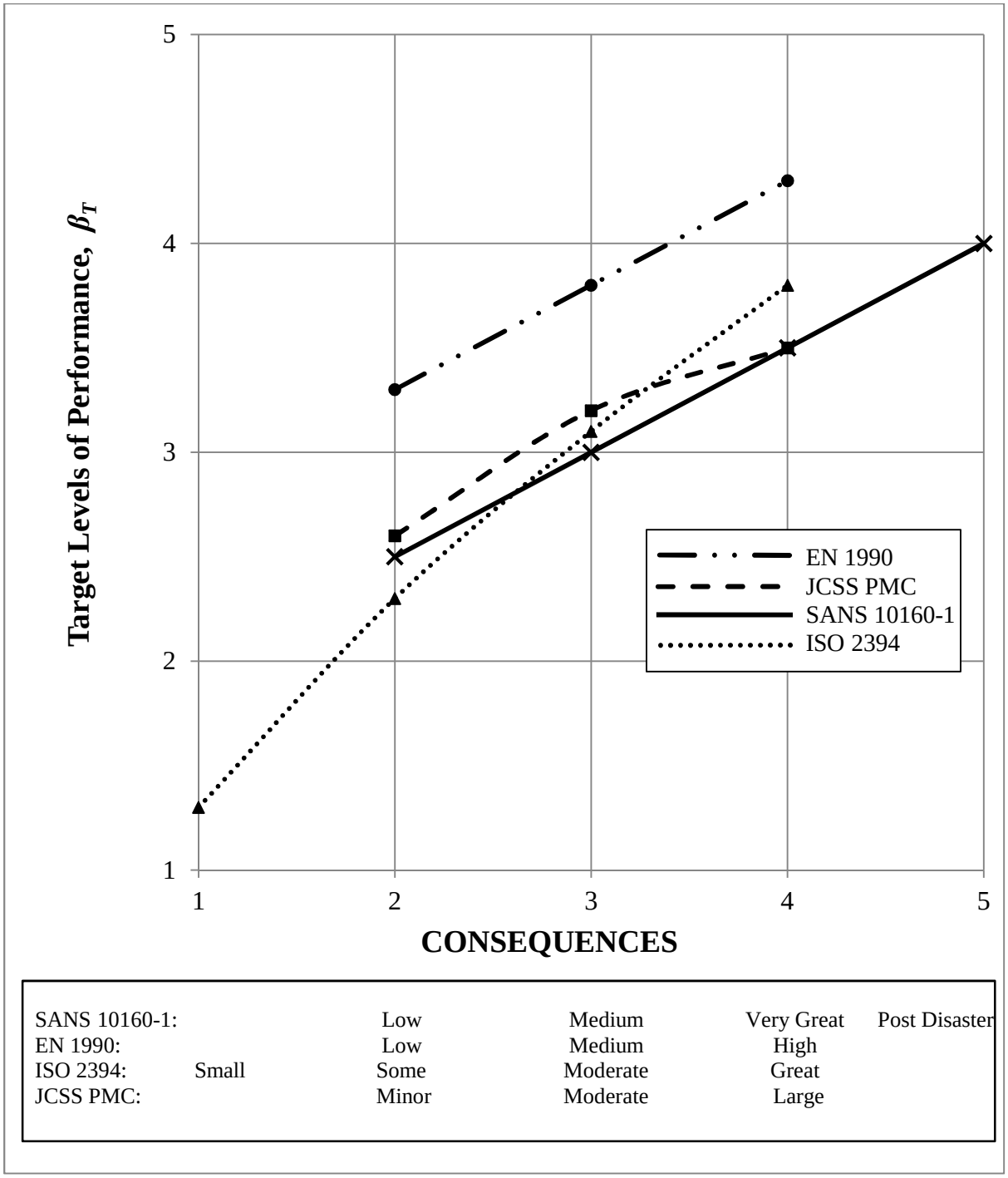

Figure 2.2. Comparison of SANS, Eurocode, ISO and JCSS levels of performance (adapted from Holický, 2013)

2.3.2 Probabilistic basis of partial factors for resistance

Due to the uncertainties associated with material properties as discussed in Table 2.3, it is generally expected (JCSS, 2001) that the resistance predictions of structural models (R) and their associated material properties (X) may be described by the Log-normal (LN) distribution with a 0-value lower bound. The Normal (N) distribution, however, finds itself readily used in reliability modelling, both for actions and material properties or resistance (usually used if geometric effects are to be modelled or quite often used to nominally represent model uncertainties); hence it is useful to also portray its effect on operational partial factors. Assuming first a Log-normal distribution in Equation 2.2, followed by a Normal distribution in Equation 2.3, the partial factors, γ_m for materials and γ_{Rd} for resistance models, are described by (European Concrete Platform, 2008a):

$$\gamma_m = \frac{X_k}{X_d} = \frac{\exp(-1.645V_X)}{\exp(-\alpha_R \beta V_X)} \quad or \quad \gamma_{Rd} = \frac{R_k}{R_d} = \frac{\exp(-1.645V_R)}{\exp(-\alpha_R \beta V_R)} \qquad [2.2]$$

$$\gamma_m = \frac{X_k}{X_d} = \frac{1-1.645V_X}{1-\alpha_R \beta V_X} \quad or \quad \gamma_{Rd} = \frac{R_k}{R_d} = \frac{1-1.645V_R}{1-\alpha_R \beta V_R} \qquad [2.3]$$

where $V_{X,R}$ is the coefficient of variation $\left(\sigma_{X,R}/\mu_{X,R}\right)$ of general resistance property X or R. Note that the characteristic values X_k and R_k are the fractiles of X and R corresponding to the 5 % fractile, hence the factor -1.645 is the fractile of the standardised normal distribution corresponding to the same 5 % fractile. Equation 2.2 provides a good approximation if the coefficient of variation $V_{X,R}$ is small, approximately $V_{X,R} < 0.20$ (Holický & Diamantidis, 2010).

Equations 2.2 and 2.3 are plotted in Figure 2.3. Figures 2.3 (a) and (b) show the general trends of the partial factors (γ_m and γ_{Rd}) with varying coefficients of variation ($V_{X,R}$) and varied levels of reliability (β) for the separate assumed cases of (1) Log-normal and, (2) Normal distributions, respectively, of material or resistance properties (X, R). Indications are given in Figure 2.3 to show the implication of the differently adopted target β-levels for RC2 structures by SANS 10160-1 and EN 1990 on partial factor requirements. Figures 2.3 (c) and (d) illustrate for the two separate cases, $\beta_{RC\,2,SANS} = 3.0$ and $\beta_{RC\,2,EN} = 3.8$ respectively, how partial factors for material and resistance properties are dependent on the coefficient of variation as well as on the reliability requirements set by SANS 10160-1 and EN 1990.

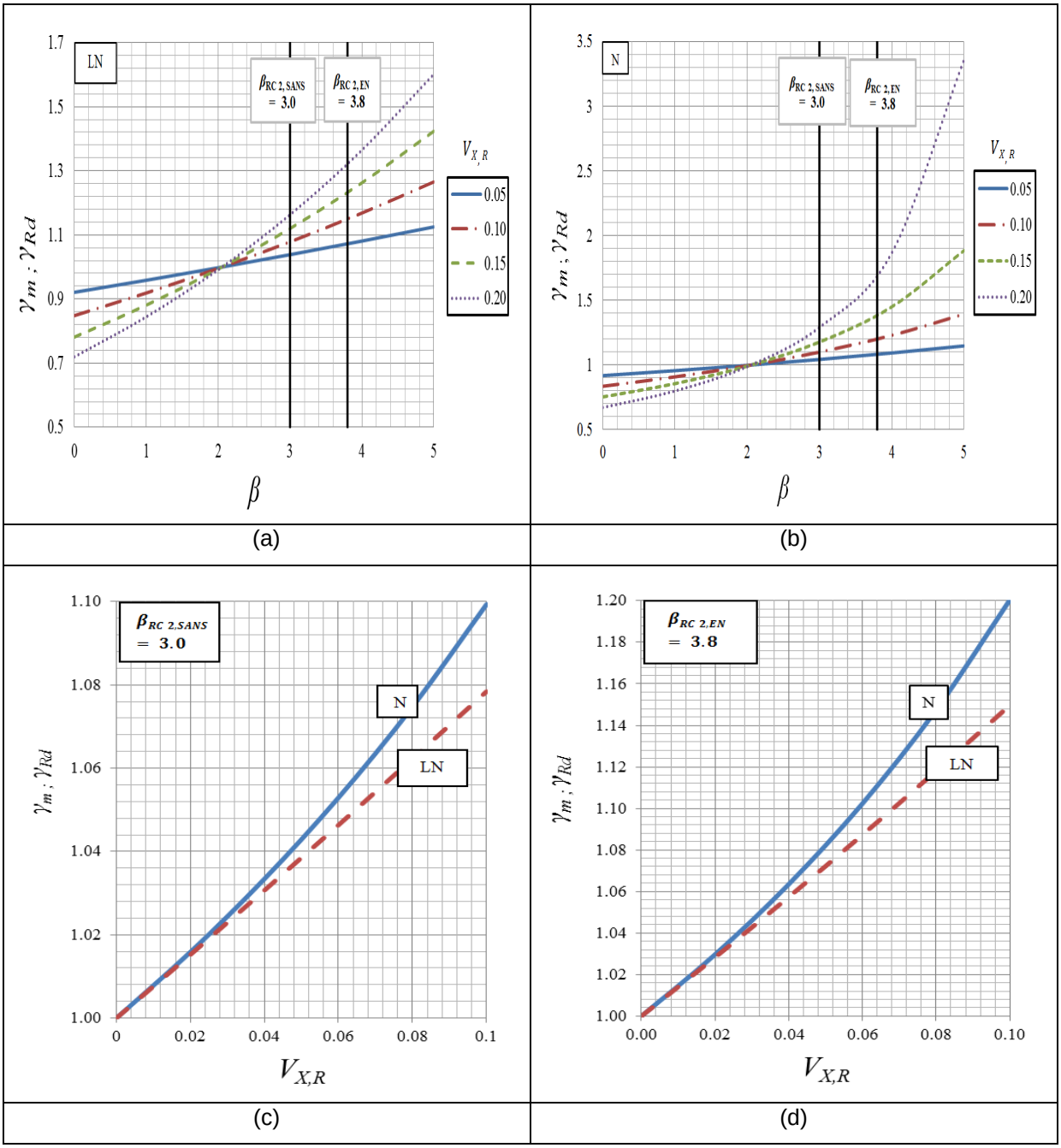

Figure 2.3. Graphs showing the trends of γ_m and γ_{Rd} : (a) for Log-normal distribution, (b) for Normal distribution of X & R, (c) at $\beta_{RC\,2,SANS} = 3.0$, (d) at $\beta_{RC\,2,EN} = 3.8$

Notice that for material properties, V_X is mostly influenced by the production quality of the material manufacturing process. Further note that production quality for the different materials also varies between countries. For resistance models, V_R on the other hand is influenced by the epistemic uncertainty or bias of the resistance model, either due to incomplete understanding or deliberate simplification.

It can be logically deduced from Figure 2.3 that reliability differentiation through specification of different Reliability Classes (RCs) should have an effect on the operational partial factors to be adopted in design. Furthermore, improved quality measures can be effective in reducing deviations of a material property by efficient control of the production process.

The use of commonly available European models of basic variables will most likely be used in most calibration studies aimed at applying EC2 in SA. This will obviously cause some additional uncertainty regarding the suitability of calibrated models for local conditions and practice, particularly concerning local aspects of production quality and management. This creates the need for a conservative approach to be applied when reviewing the outcomes of calibration studies, adjusting the results when justified to cater for the perceived higher levels of standard quality exercised in Europe than in SA.

Model uncertainties should also have an effect on the value of operational partial factors used in design, where V_R would be determined from a database of representative laboratory test results and a fitting of the appropriate resistance models. The partial factor for materials, γ_m, could then be combined with that for the resistance model, γ_{Rd}, to give rise to a bulk resistance factor, $\gamma_M = \gamma_m \cdot \gamma_{Rd}$. This is the rational way in which model uncertainties should be taken into account.

2.3.3 Initial calibration of resistance models from EC2 against SANS 10160-1 performance requirements

Holický et al. (2010) conducted a limited calibration of partial factors γ_C and γ_S for structural concrete against SANS 10160-1 performance requirements. The study considered the parametric assessment of a slab and short centrically loaded column as representative, respectively, of flexure and compressive modes of resistance. South Africa's reference level of reliability for RC2 structures, $\beta = 3.0$, formed the basis of the evaluation; seeking an adequate partial factor scheme (γ_C and γ_S-values) to apply for reference class RC2 structures in South Africa's future design code for concrete structures SANS 51992-1-1.

Furthermore, important insights gained from the results of the study by Holický et al. (2010), concerning the reliability performance of procedures for structural concrete design, were revealed. The most prominent insights shared were:

1. A number of factors influence structural concrete performance, besides concrete strength (f_c) and steel strength (f_y) which are conventionally catered for explicitly by partial factors γ_C and γ_S respectively. This implies for the current format that γ_C and γ_S are a simplification that should be calibrated to (a) cater for uncertainties associated with other less influential basic variables e.g. geometry, model uncertainty, and (b) since different influences of the various basic variables are shown for different modes of resistance, γ_C and γ_S should be assessed across all modes of resistance (shear, flexure, compression, etc.) in order to derive a partial factor scheme effective in managing structural performance.

2. Although model uncertainty statistics associated with the prediction models were selected based on expert guidance from the JCSS PMC, a significant influence was shown for model uncertainty affecting particularly compressive resistance. Hence, the results indicated that (a) model uncertainty representation could be improved by characteristaion against representative tests – for a more representative analysis, and (b) model uncertainties could be more influential on structural performance for modes of resistance where prediction accuracy is less consistent or accurate, as has classically been the case with shear resistance (with or without stirrups).

3. In light of the above points, reduced partial factors of $\gamma_S = 1.10$ & $\gamma_C = 1.40$ were found applicable for both flexure and compression; but more studies were suggested to assess the partial factor scheme γ_C and γ_S for (a) other modes of resistance, and (b) using more representative model uncertainty statistics.

2.3.4 Structural performance and present state of calibration of the EC2 models for shear resistance

Narayanan and Beeby (2005) in the Guide to EC2, state that despite the uncertainties associated with shear prediction models, shear design can be carried out with confidence as the models in EC2 have been tested against and adjusted to fit a large set of experiments.

A survey of the background publication Eurocode 2 Commentary (European Concrete Platform, 2008a) showed evidence of the calibration of EC2's shear design model for members without stirrups (reliability-based coefficient is applied to the empirically determined design formula). A similar calibration/assessment for the design model for members with stirrups has been lacking. This is surprising considering the fact that the provision of stirrups or vertical reinforcement in design signifies an important and highly routine design situation that frequently occurs in practice to prevent sudden brittle failures.

EC2 employs the Variable Strut Inclination Method (VSIM) as the analogy for stirrup design. The assessment of the general performance of the VSIM as presented by EN 1992-1-1 therefore becomes one of the essential activities of SA's adoption process.

Furthermore, investigations by Cladera & Mari (2007), confirmed later in Chapter 7 of this report, have shown the unbiased stirrup contribution of the VSIM to be sensitive to the amount of stirrups provided in design. Figure 2.4 illustrates the trend of the ratio of the failure load from a laboratory beam experiment (V_{exp}) to a corresponding unbiased VSIM prediction (V_{pred}) versus the nominal quantity of stirrups provided in design ($\rho_w f_{yw}$). The stirrup reinforcement ratio ρ_w is equivalent to the ratio of the area of the 2-legs of a stirrup (A_{sw}) over the product of the beam width (b_w) and stirrup spacing (s). f_{yw} represents the yield strength of the stirrups. The unbiased stirrup contribution of the VSIM seems to generally give excessively conservative capacity predictions when small amounts of stirrups are provided in design. Conversely, the model progresses to marginally conservative and eventually becomes unconservative as $\rho_w f_{yw}$ increases.

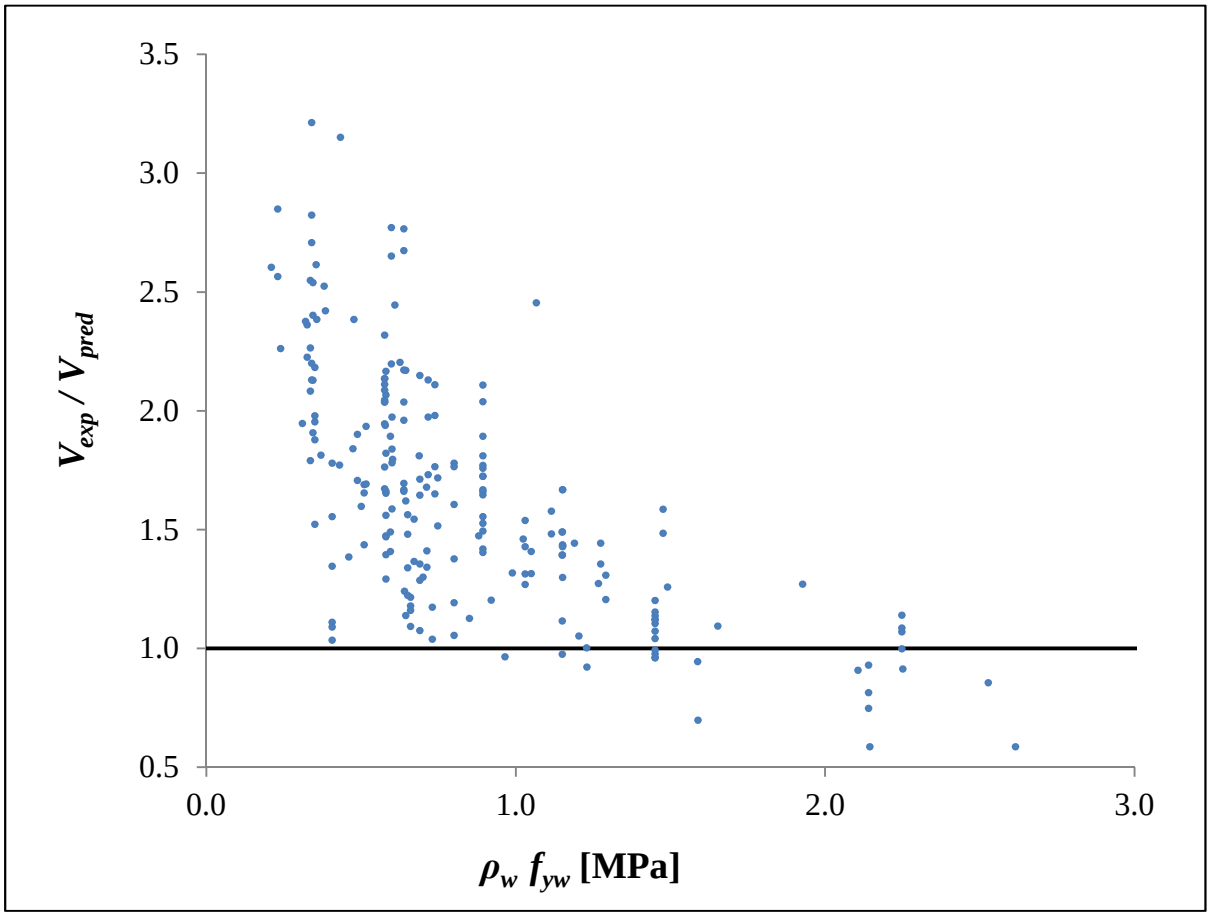

Figure 2.4. Relationship between V_{exp}/V_{pred} and $\rho_w f_{yw}$

Given the trend of shear resistance predictions shown in Figure 2.4, particularly the potentially unsafe predictions at high $\rho_w f_{yw}$, no clear mechanisms towards the appropriate reliability calibration of the VSIM, as required by modern basis of design formats, are provided in the background to EC2. The European Concrete Platform (2008a) presents evidence showing the VSIM to be in agreement with test results. Some initial results presented against the development and application of the VSIM (Bræstrup et al. 1976) also shows general agreement with results, with some test data scattered above and below the model's fit. Calibration of the model is therefore an essential task, not only to mitigate uncertainties associated with it, but to support the proper application of the VSIM in practice by ensuring adequate safety and economy of design whenever it is used.

The appropriate level of performance for the VSIM design procedure is obtained using the conventional partial factors approach ($\gamma_C = 1.5$ for concrete and $\gamma_S = 1.15$ for steel) of expressing material strength in terms of its characteristic value X_k divided by a partial

material factor γ_m. This is however not supported by reliability calibration, particularly considering the effects of modelling uncertainty.

Substantial effort is therefore directed in subsequent Chapters of this report to assess the reliability performance of the VSIM design model discharged for use by EC2. FORM analysis was applied to assess the achieved β-values primarily against $\rho_w f_{yw}$, although the sensitivity of β to concrete strength f_c was also investigated. Consequently the results confirm concerns, indicating the potential of inadequate reliability performance at high $\rho_w f_{yw}$ (estimated $\beta < \beta_T$), to be possibly mitigated by increasing concrete strength f_c since β increases with an increase in f_c. Subsequent Chapters are therefore concerned primarily with procedures for shear resistance and the design of stirrups, aiming to:

1. Give the theoretical and analytical background to the various shear resistance prediction methods used in the performance analysis of VSIM procedures (Chapters 3 & 4).
2. Based on the trend from Figure 2.4, compare the performance of alternative prediction models for shear/stirrup design, particularly against $\rho_w f_{yw}$ (Chapter 5).
3. Present the theoretical background of the FORM procedure for reliability analysis (Chapter 6).
4. Investigate various model uncertainty statistics, derived from a database of stirrup-reinforced beam tests, to incorporate as part of the rational reliability performance assessment of VSIM procedures (Chapter 7).
5. Conduct the reliability analysis of VSIM procedures according to alternative General Probabilistic Model (GPM) representations for shear resistance, and the present results (Chapters 8 and 9).

Chapters 10 and 11 then move, respectively, to share some valuable insights gained from the investigation and then conclude the study.

2.4 SUMMARY AND OBSERVATIONS ON THE BASIS OF STRUCTURAL CONCRETE DESIGN

The reliability basis of structural resistance, as should be considered for structural concrete performance in South Africa, has been reviewed. Many shortcomings inhibiting the full implementation of the general resistance basis of design requirements to structural concrete have been identified. This however reflects the current state of mature knowledge and technology of dealing with structural concrete performance, and is not peculiar to EC2. Partial factor diversity (or systematic calibration), model uncertainties and the exploitation of the reliability differentiation framework for resistance are the key issues affecting structural concrete performance that still require further international unification with reliability principles.

The currently widely adopted philosophy of applying the partial factors γ_C and γ_s to provide for all the various uncertainties and associated limit states only allows for limited calibration of the resistance models used in design codes. Although EC2 establishes that a design conforming to its general assumptions and provisions should lead to a structure of reliability class RC2, there is no explicit way to make adjustments to its provisions to achieve the other (differentiated) reliability classes.

Informative Annex A in EC2 does, however, provide recognition for improvements of variations achieved by more stringent quality control measures (exercised at controlling deviations of critical sections and concrete strength) by allowing reductions of the partial factors. Through its controlling effect on material property variations, quality control consequently plays an integral role in achieving the specified characteristic values of material properties; both these elements play an integral role in achieving a certain level of reliability.

The specification of characteristic values (or bias), as can be seen from Table 2.3, is an important step in achieving operational partial factors for materials. Strictly speaking, different quality regimes should have an influence on the value of operational partial factors used in design. The interplay between quality control, reliability classes and their differentiation (both SANS and EN RCs), and partial factor reduction as allowed in EC2 are explored by Mensah et al. (2010). It is therein shown that partial factor adjustments are warranted under the auspices of the various reliability classes and their associated quality measures.

Model uncertainties and their systematic treatment or calibration requires attention for structural concrete performance. Although provision is made in EC0 for model uncertainties, there are no clear mechanisms showing how modelling uncertainty can be, or has been, taken into account in EC2. Model uncertainty is one of the dominant factors that affect concrete performance. Recall that it varies along the various modes of structural concrete behaviour; it also varies parametrically for a single mode of resistance. Their proper characterisation and subsequent calibration (say for different RCs) is therefore an essential task which requires some attention.

It is clear that in the interim, South Africa should adopt EC2 as it is with the relevant NDPs and warnings to be provided in National annexes. A further exercise would be to advance the implementation of reliability principles in deriving guidelines for structural concrete resistance. It is not anticipated that there will be any major differences in the specification of the reliability elements in EC2 during South Africa's adoption of the standard, particularly regarding the values of the partial factors given the different SANS and EN target levels of reliability.

In addition to concerns about local quality control, there is lack of South African data on the achieved probability distributions of the common random variables affecting structural concrete performance. Hence, no credible evidence exists to reduce EC2's partial factors or revise its partial factor reduction scheme given in informative Annex A. The process could however be updated as local data becomes available. Such an instance would reduce the application of expert judgement in the process thus alleviating some additional uncertainty.

CHAPTER 3

SHEAR RESISTANCE AND THE VARIABLE STRUT INCLINATION METHOD FOR SHEAR

In practice, stirrups are provided to a majority of reinforced concrete members, save those of minor structural importance such as lintels, blinding, and etcetera. Stirrups enhance the ductility characteristics of reinforced concrete structures subjected to shear-flexure stresses by:

1. Increasing the number of cracks that occur before failure, providing increased warning of impending failure
2. Increasing section capacity due to increased post-cracking strength of the member

This Chapter is primarily concerned with the theoretical background of the analogy that EC2 recommends for the provision of stirrups to RC members, namely the Variable Strut Inclination Method (VSIM) for shear. However, alternative procedures for stirrup design and shear resistance are included as part of the performance assessment of VSIM procedures in Chapters of this report.

In Chapter 5, VSIM procedures are compared to (1) the stirrup design analogy employed in the currently operational local design standard SANS 10100-1 *The structural use of concrete*, and (2) the *fib* Model Code 2010 Modified Compression Field Theory (MCFT)-based design analogies (Levels of Approximation I & III). Sectional analysis program Response 2000, which is also based on the MCFT, served in the assessment providing best estimate capacity predictions representative of test results. Response 2000 capacity predictions were additionally utilised as an integral part of reliability performance investigations of VSIM procedures presented in latter Chapters (Chapters 7 to 9) of this report. A survey of VSIM and alternative stirrup design methods (which are based on the MCFT) is therefore presented initially in this Chapter, with the theoretical background of the MCFT given in Chapter 4.

In order to effectively discuss the background of the EC2 VSIM procedure, this Chapter:

- Reviews milestone contributions made by prominent researchers to field of shear mechanics; shaping way various analogies approach design, particularly for stirrup-reinforced concrete members
- Takes a look at the behaviour and mechanisms of failure of stirrup-reinforced concrete members

- Distinguishes between B-region and D-region shear; of which the VSIM applies to B-region shear
- Provides a general survey of some existing operational procedures to shear analysis and design
- Then, finally, presents the theoretical background of the EC2 VSIM design formula with emphasis on its basis on the theory of plasticity

3.1 EVOLUTIONARY BACKGROUND OF DESIGN PHILOSOPHIES FOR STIRRUP-REINFORCED CONCRETE MEMBERS

Proper understanding of shear, both with and without shear reinforcement, seems to elude many practitioners and researchers alike. Research efforts on understanding shear date back to as early as 1899 in which Ritter carried out an investigation to determine an effective type of stirrup reinforcement (Balázs, 2010). Inspired by crack patterns typically observed in beam tests, Ritter and later Mörsch in 1902 postulated that after a shear reinforced concrete beam cracks due to diagonal tension stresses, it can ideally be thought of as a parallel chord truss with compression diagonals inclined at 45° with respect to the longitudinal axis of the beam. The stirrups or bent-up bars and the bottom longitudinal reinforcement act as tensile members whilst virtual concrete struts and concrete in the compression zone act as compression members. The truss systems proposed by Mörsch are given in Figure 3.1, where the shaded concrete strips represent the compressed struts. The tensile forces in the shear reinforcement are then obtained by analysis of the truss itself. This model is easy to understand and has historically been used as the starting point for the development of design models.

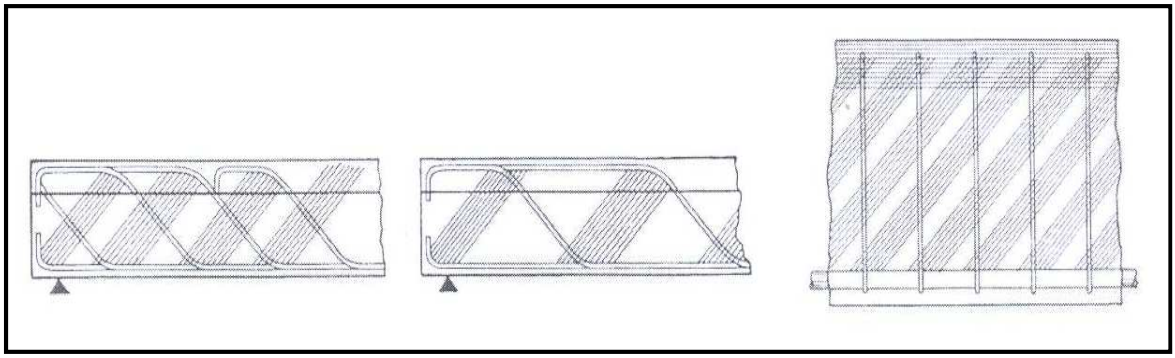

Figure 3.1. Simple or multiple truss systems with bent-up bars and stirrups. (Mörsch, 1908, as cited in Balázs, 2010)

Post 1902 to date much research effort has been directed towards the near impossible task of matching shear failure with predictions from theoretical models. Fairly recently, in October 2010, a special workshop convened in Salò, Italy, to critically discuss and review the latest research and validate shear provisions adopted by the new *fib*2010 Model Code. Over the last 50 to 60 years pivotal work by researchers such as Kupfer, Walther, Kani, Leonhardt and Mönig, Thürlimann et al., Walraven and Collins and Vecchio, amongst others, has contributed much to better understanding of shear in reinforced concrete, including the influence of prestressing on shear behaviour. The important developments of design theories for non-prestressed members with shear reinforcement are briefly reviewed.

3.1.1 Developments by Kupfer

Following his presentation in 1962 at a Colloquium on shear in Stuttgart (Balázs, 2010), Kupfer published a paper in a CEB bulletin in 1964 (ACI-ASCE Committee 445 Report, 2009) that analysed a truss model consisting of linearly elastic members and neglecting the concrete tensile strength, he provided a solution for the inclination of diagonal cracks. Kupfer proposed to select the shear reinforcement with simultaneous yielding of the longitudinal reinforcement and suggested to define the inclination of the strut by using the principle of minimum deformation work.

3.1.2 Developments by Leonhardt and Mönig, and other researchers

In 1973, Leonhardt and Mönig published a textbook that gave details on the so-called classic truss analogy by Mörsch with 45° struts as well as an improved truss analogy. They gave experimental evidence that illustrated that a lower amount shear reinforcement, expressed as ρ_w, reduces the inclination of cracks in the shear span as shown in Figure 3.2. It can also be observed that more shear reinforcement increases the number of cracks developed before failure, thus promoting more ductile behaviour of structures.

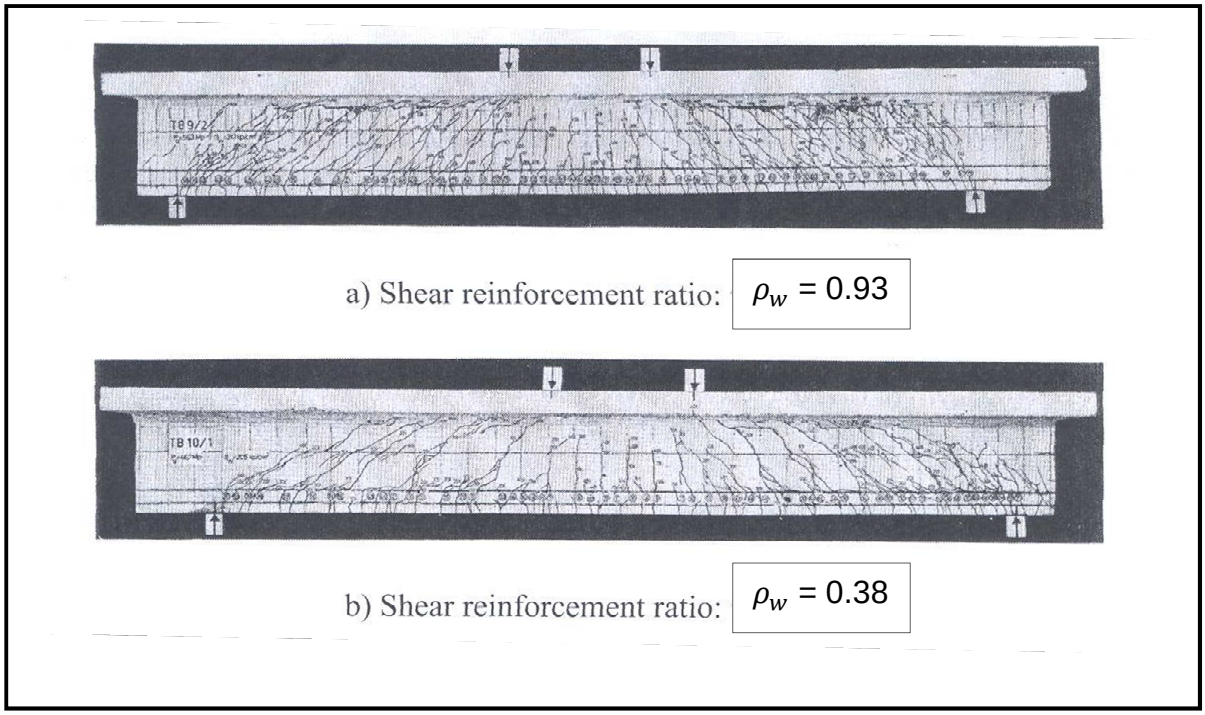

Figure 3.2. Crack patterns of T beams with very different amounts of shear reinforcement (Leonhardt & Mönig, 1973 as cited in Balázs, 2010)

Further, Leonhardt and Mönig paid special attention to the possible failure of concrete struts in I-sections with large flanges and large amounts of web reinforcement as well as relatively thin webs. It was noticed that for such a beam configuration the compressive struts may suddenly fail between inclined cracks, even before the web reinforcement yields as was the case for the I-beam shown in Figure 3.3. It was established therein that web compression failure should give the upper limit of shear resistance.

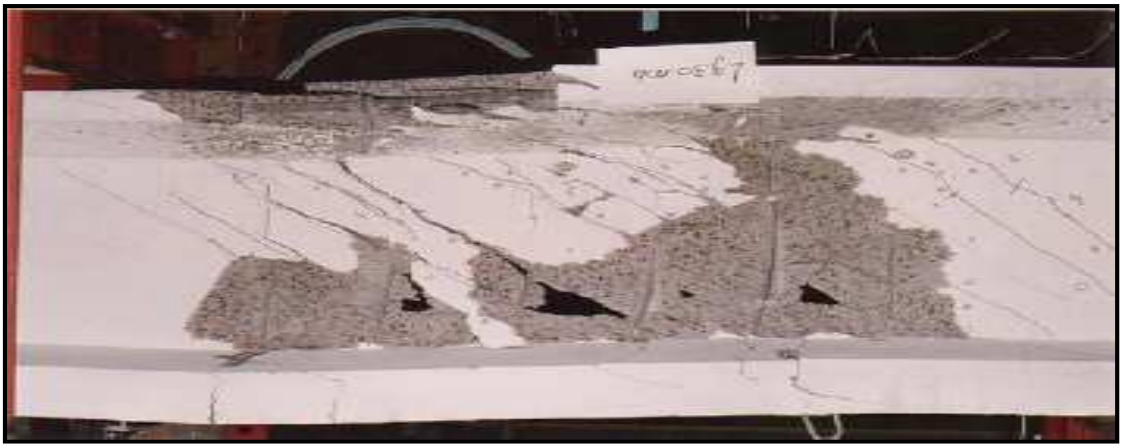

Figure 3.3. Sudden web compression failure due to large amounts of shear reinforcement. (Joint Research Centre, 2008)

Further development of plasticity theories by Nielsen and Braestrup in 1975 extended the applicability of the model to non-yielding domains. In 1987, Schlaich, Schäfer and Jennewein extended the truss model for beams with uniformly inclined diagonals. This approach is particularly relevant in regions where the distribution of strains is significantly nonlinear along the depth. Such regions are described as D-regions in Section 3.3.

3.1.3 Developments by Wagner

It must be noted that in 1929, the German engineer H.A. Wagner was the first to describe the angle of inclination of diagonal tension whilst solving an analogous problem of shear during the design of a stressed-skin aircraft (ACI-ASCE Committee 445 Report, 2009). Wagner assumed that after the thin metal skin buckled, it could continue to carry shear by a field of diagonal tension, provided that it was stiffened by transverse frames and longitudinal stringers. In an approach later termed the tension field theory and using the deformations of the system, he assumed that the angle of inclination of the diagonal tensile stresses in the buckled thin metal skin would coincide with the angle of inclination of the principal tensile strain as determined from the deformations of the skin, the transverse frames, and the longitudinal stringers.

Kupfer's work, published in 1964, only presented approaches for determining the angle of inclination of the concrete struts assuming that the cracked concrete and reinforcement were

linearly elastic. As an improvement, methods for determining the angle of inclination applicable over the full loading range and based on Wagner's developments were established for members in torsion and shear by Collins in 1974 (ACI-ASCE Committee 445 Report, 2009). This procedure became known as the Compression Field Theory (CFT).

3.1.4 Developments by Vecchio and Collins

Vecchio and Collins (1986) developed the Modified Compression Field Theory (MCFT) for reinforced concrete elements subjected to shear, which unlike the CFT, accounts for the influence of tensile stresses in the cracked concrete. The MCFT was calibrated to the so-called Toronto large panel tests. Collins et al. (2007), claim that one of the reasons it has taken so long to develop an adequate theory for shear is that the traditional type of shear test in which a simply supported beam is subjected to one or two point loads, while simple to perform, yields results which are difficult to use as the basis of a theoretical model. The MCFT was developed by testing reinforced concrete elements in pure shear using the membrane element tester as shown in Figure 3.4.

Figure 3.4. Membrane element tester (Collins et al., 2007)

3.2 THE SHEAR RESISTANCE OF STIRRUP-REINFORCED CONCRETE MEMBERS

Shear reinforcement does not prevent cracks from forming in a member. Its purpose is to ensure that the member will not undergo shear failure before the full bending capacity is reached. When inclined cracks form in a member with stirrups, only the bars that cross the cracks contribute to the shear resistance of the member as shown in Figure 3.5 below.

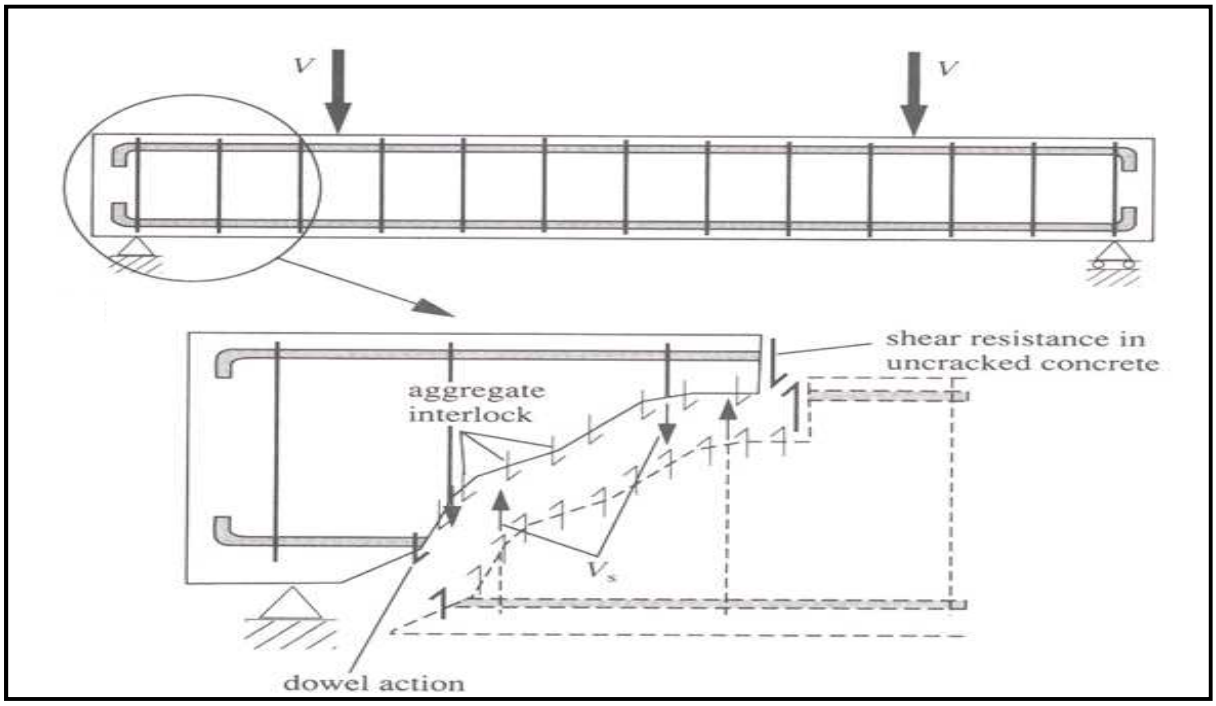

Figure 3.5. Shear resistance of member with stirrups. Elevation showing reinforcement (***top***) and transfer of shear force through the member (***bottom***). (O'Brien & Dixon, 1995)

The total shear capacity, V_u, provided by the section can be considered as a combination of the capacity of the reinforcement and that of the concrete. Therefore:

$$V_u = V_s + V_c \qquad [3.1]$$

Where V_s is the contribution of the shear reinforcement and V_c, the concrete resistance, is the contribution from dowel action, aggregate interlock and the shear stresses in the uncracked concrete. The dowel action of the reinforcement results from the resistance of the reinforcement to local bending and the resistance of the concrete to localised crushing near the reinforcement. Aggregate interlock occurs in cracked members and results from the forces transmitted across the crack by interlocking pieces of aggregate protruding at a crack. Shear stresses in the uncracked concrete refers to the resistance provided by the portion of the beam where the axial stress is compressive.

If the applied shear force is sufficiently large, the shear reinforcement will reach its yield strength. Beyond this point, the reinforcement behaves plastically and the cracks open more rapidly (O'Brien & Dixon, 1995). As the cracks widen, the proportion of the shear resisted by aggregate interlock is reduced forcing an increase in dowel action and shear stress in the uncracked portion of the section. Failure finally occurs by crushing of the concrete in the compression zone or splitting of the longitudinal tension reinforcement.

3.2.1 Post-cracking behaviour of stirrup-reinforced concrete members

In principle, after initial cracking a redistribution of forces occurs in the webs of shear reinforced concrete beams, resulting in strut inclinations smaller than 45°. If the shear reinforcement at a crack yields, the truss can, by rotation of the compression struts to a lower inclination, activate more stirrups for the transmission of the shear force and, as such, extend the zone of failure. Due to strut rotation, the stress in the concrete struts increases. Consequently, rotation can only continue until crushing of the concrete occurs. This is further discussed in Section 3.5.3. Figure 3.6 provides a schematic representation of the four steps of strut rotation experienced by a stirrup-reinforced concrete member.

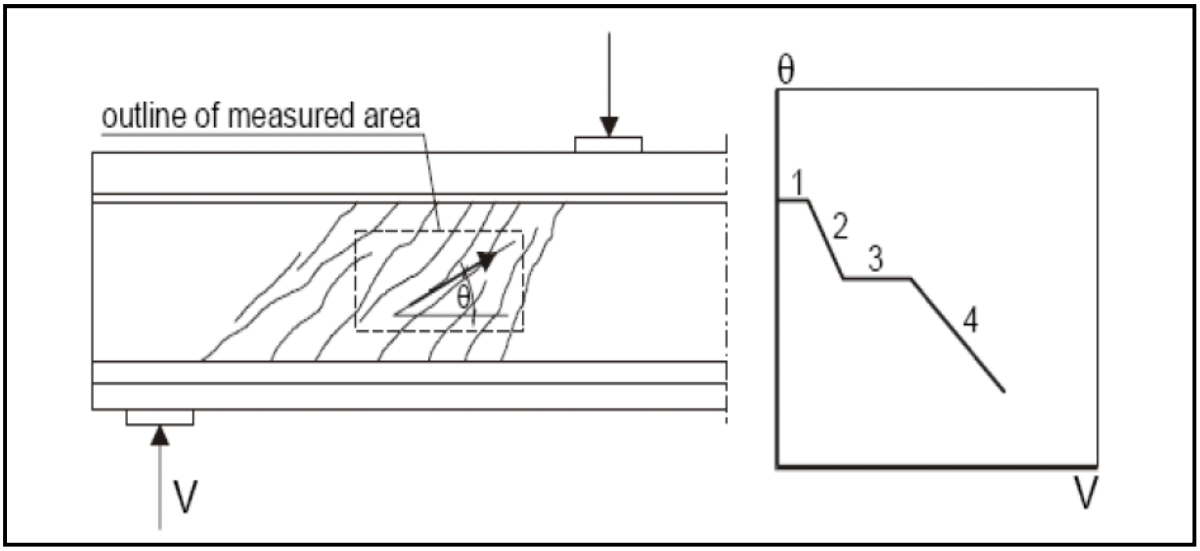

Figure 3.6. Schematic representation of the rotation of the concrete struts as measured on the web of beams with shear reinforcement (European Concrete Platform, 2008a)

In the beginning of shear loading the beams are uncracked in shear so that the principal strain direction is 45° (Line 1 from Figure 3.6). At the formation of inclined shear cracks the principal strain direction decreases (Line 2). After having reached the stabilised inclined crack pattern, a new type of elastic equilibrium is obtained. At this point, the constant principal strain direction is dependent on the stiffness ratio of the concrete member in the cracked state (Line 3). At yield of the stirrups, through rotation of the struts to a lower inclination in which the beam activates more stirrups to carry the load, the web searches for a new state of equilibrium. Simultaneously, the compressive stress in the concrete struts increases. Stress in the concrete diagonal struts will increase until the crushing strength is attained and the beam fails in shear (Line 4).

3.2.2 Causes and types of shear failure in members without shear reinforcement

Shear reinforcement is provided to control detrimental cracking behaviour that has been experienced in members not reinforced for shear. As such, the cracking or failure of members unreinforced for shear should be well understood as they mostly also affect members with shear reinforcement.

Inclined cracks must develop in a member before complete shear failure can occur (O'Brien & Dixon, 1995). Reinforced concrete structures typically undergo two forms of shear cracking, namely shear-web cracking and shear-flexure cracking. Shear-web cracking occurs at sections where the shear stress predominates throughout the depth and bending moments are negligible or where the web width of the member is small. Such situations are not very commonly encountered in practice but do sometimes occur. On the other hand, shear-flexure cracking occurs in members that are exposed to significant amounts of both bending and shear stresses. The type of shear failure which occurs in a particular member depends on various factors including (ACI-ASCE Committee 445 Report, 2009 and O'Brien & Dixon, 1995):

1. The shape of the cross section
2. The size of the cross section
3. The amount of longitudinal tension reinforcement
4. Maximum moment to shear ratio divided by the effective depth (M/Vd) or alternatively the a/d ratio
5. Axial (or prestress) force

Much of the research into shear behaviour of concrete beams and slabs, including the tests compiled to form the shear database in this thesis, have been carried out using a three-point or four-point bending test in which shear forces and moments are predominant at different locations throughout the length of the beam. Figure 3.7 shows the typical test arrangement and associated bending moment of the four point bending test. The test setup is applicable to members with or without shear reinforcement.

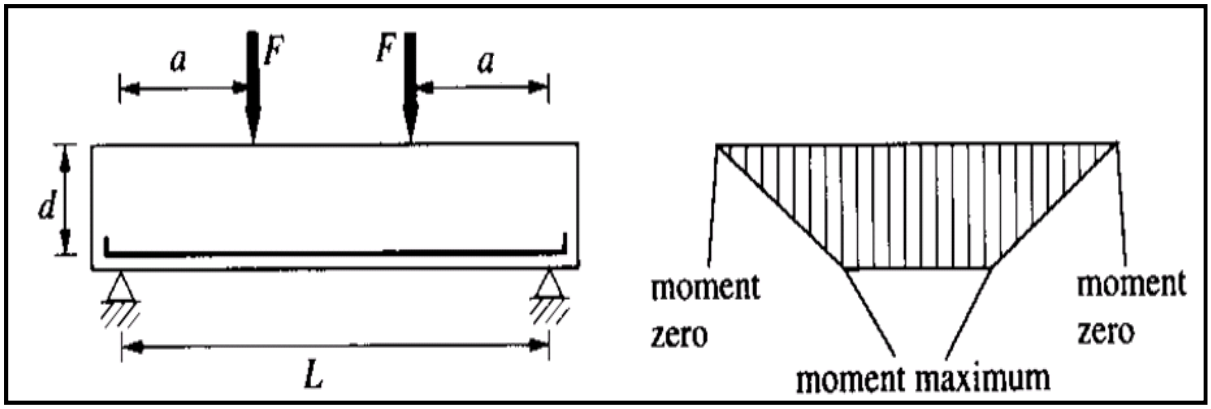

Figure 3.7. Typical test arrangement and bending moment diagram for member without shear reinforcement (O'Brien & Dixon, 1995)

Many empirical design formulae for shear to date have been derived based on the characteristics of shear potrayed in such tests. From extensive testing over the years, it is well established that the shear capacity of a member is strongly dependent on a/d. In general, the shear capacity decreases with increasing a/d. As such, shear failures can be categorised, according to a/d, as illustrated in Table 3.1 (O'Brien & Dixon, 1995). For different members falling into the same category, the sequence of events and the nature of failure are approximately the same.

Table 3.1. Categories of shear failure with associated types of failure based on a/d ratio.

Category	$\boldsymbol{a/d}$	**Type of failure**
I	$0 < a/d \leq 1$	Deep beam failure
II	$1 < a/d \leq 2.5$	Shear bond / Shear compression failures
III	$2.5 < a/d \leq 6$	Diagonal tension failure
IV	$6 < a/d$	Flexural failure

Members with very short spans or which have a large effective depth are commonly referred to as deep beams and fall into Category I of Table 3.1. Diagonal shear-web cracks form as the load is almost transferred directly to the reaction by means of compression. The crack propagates away from the support and toward the applied load. Failure may occur in several

ways; by anchorage failure, bearing failure at the support or location of the load, or by cracking failure of the arch. Failure may occur at several times the initial cracking load.

Members that fall into category II behave in a similar manner to Category I members, in that shear-web cracks develop in the region between the loaded sections and the supports. Thereafter, unlike deep beam failure, the crack propagates along the tension reinforcement destroying the bond between reinforcement and concrete in its vicinity. This form of failure is called shear-bond failure. Alternatively, Category II members may fail owing to dowel failure of the longitudinal tension reinforcement at the point of the inclined crack. Further, shear compression failure may also occur which is characterised by crushing failure of the concrete at points of load application.

Category III members are likely to develop flexural cracks before the compressive force is great enough to develop shear-web cracks. The flexural cracks occur closer to the support, where shear forces are significant compared to moments, develop into inclined shear-flexure cracks and propagate towards the applied loads thus splitting the member in the process. This type of failure is usually referred to as diagonal tension failure. The load at which diagonal tension failure occurs is approximately half that for shear compression/shear bond failure (O'Brien & Dixon, 1995). A majority of beams in practice fall into this Category hence making diagonal tension the most common type of failure.

Category IV members are so slender that shear is hardly ever an issue and as such they tend to fail in pure flexure. This implies that the longitudinal reinforcement yields and the concrete above it crushes before shear cracking occurs.

It should be noted that anchorage failure is not regarded as a shear failure but is rather viewed as a consequence of shearing action in beams. In addition to the types of shear failure considered above, web crushing may occur mostly in members with thin webs that are quite heavily reinforced for shear with wide flanges. This type of failure is more prone to occurring in T- and I-sections as opposed to occurring in beams of uniform rectangular cross-section.

3.3 SCOPE OF APPLICATION OF THE EC2 VSIM DESIGN PROCEDURE

The subject of shear design of reinforced concrete can be divided into two broad categories, known as B and D regions, where B stands for beam or Bernoulli, and D stands for discontinuous or disturbed (ACI-ASCE Committee 445 Report, 2009). In B regions the distribution of strains is linear, whereas the distribution is nonlinear in D regions.

This EC2 VSIM design procedure is applicable only to with B region shear. Design of B-regions for shear is the dominant design situation in practice. Nonetheless, EC2 does contain separate provisions for the design of D regions in shear; those are, punching shear and strut and tie models for arch action. A structural concrete member can consist entirely of a D region though it is the more common situation to have B and D regions in the same member or structure. Figure 3.8 below clearly illustrates this concept.

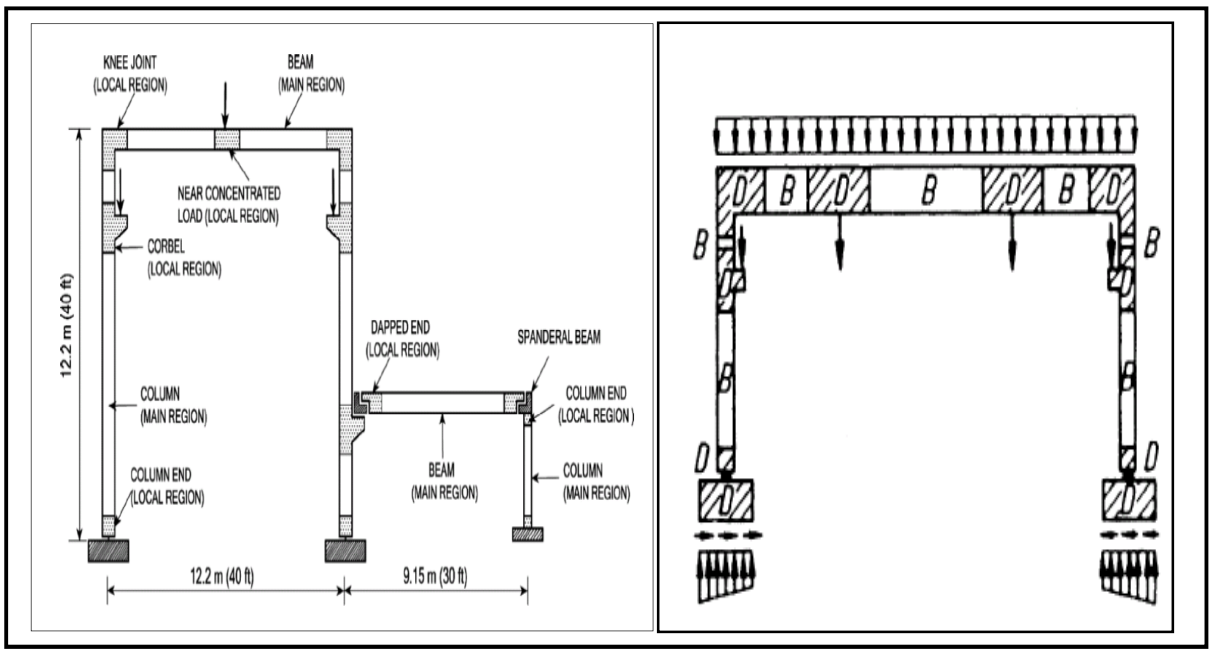

Figure 3.8. Typical frametype reinforced concrete structures. ***Left***: D regions are shaded portions of the structure and the rest are B-regions (Hsu & Mo, 2010). ***Right***: D and B regions as indicated (ACI-ASCE Committee 445 Report, 2009)

As shown in Figure 3.8, D regions extend a distance equal to the member depth away from any discontinuity, such as change in cross section or the presence of concentrated loads. Examples of B regions in shear include normally reinforced beams, prestressed beams, columns and slabs of constant cross section. Conversely, D-regions encompass regions with discontinuities in cross section, such as beam to column joints, flat slab to column connections, corbels and footings.

3.4 SURVEY OF OPERATIONAL PROCEDURES FOR STIRRUP DESIGN

For members requiring stirrups, classical Ritter-Mörsch truss model idealisations have traditionally been used as conceptual basis for design. Historical approaches based on this analogy describe the post-cracking stirrup contribution to shear resistance ($V_{Rd,s}$) by a 45° concrete strut angle (θ) truss with an empirically determined pre-cracking concrete contribution term ($V_{Rd,c}$). This is the approach followed by SA's currently operational concrete design standard SANS 10100-1. The VSIM employed in EC2 is fundamentally a truss model that allows for a variable angle of the concrete compressive struts as derived based on the theory of plasticity (Bræstrup et al., 1976; Jensen & Lapko, 2009). This model does not consider any direct contribution of the concrete to shear resistance. In EC2, the concrete compressive strut angle (θ) is assumed to vary between the confines of 21.8° and 45°.

The MCFT, unlike the conventional constant angle and plasticity-based truss model approaches, accounts directly for the components of shear failure such as aggregate interlock and friction, dowel action and longitudinal steel, and shear carried across the uncracked concrete (ACI-ASCE Committee 445 Report, 2009). The full procedure of the MCFT is described by Vecchio and Collins (1986), with applications in design standards described by Bentz & Collins (2006) and Kuchma et al. (2008) amongst a plethora of other publications.

The emerging *fib* 2010 Model Code describes the four Levels of Approximation (LoA) that could be used to determine the shear resistance of a reinforced concrete member. Both the accuracy and computational effort required to make a prediction increase as the LoA

increases. The first Level of Approximation (LoA I) is based on a simplified form of the LoA III approach and both are based on the MCFT (Bentz, 2010). LoA II is based on the principles of plasticity modified with a strain term based on the MCFT to better model the behaviour of heavily reinforced concrete beams.

LoA IV shear resistance predictions could be fulfilled by either LoA III or, if possible, higher order approximations proven to be of supreme accuracy. Response 2000 (Bentz, 2000) is an MCFT-based sectional analysis program that can predict the load deformation response of concrete sections and members subjected to a combination of shear, flexure and axial load. Response 2000 has proved to provide a more accurate and reliable prediction of the shear capacity of flexural members than any other method (Kuchma et al., 2008). R2k cannot be used as a design method, but its accurate predictions could rather serve as the equivalent of physical test predictions.

3.4.1 Appraisal of the various methods for stirrup design

The 45° constant angle strut analogy that neglects the contribution of concrete to shear resistance has been proven to be over-conservative. It is for this reason that standards like SANS 10100-1 include an empirically determined concrete contribution term. Design procedures established in such a manner usually exhibit adequate performance within the range from which it has been derived. However, due to a lack of sound conceptual and scientific basis, the results of empirically derived design cannot be generalised and apply strictly within clearly defined boundaries. The VSIM and MCFT prediction models have evolved as the more economic and rational approaches to shear analysis, prediction and design.

Modern trends in structural design tend to prescribe a variety of plasticity-based approaches for routine and conventional design situations, owing to their ease of use and quick execution times. The more computationally involving MCFT-based predictions usually suffice when more refined analyses are required or when they could yield significant economic benefits (usually for complex structures e.g. nuclear reactors, offshore structures, high-rise buildings). The approach taken by the *fib* MC 2010 for stirrup design offers a refreshing approach to the application of MCFT-based design procedures, specifically the simpler LoA I.

3.5. THEORETICAL BACKGROUND OF THE EC2 VSIM DESIGN PROCEDURE

Though not taken into account explicitly, the standard truss model with no concrete contribution is explained by the existence of aggregate interlock and dowel forces in the cracks, which allow a lower inclination of the compression diagonals and the further mobilisation of the stirrup reinforcement (ACI-ASCE Committee 445 Report, 2009). This is shown schematically in Figure 3.5. However, consistent with the principles of truss models first introduced by Ritter and Mörsch, a reinforced concrete beam in shear can be represented by an analogous truss as shown in Figure 3.8. The design equations for shear for members requiring stirrups in EC2 are derived from the relationships depicted in Figure 3.8 (Mosley et al., 2007).

In the VSIM analogy all the shear force will be resisted by the provision of stirrups with no direct contribution from the shear capacity of the concrete itself. Using the method of sections it can be seen that, at Section $X - X$ in Figure 3.8, the design force in the vertical link member $V_{Rd,s}$ must equal the design shear force V_{Ed}, that is:

$$V_{Rd,s} = \frac{f_{yk}}{1.15} A_{sw} = f_{ywd} A_{sw} = V_{Ed} \qquad [3.2]$$

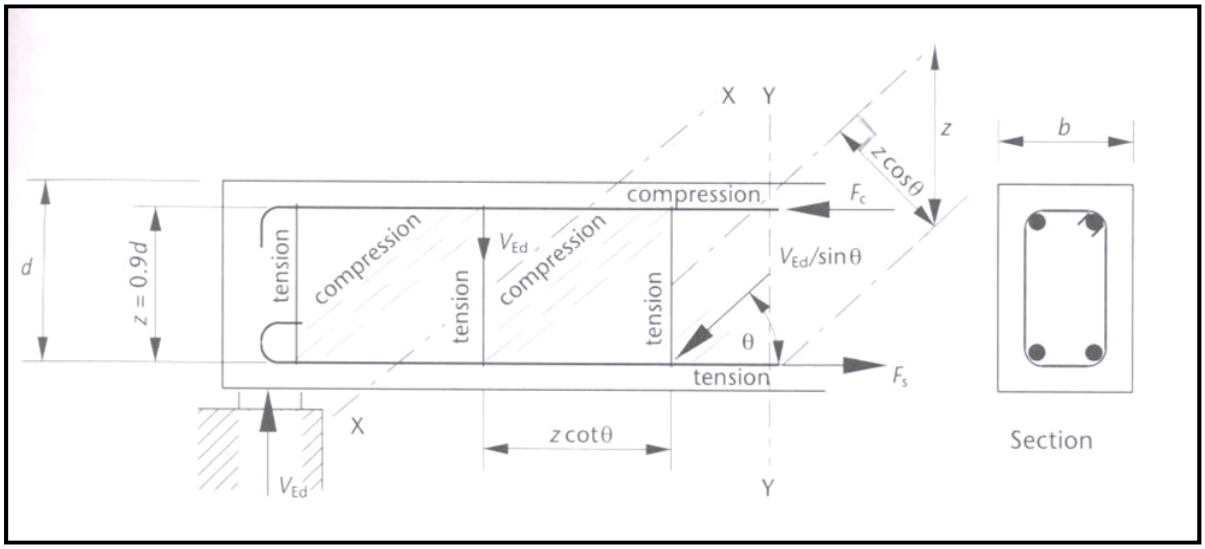

Fig 3.8. Assumed truss model for the variable strut inclination method (Mosley et al., 2007)

If the links are spaced at a distance s apart, then the force in each link is reduced proportionately and is given by:

$$V_{Rd,s}\frac{s}{z\cot\theta} = f_{ywd}A_{sw}$$

$$\therefore\ V_{Rd,s} = V_{Ed} = \frac{A_{sw}}{s} z\, f_{ywd}\ \cot\theta \qquad [3.3]$$

The angle θ increases with the magnitude of the maximum shear force on the beam and hence the compression forces in the diagonal concrete members. EC2 limits θ to occur between $21.8°$ $(\cot\theta = 2.5)$ and $45°$ $(\cot\theta = 1)$. For most cases of predominately uniformly distributed loading the angle θ will be $21.8°$ but for heavy and concentrated loads it can be higher in order to resist crushing of the concrete diagonal members (Mosley et al., 2007). The limits placed on θ, which affect the quality and performance of the model's predictions (particularly the lower limit of 21.8°), are set from applying the plasticity theory to the truss model.

It is essential to note that the VSIM procedure naturally predicts flatter angles of the concrete struts ($< 21.8°$), denoted $\theta_{Analytical}$. The lower limit of 21.8° was assumed for EC2 operational procedures (European Concrete Platform, 2008a) based on critical geometry $(a/d = 2.5)$ to introduce some conservative bias into the procedures. The lower limit of 21.8° signifies a steep limit incorporated into operational VSIM procedures to prevent flatter angles predicted by the pure analytical version of VSIM. The prevention of strut angles that are too flat avoids giving too much credit to beam stirrups, thereby introducing conservatism into the procedures. A detailed review of the manner in which the theory of plasticity is applied to the truss model to establish the limits for θ as enforced by EC2 is given in Section 3.6.

3.5.1 Upper limit of shear resistance to prevent web-crushing failures

EC2 provides an upper limit, $V_{Rd,max}$, on design shear force that is limited by the ultimate crushing strength of the diagonal concrete strut in the analogous truss resolved at its vertical component. As can be seen from Figure 3.8, the effective cross sectional area of concrete

acting as the diagonal strut can be taken as $b_w \times z\cos\theta$ and the design concrete stress, f_{cd}, is:

$$f_{cd} = \frac{\alpha_{cc} f_{ck}}{\gamma_C} \qquad [3.4]$$

Where α_{cc} is the coefficient taking account of long term effects on the compressive strength and of unfavourable effects resulting from the way the load is applied. It is a parameter open for national choice and the UK adopts a value of 0.85 (UK National Annex to EC2, 2005). γ_C is the partial material factor for concrete and is open for national determination. The UK adopts the recommended value of $\gamma_C = 1.5$ for persistent and transient design situations. Therefore:

$$\text{Ultimate strength of the strut} = \text{ultimate design stress} \times \text{cross} - \text{sectional area}$$

$$= \left(\frac{f_{ck}}{1.5}\right) \times (b_w \times z\cos\theta) \qquad [3.5]$$

$$\therefore \quad \text{its vertical component} = \left[\left(\frac{f_{ck}}{1.5}\right) \times (b_w \times z\cos\theta)\right] \times \sin\theta \qquad [3.6]$$

so that, $V_{Rd,max} = f_{cd} b_w z\cos\theta\sin\theta$ [3.7]

which by conversion of the trigonometric functions can also be expressed as (Mosley et al., 2007):

$$V_{Rd,max} = f_{cd} b_w z/(\cot\theta + \tan\theta) \qquad [3.8]$$

In EC2 Equation 3.8 is modified by two factors whose values are subject to national choice: the inclusion of a strength reduction factor, ν_1, taking account of the fact that the beam web, which is transversally in tension, is not as well suited to resist the inclined compression as for cylinder tests and a coefficient accounting for compression in the chord, α_{cw}, due to prestress. For cases where there is no prestress, the UK adopts the same value of $\alpha_{cw} = 1$ as is recommended in EC2 and is thus not further considered here. On the other hand, the UK adopts in part the recommended value of ν_1 in EC 2, maintaining:

$$\nu = 0.6\left[1 - \frac{f_{ck}}{250}\right] \qquad [3.9]$$

However, in cases where the design stress of the shear reinforcement is below 80 % of the characteristic yield stress, UK suggests a value of ν_1 different from that recommended in EC2, which is given in its national annex as:

$$\nu_1 = 0.54(1 - 0.5cos\alpha) \qquad for\ f_{ck} \leq 60\ MPa \qquad [3.10a]$$

$$\nu_1 = (0.84 - f_{ck}/200)(1 - 0.5cos\alpha) > 0.5 \qquad for\ f_{ck} \geq 60\ MPa \qquad [3.11a]$$

For the case of vertical stirrups, $\alpha = 90°$ and the Expressions above reduce to:

$$\nu_1 = 0.54 \qquad for\ f_{ck} \leq 60\ MPa \qquad [3.10b]$$

$$\nu_1 = (0.84 - f_{ck}/200) > 0.5 \qquad for\ f_{ck} \geq 60\ MPa \qquad [3.11b]$$

Equation [3.10] and [3.11] were suggested to be altered for the UK in an investigation conducted and later presented by Jackson & Salim (2006). The motivation to alter EC2's recommended limits was based on a better fit to experimental data under the 80 % yield rule using the limits presented above than those suggested for use in EC2.

3.5.2 Minimum amount of shear reinforcement

Section 9.2.2(5) of EC2 requires that a minimum amount of shear reinforcement, described by the shear reinforcement ratio ρ_w, be provided for all members requiring design shear reinforcement. This is a parameter open for national choice and the UK adopts the value recommended in EC2. For cases with less than minimum shear reinforcement, the reinforcement provided is ineffective and the shear resistance is best calculated as for a member without shear reinforcement. This, as part of the general relationship between the design shear force and the amount of shear reinforcement, is shown in Figure 3.9. The minimum amount of shear reinforcement, $\rho_{w,min}$, is given in EC2 as:

$$\rho_{w,min} = (0.08\sqrt{f_{ck}})/f_{yk} \quad [3.12]$$

An additional requirement for links, as set by EC2, is that the stirrup spacing must not exceed, in any direction, the lesser of 75 % of the effective member depth, d, and 600 mm.

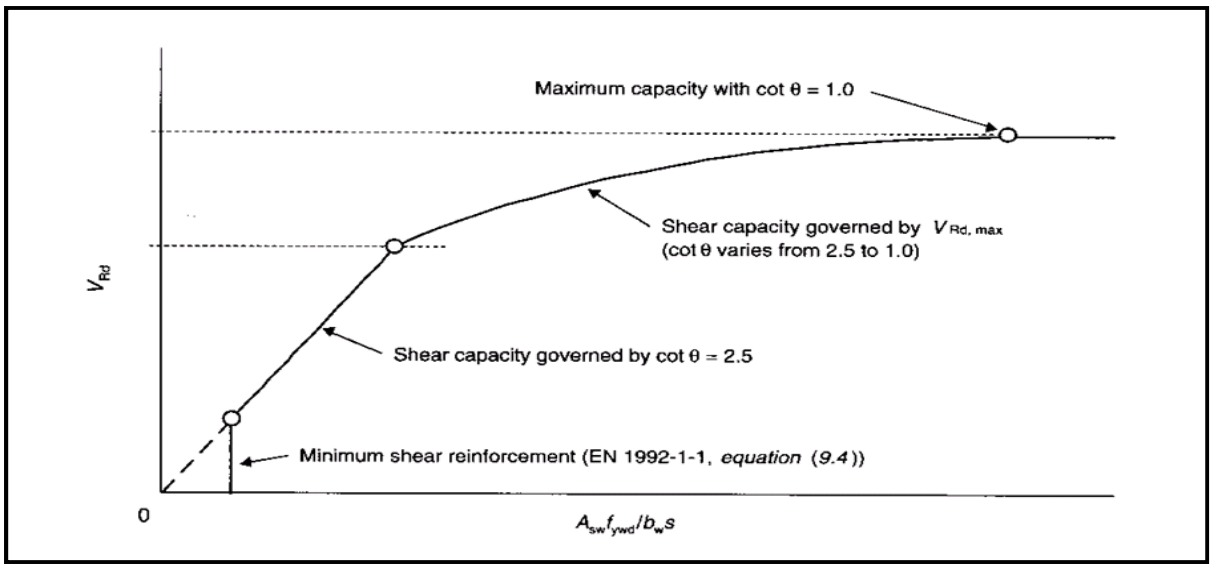

Figure 3.9. Relationship between the design shear force and the amount of shear reinforcement (Narayanan & Beeby, 2005).

3.5.3 Capacity design for VSIM

It will be noted from Equation 3.3 that the smaller the angle θ, the greater is the shear capacity based on the shear reinforcement. However, the shear capacity based on the crushing strength of the strut, given by Equation 3.8, decreases with decreasing values of θ below 45°. Hence the maximum capacity corresponds to the situation where the capacity based on the shear reinforcement just equals the capacity based on the strength of the strut (Narayanan & Beeby, 2005). According to Narayanan and Beeby (2005), this implies that the actual conditions at failure may be established using Equation 3.13 to estimate the value of θ for which $V_{Rd,s} = V_{Rd,max}$, and then using this value of θ to obtain the required amount of shear reinforcement. Therefore, at failure θ can be found by equating Equation 3.3 and Equation 3.8, thereby yielding (European Concrete Platform, 2008b):

$$\theta = sin^{-1}\sqrt{\frac{A_{sw}f_{ywd}}{b_w s v_1 f_{cd}}} \qquad [3.13]$$

Figure 3.10, taken from the European Concrete Platform (2008a), depicts the development of $V_{Rd,s}$ and $V_{Rd,max}$ for decreasing angle of strut inclination

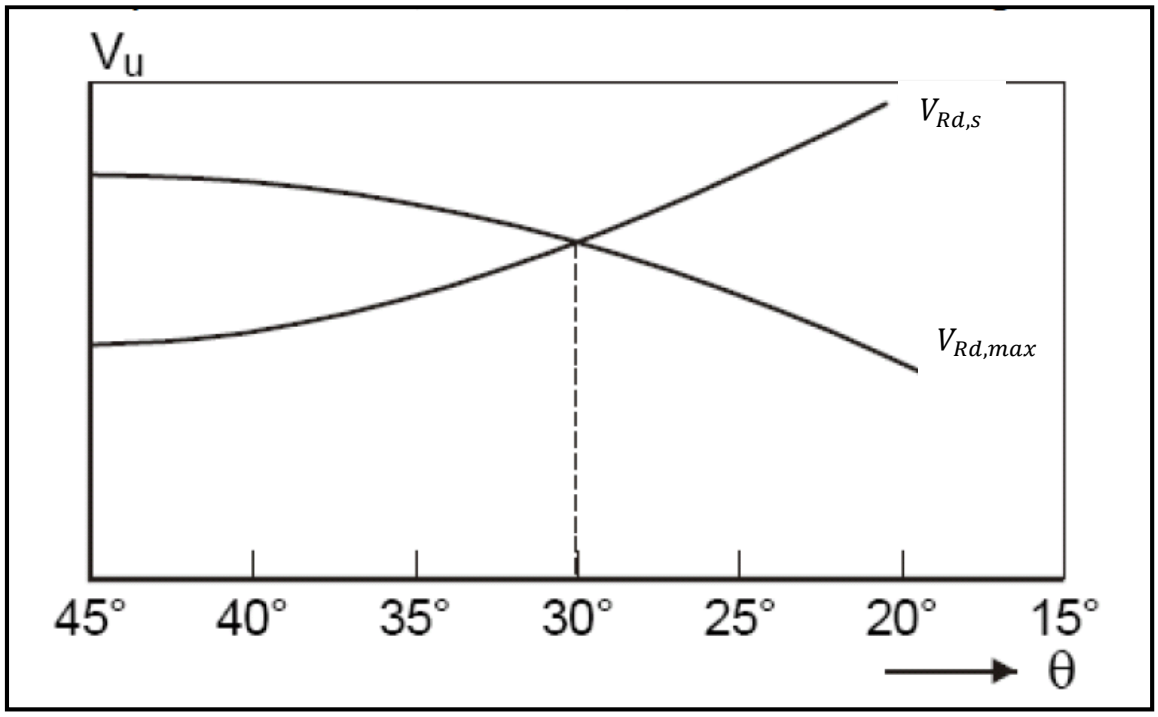

Figure 3.10. Dependence of $V_{Rd,s}$ and $V_{Rd,max}$ on the strut inclination (European Concrete Platform, 2008a)

3.6 DERIVATION OF THE EC2 VSIM STRUT ANGLE θ FROM PLASTICITY THEORY

For members requiring design shear reinforcement, stirrups in this case, EC2 incorporates a variable angle truss model based on the lower bound theory of plasticity. It should be noted that in this model of shear behaviour all the shear will be resisted by the provision of links

($V_{Rd,s}$ term) with no direct contribution from the shear capacity of the concrete itself (Mosley & Bungey, 2007). Jensen and Lapko (2009) establish that lower bound solutions are applicable when the theory of plasticity is used to find values of the carrying capacity, which are lower than or equal to the yield load by creating stress fields, which fulfill equilibrium conditions and are safe according to the failure criterions of the materials. On the other hand, upper bound solutions are applicable when a load equal to or greater than the yield load is sought by creating failure mechanisms and using the work equation on the mechanisms. An exact solution is found when the highest possible lower bound solution is equal to the lowest possible upper bound solution. In this instance, the yield load or carrying capacity is exactly satisfied. The theory of plasticity assumes the yield plateau as a typical stress-strain curve of a plain concrete specimen under compression instead of strain softening as would be more representative of highly reinforced or unreinforced concrete structures.

The plasticity truss model, as is adopted by EC 2, is based on the assumption that both the longitudinal and the transverse steel must yield before failure (Hsu & Mo, 2010). In order to ensure this mode of failure, the shear elements are divided into two types: under-reinforced and over-reinforced. The application of the theory of plasticity to under-reinforced concrete structures, where failure is governed by yielding of steel reinforcement, seems reasonable. In contrast, it is far less obvious that the theory of plasticity can be applied to over-reinforced or unreinforced concrete structures where the behaviour is governed mainly by the concrete (Ashour & Yang, 2007).

3.6.1 Application of the theory of plasticity to the truss model

The equations that Ritter and Mörsch derived are applied in the plasticity truss model. Note that the amount of steel in both directions is expressed as a ratio here, and shear stresses are used, not forces.

Shear stress at yielding of stirrups: $\nu_{sw} = \rho_w f_{yw} \cot\theta$ [3.14a]

Shear stress in concrete struts: $\nu_d = f_c \sin\theta \cos\theta$ [3.15]

Shear stress at yield of longitudinal reinforcement: $\nu_{sl} = \rho_l f_{yl} \tan\theta$ [3.16a]

Equilibrium of the beam shear element shown in Figure 3.8 illustrates that the shear force has a component in the longitudinal direction as expressed by Equation 3.16.

From the plasticity theory's assumption that the longitudinal and transverse reinforcement simultaneously yield at failure, then $\nu_{sw} = \nu_d = \nu_{sl}$ at failure. Note that the compression stress in the concrete struts f_c is not equal to the crushing strength of the concrete $f_{c,max}$. Equation 3.14a and Equation 3.16a can be expressed in terms of f_c by substituting Equation 3.15 into each of the two, as follows:

$$f_c \sin\theta \cos\theta = \rho_w f_{yw} \frac{\cos\theta}{\sin\theta} \quad \Longrightarrow \quad f_c \sin^2\theta = \rho_w f_{yw} \qquad [3.14b]$$

$$f_c \sin\theta \cos\theta = \rho_l f_{yl} \frac{\sin\theta}{\cos\theta} \Longrightarrow f_c \cos^2\theta = \rho_l f_{yl} \qquad [3.16b]$$

And:

$$\nu_d = f_c \sin\theta \cos\theta \qquad [3.15]$$

Now adding the final results from Equation 3.14b and 3.16b and utilising the identity $\sin^2\theta + \cos^2\theta = 1$, it follows that:

$$\rho_l f_{yl} + \rho_w f_{yw} = f_c \qquad [3.17]$$

The equation can be normalised in terms of the crushing strength of the diagonal compression struts, $f_{c,max}$:

$$\frac{\rho_l f_{yl}}{f_{c,max}} + \frac{\rho_w f_{yw}}{f_{c,max}} = \frac{f_c}{f_{c,max}} \Longrightarrow \omega_l + \omega_t = \frac{f_c}{f_{c,max}} \qquad [3.18]$$

Where ω_l is known as the longitudinal reinforcement index and ω_t is known as the shear reinforcement index. On this basis, the three failure conditions can be defined as follows:

Under-reinforced elements: $\omega_l + \omega_t < 1$ [3.19]

Over-reinforced elements: $\omega_l + \omega_t > 1$ [3.20]

Balanced condition: $\omega_l + \omega_t = 1$ [3.21]

Over-reinforced elements do not conform to the assumptions of the plasticity truss model and are not considered any further.

The under-reinforced condition $\omega_l + \omega_t < 1$

Substituting Equations 3.14b and 3.16b into Equation 3.15, the shear stress at simultaneous yield of shear and longitudinal reinforcement is then given by:

$$\nu = \sqrt{(\rho_l f_{yl})(\rho_w f_{yw})}$$

And dividing both sides by $f_{c,max}$:

$$\frac{\nu}{f_{c,max}} = \sqrt{\omega_l \omega_t} \quad [3.22]$$

Dividing Equation [3.14b] by Equation [3.16b], θ can be calculated by:

$$\tan\theta = \sqrt{\frac{\omega_t}{\omega_l}} \quad [3.23]$$

The variable angle truss model as applied in EC2 is based on one of the cases of the balanced condition presented below.

The balanced condition, $\omega_l + \omega_t = 1$

Three cases are distinguished within the limits of the balanced condition, where:

$Case\ (1)$: $\omega_l = \omega_t = 0.5$

For this case of the balanced condition, the yielding of both the longitudinal and transverse steel occur simultaneously with the crushing of the concrete struts at effective stress. From Equation [3.23], $\theta = 45°$ always for this case.

$Case\ (2)$: $\omega_t < 0.5$

In this case the transverse steel has yielded and is followed by the yielding of the longitudinal steel with simultaneous crushing of the concrete. The longitudinal reinforcement index becomes $\omega_l = 1 - \omega_t$, hence:

$$\frac{\nu}{f_{c,max}} = \sqrt{\omega_t(1-\omega_t)} \qquad [3.24]$$

$$\tan\theta = \sqrt{\frac{\omega_t}{(1-\omega_t)}} \qquad [3.25]$$

$\tan\theta$ in Equation 3.23 will always be less than 1, since $\omega_t < 0.5$, and thus θ is always less than 45° for this case. EC2 adopts this Case for use in its variable strut inclination method for shear design.

$Case\ (3)$: $\omega_l < 0.5$

The longitudinal steel has yielded, but the concrete crushes simultaneously with the yielding of the transverse steel. The transverse steel will then be determined by the balanced condition, $\omega_t = 1 - \omega_l$, therefore:

$$\frac{\nu}{f_{c,max}} = \sqrt{\omega_l(1-\omega_l)} \qquad [3.26]$$

$$\tan\theta = \sqrt{\frac{(1-\omega_l)}{\omega_l}} \qquad [3.27]$$

$\tan\theta$ in Equation 3.23 will always be greater than 1, since $\omega_l < 0.5$, and thus θ is always greater than 45° for this case.

3.6.2 Conditions for design

The balanced condition can also be expressed graphically by a semicircular curve in a $\frac{v}{f_{c,max}}$ vs. ω_t. Squaring both sides of Equation 3.24 and adding 0.5^2 on both sides

$$\left(\frac{v}{f_{c,max}}\right)^2 + (\omega_t - 0.5)^2 = 0.5^2 \qquad [3.28]$$

Equation [3.28] represents a circle with radius 0.5 and centre located on the ω_t axis at $\omega_t = 0.5$. This circle, half of which is shown in Figure 3.11, gives the nondimensional relationship between the shear stress v and the transverse steel stress, $\rho_w f_{yw}$. The axis pointing to the left, drawn to represent ω_l, represents of appropriate values of longitudinal steel that satisfies the balanced condition.

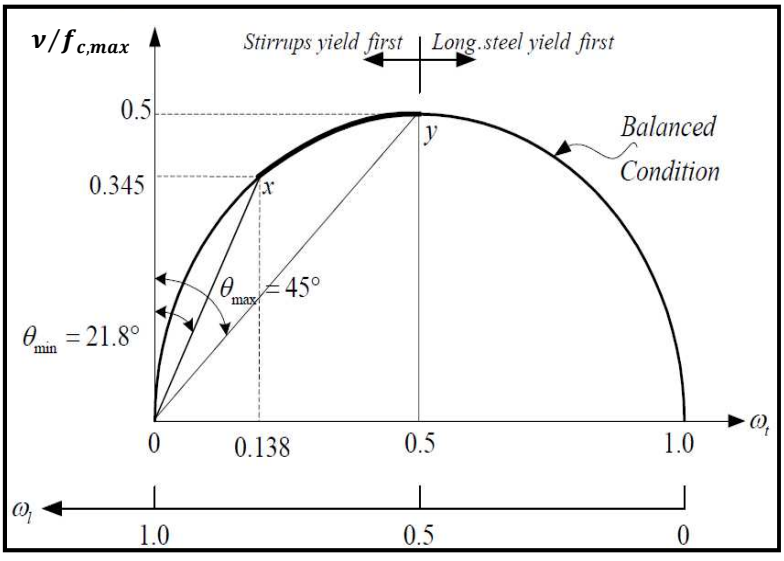

Figure 3.11. Relationship for shear stress ratio *vs.* reinforcement ratios for the balanced condition (Hsu, 1993, as cited in Huber, 2005)

Figure 3.11 shows that, for given amounts of transverse or shear reinforcement, much larger capacities are predicted than those based on the traditional Mörsch model, which assumes a strut inclination of 45°. Further, it can be noticed that for low amounts of shear reinforcement very flat angles of θ are predicted so that mostly lower limits are given to avoid under-reinforced members.

When Equation 3.22 is substituted into Equation 3.23 and ω_l is eliminated, then we get that θ can be calculated from:

$$\tan\theta = \frac{\omega_t}{\nu/f_{d,max}} \qquad [3.29]$$

Design of reinforcement within the semicircle will give an under-reinforced element, while the region outside the semicircle represents over-reinforcement. The EC2 shear prediction model requires stirrups to be designed in order to satisfy Case 2 of the balanced condition: That is, the case where the shear reinforcement yields before simultaneous crushing of the diagonal concrete struts and yielding of the longitudinal reinforcement.

For Case 2, θ is always less than45°. In addition, EC2 places a lower limit on θ which corresponds to ω_t of 0.138 as calculated from Equation 3.29. From Figure 3.11 it is evident that the EC2 shear design procedure is a blend of a constant θ method and a variable angle method. For reinforced concrete members with $\omega_t \leq 0.138$, the normalised shear resistance $\nu/f_{c,max}$ increases linearly with increasing ω_t, due to constant value of θ of 21.8°. In the instance that ω_t exceeds 0.138, θ gradually increases from 21.8° to 45° in a non-linear manner. This implies that the shear resistance increases non-linearly with increasing amount of shear reinforcement.

CHAPTER 4

As established in Chapter 3, the alternative methods for stirrup analysis and design used in the performance assessment of VSIM procedures were based on the MCFT. Both (1) *fib* MC 2010 LoA I and LoA III stirrup design methods, and (2) capacity predictions from sectional analysis program Response 2000 (R2k) are based on the MCFT. This Chapter serves to conveniently provide the theoretical background of the MCFT, as well as give a brief description of the Response 2000 program.

4.1 CONCEPTUAL BACKGROUND OF THE MCFT

The Modified Compression Field Theory (MCFT) was developed from the Compression Field Theory (CFT) for reinforced concrete in torsion and shear. In both models, the cracked concrete is treated as a new material with its own stress-strain characteristics. The CFT and the MCFT both have an extended rational base as compared to conventional truss models that arises from not just considering equilibrium, but additionally treating compatability as well as more general stress-strain relationships of the steel and concrete, all of which are formulated in terms of average stresses and average strains.

The angle of inclination of the concrete compressive struts, θ, is determined by considering the cross-sectional dimensions of a member and its deformations, caused by bending moments concomitant with shear at the studied section, of the transverse reinforcement, the longitudinal reinforcement and the diagonally stressed concrete (Cladera & Mari, 2007). With these methods alongside equilibrium conditions, compatability conditions, and stress-strain relationships for both the reinforcement and the diagonally cracked concrete, the load deformation response of a member subjected to shear can be determined.

The MCFT is a further development of the CFT that accounts for the influence of tensile stresses in cracked concrete. It recognises that the local stresses in both the concrete and the

reinforcement vary from point to point in the cracked concrete, with high reinforcement stresses but low concrete tensile stresses occurring at crack locations.

4.1.1 Main assumptions of the MCFT

The MCFT may be explained as a truss model in which the shear strength is the sum of the steel and concrete contribution. As such, it provides itself as a general model for the load-deformation behaviour of two-dimensional cracked reinforced concrete subjected to shear. It models concrete considering concrete stresses in principal directions summed with reinforcing stresses assumed to be only axial. A key assumption used to simplify the development of the MCFT is that the principal strain coincides with the principal stress directions. This assumption is confirmed by experimental measurements, which show that the principal directions of stress and strain are parallel within $\pm 10°$ (Vecchio & Collins, 1986).

The most important assumption in the model is that the cracked concrete in a reinforced member can be treated as a new material with empirically defined stress-strain behaviour. This behaviour differs from the traditional stress-strain behaviour as determined from conventional cylinder compressive strength tests. The strains used for these stress-strain relationships are average strains; that is, they lump together the combined effects of local strain at cracks, strains between cracks, bond-slip, and crack slip (Bentz, 2000).

According to Bentz (2000), the calculated stresses are also average stresses in that they implicitly include stresses between cracks, stresses at cracks, interface shear transfer on cracks, and dowel action. In contrast, failure of reinforced concrete elements may not be governed by average stresses, but rather by considering the steel stress at the crack and the ability of the crack surface to resist stresses. Therefore, an explicit check must be made to ensure that the average stresses are compatible with the actual cracked condition of the concrete.

4.2 ANALYTICAL FORMULATION OF THE MCFT

In accordance with the conceptual scheme of the MCFT presented above, the Equations of the MCFT are developed below with reference to Figure 4.1, which shows the free body diagrams for stress and strains and their associated Mohr's circles.

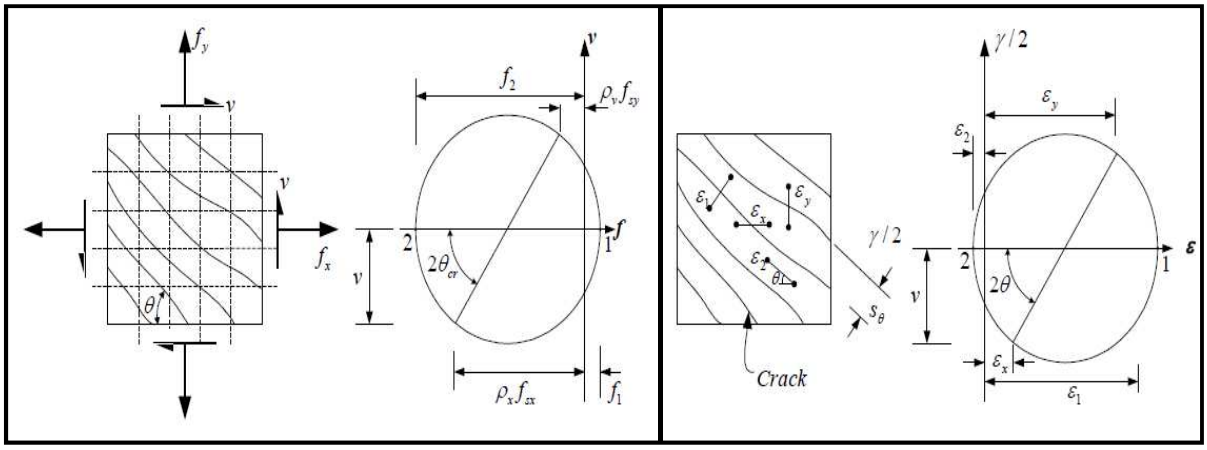

Figure 4.1. Average stress (***left***) and average strain (***right***) free body diagrams with associated mohr's circles in a reinforced concrete element (Vecchio & Collins, 1986).

4.2.1 Equilibrium

By considering force equilibrium, the stress in the transverse and longitudinal reinforcement are related to the shear stress and tensile stresses in the cracked concrete by Mohr's circle for concrete stresses. Therefore, shear in the section is resisted by the diagonal compressive stresses, f_2, together with the diagonal tensile stresses, f_1. The tensile stresses vary from 0 at the cracks to a maximum between cracks. From the left portion of Figure 4.1, the following Equations are derived:

$$\rho_y f_{sy} = f_y + v \tan\theta - f_1 \qquad [4.1]$$

$$\rho_x f_{sx} = f_x + v \cot\theta - f_1 \qquad [4.2]$$

$$f_2 = v(\tan\theta + \cot\theta) - f_1 \qquad [4.3]$$

Where ρ_x and ρ_y are the reinforcement ratios in the longitudinal and transverse directions, f_x and f_y are the stresses in concrete in the x- and y-directions respectively, and ν is the shear stress on the element.

4.2.2 Compatability

Compatability requires that any deformation experienced by the concrete must be matched by an identical deformation of the reinforcement. Thus, it holds that:

For the transverse direction, $\varepsilon_{sy} = \varepsilon_{cy} = \varepsilon_y$ [4.4a]

For the longitudinal direction, $\varepsilon_{sx} = \varepsilon_{cx} = \varepsilon_x$ [4.4b]

From the Mohr's circle on the right of Figure 4.1, the strains in the transverse and longitudinal directions (ε_y and ε_x) are related to the principal tensile strain ε_1 and the principal compressive strain ε_2 as follows:

$$\varepsilon_x + \varepsilon_y = \varepsilon_1 + \varepsilon_2 \quad [4.5]$$

$$\tan^2\theta = \frac{\varepsilon_x - \varepsilon_2}{\varepsilon_y - \varepsilon_2} \quad [4.6]$$

The stress-strain relationship for steel and cracked concrete are needed to relate the stresses (Equations 4.1 to 4.3) to the strains (Equations 4.4a and 4.4b)

4.2.3 Reinforcement stress-strain relationship

The reinforcement stress-strain relationship is a typical bilinear diagram, of which linear pre-yield stresses can be determined from hooke's law as:

$$f_{sx} = E_s\varepsilon_x \leq f_{x,yield} \quad [4.7a]$$

$$f_{sy} = E_s \varepsilon_y \leq f_{y,yield} \quad [4.7b]$$

Where E_s is the modulus of elasticity of the reinforcement, $f_{x,yield}$ and $f_{y,yield}$ are the yield points of the reinforcement in the $x-$ and $y-$directions respectively, and f_{sx} and f_{sy} are the service stresses in the reinforcement in the $x-$ and $y-$directions respectively.

4.2.4 Concrete stress-strain relationship

It can be observed from Figure 4.1 that the concrete web acts not only in compression in direction 2, but also acts in tension in direction 1. The stress-strain relationships for diagonally cracked concrete, applied in the MCFT, are given by the following relationships derived from experiments:

$$\varepsilon_2 = -0.002\left(1 - \sqrt{1 - f_2/f_{2,max}}\right) \quad [4.8]$$

$$Where,\ \ f_{2,max} = f_c/(0.8 + 170\varepsilon_1) \quad [4.9]$$

$$And,\ \ f_1 = \frac{f_{cr}}{1+\sqrt{500\varepsilon_1}} \quad [4.10]$$

$$But\ with\ the\ limitation\ that,\ \ f_1 \leq \frac{0.18\sqrt{f_{c,max}}\tan\theta}{0.3+\frac{24w}{agg+16}} \quad [4.11]$$

$$Where,\ \ w = \frac{s_x}{\sin\theta}\varepsilon_1 \quad [4.12]$$

f_{cr} is the principal compressive stress at initial cracking taken as $0.33\sqrt{f_{c,max}}$ in MPa units, $f_{2,max}$ is the crushing strength of the diagonally compressed strut, w is the crack width in mm, s_x is the perpendicular spacing of cracks inclined at θ. The concrete and reinforcement stress-strain graphs are presented in Figure 4.2. Figure 4.2 illustrates that the behaviour of cracked concrete subjected to tensile straining differs from that of the cylinder test where no tensile straining takes place. The peak compressive stress is much reduced compared to that of the cylinder test where no tensile straining takes place.

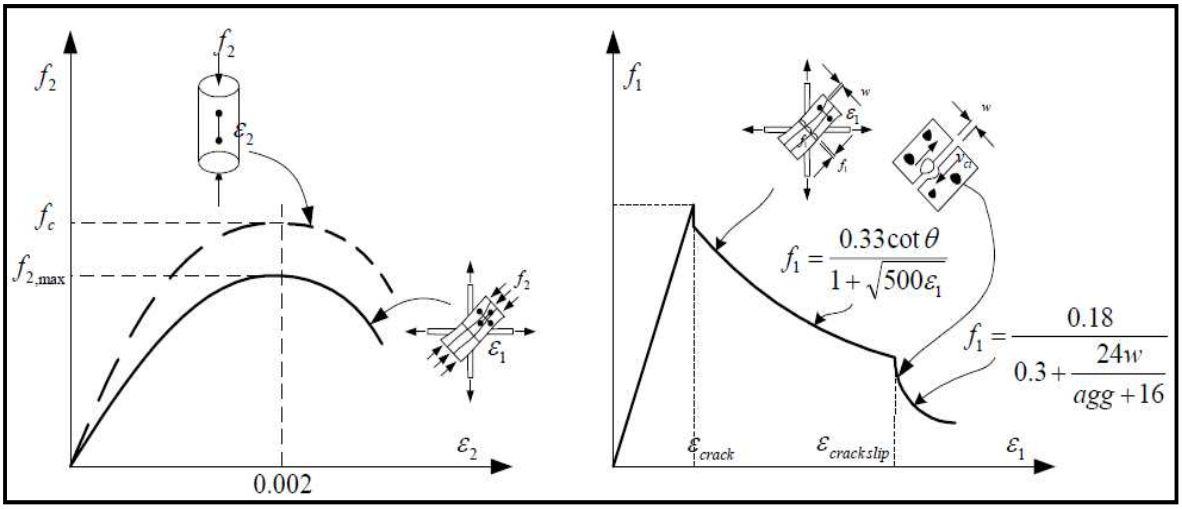

Figure 4.2. Stress strain relationship for cracked concrete in compression (***left***) and tension (***right***). (Collins et al., 1996, as cited in Huber, 2005).

4.2.5 Crack check

In checking the conditions at the crack, the actual complex crack pattern is idealised as a series of parallel cracks, all occurring at an angle θ to the longitudinal reinforcement and spaced a distance s_θ apart. Figure 4.3 depicts, in terms of free body diagram and associated mohr's circle, the equilibrium in terms of local stresses at a crack.

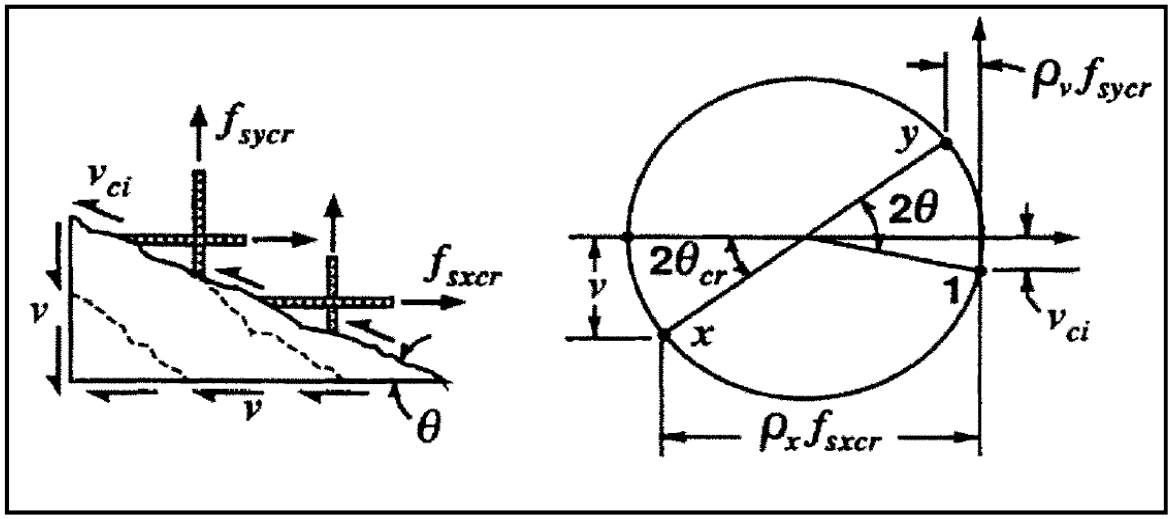

Figure 4.3. Equilibrium in terms of local stresses at a crack (ACI-ASCE Committee 445 Report, 2009)

From Figure 4.3, the reinforcement stresses at a crack can be determined as:

$$\rho_x f_{sxcr} = f_x + \nu \cot\theta + \nu_{ci} \cot\theta \quad [4.13]$$

$$\rho_y f_{sycr} = f_y + \nu \tan\theta - \nu_{ci} \tan\theta \quad [4.14]$$

The ability of the crack interface to transmit the shear stress, ν_{ci}, depends on the crack width, w. The limiting value of ν_{ci} is given by the inequality (ACI-ASCE Committee 445 Report, 2009):

$$\nu_{ci} \leq 0.18 \frac{\sqrt{f_{c,max}} \tan\theta}{0.3 + \frac{24w}{agg+16}} \quad [4.15]$$

4.3 MODELLING OF CONCRETE MEMBERS USING RESPONSE 2000

Response 2000 (Bentz, 2000) – hereafter referred to a R2k – is a sectional analysis program that calculates the strength and ductility of a reinforced concrete cross-section subjected to shear, moment and axial load. All the three loads are considered simultaneously to find the full load-deformation response using the latest research based on the MCFT. The Program is available for free download at: http://www.ecf.utoronto.ca/~bentz/r2k.htm

The following three assumptions are made in R2k:

1. The beam theory is applicable to all sections modelled, that is plane sections remain plane even at the ultimate limit state.
2. No significant clamping stress is taken as acting through the depth of the beam. This implies that fixed supports cannot be modelled in R2k. If there is transverse clamping, the real strength will be higher than that predicted by the program.

3. The MCFT can be used for biaxial stress-strain behaviour throughout the depth of the beam.

Through the use of the assumptions stated above, the generally well known fibre model of sectional analysis is extended to include the effects of shear. In order to carry out an ultimate shear strength prediction based on the MCFT using R2k the following input parameters have to be specified:

1. Concrete cylinder compressive strength
    a. *Aggregate size*
    b. *Compression softening characteristic equation*
2. Longitudinal steel yield strength
3. Transverse steel yield strength
4. Stirrup spacing
5. Clear cover
6. Section breadth
7. Section height
8. Number of bars and area of top non-prestressed reinforcement
9. Number of bars and area of bottom non-prestressed reinforcement
10. Stirrup type (None, single leg, open stirrup, closed stirrup, hoop, T-headed single leg, interlocking hoops)
11. Loading configuration

Some additional parameters are determined automatically based on specific inputs of the parameters listed above. In most cases the automatically determined values are maintained for the analysis of ultimate shear strength, save for the case of Aggregate size and Compression softening as shown in the bullet list above. Important aspects and any changes in these settings will be discussed below. Other unaltered parameters are not discussed here and reference can be made to the program user manual for default settings.

4.3.1 Crack spacing

R2k automatically calculates the crack spacing based on the CEB crack spacing provision that has been adopted from work done by Walraven. However, the program has the flexibility of allowing the user to input crack spacing as desired depending on the aim of the investigation. The recommended CEB crack spacing at a given depth z is given by:

$$Crack\ spacing = 2c + 0.1\, d_b/\rho \qquad [4.16]$$

Where c is the diagonal distance to the nearest reinforcement in the section from current depth, d_b is the diameter of the nearest bar, and ρ is the percentage of steel within a depth of $z \pm 7.5d_b$. The recommended value of the crack spacing is maintained in this investigation, so as to model as best as possible the real behaviour of the section or member.

4.3.2 Definition of concrete cylinder strength

On specifying the concrete cylinder compressive strength, other parameters are automatically determined as shown in Figure 4.4

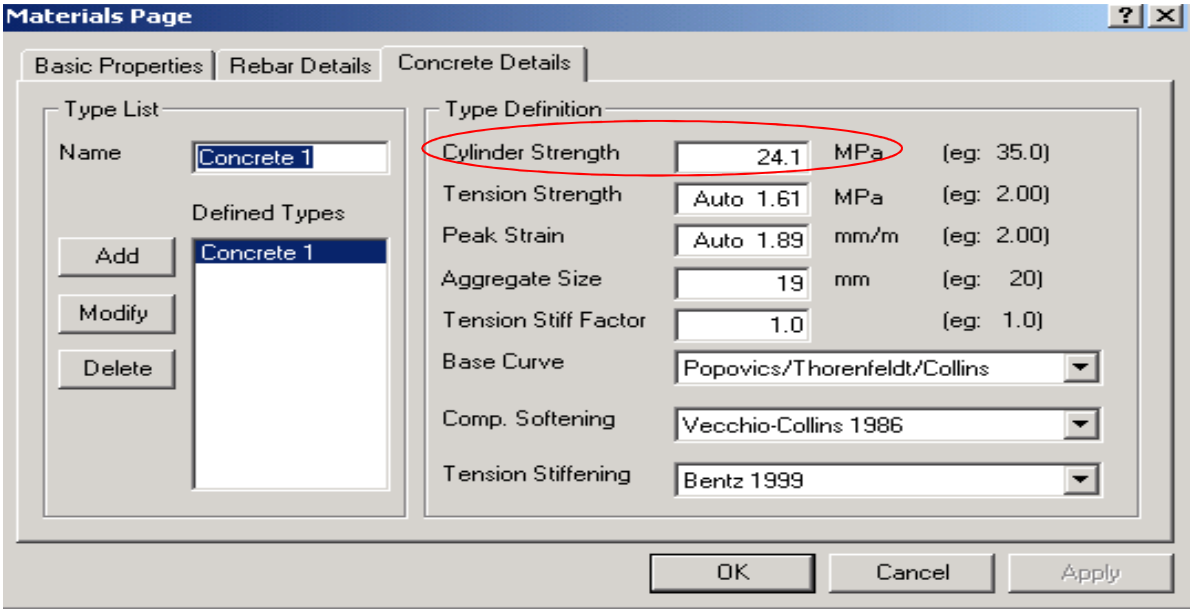

Figure 4.4. Concrete Details tab showing cylinder strength input with associated automatically defined parameters

The Aggregate size and Compression softening parameters are altered form default specifications. The basis and the way in which these parameters were altered are discussed.

4.3.3 Aggregate size

Appropriate aggregate sizes as reported in the literature sources and publications used to compile the database were input into R2k for ultimate shear strength analysis. Aggregate sizes were not always reported and were reasonably estimated in a select few cases. The estimation of aggregate sizes was centred on the concrete cylinder compressive strength values of the tests. It is common worldwide convention to use larger aggregates for normal strength concretes and smaller aggregates for high strength concretes. For normal strength concretes of about $40\,MPa$ characteristic cylinder strength and less, $19\,mm$ maximum aggregate size is normally used in the mix design.

For high and very high strength concretes above $40\,MPa$ cylinder strength, maximum aggregate sizes are commonly specified between 7 and $12\,mm$. This reduction in aggregate size affects the interface shear transfer mechanism as rough cracks no longer form around the aggregates for high strength concrete as in normal concrete. Rather, for high strength concrete, smooth cracks occur through the aggregate. To appropriately model this effect, the maximum aggregate size was linearly reduced to $0\,mm$ in the concrete cylinder strength range between 60 and $80\,MPa$ as suggested by the R2k user manual. Thus, for high strength concretes of 80 MPa and above, $0\,mm$ maximum aggregate size was prescribed for use in the analysis regardless of the aggregate size in the physical member.

4.3.4 Compression softening

As shown in Figure 4.4, the Vechio-Collins 1986 equation is set as the program default setting to describe compression softening. The R2k user manual, however, suggests the use of the Porasz-Collins 1988 Equation for very high strength concretes above $90\,MPa$. This recommendation was set for use in the investigation for the sections made from high strength concretes.

4.3.5 Definition of reinforcement bar yield strength

On specifying the steel yield strength for the reinforcing bars, both longitudinal and transverse, other parameters as shown in Figure 4.5 are automatically determined by the Program. No alteration was made to any of the parameters based on reinforcement yield strength.

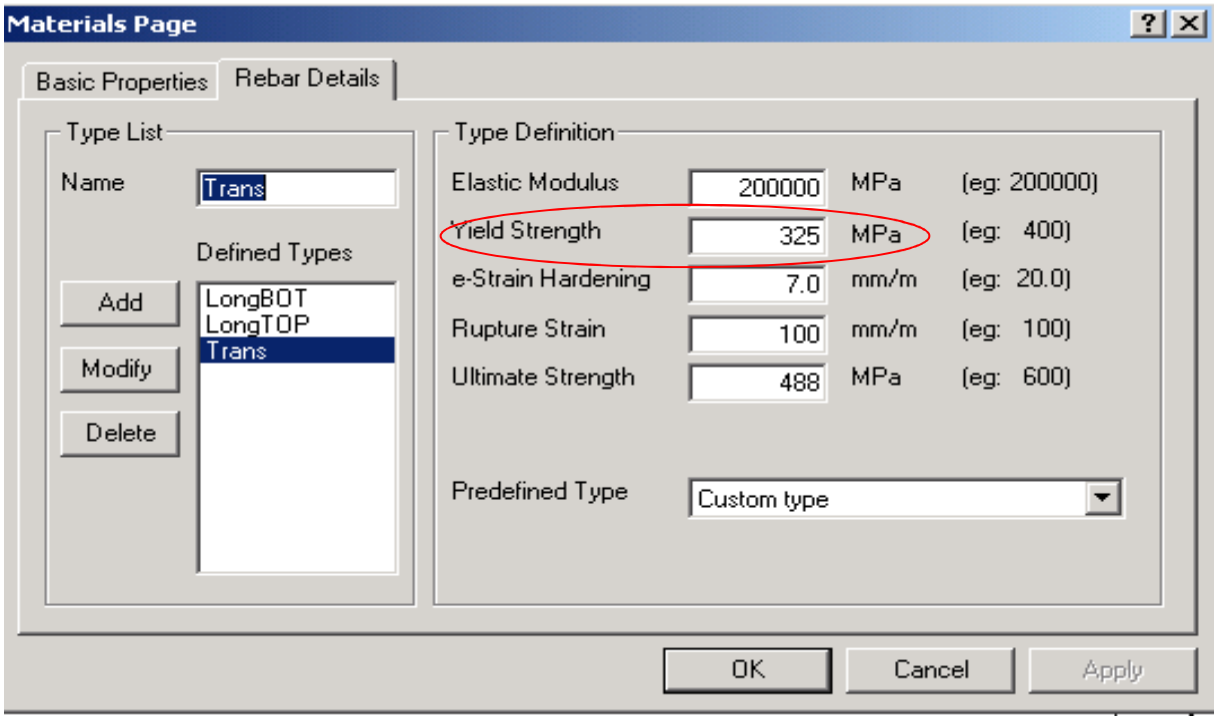

Figure 4.5. Reinforcement bar details showing steel yield strength input and other automatically determined parameters

4.3.6 Loading, geometry and the specification of other member properties

For shear analysis, R2k allows the analysis of one or two point loads between supports. This is typical of test setups used for investigating shear. Figure 4.6 shows the Full Member Properties window from the program where loads, some geometry and other member properties are specified.

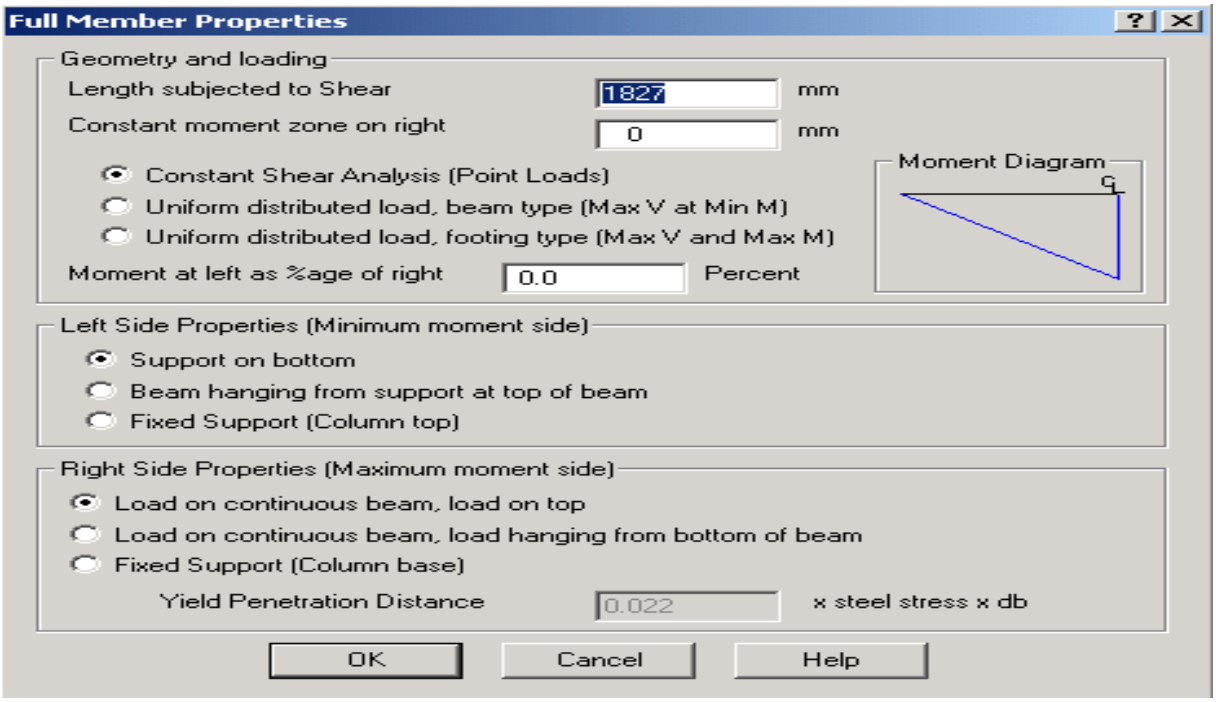

Figure 4.6. Full member properties window showing input of loads and other member properties for analysis

4.3.7 Outputs from R2k

Once all the input parameters were adequately specified for analysis, R2k provided a cross-sectional plot, an example of which is shown in Figure 4.7, to give a clear depiction of the section. As a result, any errors between the modelled cross section and the test setup reported in literature were easily recognisable.

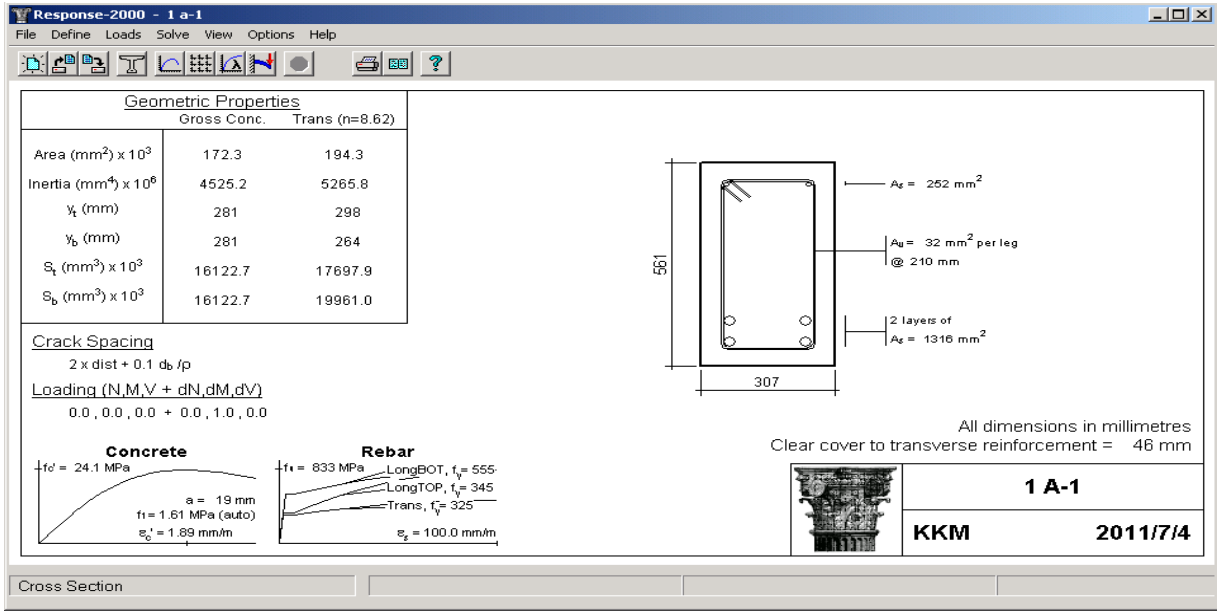

Figure 4.7. Cross-sectional plot and parameter output from R2k

Following satisfactory modelling of the cross-section, a member response analysis is conducted using the cross section details and the member as described in Section. The results of the analysis are given in Figure 4.8.

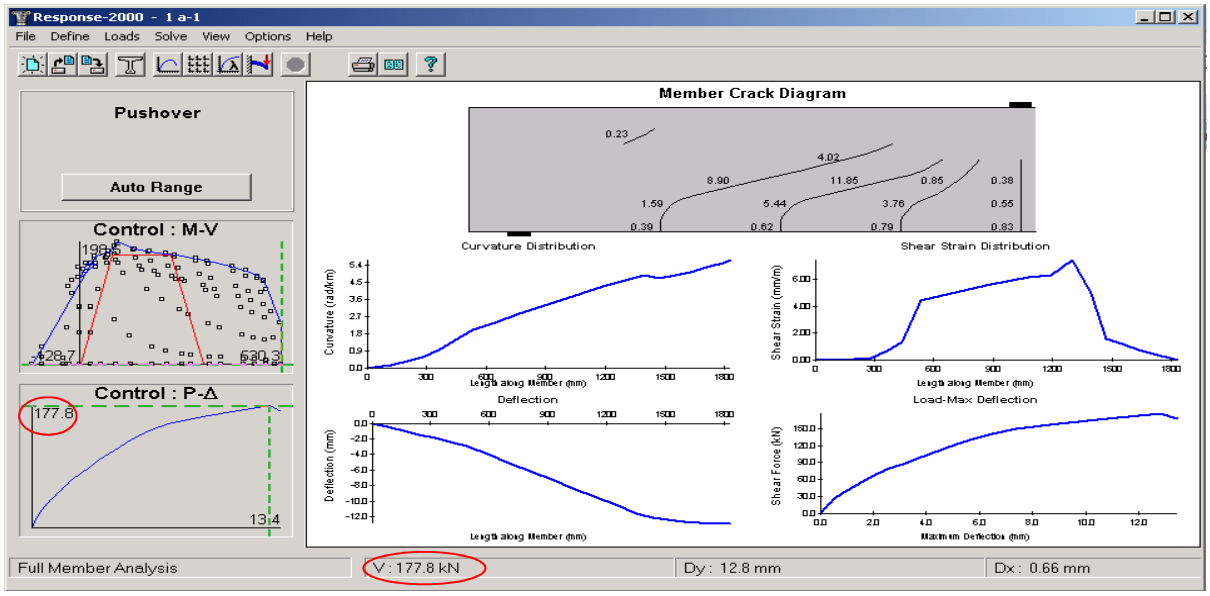

Figure 4.8. Results of the member response analysis with ultimate shear load given as indicated by the red ovals

CHAPTER 5

A COMPARISON OF THE VARIABLE STRUT INCLINATION AND ALTERNATIVE STIRRUP DESIGN METHODS

The inconsistent behaviour of the VSIM at varied amounts of stirrup reinforcement $\rho_w f_{yw}$ was highlighted in Section 2.3.4. To mitigate uncertainties and promote its economic use in SA, an extensive reliability investigation has been commissioned to calibrate the VSIM against local conditions and practice.

As part of the general assessment of the performance of the VSIM, this Chapter presents a comparison of the EC2 mean and design value predictions to those from, (1) the semi-empirical Ritter-Mörsch-based stirrup design analogy employed in the currently operational local design standard SANS 10100-1, and (2) the *fib* MC 2010 MCFT-based LoA I and LoA III design analogies.

The mean (unbiased) (V_{Rm}) and design (V_{Rd}) shear capacity predictions of the aforementioned procedures were compared for a beam of known cross-sectional and longitudinal geometry. Motivated by the systematic sensitivity of the VSIM portrayed in Figure 2.4, the design values of the different design methods were compared at parametric variations of $\rho_w f_{yw}$ for the chosen Test Case. Furthermore, the performance of the V_{Rm} trend with $\rho_w f_{yw}$ for the various design approaches were compared to equivalent R2k predictions; with the R2k predictions serving as LoA IV or representative best estimate results across the parametric range considered. The objectives of the investigation were thus to;

1. Assess the trend of EC2 V_{Rm} predictions to the other approaches over the parametric range considered, and
2. Assess the trend of EC2 V_{Rd} predictions compared to the different approaches at varied amounts of $\rho_w f_{yw}$ in comparison to point (1) above. This analysis showcased the effect

of the bias incorporated by partial factors and characteristic values for the different design methods across the parametric range considered.

5.1 DESIGN VALUE FUNCTIONS FOR THE VARIOUS APPROACHES

As previously established in Chapter 3, the design shear resistance V_{Rd} of the web of a reinforced concrete member may be generally described by:

$$V_{Rd} = V_{Rd,c} + V_{Rd,s} \leq V_{Rd,max} \quad [5.1]$$

where $V_{Rd,max}$ is an upper limit to shear resistance aimed at avoiding premature web-crushing failures of the concrete compressive struts. The $V_{Rd,c}$, $V_{Rd,s}$ and $V_{Rd,max}$ components of Equation 5.1 for the different design approaches are reported in Table 5.1. The strut angle (θ) specified by each design approach is also presented in Table 5.1. It should be noted that Table 5.1 presents simplifications of the general design equations that are applicable to stirrup design. Salient features regarding the application of the various design procedures are discussed in the following Sections.

Table 5.1. Design functions for determining shear resistance according to EC2, SANS 10100-1 and *fib* LoA I & LoA III.

No.	Approach	$V_{Rd,s}$	$V_{Rd,c}$	$V_{Rd,max}$	Strut angle (θ)
1	EN 1992	$\frac{A_{sw}}{s} z \frac{f_{ywk}}{\gamma_S} \cot\theta$	0	$\frac{b_w z \nu_1 (f_{ck}/\gamma_C}{\cot\theta + \tan\theta}$	$21.8° \leq \theta \leq 45°$, or $1 \leq \cot\theta \leq 2.5$
2	SANS 10100-1	$\frac{A_{sw} f_{ywk}}{\gamma_S \cdot s} d$	$\frac{0.75}{\gamma_C}\left(\frac{f_{cu}{}^*}{25}\right)^{\frac{1}{3}}\left(\frac{100A_s}{b_w d}\right)^{\frac{1}{3}}\left(\frac{400}{d}\right)^{\frac{1}{4}} b_v$	Lesser of $0.75\sqrt{f_{cu}}$ or $4.75\ MPa$	45°
3	*fib* MC LoA I & III	$\frac{A_{sw}}{s} z \frac{f_{ywk}}{\gamma_S} \cot\theta$	$k_v{}^{**} \frac{\sqrt{f_{ck}}}{\gamma_C} z$	$k_c{}^{**} \frac{f_{ck}}{\gamma_C} \frac{b_w z}{2}$	$= 36°$ (LoA I) $= 29° + 7000\varepsilon_x$ (LoA III)

*f_{cu} is the characteristic 28-day concrete cube strength / ** different values of k_v and k_c for LoA I & III

5.1.1 EC2

For resistance capacity predictions, θ for non-prestressed reinforced concrete members can be determined by Equation 3.13 (European Concrete Platform, 2008b), which is repeated for convenience as:

$$\theta = \sin^{-1}\left[\left(A_{sw}\left(\frac{f_{ywk}}{\gamma_S}\right)/b_w s \nu_1 \left(\frac{\alpha_{cc} f_{ck}}{\gamma_C}\right)\right)^{1/2}\right] \qquad [5.2]$$

where f_{ck} and f_{ywk} are, respectively, the characteristic compressive cylinder strength of concrete and the characteristic stirrup yield strength; γ_C and γ_S are the partial material safety factors for concrete and steel. Recall that EC2 recommends the values of $\gamma_C = 1.5$ and $\gamma_S = 1.15$. The description of all other basic variables is given in Section 3.5. Detailed parameters of the investigated Test Case are given in Section 5.3. The minimum stirrup reinforcement ratio is given by:

$$\rho_{w,min} = 0.08\frac{\sqrt{f_{ck}}}{f_{yk}} \qquad [5.3]$$

Figure 5.1 shows, for different concrete strengths, the variation of θ across the parametric range of $\rho_w f_{ywk}$ considered in this investigation. The Figure clearly shows that the performance of VSIM is controlled predominantly by the lower limit ($\theta = 21.8°$) of the concrete strut angle.

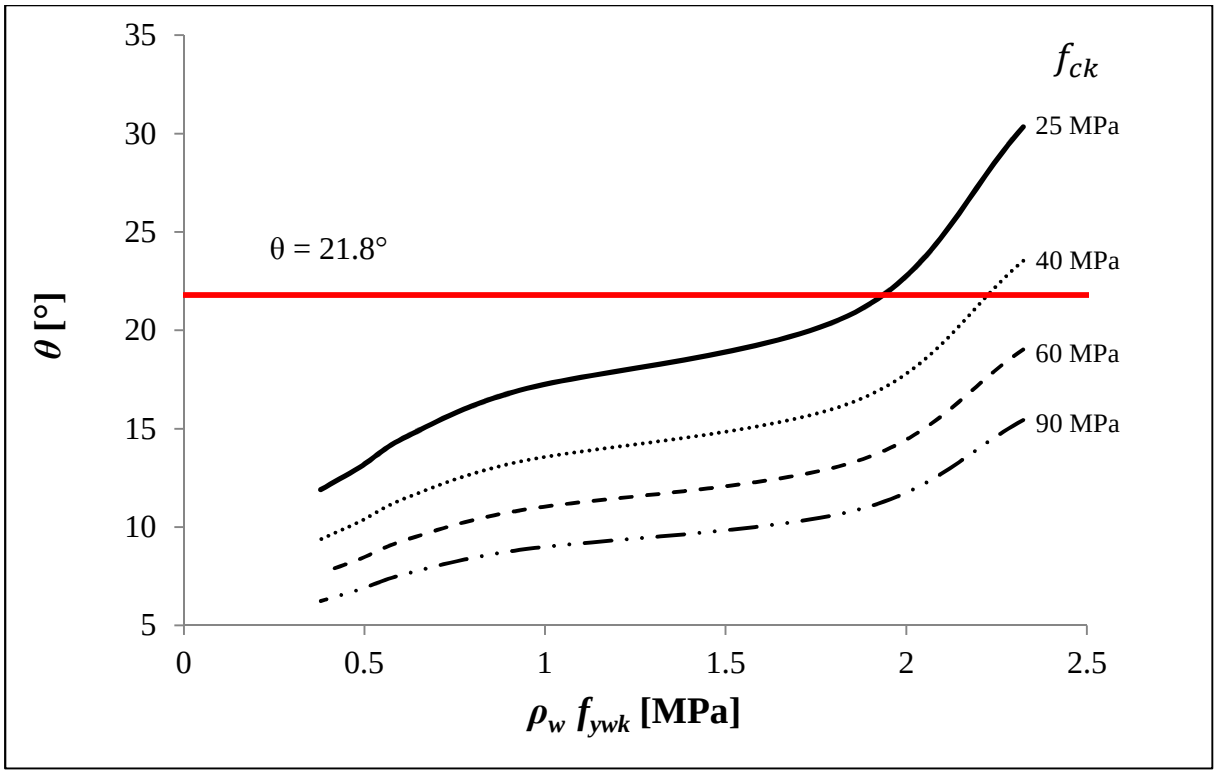

Figure 5.1. Variation of θ with $\rho_w f_{ywk}$ and f_{ck}

Figure 5.1 vividly illustrates that the pure analytical version of VSIM naturally predicts flatter angles ($< 21.8°$) as discussed in Section 3.5, with the 21.8° limit imposed to ensure $\cot\theta$ does not exceed 2.5 (see the EC2 design equation in Table 5.1). it can be witnessed that θ only exceeds 21.8° at combined situations of low f_{ck} (e.g. 25 MPa) and high $\rho_w f_{ywk}$ (e.g >1.8 MPa). However, for situations when $\theta > 21.8°$, $\cot\theta$ assumes values less than 2.5.

5.1.2 SANS 10100-1

SANS 10100-1 stipulates the same maximum spacing requirement as EC2, but suggests $\rho_{w,min}$ as 0.0012 when mild strength stirrups are used. $\rho_{w,min}$ assumes a larger value of 0.002 when high strength stirrups are used. The characteristic yield strength of SA's commercially available mild and high strength steel is 250 and 450 MPa, respectively. γ_C for shear is recommended as 1.4, whereas the same value of γ_S recommended in EC2 applies.

5.1.3 *fib* MC 2010 LoA I

Although the design function for the LoA I and LoA III design approaches is fundamentally the same, different values of k_v and k_c are applicable to either of the methods. k_v indicates the ability of the web to resist aggregate interlock stresses which provide the concrete contribution to shear strength. For LoA I, k_v can be taken as 0.15 when the stirrups provided exceed $\rho_{w,min}$ as defined in Equation 5.3. k_c is a term that shall be taken as:

$$k_c = 0.5\left(\frac{30}{f_{ck}}\right)^{\frac{1}{3}} \qquad [5.4]$$

where f_{ck} is expressed in MPa. The maximum spacing of stirrups should be taken as the lesser of $0.54d$ or 500 mm. The $\rho_{w,min}$ limit described by Equation 5.3 provides the minimum threshold ratio to which the *fib* LoA design functions apply to members with stirrups. However, for the design of new members MC 2010 requires that the 0.08 term from Equation 5.3 be replaced by 0.12. Both LoA I and LoA III apply the same values of γ_C and γ_S suggested for use by EC2.

5.1.4 *fib* MC 2010 LoA III

For LoA III, both k_v and θ are dependent on the calculated longitudinal strain, ε_x, at the mid-depth of the member. θ is defined in Table 1 and k_v is defined by:

$$k_v = 0.4/(1 + 1500\varepsilon_x) \quad [5.5]$$

provided the amount of stirrups exceeds $\rho_{w,min}$ from Equation 5.3. The expression for k_c for LoA III is similar to that given by Equation 5.4, save for the difference that 0.5 is replaced by 0.55. ε_x for non-prestressed members without axial forces is evaluated from:

$$\varepsilon_x = \frac{M_{Ed}/z + V_{Ed}}{2E_S A_S} \quad [5.6]$$

where M_{Ed} and V_{Ed} are the factored design forces for moment and shear, respectively. z is the inner lever arm and all design approaches commonly recommend its value as $0.9d$. E_s is the elastic modulus for steel and A_s represents the area of sufficiently anchored longitudinal tension reinforcement.

5.2 UNBIASED MEAN VALUE PREDICTIONS

Characteristic values (f_{ck}, f_{ywk}) and partial factors (γ_C, γ_S) are introduced into design equations to incorporate some safety bias into the design process. For material and resistance models, the safety bias reduces the unbiased or best estimate resistance prediction of the analytical (or conceptual) function under investigation. Equations 5.1 through 5.6, as well as those presented in Table 5.1, can all be represented at their unbiased values by, where applicable, (1) expressing f_{ck} and f_{ywk} at their mean values f_{cm} and f_{ywm}, respectively, and (2) not applying the partial factors γ_C and γ_S. The safety bias for the all other basic variables (A_{sw}, b_w, s etc.) is conventionally assumed as 1.0. For concrete strength, both EC2 and *fib* MC 2010 recommend the relationship:

$$f_{cm} = f_{ck} + 8\ MPa \quad [5.7]$$

For steel strength, Holický (2009) reports the following relationship:

$$f_{ywm} = f_{ywk} + 2\sigma_{f_{yw}} \;\; \& \;\; \sigma_{f_{yw}} = 0.1 f_{ywm} \qquad [5.8]$$

where $\sigma_{f_{yw}}$ is the standard deviation of steel yield strength as observed from standard European steel production practice.

5.3 PARAMETERS FOR THE INVESTIGATED TEST CASE

V_{Rm} and V_{Rd} predictions were compared at parametric variations of $\rho_w f_{yw}$. Recall that $\rho_w = \frac{A_{sw}}{b_w s}$. The parametric variation of $\rho_w f_{yw}$ was achieved by varying the stirrup spacing, s, whilst keeping fixed the values of all other parameters.

Parametric correlation and regression analyses were performed to investigate the underlying sensitivities of VSIM predictions. The results of this assessment are presented in Chapter 7 (Figure 7.7 in particular). The results of the analysis showed that the $V_{test} \,/\, V_{pred}$ ratio of VSIM predictions discussed in Section 2.3.4 are not significantly correlated to parameters such as concrete strength (f_c), beam width (b_w), shear span (a)-to-depth (d) ratio etc.

Since other design parameters do not show any systematic trends in comparing VSIM to experimental results, a typical section geometry should provide representative indication of the performance of the shear design method. The parameters of the beam cross-section required to make a prediction according to either of prediction methods presented in Table 5.1, are reported in Table 5.2. It should be noted that f_{ck} was converted to the equivalent characteristic cube strength f_{cu} to enable a SANS 10100-1 prediction.

Table 5.2. Basic parameters of the Test Case

Parameter*:	A_{sw} [mm^2]	b_w [mm]	d [mm]	f_{ck} [MPa]	f_{ywk} [MPa]	A_s [mm^2]
Quantity:	157.1	350	412	25	250	1885**

*spacing, s, varies / ** 6 Y20 bars – 2 layers of 3 bars each

LoA III additionally required the shear span-to-depth ratio (a/d), specified in Table 5.3, to enable a resistance prediction. The traditional beam setup with a single central point load on simple supports was assumed for longitudinal geometry. R2k was also implemented for a best estimate analysis of the beam. R2k, however, provides a complete implementation of the MCFT for flexural members, and consequently required the specification of additional information to enable a resistance prediction. Some of the additionally required parameters are given in Table 5.3. f_{yl} represents the yield strength of the longitudinal tension reinforcement, C the clear concrete cover from beam soffit to outermost seal of the stirrups, and h represents the beam height.

Table 5.3. Additional information required by R2k.

Parameter:	a/d	f_{yl} [MPa]	C [mm]	h [mm]
Quantity:	2.5	450	30	500

According to O'Brien et al. (2012), shear-flexure cracks that propagate towards the load (splitting the member in the process) become frequent above a value of a/d of 2.5. For lower values of a/d, direct strut action or compression forces are prevalent and such situations are best analysed by strut-and-tie approaches for efficient design. The approaches discussed here would be overly-conservative. Beyond a value of a/d of 2.5, the influence of flexure becomes more pronounced in the moment-shear interaction and flexural failures gradually become of primary concern. The value of a/d of 2.5 therefore represents a regime where shear stresses are prominent and shear strength is critical. It is for this reason that the value of a/d of 2.5 was selected for the LoA III and R2k analyses.

5.4 RESULTS OF THE MEAN AND DESIGN VALUE ANALYSIS

5.4.1 Mean values

The mean predictions of shear capacity (V_{Rm}) provided by the different design approaches are shown in Figure 5.2. By treating R2k observations as test results or the best possible prediction, the unbiased predictions offered by the different design approaches all tend to become unconservative at increased amounts of $\rho_w f_{ywm}$. This trend of results, particularly for the EC2 model, agrees with the observation reported in Figure 2.4.

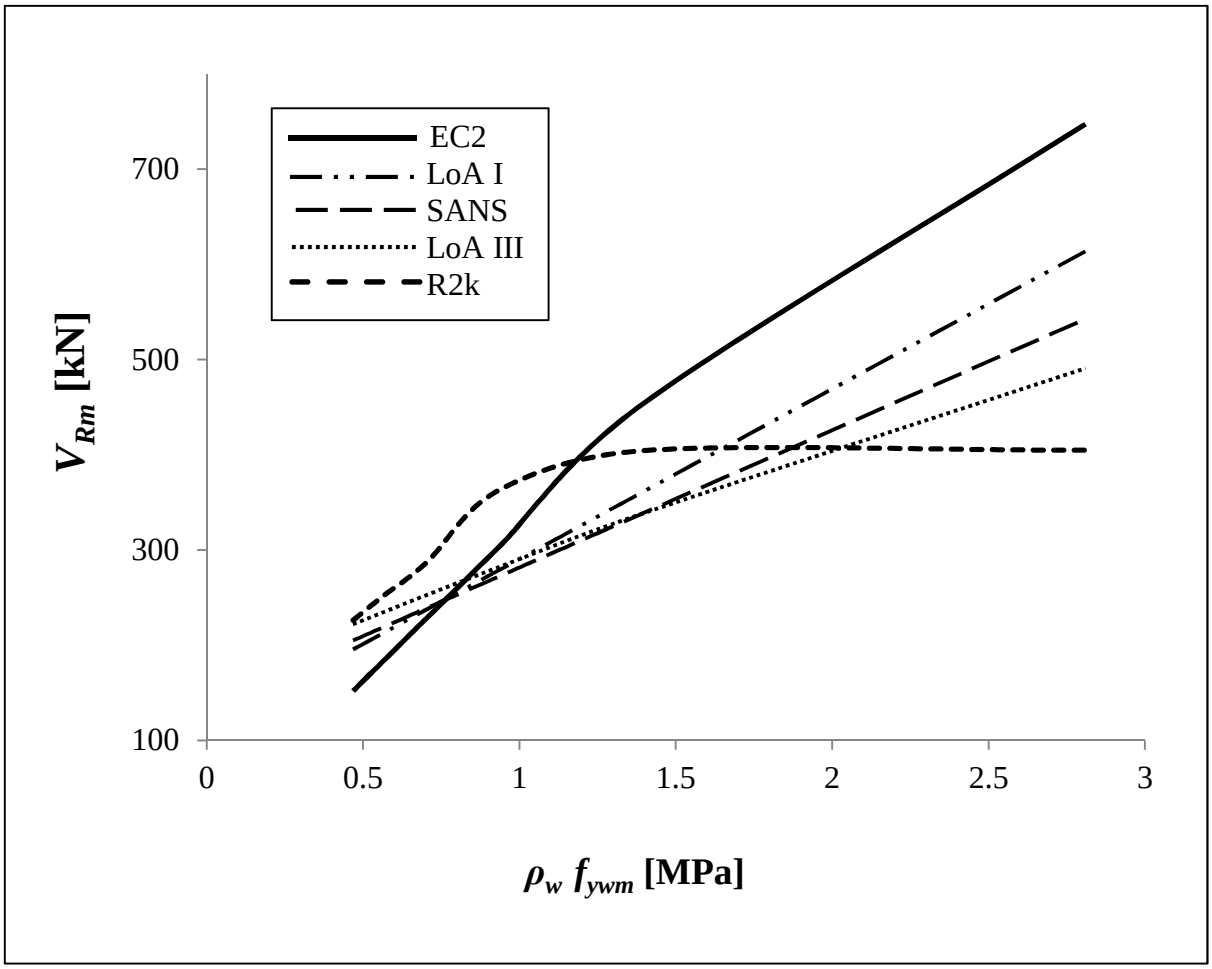

Figure 5.2. V_{Rm} for the various approaches and R2k *vs.* $\rho_w f_{ywm}$.

The EC2 VSIM is the first to exceed the R2k predictions and become unconservative at a value of $\rho_w f_{ywm}$ of approximately 1.2 MPa. The LoA III predictions provide the best approximation of the R2k predictions. Consequently, the LoA III predictions exceed those of R2k at the highest value of $\rho_w f_{ywm}$ of about 2 MPa. The SANS 10100-1 model, although semi-empirical, provides a closer match to the more accurate LoA III and R2k predictions than both EC2 and LoA I. This is an indication that the SANS model has been appropriately calibrated (empirically) for the parametric range considered in this investigation.

It is important to note that V_{Rm} predictions provided by R2k reach a maximum value at a specific $\rho_w f_{ywm}$ situation. R2k V_{Rm} predictions are shown in Figure 5.2 to increase to a maximum of about 400 kN at $\rho_w f_{ywm}$ of approximately 1.4 MPa. Beyond 1.4 MPa, R2k V_{Rm} predictions flatten-off giving no extra credit to additional quantities of stirrup reinforcement, serving only as ductility or crack control reinforcement. This behaviour of R2k best-estimate predictions is confirmed by experimental results, as discussed in Section 7.4.5. None of the compared operational approaches for shear design (EC2 VSIM, SANS, *fib* LoA I & III) seem to predict or enforce such a point of maximum shear resistance. They rather continuously give credit for increasing amounts of stirrup reinforcement.

Nevertheless, the early rise in EC2 VSIM predictions, making it the foremost model to become unconservative as $\rho_w f_{ywm}$ increases, became an issue of concern surrounding SA's adoption of EC2.

5.4.2 Design values

Figure 5.3 shows the design value shear strength predictions yielded by the different design approaches for the characteristic range of $\rho_w f_{ywk}$, since design values and safety bias are now of concern. Notice that R2k capacity predictions are absent from the design value analysis, since R2k offers a best-estimate procedure and not a design method.

Figure 5.3 shows that the EC2 design function is initially conservative and comparable with the other design methods below a value of $\rho_w f_{ywk}$ of 1 MPa. The model however rapidly progresses to become the least conservative design method by providing the highest capacity

predictions at $\rho_w f_{ywk}$ in excess of 1.2 MPa. On the other hand, the SANS 10100-1, LoA I and LoA III design approaches provided very similar capacity predictions over the parametric range, although the LoA III design values are slightly less conservative.

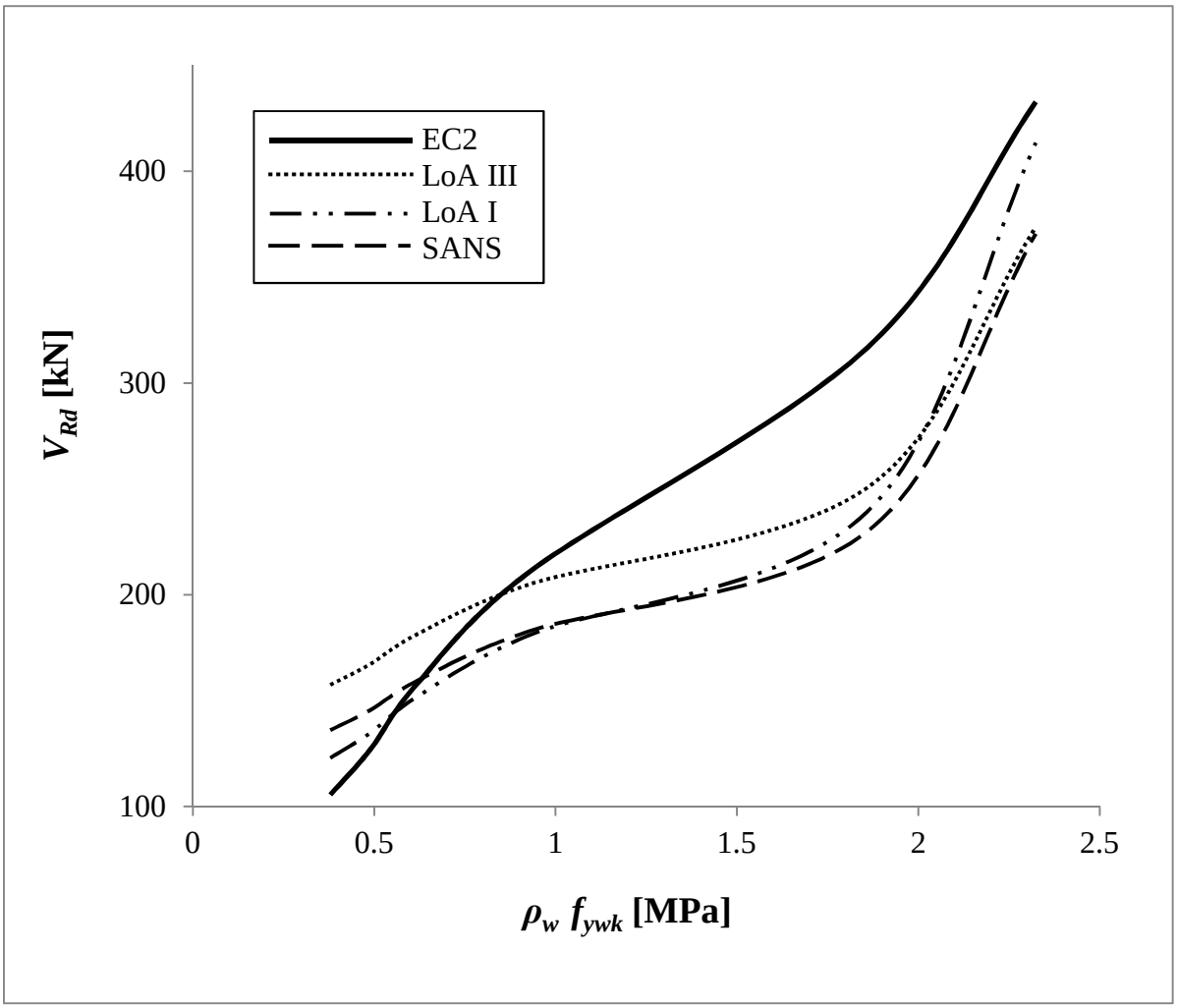

Figure 5.3. V_{Rd} for the various approaches *vs.* $\rho_w f_{ywk}$.

5.4.3 General observations and comments

The scatter of the different curves shown particularly by Figure 5.2, and to some degree for Figure 5.3 as well, indicate the wide-spread uncertainty and problems of the accurate prediction of shear resistance in structural design. Not only do the capacity predictions of the different methods vary from one another, they also vary from the actual value of resistance in a physical structure. Given these uncertainties, the issue of calibration of appropriate partial

factors and characteristic values for shear design models becomes critical to ensure their safe and economic application in practice.

Although all the models deviate from the LoA IV R2k predictions in Figure 5.2, the EC2 VSIM portrays behaviour that is not only somewhat distinct from the others, but has the potential to become unsafe at lower quantities of $\rho_w f_{yw}$ than the other models.

5.5 CONCLUDING REMARKS

The EC2 VSIM was found to be in general agreement with the other design methods, but tends to offer higher capacity predictions at stirrup amounts in excess of 1 MPa. The practical implication is that the EC2 VSIM offers economic performance stirrup amount above 1 MPa as compared to SA's currently operational concrete design standard SANS 10100-1. The comparison to the *fib* LoA I & III approaches was included as part of the investigation to gain some insight of the relative performance of internationally available alternatives for stirrup design. The different prediction methods are not only conceptually different, but also offer different V_{Rm} and V_{Rd} trends as $\rho_w f_{yw}$ varies. This is a reflection of the existing contention in the fraternity on how to approach shear analysis, prediction and design.

Whatever the motivations for applying any given design approach, the method should be calibrated to incorporate sufficient conservative bias into the procedure. This would mitigate the various uncertainties associated with any given approach and support its safe and economic application in practice. The use of the EC2 VSIM is thus warranted for use in SA, but it should be calibrated to local conditions and practice to optimise its performance for designed structures.

CHAPTER 6

BACKGROUND TO THE RELIABILITY ANALYSIS OF THE EC2 STIRRUP DESIGN PROCEDURE

6.1 STRUCTURAL RELIABILITY THEORY

In accordance with Holický (2009), the fundamental task of the theory of structural reliability is the analysis of a simple requirement that the action effect, E, is smaller than the structural resistance, R. It therefore holds that:

$$E < R \qquad [6.1]$$

The reliability of any mode of structural resistance, in this case shear of members with stirrups, derives from the difference between the expected values of the resistance and that of the applied loads effect (Huber, 2005). Equation 6.1 enables the description of a safe state, limit state and failure state of any structural component. The limit state forms the distinction between the safe and failure states of a structure and is defined by the limit state function as:

$$R - E = 0 \qquad [6.2]$$

To reflect uncertainties inherent in design, the resistance and load effect are subject to statistical distributions that reflect the central tendencies of occurrence of their mean values relative to one another and the dispersion of the respective mean values. Of particular interest is the region of expected failure at which the higher end tails of load models or distributions overlap with the lower end tails of the resistance models. This is illustrated in Figure 6.1. It can be deduced from Figure 6.1 that the probability of failure denoted as P_f, can be reduced if the difference in the central tendency of occurrence of the mean values of E and R were increased or if the spread of realisations around the mean is reduced in either or both of E and R. Further, the concept of the reliability index is illustrated for a case where both E and R are assumed to be normally distributed. This example is applicable to very simple cases in reality and is only provided here to aid in defining the reliability index, β. In

general, the reliability index is the distance, expressed in terms of standard deviations, σ_{R-E}, from the mean value of the safety margin, $\mu_R - \mu_E$, from the limit state condition or failure point $G = R - E = 0$.

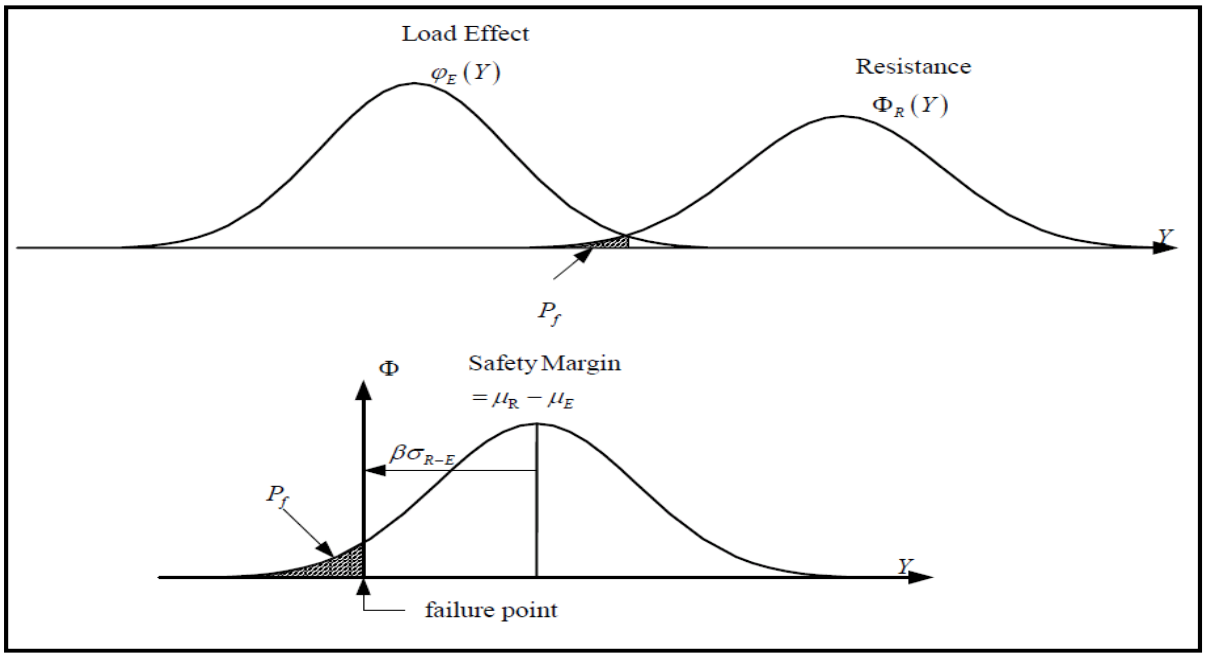

Figure 6.1. Probability Density Function of the Limit State function (Huber, 2005)

A general performance function for any mode of resistance can be defined by:

$$g(\boldsymbol{X}) = R - E \qquad [6.3]$$

Where $\boldsymbol{X} = (X_1, X_2, \dots, X_n)$ is a vector of basic state (or design) variables on which both the load E and resistance R are dependent. A structure is safe as long as $g(\boldsymbol{X}) > 0$ and has failed to meet its intended function if $g(\boldsymbol{X}) \leq 0$. In this general case, the probability of failure can be given by:

$$P_f = Probability\,(g(X) \leq 0) = \int_{g(\boldsymbol{X})\leq 0} \varphi_g(\boldsymbol{X})\, dX \qquad [6.4]$$

Where $\varphi_g(\boldsymbol{X})$ denotes the joint probability density distribution of the vector of basic variables X. In practice, evaluation of the joint probability density functions of actions and resistances is a formidable task as information is often unavailable or difficult to obtain for reasons of insufficient data (Ang & Tang, 1984). Furthermore, even in cases where the required distributions are specified, the determination of Equation 6.4, which requires numerical integration, may be impractical as much effort is required. As such, the First Order Reliability Method (FORM) method is implemented as a practical tool of conducting reliability analyses (Ang & Tang, 1984). An added advantage of the FORM method is that the reliability index, β, may be measured entirely as a function of the mean and standard deviation of basic variables when there is no information on the probability distributions. The FORM procedure is outlined in Section 6.2. The relation between β and P_f is described by:

$$P_f = \Phi(-\beta) \qquad [6.5]$$

Where Φ is the cumulative distribution function of the standardised Normal distribution.

6.1.1 Performance concepts for structural design

It may be assumed that the overall reliability index β may be split into the resistance part, expressed by the resistance index $\beta_R = \alpha_R\beta$, and the load effects part, expressed by the load effect index $\beta_E = -\alpha_E\beta$. α_R and α_E are the FORM sensitivity factors which have been recommended in EC0 as $\alpha_R = 0.8$ and $\alpha_E = -0.7$. The most important feature of reliability separation is that material codes, or resistance performance, can be calibrated independent of loading codes and loading considerations in general. The mutual relationship between the resistance failure probability, P_R, and the resistance index, β_R, is given as (Holický et al., 2010):

$$P_R = \Phi\,(-\beta_R) = P\{R(\boldsymbol{X}) < R_d(\boldsymbol{X_k}, \boldsymbol{\gamma})\} \qquad [6.6]$$

Where $R(\boldsymbol{X})$ is a General Probabilistic Model (GPM), for shear in this case, representing the resistance side of the limit state equation, similar to R in Equation 6.3. $R_d(\boldsymbol{X_k}, \boldsymbol{\gamma})$ is the

deterministic code design shear resistance for a specific case for which the reliability is to be determined. Therefore, $\boldsymbol{X}$ denotes the vector of basic variables, $\boldsymbol{X_k}$ represents the vector of their characteristic values, and $\boldsymbol{\gamma}$ the vector of relevant partial factors. By FORM analysis, the resistance reliability index, β_R, may be determined through the assessment of the performance function:

$$g(\boldsymbol{X}) = R(\boldsymbol{X}) - R_d(\boldsymbol{X_k}, \boldsymbol{\gamma}) \qquad [6.7]$$

König et al. (1985) establish that highly sophisticated models, such as GPMs can be used as models of true shear resistance in the absence of valid tests and measurements from practice.

6.1.2 Alternative forms of GPM representation for shear resistance

Two alternative forms of GPM representation $R(\boldsymbol{X})$ were adopted in this investigation as presented in Chapters 8 and 9, and are distinguished, respectively, as follows:

1. The primary GPM was based on the probabilistic representation of the analytical formulation of the VSIM, denoted $V_{VSIM-Analytical}(\boldsymbol{X})$
2. A secondary GPM representation based on R2k capacity predictions was employed as a separate checking procedure to the basic investigations described in (1) above.

6.1.3 First Order Reliability Method (FORM)

Coupled with easier assessment of the probability of failure through the determination of β, the FORM method is also an effective decision tool as it provides more insight into the reliability process than numerical integration or simulation methods. By the use of numerical examples, various reliability elements such as partial factors and direction cosines of basic variables can be investigated to determine which basic variables mostly affect the reliability performance for shear or any other mode of structural resistance. Holický et al. (2010) establish that effective management of reliability performance, in terms of attaining specified reliability levels, can be achieved by applying partial factors to the variables that most affect reliability performance. The relative importance of basic variables is reflected by the relative values of their direction cosines; that is, the greater the value of the direction cosine, the greater the influence of the parameter on reliability performance of the structure considered.

It should be emphasised that the FORM method is consistent with the equivalent normal representation of non-normal distributions. Only the mean and standard deviation of the normal distribution are required for FORM analyses, hence non-normal distributions only need to be transformed to normal distributions at specific points where the performance is being assessed. Hence, an essential step in using the FORM method is first transforming the basic variables of various distributions into a transformed space of equivalent normal variables.

6.2 PROCEDURE FOR THE FORM ANALYSES

The FORM algorithm outlined in Holický (2009) was programmed in Excel spreadsheets to conduct the reliability analysis of the EC2 stirrup design method. Elaborate details of the application of the FORM algorithm as executed in the spreadsheet during the basic performance assessment and validation, respectively, of EC2's VSIM design procedure is elaborated in Chapters 8 and 9. The generic steps of the FORM algorithm (Holický, 2009) applied throughout the study are outlined below:

1. The limit state function $g(\boldsymbol{X}) = 0$ was formulated and theoretical models for basic variables $\boldsymbol{X} = \{\boldsymbol{X_1}, \boldsymbol{X_2}, \ldots, \boldsymbol{X_n}\}$ specified:

$$g(\boldsymbol{X}) = R(\boldsymbol{X}) - R_d(\boldsymbol{X_k}, \boldsymbol{\gamma}) = 0 \qquad [6.8]$$

2. The design point $\boldsymbol{x}^* = \{x_1^*, x_2^*, \ldots, x_n^*\}$, was estimated initially using the means of $n-1$ basic variables, and the value of the last basic variable was calculated from $g(\boldsymbol{x}^*) = 0$.

3. The equivalent normal distribution for all basic variables at $\boldsymbol{x^*}$ were evaluated. For an individual variate, the equivalent normal dsitribution for a nonnormal variate may be obtained such that the cumulative probability as well as the probability density ordinate of the equivalent normal distribution are equal to those of the correspnding

nonnormal distribution at the appropriate point, x_i^*, on the failure surface (Ang & Tang, 1984). Hence, equating the cumulative probabilities, we get:

$$\Phi\left(\frac{x_i^* - \mu_{X_i}^N}{\sigma_{X_i}^N}\right) = F_{X_i}(x_i^*) \quad [6.9]$$

Where $\mu_{X_i}^N \; and \; \sigma_{X_i}^N$ are the mean value and standard deviation, respectively, of the equivalent normal distribution for X_i. $F_{X_i}(x_i^*)$ is the original Cumulative Distribution Function (CDF) of X_i evaluated at x_i^*

Transposing Equation 6.9 and making the equivalent normal mean subject yields:

$$\mu_{X_i}^N = x_i^* - \sigma_{X_i}^N \Phi^{-1}\left[F_{X_i}(x_i^*)\right] \quad [6.10]$$

Furthermore, equating the corresponding probability density ordinates at x_i^* means yields,

$$\frac{1}{\sigma_{X_i}^N}\varphi\left(\frac{x_i^* - \mu_{X_i}^N}{\sigma_{X_i}^N}\right) = f_{X_i}(x_i^*) \quad [6.11]$$

Transposing Equation 6.11 and making the equivalent normal standard deviation subject:

$$\sigma_{X_i}^N = \frac{\varphi\left\{\Phi^{-1}\left[F_{X_i}(x_i^*)\right]\right\}}{f_{X_i}(x_i^*)} \quad [6.12]$$

Equations 6.9 to 6.12 only give superficial treatment of how basic variables are transformed. Similar transformations for non-normal distributions are further elaborated on in Section 6.3.

4. The transformed design point $\boldsymbol{u^*} = \{u_1^*, u_2^*, \ldots u_n^*\}$ of standardised normal variables $\boldsymbol{U} = \{U_1, U_2, \ldots U_n\}$ corresponding to $\boldsymbol{x^*} = \{x_1^*, x_2^*, \ldots x_n^*\}$ was determined using Equation:

$$\boldsymbol{u_i^*} = \frac{x_i^* - \mu_X^N}{\sigma_X^N} \qquad [6.13]$$

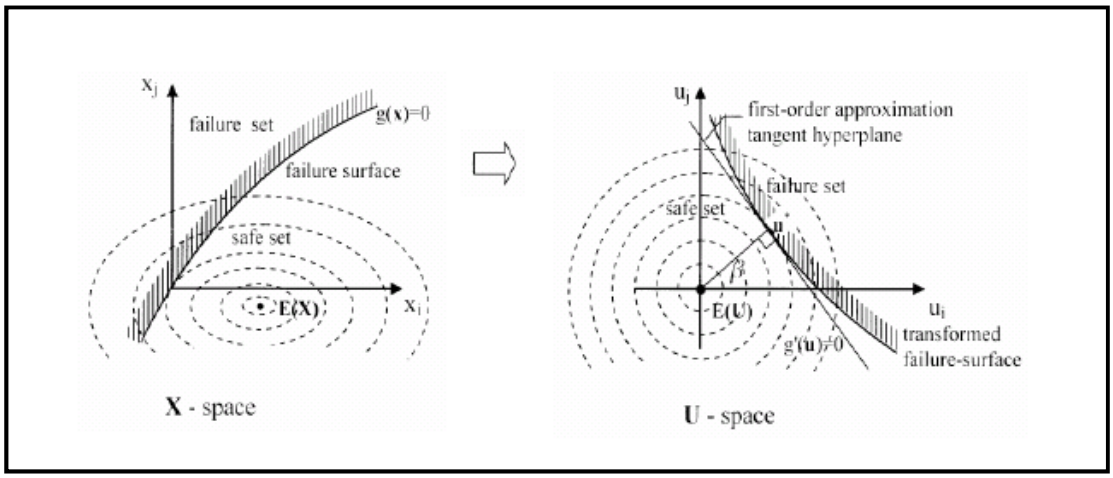

Figure 6.2. Schematic representation of the standard normal transformation process (Taken from Dithinde, 2007)

5. Partial derivatives of the limit state function with respect to $\boldsymbol{U} = \{U_1, U_2, \ldots, U_n\}$ were determined at the design point and denoted as the vector $\boldsymbol{D} = \{D_1, D_2, \ldots, D_n\}$ and:

$$D_i = \frac{\partial G}{\partial U_i} = \frac{\partial G}{\partial X_i}\frac{\partial X_i}{\partial U_i} = \frac{\partial G}{\partial X_i} \cdot \sigma_X^N \qquad [6.14]$$

6. The reliability index β was estimated as:

$$\beta = -\frac{\{D\}^T\{u^*\}}{\sqrt{\{D\}^T\{D\}}} \qquad [6.15]$$

For non-linear performance functions, there is no unique distance from the failure surface to the origin of the reduced varaites but rather a linear approxiamtion by the use of a tangent plane to the failure surface at $\{x_1^*, x_2^*, \ldots, x_n^*\}$ to approximate the failure surface.

7. The vector of sensitivity factors was determined as:

$$\alpha = \frac{\{D\}}{\sqrt{\{D\}^T\{D\}}} \quad or \quad \alpha_i^* = \frac{\left(\frac{\partial g}{\partial X_i}\right)_*}{\sqrt{\sum_i \left(\frac{\partial g}{\partial X_i}\right)_*^2}} \qquad [6.16]$$

8. The new design point for *n*-1 standardised variables and original variables was given as:

$$u_i^* = \alpha_i \beta_i \qquad [6.17]$$

$$x_i^* = \mu_{Xi}^N - u_i^* \sigma_{Xi}^N \qquad [6.18]$$

9. The new checking point value of the n^{th} variable followed from solving $g(\boldsymbol{x}^*) = 0$.

10. Steps 3 to 9 were repeated until β and design point values $\{\boldsymbol{x}^*\}$ were achieved with acceptable convergence.

6.3 THEORETICAL MODELS OF BASIC VARIABLES

Holický (2009) presents a compilation of several theoretical models that can be used for the representation of basic random variables in structural reliability assessments. This is considered a sound compilation as it is extracted from renowned sources as the JCSS probabilistic model code, CIB reports, the SAKO report and other significant contributions. Direct cross reference is also made to the JCSS probabilistic model code (2001) and to the SAKO report (1999). The models prescribed by Holický (2009) are given in Table 6.1

below. For the distributions, the symbol N denotes the normal distribution, GU the gumbel distribution, LN the Log-normal distribution, and BET the beta distribution. Though not shown in the Table, some basic variables that have negligible uncertainty or effect on reliability performance may be treated as deterministic values. Deterministic values are defined by a single (exact) value with no associated uncertainty (or standard deviation) of the statistical distribution to reflect such.

Table 6.1. Conventional models of basic variables for time-invariant reliability analyses (Holický, 2009)

No.	Category of variables	Name of basic variables	Sym. X	Dimension	Distrib.	Mean μ_X	St. dev. σ_X	Prob. $\Phi_X(X_k)$
1	Actions	Permanent	G	KN/m^2	N	G_k	0.03 - 0.10μ_X	0.5
2		Imposed - 5 years	Q	KN/m^2	GU	0.2Q_k	1.1μ_X	0.995
3		Imposed - 50 y	Q	KN/m^2	GU	0.6Q_k	0.35μ_X	0.953
4		Wind - 1 year	W	KN/m^2	GU	0.3W_k	0.5μ_X	0.999
5		Wind - 50 years	W	KN/m^2	GU	0.7W_k	0.35μ_X	0.89
6		Snow - 1 year	S	KN/m^2	GU	0.35 S_k	0.70μ_X	0.998
7		Snow -50 year	S	KN/m^2	GU	1.1 S_k	0.30μ_X	0.437
8	Material Strengths	Steel yield point	f_y	MPa	LN	f_{yk} + 2σ	0.07 - 0.10μ_X	0.02
9		Steel strength	f_u	MPa	LN	$\kappa\,\mu_{fy}$	0.05μ_X	-
10		Concrete	f_c	MPa	LN	f_{ck} + 2σ	0.10 - 0.18μ_X	0.02
11		Reinforcement	f_y	MPa	LN	f_{yk} + 2σ	30 MPa	0.02
12	Geometry steel sect.	IPE profiles	A, W, I	m	N	0.99 X_{nom}	0.01 - 0.04 μ_X	≈0.73
13		L-section. rods	A, W, I	m	N	1.02 X_{nom}	0.01 - 0.02 μ_X	≈0.16
14	Geometry	Cross-section	b, h	m	N	b_k, h_k	0.005 - 0.01	0.5
15	concrete	Cover of reinf.	a	m	BET	a_k	0.005 - 0.015	0.5
16	cross-sect.	Additional ecc.	e	m	N	0	0.003 - 0.01	-
17	Model uncertainties	Load effect factor	θ_E	-	N	1	0.05 - 0.10	-
18		Resistance factor	θ_R	-	N	1 - 1.25	0.05 - 0.20	-

Once the distributions of each of the basic variables had been identified, the next task was to understand the transformation of non-normal variates into equivalent normal form in order to enable their use during the FORM assessment. The Sections below treat the non-normal distributions used in the study, showing how they were transformed to equivalent normals.

6.3.1 Background of the general three parameter log-normal distribution

In general, a random variable X has a three-parameter log-normal distribution if the transformed variable, Y, has a normal distribution., where:

$$Y = \ln|X - x_0| \qquad [6.19]$$

In this relation x_0 denotes the lower or upper bound of the variable X, which depends on the skewness, s_k. If the variable has a mean, μ_X, and a standard deviation, σ_X, and a measure of skewness, c, then the lower or upper bound can be expressed as:

$$x_0 = \mu_X - \frac{\sigma_X}{c} \qquad [6.20]$$

Note that for negative skewness, c is a negative quantity and in that case x_0 is indicative of the upper bound of the distribution. The coefficient, c, is obtained from the value of the skewness, s_k, according to the relation:

$$s_k = c^3 + 3c \qquad [6.21]$$

From which follows an explicit relation for c:

$$c = \left[\left(\sqrt{s_k^2 + 4} + s_k\right)^{1/3} - \left(\sqrt{s_k^2 + 4} - s_k\right)^{1/3}\right] 2^{-1/3} \qquad [6.22]$$

Thus, when specifying a theoretical model, it is therefore possible to consider the skewness s_k or alternatively the lower or upper bound of the distribution x_0 (besides the mean μ_X and standard deviation σ_X). In general, the skewness provides better characteristic of the overall distribution of the population (particularly of large populations) than the lower or upper bounds (Holický, 2009).

The probability density function and distribution function of the general three-parameter log-normal distribution may be obtained from the well-known normal distribution using a

modified (transformed) standardised variable u'_N obtained from the original standardised random variable $u' = (x - \mu_X)/\sigma_X$ as:

$$u'_N = \frac{\ln\left(\left|u' + \frac{1}{c}\right|\right) + \ln\left(|c|\sqrt{1+c^2}\right)}{\sqrt{\ln(1+c^2)}} sign(s_k) \quad [6.23]$$

Where $sign(s_k)$ equals $+1$ for $s_k > 0$ and -1 for $s_k < 0$. The probability density function $\varphi_{LN,U}(u)$ and the distribution function $\Phi_{LN,U}(u) = \Phi_{LN,X}(x)$ of the log-normal distribution are given as:

$$\varphi_{LN,U}(u) = \frac{\varphi(u'_N)}{\sigma_U\left(\left|u' + \frac{1}{c}\right|\right)\sqrt{\ln(1+c^2)}} \quad [6.24]$$

$$\Phi_{LN,X}(x) = \Phi_{LN,U}(u) = \Phi(u'_N) \quad [6.25]$$

Where $\varphi(u'_N)$ and $\Phi(u'_N)$ denote the probability density and distribution function of the standardised normal variable.

A special case of the three-parameter log-normal distribution is the log-normal distribution with the lower bound at zero ($x_0 = 0$). This distribution depends on two parameters only – the mean, μ_X, and standard deviation, σ_X. In such a case the coefficient, c, is equal to the coefficient of variation, Ω_X. It further follows from Equation 6.21 that:

$$s_k = \Omega_X^3 + 3\Omega_X \quad [6.26]$$

Thus, the log-normal distribution with the lower bound at zero always has a positive skewness.

6.3.2 Background of the two-parameter log-normal distribution

Ang and Tang (1975) give the density function, $f_x(x)$, and distribution function between limits a and b of an arbitrary random variable, X, that follows the two parameter log-normal distribution as:

$$f_x(x) = \frac{1}{\sqrt{2\pi}\zeta x} exp\left[-\frac{1}{2}\left(\frac{\ln x-\lambda}{\zeta}\right)^2\right] \qquad 0 \le x \le \infty \qquad [6.27]$$

$$P(a < X \le b) = \frac{1}{\sigma\sqrt{2\pi}}\int_a^b \exp\left[-\frac{1}{2}\left(\frac{x-\mu}{\sigma}\right)^2\right] dx \qquad [6.28]$$

Where $\lambda = E(\ln X)$ and $\zeta = \sqrt{Var(\ln X)}$ are, respectively, the mean and standard deviation of $\ln X$, and are the parameters of the distribution. The mean, λ, and the standard deviation, ζ, of $\ln X$ are defined as:

$$\lambda = \ln \mu_X - \frac{1}{2}\zeta^2 \qquad [6.29]$$

$$\zeta = \sqrt{\ln\left(1 + \frac{\sigma_X^2}{\mu_X^2}\right)} = \sqrt{\ln(1 + \Omega_X^2)} \qquad [6.30]$$

Note that ζ will have to be determined before the solution to Equation 6.29 is sought.

The density function and probability generating function of the two-parameter log-normal distribution can be found by use of the standardised normal distribution:

$$\text{Let } \; s = \frac{\ln x-\lambda}{\zeta} \qquad [6.31]$$

Then $dx = x\zeta ds$, and:

$$\text{Then } f_x(x) = \frac{1}{\sqrt{2\pi}\zeta x} exp\left[-\frac{1}{2}\left(\frac{\ln x-\lambda}{\zeta}\right)^2\right] \qquad 0 \le x \le \infty \qquad [6.32]$$

$$P(a < X \le b) = \frac{1}{\sqrt{2\pi}}\int_{(\ln a-\lambda)/\zeta}^{(\ln b-\lambda)/\zeta} e^{-(1/2)s^2}\, ds = \Phi\left(\frac{\ln b-\lambda}{\zeta}\right) - \Phi\left(\frac{\ln a-\lambda}{\zeta}\right) \qquad [6.33]$$

Where $\Phi(-)$ denotes the cumulative distribution function of the standard normal distribution.

Ang and Tang (1984) then proceed to represent the density function and distribution function of the log-normal distribution in the form of the standardised normal distribution, similar to the end results Equation 6.10 and 6.12, as:

$$\Phi_{LN,X}(x_i^*) = \Phi\left(\frac{\ln x^* - \lambda_X}{\zeta_X}\right) \quad [6.34]$$

$$\varphi_{LN,X}(x^*) = \frac{1}{x^*\zeta_X}\varphi\left(\frac{\ln x^* - \lambda_X}{\zeta_X}\right) \quad [6.35]$$

Where $\Phi_{LN,X}(x_i^*)\ and\ \varphi_{LN,X}(x_i^*)$ denote the cumulative distribution and probability density function of the lognormal distribution of the original variate at the checking point x_i^*. Therefore, for the two-parameter log-normal distribution:

$$\sigma_{X_i}^N = \frac{\varphi\left\{\Phi^{-1}\left[\Phi\left(\frac{\ln x^* - \lambda_X}{\zeta_X}\right)\right]\right\}}{\frac{1}{x^*\zeta_X}\varphi\left(\frac{\ln x^* - \lambda_X}{\zeta_X}\right)} = \frac{x^*\zeta_X\left[\varphi\left(\frac{\ln x^* - \lambda_X}{\zeta_X}\right)\right]}{\varphi\left(\frac{\ln x^* - \lambda_X}{\zeta_X}\right)} = x^*\zeta_X \quad [6.36]$$

$$\mu_{X_i}^N = x^* - x^*\zeta_X\left(\frac{\ln x^* - \lambda_X}{\zeta_X}\right) = x^* - x^*(\ln x^* - \lambda_X) = x^*(1 - \ln x^* + \lambda_X) \quad [6.37]$$

6.3.3 Model uncertainties

Since in developing a resistance model certain influences are either consciously or unconsciously neglected, deviations between analysis and tests are to be expected. An analysis and assessment of uncertainty must include the uncertainties in the design variables as well as in the prediction models (Ang & Tang, 1984). For good models the Model Factor, defined as the ratio of experimental to predicted capacity, is approximately equal to one. Since, however, conservative models are used it often results in Model Factors greater than one. For good models, such as bending resistance of concrete and even steel, the coefficient of variation is just a few percent, whereas for poor models such as shear and punching shear, values in the region of 10 to 20 % are typical (Schneider, 2006). Taerwe (1993) states that special calibration of the model uncertainty as part of the global resistance factor is warranted for coefficients of variation of 20 % and above. For smaller coefficients of variation it could be tentatively suggested that the model uncertainties don't require an additional safety factor if safe side models are used.

Figure 6.3 gives a schematic overview of how model uncertainties can be treated. It is illustrated in Figure 6.3 that model uncertainties can be treated at different levels of refinement ranging from the top of the chart with experience or judgement based treatment, going down to the more rigorous and rational methods of full probabilistic analysis. The way

in which model uncertainties are dealt with during calibration exercises is largely dependent on whether or not statistical information on the model uncertainty is available, and if thereafter, severe trends exist between the model factor and any of the shear parameters. In the event that sufficient information is available for a statistical evaluation of model uncertainty, as is the case for shear, and it is found to be dominating or important to structural performance, it should be sufficiently accounted for and properly calibrated into the resistance model or the global partial safety factor.

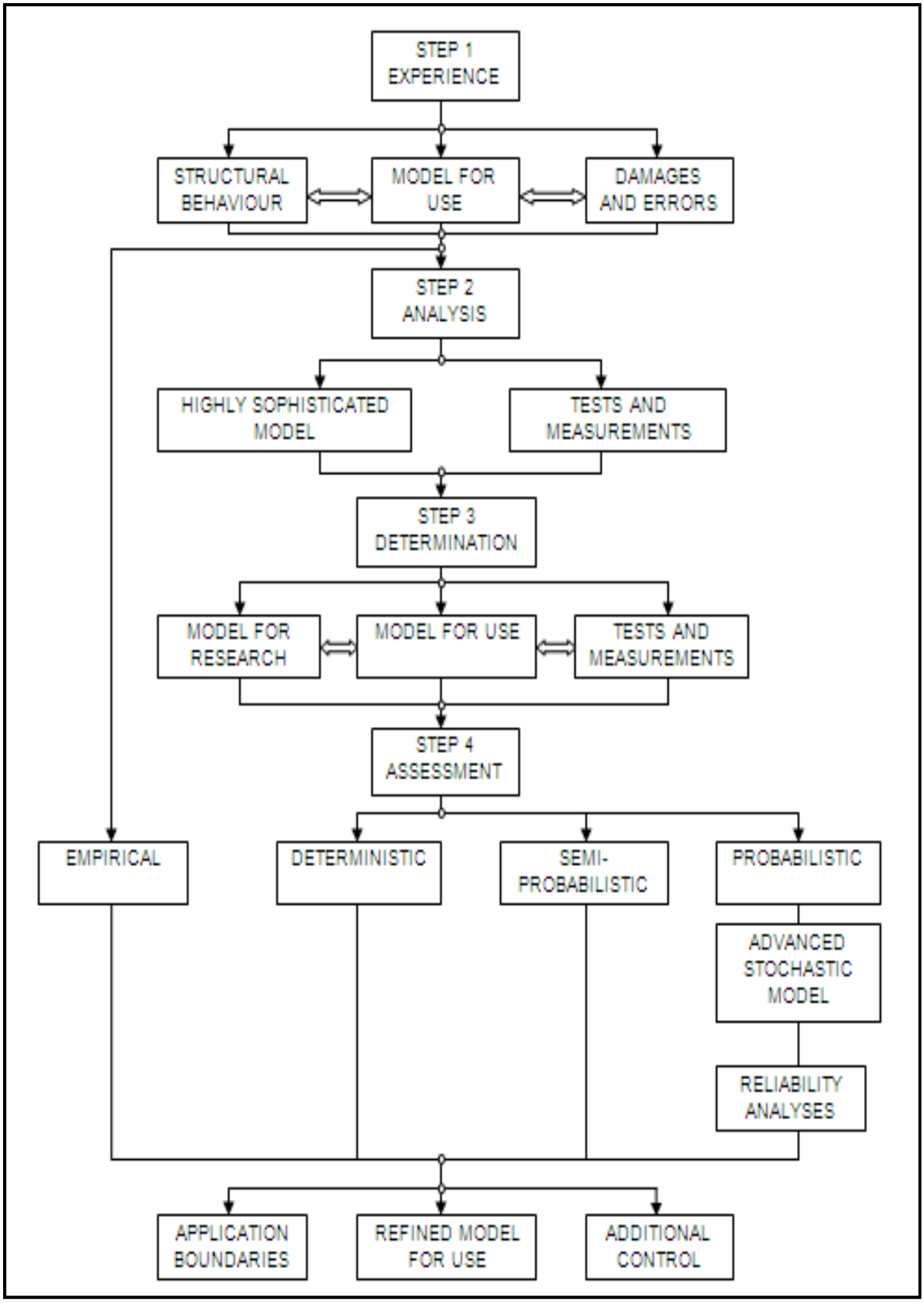

Figure 6.3. Flow chart for treatment of model uncertainties (König et al, 1985)

CHAPTER 7

DERIVATION OF MODEL STATISTICS FOR RELIABILITY ANALYSIS

Model uncertainties, which reflect the accuracy of predictions of uncalibrated resistance models, have been shown to have a significant influence on resistance reliability performance. Holický, Retief, and Dunaiski (2007), for example, presented and discussed specific examples of various modelling uncertainties in an attempt to demonstrate their importance/influence in the structural design process. Model uncertainty was therein shown not only to vary across the different modes of structural concrete resistance (mean and standard deviation $\mu = 1.08,\ \sigma = 0.10$ for flexure; $\mu = 1.23, \sigma = 0.38$ for EN 1992-1-1 shear with no links) but also varies along the parametric range of a single mode of resistance (showing sensitivity to design parameters).

Model uncertainties are, however, still applied rather approximately in reliability analyses, usually lacking proper characterisation according to a representative database of associated laboratory tests. As a result, there is some concern as to whether the conventional partial safety factors for concrete γ_C and steel γ_S are appropriately calibrated to cater for model and other uncertainties, with particular concern toward provisions for stirrup design.

This Chapter describes the derivation of key statistics for various Model Factors (MF) that both guided and formed an integral part of the reliability performance assessment of the EC2 stirrup design procedure. The failure loads ($V_{experiment}$) from a database of stirrup-reinforced beam experiments were compared against unbiased ultimate shear strength predictions obtained from (1) two variations of the Variable Strut Inclination Method (VSIM), resulting in two separate Model Factors ($MF_{VSIM-Analytical}$ & $MF_{VSIM-Limit\theta}$), and (2) from Response-2000 (R2k), resulting in the Model Factor MF_{R2k}. This Chapter presents the detailed statistics of the three Model Factors (MFs) obtained from this assessment. Table 7.1 gives key attributes for each case of the MF.

Table 7.1. Key attributes of the three alternative Model Factors.

Model Factor (MF)	**Key Attributes**
$MF_{VSIM-Analytical}$	Characterised by the ratio $\frac{V_{experiment,i}}{V_{VSIM-Analytical,i}}$ against the entire database of 222 experiments. $V_{VSIM-Analytical}$ represents the unbiased ultimate stirrup resistance prediction of the analytical formulation of the VSIM.
$MF_{VSIM-Limit\theta}$	Characterised by the ratio $\frac{V_{experiment,i}}{V_{VSIM-Limit\theta,i}}$ against the entire database of 222 experiments. $V_{VSIM-Limit\theta}$ is the unbiased ultimate stirrup resistance prediction of the operational version of the VSIM. This version of VSIM limits the virtual concrete strut angle θ within confines $21.8° \leq \theta_{Limited} \leq 45°$.
MF_{R2k}	Characterised by the ratio $\frac{V_{experimental,i}}{V_{R2k,i}}$ against a subset of 116 experiments. V_{R2k} is the equivalent unbiased shear capacity prediction of a stirrup-reinforced beam as per the sectional analysis program R2k.

Characteristics of the Model Factor related to failure modes indicative of stirrup yielding in beam experiments were sought in this investigation. To achieve this goal, reported anchorage and flexural failures were excluded from the database of compiled beam tests. Shear Compression was the predominantly accepted mode of failure used for selecting beam tests for the database, with failure of the dowel bars through splitting action being acceptable in some instances.

Derived Model Factor (MF) statistics guided reliability investigations as well as formed an integral part of the rational models for reliability analysis of EC2's stirrup design procedure discussed in Chapters 8 and 9. It is worth noting that only $MF_{VSIM-Analytical}$ and MF_{R2k} were applied, respectively, for the reliability performance assessment of the EC2 stirrup design procedure presented in Chapters 8 and 9.

$MF_{VSIM-Limit\theta}$, on the other hand, was investigated to (1) determine the influence the condition $21.8° \leq \theta_{Limited} \leq 45°$ has on the performance of VSIM, and (2) to determine the factors affecting shear strength against which $V_{VSIM-Limit\theta}$ predictions are sensitive. The

assessment concluded that $MF_{VSIM-Limit\theta}$ is particularly sensitive to the amount of stirrup reinforcement provided in design, denoted $\rho_w f_{ywm}$, with no similar sensitive trends portrayed against other important factors affecting shear strength i.e. a/d, ρ_l, b_w, d, and f_{cm}. However, the tendency of $V_{VSIM-Limit\theta}$ predictions to become mildly unconservative for heavily stirrup-reinforced concrete beams caused serious concern about the performance of the EC2 stirrup design procedure in such situations. This result led to the commissioning of reliability investigations to assess the consistency of the achieved level of reliability (β-values) across a parametric range of $\rho_w f_{ywm}$.

Furthermore, β-values were also assessed across a range of concrete strengths f_{cm}. However, this sensitivity of estimated β-values to concrete strength was not exposed by characteristics of the Model Factor. Recall that the Model Factor (MF) consists of the comparison of the resistance from an experimental beam to the equivalent prediction offered by a resistance model i.e. the inherent uncertainty of the prediction model is sought, and not the sensitivity of the prediction model to its component parameters. Cognizance must be taken of the fact that, in general, shear resistance predictions V are proportionally sensitive to changes in concrete strength. That is, the higher the concrete strength, the greater the resistance predictions, and vice versa holds true.

Parametric assessments of the various prediction methods (VSIM-Analytical, VSIM-Limitθ, and R2k) applied to the database of beam experiments were conducted based on a combination of (1) observations of systematic behaviour from the scatter plots of MF realisations versus important factors affecting shear strength, (2) statistical correlation analysis, and (3) fitted regression trendlines to the scattered data.

7.1 THE EXPERIMENTAL DATABASE

The experimental database compiled for determining MF statistics for each of the prediction methods was compiled from research published in most part by the American Concrete Institute (ACI) Structural Journal over the past 50 years. The different experiments, conducted by different researchers, were aimed and hence designed to reflect different

aspects of performance of stirrup-reinforced concrete beams. Many of the experimental studies on shear from the ACI Structural Journal have resulted in the use of different design rules and approaches worldwide. As a result, the database does provide some representation of beams in practice. Detailed statistical properties of the database are reported and discussed throughout the Chapter. Some detail of the database is given in Appendix A, citing (1) the main factors affecting shear strength captured by the database ($b_w, d, f_{cm}\ etc.$), presented alongside (2) unbiased shear resistance predictions offered by the respective approaches ($V_{VSIM-Analytical}$, $V_{VSIM-Limit\theta}$, V_{R2k}), and (3) giving each of their Model Factors when compared to the failure loads ($V_{experiment}$) of the beam tests from the compiled experimental database. An extensive version of the database is provided on the CD affixed at the end of this document.

R2k predictions could not be made against every test result in the compiled experimental database, owing to the fact that a wealth of data is required for such R2k predictions, some of which was not reported in a number of studies. Therefore, two sets of the data were created; the first was the complete database of 222 beam tests to which VSIM predictions were possible, and the other a subset of 116 beam tests which could be modelled in R2k. Statistical comparisons of the two sets of data are given in Sections 7.1.3 and 7.3.1.

7.1.1 Composition of the database

The entire database consisted of 222 reinforced concrete beams with stirrups, which were collected from published experimental data from some 24 literature sources. The most salient features of the beam experiments included in the database are summarised in the list below.

1. Range of shear span (a)-to-depth (d) ratios: Most beams in the database were in the range $2.5 \leq \mathrm{a}/d \leq 6.0$. Beams without stirrups in this range would typically experience Diagonal Tension failures (O'Brien, Dixon & Sheils, 2012; see also Section 3.2.2). The provision of stirrups averts the occurrence of brittle diagonal tension failures, promoting ductile behaviour through increased diagonal and flexural cracking. Ultimate ductile failures would typically occur by Shear-Compression as described in the next point.

2. Failure Modes: Beam experiments in the database failed predominantly by Shear-Compression, which is typically a ductile failure mode characterised by splitting in the compression zone (usually close to point of applied loading) of the concrete member following from a critical diagonal tension crack formed in the shear span. In addition to splitting in the compression zone, the diagonal cracks could possibly also extend toward the bottom face of the beam; depending on (1) the quantity of longitudinal tension reinforcement, (2) the multi-layer arrangement of reinforcement, and (3) the effectiveness of the longitudinal reinforcement (if stressed below yield point), as expressed in Bresler and Scordelis (1963). Beam experiments that showed any signs of Flexure-Compression, anchorage, deep beam, or flexural yielding failures were excluded from the database. The accepted modes of failure characteristic for beams included in the database were considered ductile failure modes that occur post-yield of the stirrups.

3. Beam geometries: All beams in the compiled database were simply supported and had predominantly 1 or 2 gravity point loads between supports, although 4 gravity point loads were placed between the supports in only four tests.

4. Minimum amount of stirrups: All beams had to have at least the minimum amount of stirrups as set by EC2. This is a parameter left open for national choice and the UK adopts the value given in Equation 3.12. This implies that all beams in the database satisfied the condition:

$$\rho_w \geq 0.08 \frac{\sqrt{f_{cm}}}{f_{ywm}} \quad , \quad \text{and} \quad \rho_w = \frac{A_{sw}}{b_w s} \qquad [7.1]$$

where ρ_w is the stirrup reinforcement ratio; f_{cm} and f_{ywm} are, respectively, the mean concrete and mean steel yield strengths as reported in the literature.

5. Maximum spacing of stirrups: The maximum spacing limit for stirrups of $0.75d$ or 600 mm as recommended by EC2 and maintained for use in the UK was enforced for all beams in the database.

6. Upper limit to check Web-Crushing failures: For both VSIM calculations (VSIM-Analytical and VSIM-Limitθ), it was ensured that the conditions $V_{VSIM-Analytical} \leq V_{Rd,max}$ and $V_{VSIM-Limit\theta} \leq V_{Rd,max}$ were satisfied. $V_{Rd,max}$ represents the upper limit to shear resistance enforced as part of the VSIM procedure to prevent the occurrence of web-crushing failures. Note that $V_{Rd,max}$ was merely treated as a constraint set, with operational resistance provided solely by the contribution of the stirrups ($V_{VSIM-Analytical}$ or $V_{VSIM-Limit\theta}$).

7. Subset of 116 stirrup-reinforced beam tests: R2k could only be used to model 116 beam experiments for which sufficient data was available to enable its use. R2k required the specification of more input variables to enable an ultimate strength prediction as compared to VSIM calculations. Examples of additional parameters required to enable R2k ultimate strength predictions include concrete cover, maximum aggregate size, yield strength and arrangement of longitudinal reinforcement, etc.

7.1.2 Ranges and distributions of factors affecting shear strength

Separate histogram plots for each of the shear parameters against the entire database of 222 tests are given in Figure 7.1 to Figure 7.6 below. The investigated shear parameters are listed below.

1. The stirrup quantity, $\rho_w f_{ywm}$, expressed in MPa
2. Shear span to depth ratio, a$/d$
3. Percentage of longitudinal tension reinforcement, $\rho_l = 100A_s/b_w d$
4. Breadth of the member, b_w
5. Member effective depth, d
6. Concrete (mean) cylinder compressive strength, f_{cm} (mean strengths reported for experiments)

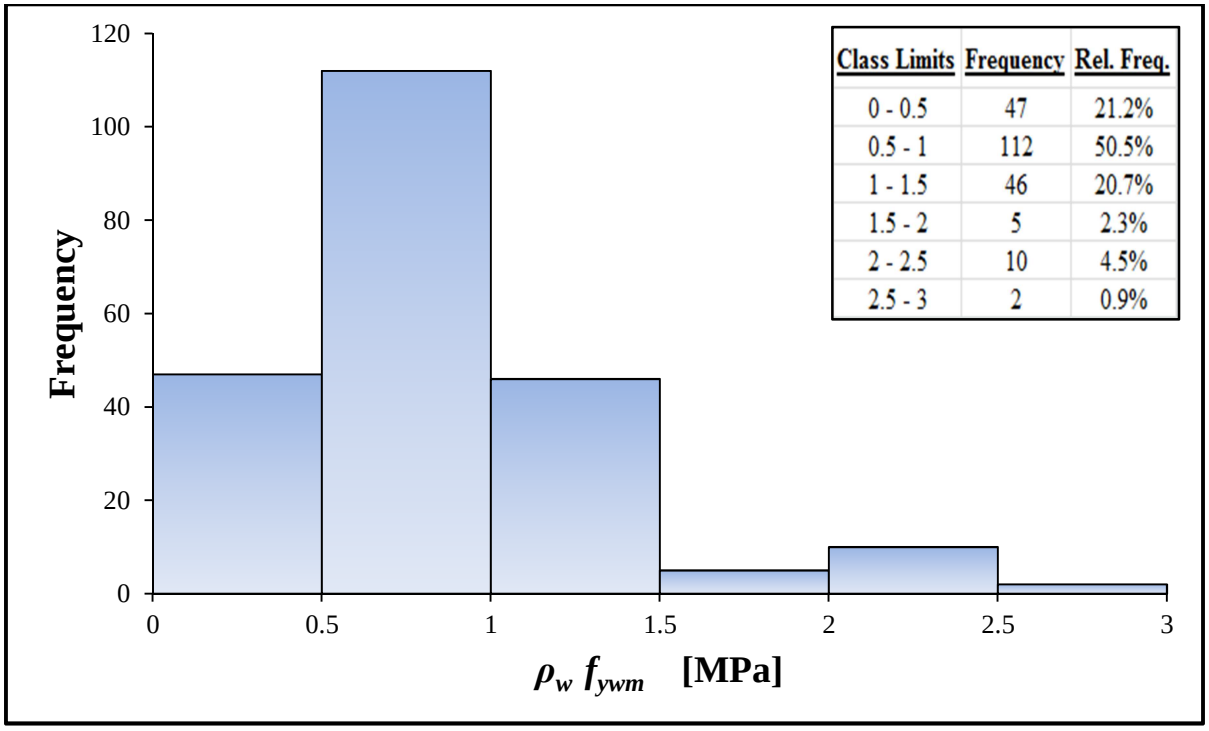

Figure 7.1. Distribution of for the entire database of 222 experiments

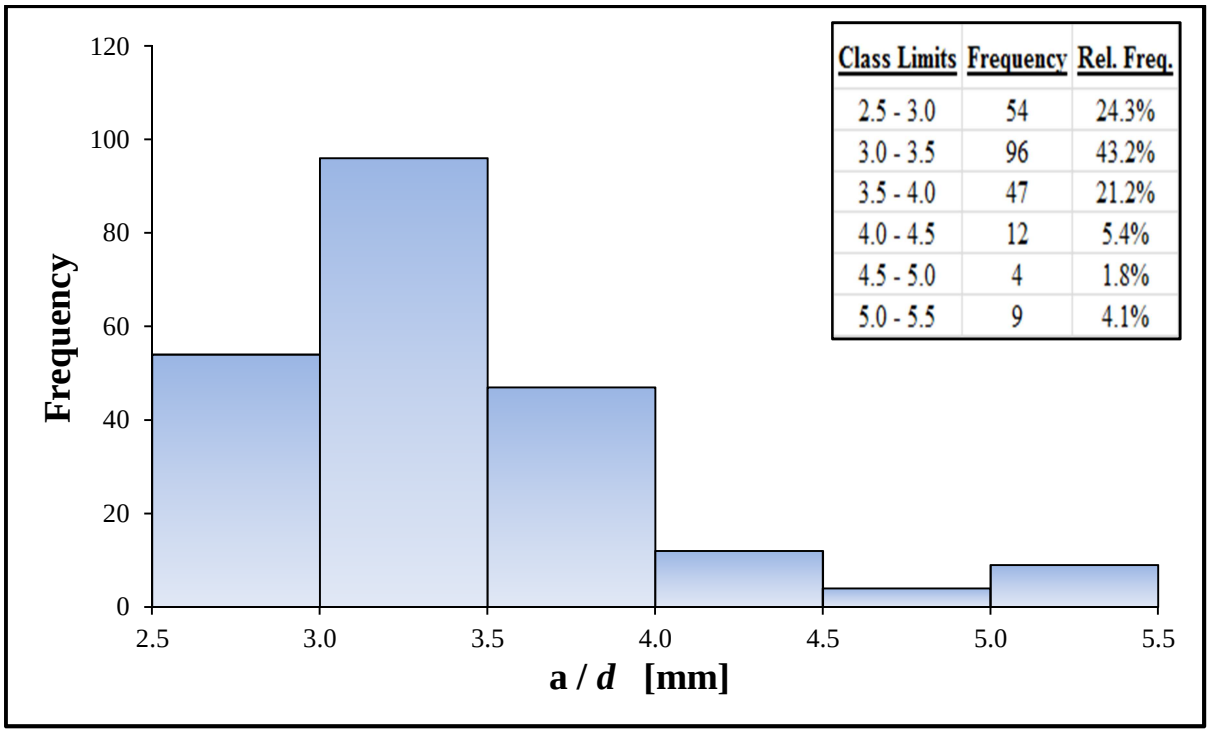

Figure 7.2. Distribution of for the entire database of 222 experiments

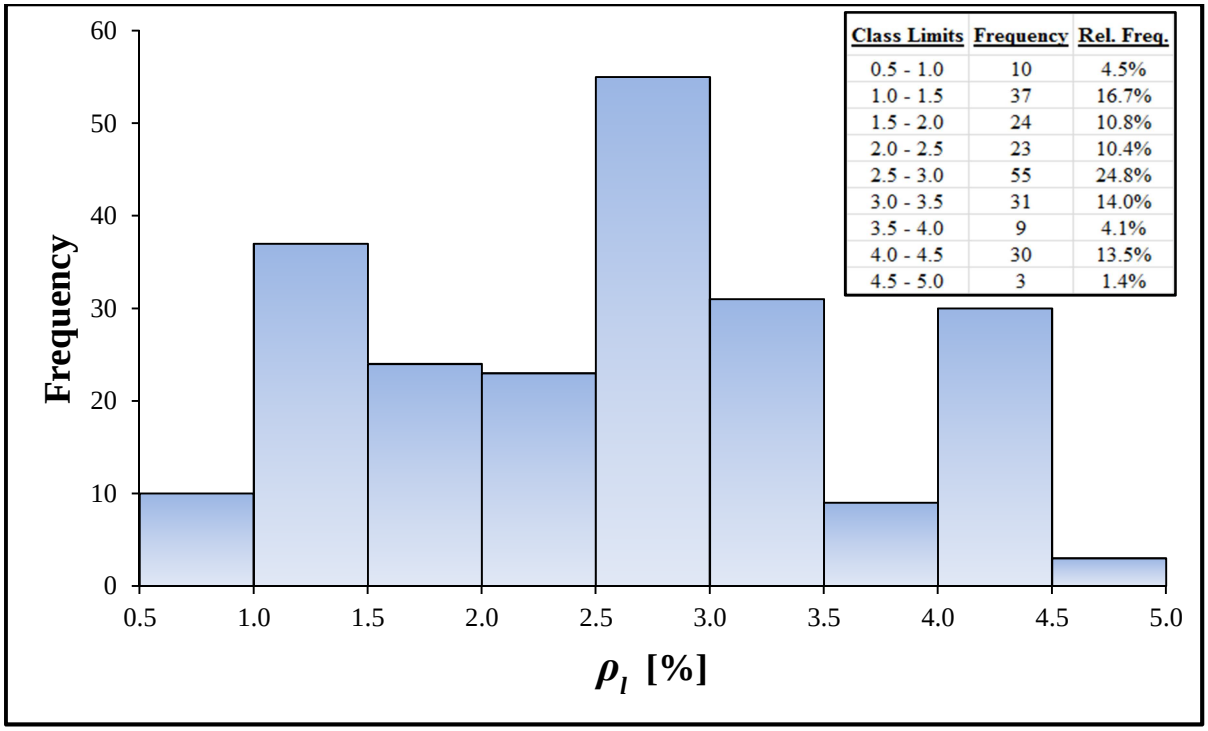

Figure 7.3. Distribution of for the entire database of 222 experiments

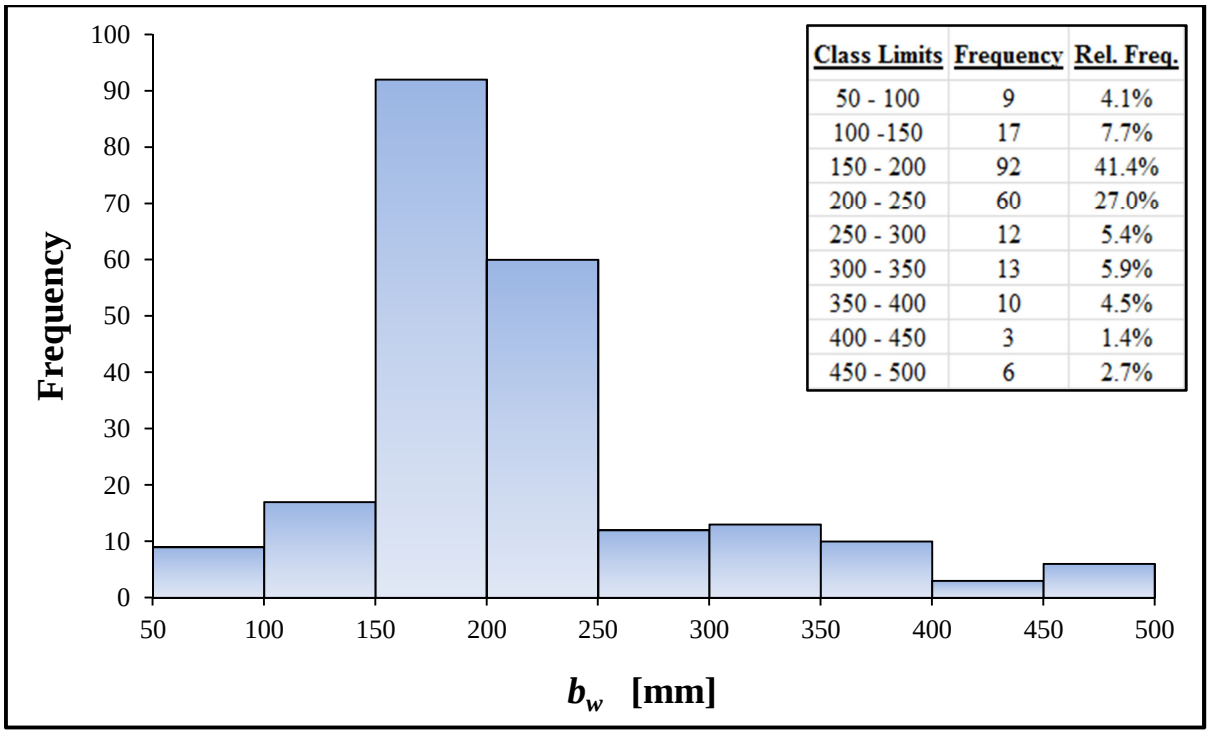

Figure 7.4. Distribution of for the entire database of 222 experiments

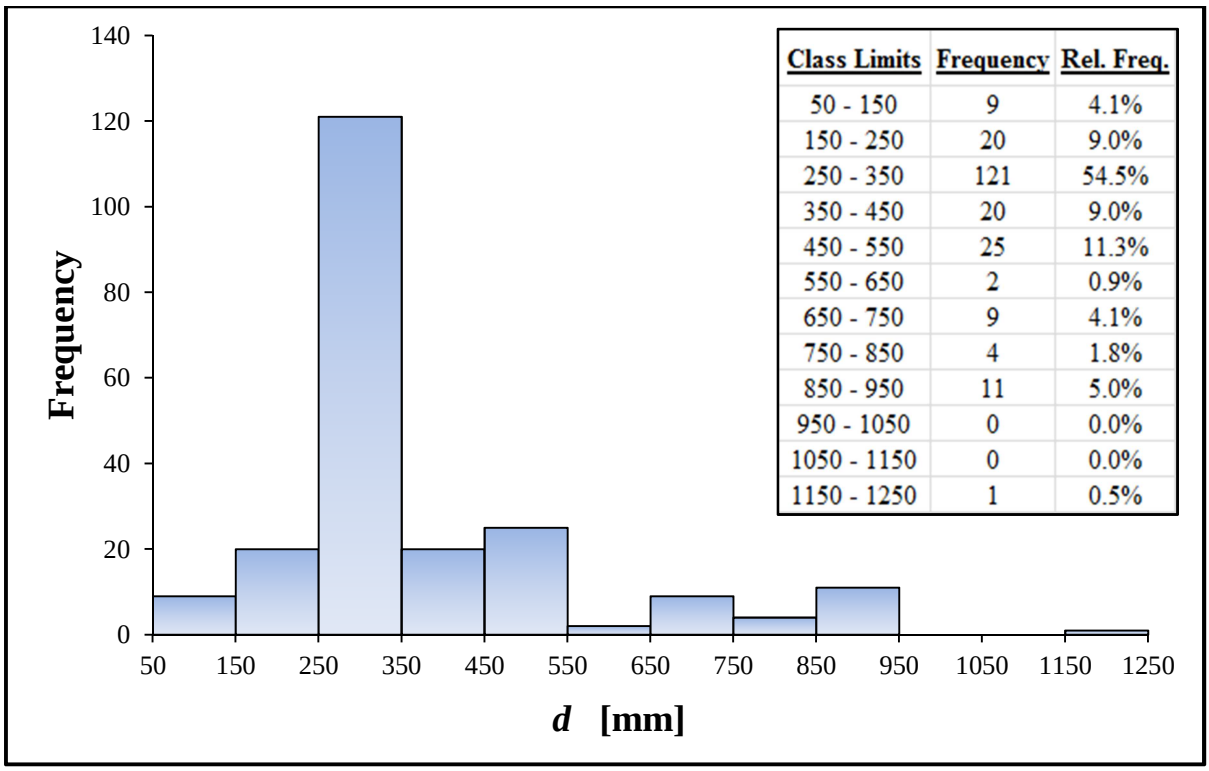

Class Limits	Frequency	Rel. Freq.
50 - 150	9	4.1%
150 - 250	20	9.0%
250 - 350	121	54.5%
350 - 450	20	9.0%
450 - 550	25	11.3%
550 - 650	2	0.9%
650 - 750	9	4.1%
750 - 850	4	1.8%
850 - 950	11	5.0%
950 - 1050	0	0.0%
1050 - 1150	0	0.0%
1150 - 1250	1	0.5%

Figure 7.5. Distribution of for the entire database of 222 experiments

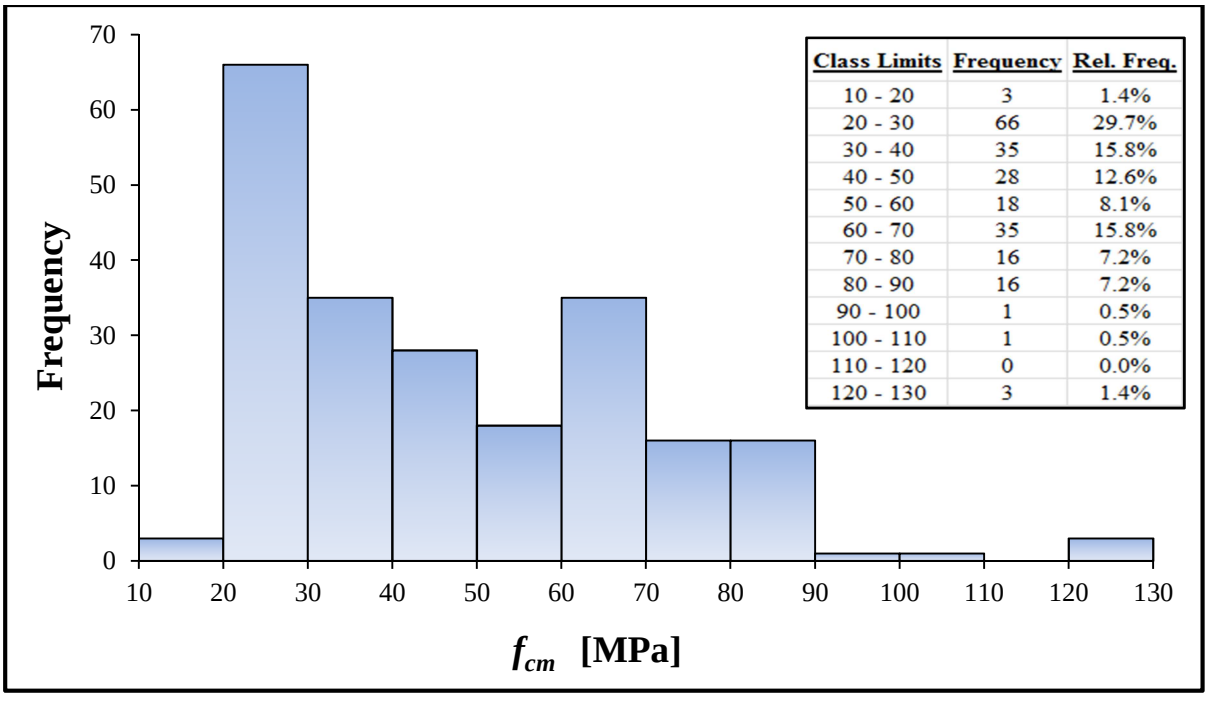

Class Limits	Frequency	Rel. Freq.
10 - 20	3	1.4%
20 - 30	66	29.7%
30 - 40	35	15.8%
40 - 50	28	12.6%
50 - 60	18	8.1%
60 - 70	35	15.8%
70 - 80	16	7.2%
80 - 90	16	7.2%
90 - 100	1	0.5%
100 - 110	1	0.5%
110 - 120	0	0.0%
120 - 130	3	1.4%

Figure 7.6. Distribution of for the entire database of 222 experiments

7.1.3 Statistical comparison of the full database and subset of 116 beam experiments

Table 7.2 presents a summary of minimum and maximum values of the investigated factors affecting shear strength for the full database of 222 tests, whereas Table 7.3 provides similar statistics for the subset of 116 beam experiments. A comparison of the values from the two Tables highlights some of the similarities and differences between the full database and the subset of 116 experiments.

Table 7.2. Descriptive statistics of factors affecting shear strength for 222 experiments

Descriptive statistics	b_w **[mm]**	d **[mm]**	f_{cm} **[MPa]**	ρ_l **[%]**	$\rho_w f_{ywm}$ **[MPa]**	a/d
Minimum	76.2	95	12.0	0.50	0.21	2.49
Maximum	457.2	1200	125.4	4.54	2.62	5.40

Table 7.3. Descriptive statistics of factors affecting shear strength for 116 experiments

Descriptive statistics	b_w **[mm]**	d **[mm]**	f_{cm} **[MPa]**	ρ_l **[%]**	$\rho_w f_{ywm}$ **[MPa]**	a/d
Minimum	76.2	95	20.7	0.50	0.33	2.49
Maximum	457.2	925	125.4	4.54	2.62	5.00

In terms of extreme values of the factors affecting shear strength, the subset of 116 experiments compared well with the full database of 222 experiments, capturing a majority of the maximum and minimum values from the full database.

7.1 CALCULATIONS TO ESTABLISH THE THREE CASES OF THE MODEL FACTOR

The Model Factor, MF, for any prediction method associated with a single experiment, i, was calculated as:

$$MF_i = \frac{V_{experiment,i}}{V_{predicted,i}} \quad [7.2]$$

where $V_{experiment,i}$ is the failure load for a single beam experiment, i. $V_{predicted,i}$ is the equivalent unbiased prediction of ultimate shear resistance for the same experimental beam, i, offered by either of:

(1) The analytical formulation of the VSIM describing stirrup resistance, denoted $V_{VSIM-Analytical,i}$, resulting in the Model Factor realisation $MF_{VSIM-Analytical,i}$

(2) The operational version of the VSIM describing stirrup resistance by enforcing the limit $21.8° \leq \theta_{Limited} \leq 45°$ to concrete strut angle θ, denoted $V_{VSIM-Limit\theta,i}$, resulting in the Model Factor realisation $MF_{VSIM-Limit\theta,i}$

(3) Capacity predictions provided by the MCFT-based sectional analysis program R2k; denoted $V_{R2k,i}$, resulting in the Model Factor realisation $MF_{R2k,i}$.

It follows from Equation 7.2 that a value of $MF > 1$ implies that the prediction model yields a lower value of ultimate shear strength than the failure load of a beam experiment and is thus conservative. Conversely, a value of $MF < 1$ implies that the prediction model yields higher ultimate strength than is actually available and is thus unconservative.

7.2.1 Calculation of the unbiased stirrup resistance terms $V_{VSIM-Analytical}$ and $V_{VSIM-Limit\theta}$

(i) Calculation of $V_{VSIM-Analytical}$

The unbiased contribution of the stirrups as described by the analytical formulation of the VSIM is based on the expression:

$$V_{VSIM-Analytical} = \frac{A_{sw}}{s} z f_{ywm} \cot\theta_{Analytical}$$

where, $\theta_{Analytical} = \sin^{-1}\sqrt{\frac{A_{sw} f_{ywm}}{b_w s \nu_1 \alpha_{cc} f_{cm}}}$ [7.3]

$\theta_{Analytical}$ is the concrete strut angle as determined directly from Equation 7.3 with no constraints applied to the obtained result. f_{ywm} and f_{cm} are the mean measured strengths of the steel yield and concrete compressive cylinder (150×300 mm) strengths, respectively. In cases where *cube strength* tests for concrete compressive strength were reported in literature, the necessary conversions to equivalent compressive *cylinder strengths* were made. Furthermore, the strengths of non-conventional cylinder sizes (say, 100×200 mm) used in determining compressive strength were converted to represent the strength of the conventional 150×300 mm cylinder. These adjustments were carried out with guidance from research by French and Mokhtarzadeh (1993); Aïtcin, Miao, Cook and Mitchell (1994); Carrasquillo and Carrasquillo (1998); and Mphonde and Frantz (1985).

No partial safety factors (γ_C for concrete & γ_S for steel) were applied to either the steel or concrete strengths in the assessment of $V_{VSIM-Analytical}$. The coefficient ν_1 taking account of the reduced strength of concrete cracked in shear was calculated as $0.6(1 - f_{cm}/250)$, and the scale effects coefficient α_{cc} was assigned the conservative value of 0.85 throughout the study.

(ii) Calculation of $V_{VSIM-Limit\theta}$

$V_{VSIM-Limit\theta}$ was determined in essentially the same manner as $V_{VSIM-Analytical}$, save for the difference that $\theta_{Analytical}$ from Equation 7.3 is replaced by a restricted angle $\theta_{Limited}$. $\theta_{Limited}$ is still determined as in Equation 7.3, but the outcome is limited within the confines of $21.8° \leq \theta_{Limited} \leq 45°$. It was observed from the database of beam tests that Equation 7.3 predominantly predicted strut angles below 21.8° (see the values of $\theta_{Analytical}$ in Appendix A) , requiring in most cases that the lower limit of $\theta_{Limited} = 21.8°$ be enforced when calculating $V_{VSIM-Limit\theta}$ (i.e. $\cot\theta = 2.5$). There were no instances in which Equation 7.3 yielded strut angles above 45° when applied to the database of beam tests.

7.2.2 Determination of V_{R2k} from R2k

It should be noted that sectional analysis program R2k does not provide/offer a design procedure for shear; rather, it provides best-estimate predictions of shear capacity that are based on mean quantities of the input variables required to enable an R2k prediction. R2k therefore provides unbiased estimates of shear capacity as an attempt to accurately reflect failures in actual/physical/real reinforced concrete members (i.e. R2k predictions are therefore not associated with the design bias introduced by characteristic values and partial safety factors as would typically be incorporated into a design procedure to achieve adequate safety performance).

The detailed procedure on the use of R2k to obtain V_{R2k} is given in Section 4.3. In order to obtain unbiased estimates of ultimate shear capacity from R2k, mean values of beam experimental parameters as outlined in 4.3 were used in the Program.

7.1 STATISTICAL PROPERTIES OF THE MODEL FACTORS

The Equations in this Section use the symbol MF to represent a generic case of the Model Factor, i.e. applies to either of $MF_{VSIM-Analytical}$, $MF_{VSIM-Limit\theta}$, or MF_{R2k}. Basic statistical properties of each MF that were determined, ultimately, for use in reliability analysis of the EC2 stirrup design procedure, are reported in Table 7.4. Following from Equation 7.2, each MF can be considered a random variable having mean value (μ_{MF}), standard deviation (σ_{MF}) and skewness (Ω_{MF}). μ_{MF}, σ_{MF}, and Ω_{MF} were calculated according to Equations 7.4, 7.5, and 7.6, respectively:

$$\mu_{MF} = \frac{1}{n}\sum MF_i \qquad [7.4]$$

$$\sigma_{MF} = \sqrt{\frac{\sum(MF_i-\mu_{MF})^2}{n-1}} \qquad [7.5]$$

$$\Omega_{MF} = \frac{n}{(n-1)(n-2)}\sum\left(\frac{MF_i-\mu_{MF}}{\sigma_{MF}}\right)^3 \qquad [7.6]$$

where n is the number of beam experiments used in the characterisation of each MF i.e. $n = 222$ for $MF_{VSIM-Analytical}$ & $MF_{VSIM-Limit\theta}$, and $n = 116$ for MF_{R2k}. The Coefficient of Variation ($C.o.V$) for the MF was taken equal to (σ_{MF}/μ_{MF}). Probability distributions are defined in Table 7.4 only for the Model Factors $MF_{VSIM-Analytical}$ and MF_{R2k}. $MF_{VSIM-Analytical}$ and MF_{R2k} were both best represented by the Two-parameter Log-normal distribution with a 0-value lower bound, denoted for convenience as 2P-LN. The choice of probability distribution is, however, a special topic given attention in Section 7.5 and is mentioned here for convenience only. It is important to note that the skewness reported in Table 7.4, as determined according to Equation 7.6, is representative of the scatter of MF realisations and is not that associated with the 2P-LN distribution. The 2P-LN distribution has its own skewness, and a brief discussion on the implications of the mis-match of skewness between data points and assigned distributions is given in Section 7.5.

Table 7.4. Statistical properties of Model Factors $MF_{VSIM-Analytical}$, $MF_{VSIM-Limit\,\theta}$ and MF_{R2k}.

Statistics of the Model Factor	**222 experiments**		**Subset of 116 experiments**		
	$\boldsymbol{MF_{VSIM-Limit\theta}}$	$\boldsymbol{MF_{VSIM-Analytical}}$	$\boldsymbol{*MF_{VSIM-Limit\theta}}$	$\boldsymbol{MF_{VSIM-Analytical}}$	$\boldsymbol{MF_{R2k}}$
Minimum (min. MF_i)	0.65	0.43	0.64	0.43	0.72
Mean (μ_{MF})	1.65	0.84	1.70	0.78	1.14
Maximum (max. MF_i)	3.21	1.53	3.21	1.25	1.76
Std. Dev. (σ_{MF})	0.50	0.18	0.53	0.14	0.20
$C.o.V$	0.30	0.21	0.31	0.18	0.18
Skewness (Ω_{MF})	0.50	0.66	0.37	0.16	0.61
Probability distribution	N/A	2P-LN	NOT APPLICABLE		2P-LN

*Shaded columns are provided for comparative purposes only, as discussed in Section 7.3.1

7.3.1 Comments on the adequacy of the subset of 116 beam experiments used for determining MF_{R2k} statistics

The results of the shaded columns from Table 7.4 ($MF_{VSIM-Limit\theta}$ and $MF_{VSIM-Analytical}$ for 116 beam experiments) are comparable, respectively, with the results of $MF_{VSIM-Limit\theta}$ and $MF_{VSIM-Analytical}$ for 222 beam experiments. Although the subset of 116 beam experiments contained far less than 222 experiments, it captured experiments with sufficient quality and

diversity such that key statistical parameters μ_{MF} and σ_{MF} associated with either of the Model Factors ($MF_{VSIM-Limit\theta}$ and $MF_{VSIM-Analytical}$) did not vary by any significant amount i.e. the subset of 116 tests was sufficiently representative of the full data database of 222 experiments.

$MF_{VSIM-Analytical}$ portrayed the largest variation in its μ_{MF}-value between the two sets of data, with a decrease of 7 % when μ_{MF} for the subset of 116 experiments ($\mu_{MF} = 0.78$) is compared to that derived from 222 experiments ($\mu_{MF} = 0.84$). Variations in σ_{MF} were non-uniform and somewhat more severe, but not alarmingly so. σ_{MF} associated with $MF_{VSIM-Analytical}$ portrayed the largest variation of 22 %, with $\sigma_{MF} = 0.14$ for 116 experiments compared to $\sigma_{MF} = 0.18$ for the full database of 222 experiments. A similar comparison for $MF_{VSIM-Limit\theta}$ indicated only a 6 % difference in σ_{MF}. These results provided confirmation that statistics of MF_{R2k}, which were only possible for the subset of 116 tests, could be relied upon for performance assessments of R2k and used in establishing the R2k-based GPM for stirrup resistance as detailed in Chapter 9.

The skewness (Ω_{MF}) of both $MF_{VSIM-Limit\theta}$ and $MF_{VSIM-Analytical}$ was more sensitive to the number of experiments used in its determination (i.e. 116 tests versus 222 tests) as can be witnessed from Table 7.4. Such behaviour is typical of skewness as reported in Holický (2009), emphasising that skewness is very sensitive to extreme values of a sample as can be observed by inspecting Equation 7.6 (sensitive to extreme deviations $MF_i - \mu_{MF}$ to the 3rd power). It is for this reason that the difference in skewness due the reduced subset of 116 tests does not cause much concern about its representation of the full database of 222 tests.

7.3.2 Discussion of $MF_{VSIM-Limit\theta}$ statistics

$MF_{VSIM-Limit\theta}$ was found to have mean value $\mu_{MF} = 1.65$, implying that the unbiased stirrup resistance function $V_{VSIM-Limit\theta}$ is generally very conservative in its predictions. However, the large spread of $\sigma_{MF} = 0.51$ suggested also a large dispersion of $MF_{VSIM-Limit\theta,i}$ realisations (point estimates) about μ_{MF}. Various parametric scatter plots for $MF_{VSIM-Limit\theta}$, $MF_{VSIM-Analytical}$, and MF_{R2k} against the important factors affecting shear strength are shown in Figures 7.7, 7.8, and 7.9, respectively. The scatter plots for $MF_{VSIM-Limit\theta}$ depict the dispersion of its realisations about the mean $\mu_{MF} = 1.65$, even indicating instances where

$V_{VSIM-Limit\theta}$ predictions are unconservative. Detailed discussions of the parameter scatter plots, supported by correlation and regression analyses, are presented in Section 7.4.

7.3.3 Discussion of $MF_{VSIM-Analytical}$ statistics

$MF_{VSIM-Analytical}$ was found to have mean value $\mu_{MF} = 0.84$, implying that $V_{VSIM-Analytical}$ stirrup resistance predictions are generally unconservative (with a 16 % inherent unconservative bias). In terms of scatter, the $MF_{VSIM-Analytical,i}$ realisations are however more precise than those of $MF_{VSIM-Limit\theta,i}$, boasting a lower standard deviation of $\sigma_{MF} = 0.18$ ($C.o.V = 0.21$). A comparison of Figure 7.7 ($MF_{VSIM-Limit\theta}$ scatter plots) and Figure 7.8 ($MF_{VSIM-Analytical}$ scatter plots) provide a vivid depiction of the lower dispersion associated with $MF_{VSIM-Analytical}$ realisations about its mean $\mu_{MF} = 0.84$. No sensitive trend was observed from the graph of $MF_{VSIM-Analytical}$ versus $\rho_w f_{ywm}$ (Figure 7.8a), enabling the application of the single mean value $\mu_{MF} = 0.84$ when implementing the GPM for stirrup resistance based on this version of VSIM as shown in Chapter 8.

7.3.4 A comparison of the mean predictions of $MF_{VSIM-Limit\theta}$ and $MF_{VSIM-Analytical}$

A comparison of the mean values of $MF_{VSIM-Limit\theta}$ and $MF_{VSIM-Analytical}$ ($\mu_{MF} = 1.65$ & $\mu_{MF} = 0.84$, respectively) makes it clear that the restriction of $21.8° \leq \theta_{Limited} \leq 45°$ on the concrete strut angle is implemented as part of the operational 'VSIM-Limitθ' procedure to achieve a 'safe side' model. The scatter plots of $MF_{VSIM-Limit\theta}$ versus each of the factors (1) a/d, (2) ρ_l, (3) b_w, (4) d, and (5) f_{cm}, shown in Figure 7.7(b) to 7.7(d), respectively, provided indication that the restriction on $\theta_{Limited}$ leads to generally conservative $MF_{VSIM-Limit\theta}$ realisations (realisations lie predominantly above the $MF = 1.0$ line). Furthermore, no sensitive trends of $MF_{VSIM-Limit\theta}$ realisations were observed for the aforementioned parameter plots, somewhat justifying the enforcement or implementation of $\theta_{Limited}$ as part of the operational VSIM procedure.

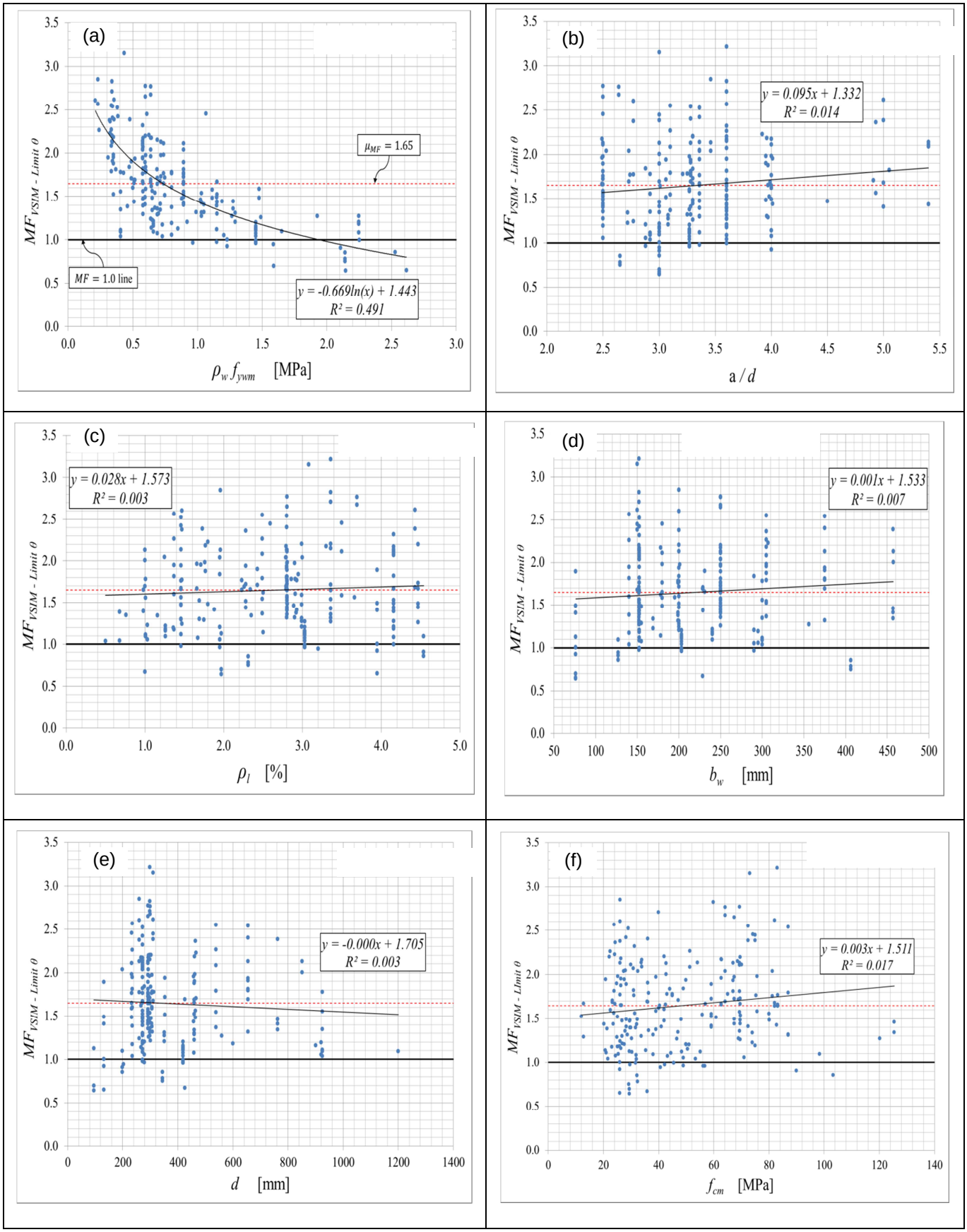

Figure 7.7. Scatter plots, with regression trendlines and correlations statistics, of versus (a) , (b) , (c) , (d) , (e) , and (f) .

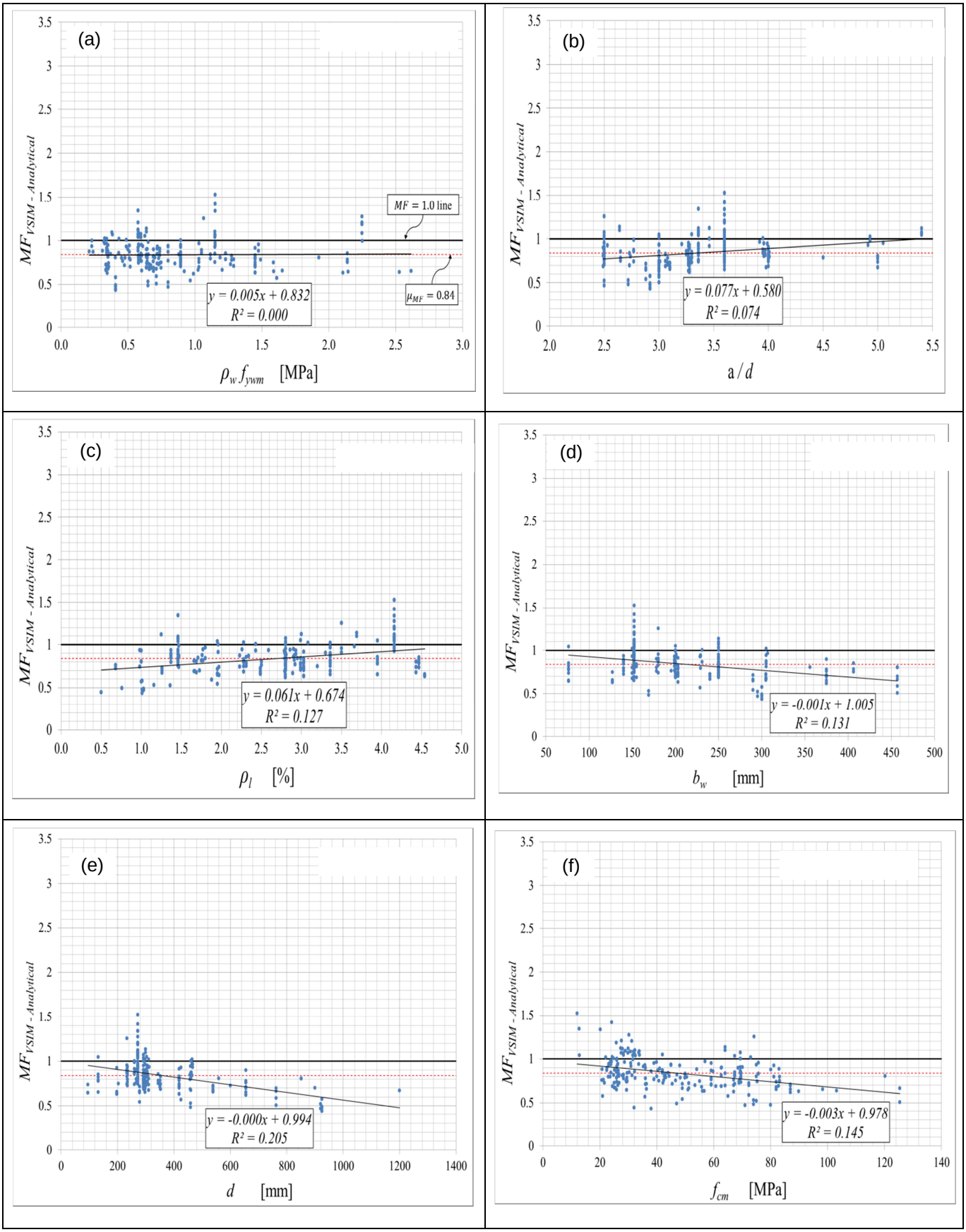

Figure 7.8. Scatter plots, with regression trendlines and correlations statistics, of versus (a) , (b) , (c) , (d) , (e) , and (f) .

However, a sensitive trend was portrayed in the plot of $MF_{VSIM-Limit\theta}$ versus $\rho_w f_{ywm}$ shown in Figure 7.7(a). $MF_{VSIM-Limit\theta}$ realisations were excessively conservative at low $\rho_w f_{ywm}$, but progressed to become unconservative as $\rho_w f_{ywm}$ increased. This trend led to concerns about the performance of the operational VSIM procedure, particularly at higher $\rho_w f_{ywm}$ situations where $MF_{VSIM-Limit\theta}$ realisations start to become marginally conservative, then eventually become unconservative. Further investigations were therefore commissioned to assess the consistency of the reliability index β at parametric variations of $\rho_w f_{ywm}$, as presented in Chapters 8 and 9. A more detailed discussion of the parameter plots is given in Section 7.4.

7.3.5 Discussion of MF_{R2k} statistics

MF_{R2k} was found to have mean value $\mu_{MF} = 1.14$, making it the most accurate of the ultimate strength prediction models applied to the experimental database (14% inherent conservative bias). MF_{R2k} realisations had a relatively low standard deviation of $\sigma_{MF} = 0.20$ ($\sigma_{MF} = 0.51$ for $MF_{VSIM-Limit\theta}$; $\sigma_{MF} = 0.18$ for $MF_{VSIM-Analytical}$) ; a value of dispersion slightly larger than that associated with $MF_{VSIM-Analytical}$. The relative dispersions of MF_{R2k} realisations about its mean $\mu_{MF} = 1.14$ for the various parametric scatter plots are shown in Figure 7.9, which can be compared to the scatter given in Figures 7.7 and 7.8 for other cases of MF.

The high accuracy displayed by MF_{R2k} realisations, coupled with its relatively low dispersions, are features that warranted the use of the R2k-based GPM in a separate reliability performance assessment of the EC2 VSIM-based stirrup design procedure. Although MF_{R2k} realisations represented an improvement of shear capacity predictions (compared to $MF_{VSIM-Limit\theta}$), the graph shown in Figure 7.9(a) shows a sensitive trend of MF_{R2k} realisations in the captured parametric range of $\rho_w f_{ywm}$. The trend of decreasing conservative bias in MF_{R2k} realisations versus increasing $\rho_w f_{ywm}$ is visibly milder than that of $MF_{VSIM-Limit\theta}$ versus $\rho_w f_{ywm}$ (Figure 7.7(a)), but still tends to similarly become unconservative at values of $\rho_w f_{ywm}$ above approximately 2 MPa. This sensitivity of MF_{R2k} realisations was taken into account when implementing the R2k-based GPM for stirrup resistance during reliability modelling/investigations, as discussed in Chapter 9.

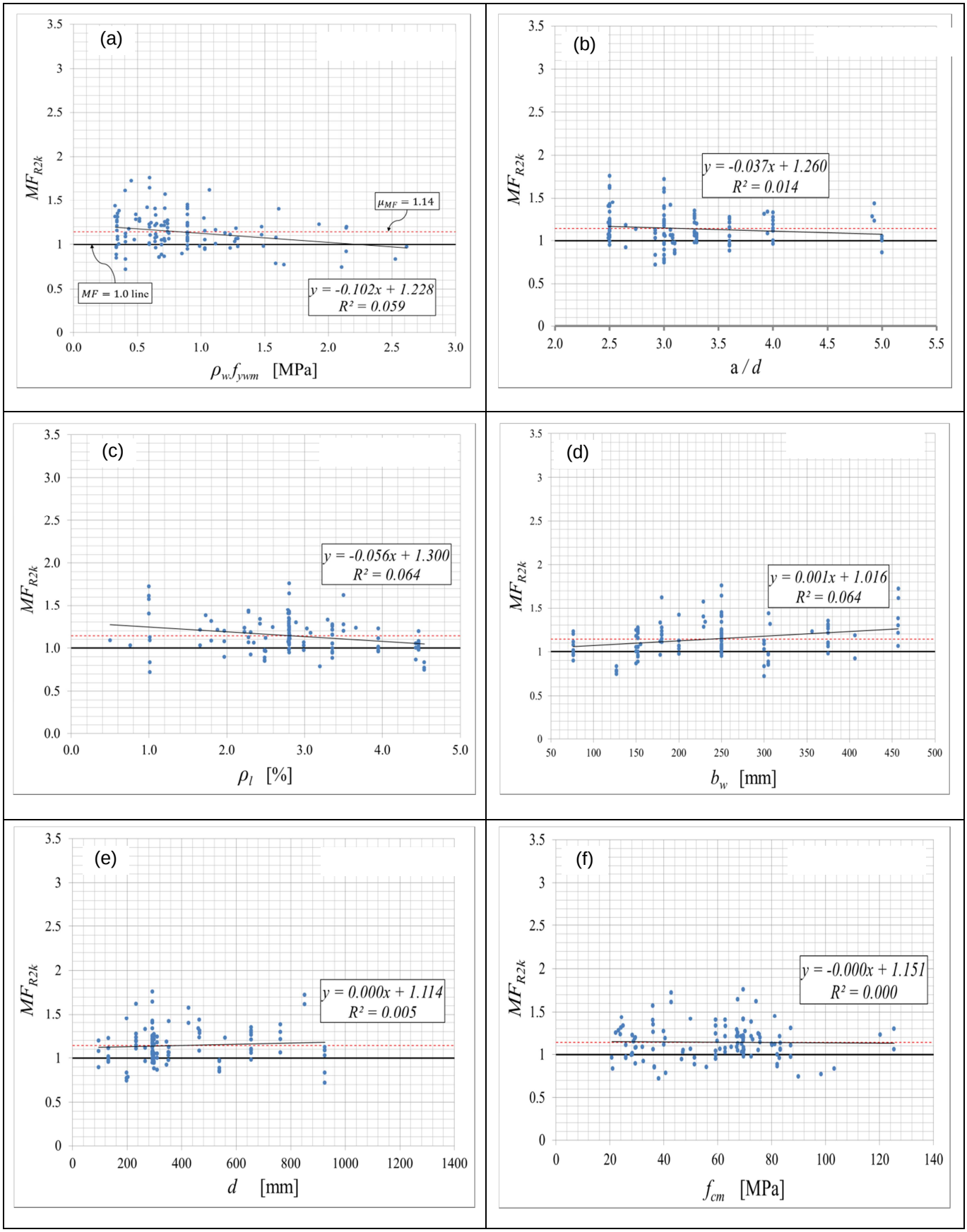

Figure 7.9. Scatter plots, with regression trendlines and correlations statistics, of versus (a) , (b) , (c) , (d) , (e) , and (f) .

7.4. PERFORMANCE ASSESSMENTS OF $V_{VSIM-Limit\theta}$, $V_{VSIM-Analytical}$, and V_{R2k} UNBIASED CAPACITY PREDICTIONS

Performance assessments of the different prediction models (VSIM-Limitθ, VSIM-Analytical & R2k) applied to the database of stirrup-reinforced beam experiments, based on Figures 7.7 to 7.9, are given in this Section. Trends of any MF ($MF_{VSIM-Limit\theta}$, $MF_{VSIM-Analytical}$, or MF_{R2k}) against the important factors affecting shear strength outlined in Section 7.1.2 were investigated by a combination of (1) visual inspection of Figures 7.7 to 7.9, (2) statistical correlation analysis, and (3) Regression trendline fitting to scattered data. Brief descriptions of (2) and (3) are given in Sections 7.4.1 and 7.4.2 below.

Since EC2's operational VSIM stirrup design procedure is an adaptation of the $V_{VSIM-Limit\theta}$ calculation procedure, performance assessments of $V_{VSIM-Limit\theta}$ directly relate to the performance of the EC2 operational design procedure. The performance assessments of $V_{VSIM-Analytical}$ and V_{R2k} capacity predictions were conducted to investigate the suitability of the VSIM-Analytical formulation and R2k, respectively, to generate General Probabilistic Models (GPMs) for stirrup resistance.

7.4.1 Correlation analysis

Correlation analyses were carried out by determining Pearson's correlation coefficient, denoted generally as r. The correlation between each MF and each important factor x affecting shear strength was calculated from:

$$r = \frac{\sum(x_i-\mu_x)(MF_i-\mu_{MF})}{\sqrt{\sum(x_i-\mu_x)^2}\sqrt{\sum(MF_i-\mu_{MF})^2}} \qquad -1 \le r \le 1 \qquad [7.7]$$

where x_i and μ_x are the i^{th} observation and mean value, respectively, for a specific factor affecting shear strength e.g. $\rho_w f_{ywm}$, a/d, ρ_l etc. The determined r-value gave an indication of the strength of the linear relationship (if any) between the MF and any shear factor x. In general, an r-value of -1 indicates a perfect negative linear relationship between variables, an r-value of 0 indicates no linear relationship between variables, and an r-value of 1 indicates a positive perfect linear relationship between variables. Correlation r-values are presented as appropriate for all the graphs shown in Figures 7.7, 7.8 and 7.9.

7.4.2 Regression analysis (trendline analysis)

The coefficient of determination, R^2, was used to test the adequacy of the various regression trendline options to the scatter plots shown in Figures 7.7, 7.8, and 7.9. R^2 can be closely approximated as the square of the r-value for a given correlation. It can be witnessed from the Figures that the trendlines were essential in making two performance assessments, namely (1) the inherent bias of systematic predictions for given situations (conservative or unconservative), and (2) the consistency of the bias of systematic predictions at parametric variations of factors affecting shear strength as shown in the Figures. The manner in which suitable trendlines were chosen to represent the systematic trends of MF realisations was therefore an important issue, discussed below.

The choice of suitable trendline options chosen to represent systematic trends in Figures 7.7, 7.8, and 7.9 were basically contested (by comparing R^2-values), between the Linear and Logarithmic regression trendline options. The suitability of alternative and higher-order regression fits (Exponential, Power-fit, Polynomial-fit) was explored, but were disqualified from the investigation for the following reasons:

1. Improvements in the R^2-value, if any, were not of a substantial nature to cause the neglect of the simpler Linear or Logarithmic trendline fits
2. In any case, for higher order Polynomial-fits, the increase in R^2-value was accompanied by more complex trendline functions. Furthermore, higher-order trendlines did not necessarily always provide any logical representation of systematic behaviour of MF realisations i.e. the fit becomes purely mathematical, trendlines cannot be used to draw inferences. Montgomery and Runger (2007) advise that the R^2 statistic be used with caution, because it is always possible to make R^2 close to unity by simply adding enough terms to the model.

It should be noted that a combination of a strong r-value (say > 0.5) and strong R^2 (say also > 0.5) was taken to indicate a significant relationship between any MF and given shear factor X. A strong r-value with relatively weak R^2 suggests a non-linear relationship (Huber, 2005).

7.4.3 Parametric performance assessments of $V_{VSIM-Limit\theta}$ predictions

The graphs presented in Figure 7.7 (particularly graphs 7.7(b) to 7.7(f)) demonstrate that $V_{VSIM-Limit\theta}$ predictions are generally systematically over-conservative for the ranges of the parameters considered. In contrast, Figure 7.7(a) showed an alarming systematic decay of conservative bias of $V_{VSIM-Limit\theta}$. Serious concerns arose at $\rho_w f_{ywm}$ of approximately 1.9 MPa as $V_{VSIM-Limit\theta}$ predictions tended to become potentially unsafe.

A discussion of the important $MF_{VSIM-Limit\theta}$ versus $\rho_w f_{ywm}$ trend, which is portrayed in Figure 7.7(a), is first discussed in detail below. Graphs 7.7(b) to 7.7(f) are thereafter collectively discussed as classes of systematically over-conservative predictions falling into categories of either (1) increasing, or (2) decreasing bias with an increase in the ranges of the parameters considered.

(i) $MF_{VSIM-Limit\theta}$ versus $\rho_w f_{ywm}$ (Figure 7.7(a))

This was the most significant trend identified from capacity predictions during the investigation. $V_{VSIM-Limit\theta}$ capacity predictions were initially excessively conservative at low $\rho_w f_{ywm}$, with generally decreasing conservatism at increased $\rho_w f_{ywm}$ quantities. The Logarithmic trendline fit was chosen to reflect this inconsistent behaviour of $V_{VSIM-Limit\theta}$ predictions. An r-value of -0.66 further suggested significant correlation between $V_{VSIM-Limit\theta}$ predictions and $\rho_w f_{ywm}$, implying statistical dependence of $V_{VSIM-Limit\theta}$ on $\rho_w f_{ywm}$ (not desirable!).

Cognizance should be taken of the fact that there were significantly more beam experiments in the database with $\rho_w f_{ywm} < 1.5$ MPa, thereby giving more confidence in trends observed in this range. The fewer experiments in the range $\rho_w f_{ywm} > 1.5$, nonetheless, yielded $MF_{VSIM-Limit\theta}$ realisations that were dispersed almost equally above and below the trendline in this region. This gave confidence in drawing the inference that $V_{VSIM-Limit\theta}$ predictions were becoming unconservative in this region.

Since the EC2 operational stirrup design method is based on the VSIM-Limitθ calculation procedure, the potentially unsafe performance of $V_{VSIM-Limit\theta}$ directly relates to that of the EC2 design method. Background documents to EC2 did not provide any evidence indicating

that the operational VSIM design method was calibrated to cater for the potentially unsafe trend. Reliability investigations were therefore commissioned to assess the consistency of performance in terms of the reliability index β across a practical range of $\rho_w f_{ywm}$.

(ii) Systematically over-conservative $V_{VSIM-Limit\theta}$ predictions with increasing bias (Graphs 7.7(b), (c), (d) & (f))

$V_{VSIM-Limit\theta}$ predictions versus a/d, ρ_l, b_w and f_{cm} were all systematically over-conservative, displaying very slight increases in conservative bias about the mean $\mu_{MF} = 1.65$ line for the parametric ranges investigated. All correlation r-values against $V_{VSIM-Limit\theta}$ predictions were very low (close to 0) which suggested the absence of any significant trends with a/d, ρ_l, b_w and f_{cm}. The strongest r-value was that of 0.13 for the relationship $MF_{VSIM-Limit\theta}$ versus f_{cm}.

Graphs 7.7(b), (c) and (d) all showed that $MF_{VSIM-Limit\theta}$ realisations were dispersed quite evenly above and below the linear trendline fits, thereby giving confidence in the systematic effects displayed by the trendlines. It can be witnessed from Graphs 7.7(b), (c), (d) and (f) that the systematic effect of $V_{VSIM-Limit\theta}$ predictions tended to range from slightly below the $\mu_{MF} = 1.65$ line in lower regions of the parameter plots to slightly above the $\mu_{MF} = 1.65$ line at higher regions of the parameter plots.

(iii) Systematically over-conservative $V_{VSIM-Limit\theta}$ predictions with decreasing bias (Graph 7.7(e))

$V_{VSIM-Limit\theta}$ predictions versus the effective depth d were all systematically over-conservative, displaying a slight decrease in conservative bias about the mean $\mu_{MF} = 1.65$ line for the parametric ranges investigated. The correlation r-value between $V_{VSIM-Limit\theta}$ predictions and d was -0.06, which suggested the absence of any significant trends between the variables.

$V_{VSIM-Limit\theta}$ predictions tended to range from slightly above the $\mu_{MF} = 1.65$ line in lower regions of the parameter plots to slightly below the $\mu_{MF} = 1.65$ line at higher values of d. Inferences about systematic effects of $V_{VSIM-Limit\theta}$ predictions versus d were only reliable in

the range of approximately $d < 880$ mm, due to the availability of a number of observations. The compiled database lacked experiments with d in the range of 900 mm and beyond.

7.4.4 Comparison of $V_{VSIM-Analytical}$ and V_{R2k} capacity predictions

A comparison of Figure 7.8 and Figure 7.9 revealed two facts, (1) that $V_{VSIM-Analytical}$ predictions are on average unconservative ($\mu_{MF} = 0.84$), and (2) conversely, that V_{R2k} predictions are on average conservative ($\mu_{MF} = 1.14$) for the parametric ranges considered. The MF_{R2k} realisations were on average slightly more accurate (14 % above 1.0 line on average) compared to $MF_{VSIM-Analytical}$ (16 % below 1.0 line on average). However, in terms of scatter, $MF_{VSIM-Analytical}$ realisations were more accurate, with $\sigma_{MF} = 0.18$ as compared to the scatter of $\sigma_{MF} = 0.20$ associated with MF_{R2k} realisations.

$MF_{VSIM-Analytical}$ ($\sigma_{MF} = 0.18$) was therefore judged to be the better predictor of shear resistance for stirrup-reinforced concrete beams based on its lower standard deviation. As a consequence, the $V_{VSIM-Analytical}$ calculation procedure was implemented as the primary General Probabilistic Model (GPM) for the reliability assessment of the EC2 stirrup design procedure, described in Chapter 8. An R2k based GPM was subsequently developed and applied as a check (Chapter 9) to the basic reliability investigations presented in Chapter 8.

7.4.5 Trends of normalised shear resistance predictions compared to experimental results

Figure 7.10 shows the trendline of normalised failure loads $V_{exp}/b_w d$ of the 222 beam experiments versus the quantity of stirrup reinforcement $\rho_w f_{ywm}$. The trendline representing experimental failures is compared primarily to the trendlines of equivalent predictions offered by (1) VSIM-Analytical ($V_{VSIM-Analytical}/b_w d$), and (2) R2k ($V_{R2k}/b_w d$) procedures. Additionally, the Figure shows the trendline of VSIM-Limitθ predictions ($V_{VSIM-Limit\theta}/b_w d$), which are given to show the influence the lower limit of 21.8° for concrete struts has on the the performance of operational VSIM procedures.

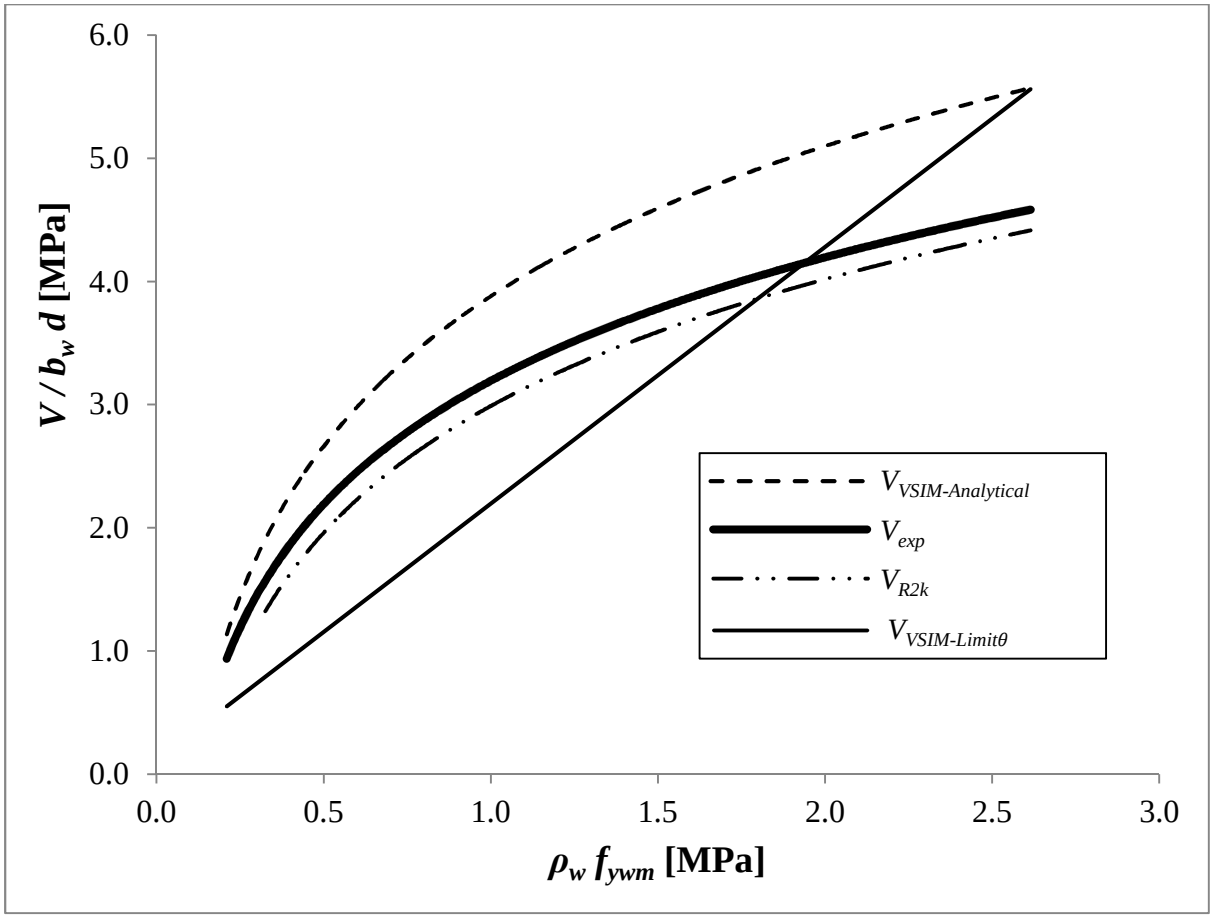

Figure 7.10. Trend of $V/b_w d$ *vs.* $\rho_w f_{ywm}$ for experimental results compared to trends of VSIM-Analytical, R2k and VSIM-Limitθ predictions

The trend of R2k capacity predictions ($V_{R2k}/b_w d$) are shown clearly in the Figure to bear the closest comparison to the trend of experimental results ($V_{exp}/b_w d$) for the range of $\rho_w f_{ywm}$ considered. This similarity in trends proves that R2k capacity predictions provide the most accurate representation of both the behaviour and ultimate strength of stirrup reinforced concrete members. To a lesser extent than R2k, the trend of VSIM-Analytical predictions portrays some agreement with the trend of experimental results; however, notice that the bias/difference between the trends tends to increase as $\rho_w f_{ywm}$ increases. The trend of VSIM-Limitθ predictions, on the other hand, predicts a linear increase of resistance predictions as $\rho_w f_{ywm}$ increases, thereby failing to capture the natural non-linear increase in resistance exhibited by experimental results.

The trendlines of V_{exp} and V_{R2k}, and to a comparable extent $V_{VSIM-Analytical}$ as well, indicate a flattening-off of normalised resistance predictions $V/b_w d$ as $\rho_w f_{ywm}$ increases. The occurrence of the plateau in the results implies that maximum shear resistance can be attained at a specific quantity of stirrup reinforcement $\rho_w f_{ywm}$. Beyond this point additional stirrup reinforcement would not result in increased member capacity, but would merely serve as ductility or crack control reinforcement. This behaviour is portrayed distinctively for the Test Section of known geometry analysed by R2k in Figure 5.2 (see Tables 5.2 and 5.3 for the parameters of the Test Case).

Figure 7.10 shows clearly that the concrete strut angle limit of 21.8° results in conservative performance of VSIM procedures, as discussed in Section 7.3.4. However, the strut angle limit does not provide good representation of the mechanism of shear failure, particularly at the different $\rho_w f_{ywm}$ situations. VSIM-Limitθ predictions are shown in Figure 7.10 to continually give credit to increasing stirrup reinforcement, thereby not capturing the plateau effect shown by experimental results.

7.5. PROBABILITY DISTRIBUTIONS FOR $MF_{VSIM-Analytical}$ and MF_{R2k}

Both $MF_{VSIM-Analytical}$ and MF_{R2k} were assigned the 2P-LN distribution, as shown in Table 7.4, to enable their representation as part of the GPM models for stirrup resistance described in Chapters 8 and 9. The choices of suitable probability distributions for MF were based on the Kolmogorov-Smirnov goodness of fit test, which was implemented using EasyFit distribution fitting software. The trial version of EasyFit is available for free download at: http://www.mathwave.com/. It is worth noting that more accurate fits to MF realisations were possible, but the 2P-LN distribution was implemented for practical reasons. Motivations for implementing the 2P-LN distribution for both $MF_{VSIM-Analytical}$ and MF_{R2k} were two-fold, described as follows:

1. It had a higher ranking in terms of the Kolmogorov-Smirnov statistic than the other practical choices of the Normal (N) or 3P-LN distributions

2. It could readily be manipulated for reliability modelling, compounded by the fact that it is a commonly recommended model for resistance properties recommended by renowned literature sources (JCSS, 2001; EN 1992-1-1, 2004).

7.5.1 Comments on the skewness representation of the 2P-LN distribution

The skewness of any MF (s_{k-MF}) represented by the 2P-LN distribution is described by Equation 6.26, repeated here for convenience as:

$$s_{k-MF} = 3 \cdot (C.o.V) + (C.o.V)^3 \qquad [7.7]$$

Using relevant data from Table 7.4, and according to Equation 7.7, Ω_{MF} for $MF_{VSIM-Analytical}$ was determined as 0.64 (compared to 0.66 of the realisations shown in Table 7.4), whereas that for MF_{R2k} was determined as 0.55 (compared to 0.61 from Table 7.4). The preceding results give indication that the 2P-LN distribution provided reasonably accurate representation of the skewness inherent to the MF realisations, although the general trend was that it under-estimated the skewness of the actual data. Under-estimating the skewness has the effect of increasing the tail end of the resistance distribution, hence increasing probability of failure P_f (resulting in lower or conservative estimates of β).

7.6. SUMMARY OF THE IMPORTANCE OF $MF_{VSIM-Limit\theta}$, $MF_{VSIM-Analytical}$, and MF_{R2k}

Table 7.5 below summarises the significance of each of the Model factors ($MF_{VSIM-Analytical}$, $MF_{VSIM-Limit\,\theta}$ and MF_{R2k}) presented and discussed throughout the Chapter. This summary is useful to highlight important conclusions obtained from this Chapter that guided the reliability investigations of the EC2 stirrup design procedure presented in Chapters 8 and 9.

Table 7.5. Significance of the three Model Factors.

Model Factor	Significance of statistical properties
$MF_{VSIM-Limit\theta}$	Its systematic sensitivity to $\rho_w f_{ywm}$ shown in Figure 7.7(a) led to the commissioning of reliability investigations to assess the consistency of the reliability index β at parametric variations of $\rho_w f_{ywm}$. Concerns about potentially unsafe performance at high $\rho_w f_{ywm}$!
$MF_{VSIM-Analytical}$ (Chapter 8)	As discussed in Section 7.4.4, the VSIM-Analytical calculation procedure was selected to represent the primary GPM model for stirrup resistance, owing to the relatively low standard deviation $\sigma_{MF} = 0.18$ associated with $MF_{VSIM-Analytical}$ realisations. Cognizance should be taken of the fact that the statistics of the MF – which were determined primarily to incorporate their characteristics as part of a rational reliability performance assessment of VSIM procedures – were derived according to a database of representative beam tests.
MF_{R2k} (Chapter 9)	R2k predictions of ultimate shear capacity were comparably accurate, warranting that a separate GPM for shear resistance based on R2k capacity predictions be used to assess the reliability performance of EC2 stirrup design procedure (see Section 7.4.4)

CHAPTER 8

RELIABILITY ANALYSIS USING VSIM-ANALYTICAL TO GENERATE THE GPM FOR STIRRUP RESISTANCE

The unbiased VSIM-Limitθ calculation procedure, on which the operational EC2 stirrup design procedure is based, was shown in Chapter 7 to be systematically sensitive to $\rho_w f_{ywm}$ when compared to the database of beam experiments. Figure 7.7(a) shows that VSIM-Limitθ predictions are initially excessively conservative at low $\rho_w f_{ywm}$ then, conversely, progress to become mildly unconservative at higher amounts of $\rho_w f_{ywm}$ (heavily stirrup-reinforced concrete beams). This was true for the range 0.3 MPa to approximately 2.5 MPa of $\rho_w f_{ywm}$ captured by the experimental database of stirrup-reinforced beam tests.

Given the trend of unbiased VSIM-Limitθ predictions with $\rho_w f_{ywm}$, no evidence was traceable from background documents and related relevant literature that the currently operational EC2 VSIM procedure was calibrated to account for this systematic sensitivity. Serious concerns at high $\rho_w f_{ywm}$ where the model is potentially unsafe (Immediately causes concerns about sufficient safety performance at ULS for relatively heavily stirrup reinforced concrete beams in practice, since shear is essentially a brittle failure mode). The investigations presented in this Chapter were therefore developed to primarily assess the consistency of β-values at parametric variations of $\rho_w f_{ywm}$.

β-values were also assessed across a range of concrete strengths f_{cm}. However, this sensitivity of estimated β-values to concrete strength was not exposed by characteristics of the Model Factor. Recall that the Model Factor (MF) consists of the comparison of the resistance from an experimental beam to the equivalent prediction offered by a resistance model i.e. the inherent uncertainty of the prediction model is sought, and not the sensitivity of the prediction model to its component parameters. Cognizance must be taken of the fact that, in general, shear resistance predictions V are proportionally sensitive to changes in concrete strength. That is, the higher the concrete strength, the greater the resistance predictions, and vice versa holds true.

The conventional reliability model which was developed and used as the primary tool during the performance assessment of EC2's VSIM stirrup design procedure is presented in this Chapter. The General Probabilistic Model (GPM) for stirrup resistance in the conventional performance function $g(\boldsymbol{X})$ was based on the probabilistic representation of the VSIM-Analytical calculation procedure, denoted $V_{VSIM-Analytical}(\boldsymbol{X})$ i.e. by allowing its input random variables to assume suitable probability models. $g(\boldsymbol{X})$ was set up to conduct a safety assessment of the EC2 VSIM stirrup design procedure, in which the First Order Reliability Method (FORM) was used to determine the reliability index β for specific situations.

The achieved β-values for the parametric range considered were compared primarily to the performance requirements for buildings and similar structures stipulated by the South African Basis of Design Standard SANS 10160-1. SANS 10160-1 offers four Reliability Classes (RC1 – RC4), of which RC2 ($\beta_{RC2} = 3.0$) and RC3 ($\beta_{RC3} = 3.5$) mostly apply to the design of conventional buildings and routine structures. Implications of the results according to Euocode's more conservative performance requirements are also discussed. The Eurocodes are based on a more stringent default value of β = 3.8 for their reference class RC2 structures.

Figure 8.1 maps out the approach taken in this Chapter to report the performance assessment of EC2's stirrup design procedure. A similar approach is taken in Chapter 9, where an alternate GPM for stirrup resistance based on unbiased shear capacity predictions from R2k is used in the performance assessment of EC2's stirrup design procedure.

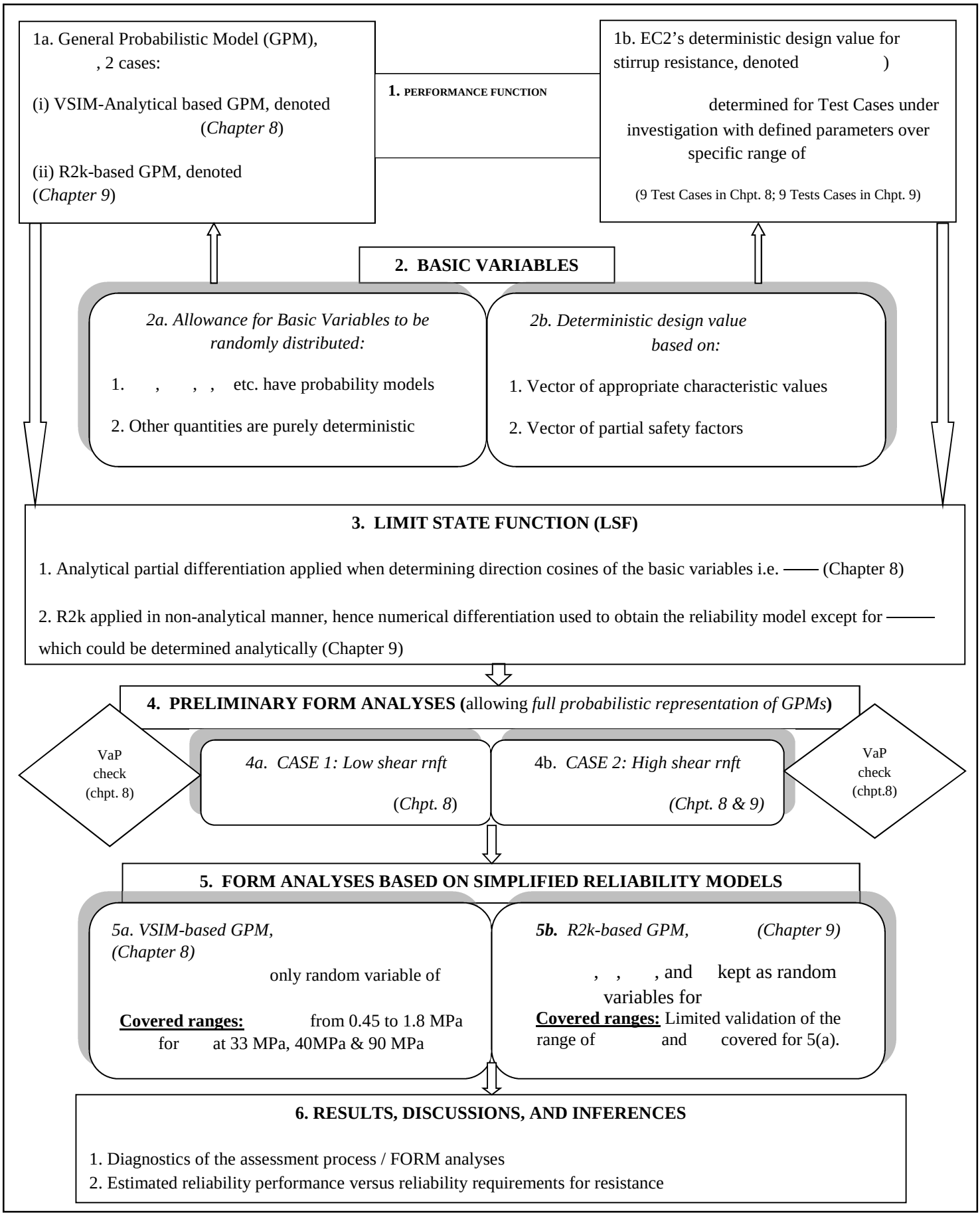

Figure 8.1. Flowchart outlining the approach taken to reliability investigation in Chapters 8 and 9

8.1 VSIM-ANALYTICAL BASED PERFORMANCE FUNCTION FOR STIRRUP RESISTANCE

The performance function, $g(\boldsymbol{X})$, was set up for a beam cross-section of typical geometry (a Test Case), with common dimensions shown in Figure 8.2. β-values, obtained from FORM evaluations of the Limit State Function $g(\boldsymbol{X}) = 0$, were determined for 9 Test Cases covering the range of $\rho_w f_{ywm}$ of 0.45 MPa to 1.8 MPa. An assessment of β-values in this range provided sufficient indication of the reliability performance of the EC2 stirrup resistance function $V_{Rd,s}(\boldsymbol{X_k}, \boldsymbol{\gamma})$ according to SANS 10160-1 and EC0 requirements for resistance (see Section 8.2.1). A detailed discussion of the Test Cases used for the performance assessment is given in Section 8.1.4.

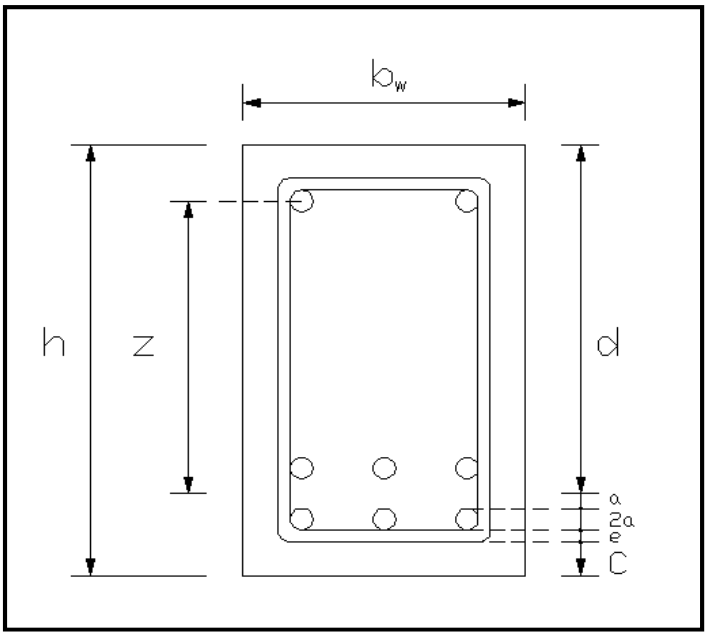

Figure 8.2. Typical beam cross-section geometry for a Test Case

8.1.1 The performance function $g(\boldsymbol{X})$ for stirrup resistance

Performance function $g(\boldsymbol{X})$ was used to determine the level of reliability β (or exceedance probability P_f) of EC2's deterministic design stirrup resistance, $V_{Rd,s}(\boldsymbol{X_k}, \boldsymbol{\gamma})$, as a function of the probability distribution of true shear strength $V_{VSIM-Analytical}(X)$ i.e. General

Probabilistic Model (GPM) – see Figure 8.3. Note that for the instance reported in this Chapter, the GPM was generated by allowing the random variables of the VSIM-Analytical calculation procedure to assume appropriate probability distributions. Consistent with the background to reliability analysis presented in Chapter 6, the performance function for stirrup resistance was expressed as:

$$g(\boldsymbol{X}) = V_{VSIM-Analytical}(\boldsymbol{X}) - V_{Rd,s}(\boldsymbol{X_k}, \boldsymbol{\gamma}) \quad [8.1a]$$

$$\therefore \quad g(\boldsymbol{X}) = MF_{VSIM-Analytical} \cdot \left[\frac{A_{sw}}{s} z f_{ywm} \cot\theta_{Analytical}\right] - V_{Rd,s}(\boldsymbol{X_k}, \boldsymbol{\gamma}) \quad [8.1b]$$

with secondary terms z and $\theta_{Analytical}$ comprised of primary terms as elaborated in Table 8.1 below. The internal lever arm, z, of the GPM was conventionally considered as $0.9d$ i.e. $z = 0.9 \cdot d$. No theoretical probability distribution was traceable for d from relevant literature. The decision was therefore taken to model d as a sum of its components, as shown in Table 8.1 (see also Fig. 8.2).

Table 8.1. Elaboration of secondary terms z and $\theta_{Analytical}$ from Equation 8.1b

Variable X_i (Secondary term)	**Primary terms**
Internal lever arm, z	$z = 0.9 \cdot d = 0.9 \cdot (h - C - n_l \cdot a - e)$, where n_l is some multiple of a half diameter of flexural reinforcement bar ($n_l = 3$ in Fig. 8.2)
Theoretical concrete strut angle $\theta_{Analytical}$	$= \sin^{-1}\sqrt{\frac{A_{sw}f_{yw}}{b_w s \nu_1 \alpha_{cc} f_c}}$, freely assuming any calculated value

Substituting primary terms from Table 8.1 into Equation 8.1b, yielded:

$$g(\boldsymbol{X}) = MF_{VSIM-Analytical} \cdot \left[\frac{A_{sw}}{s} \cdot 0.9 \cdot (h - C - n_l \cdot a - e) \cdot f_{yw} \cdot \cot\left(\sin^{-1}\sqrt{\frac{A_{sw}f_{yw}}{b_w s \nu_1 \alpha_{cc} f_c}}\right)\right] - V_{Rd,s}(\boldsymbol{X_k}, \boldsymbol{\gamma}) \quad [8.1c]$$

$MF_{VSIM-Analytical}$, A_{sw}, s, m, h, C, a, e, f_c, f_{yw} and α_{cc} in Equation 8.1c are probability models of the basic random variables as discussed in Section 8.1.2.

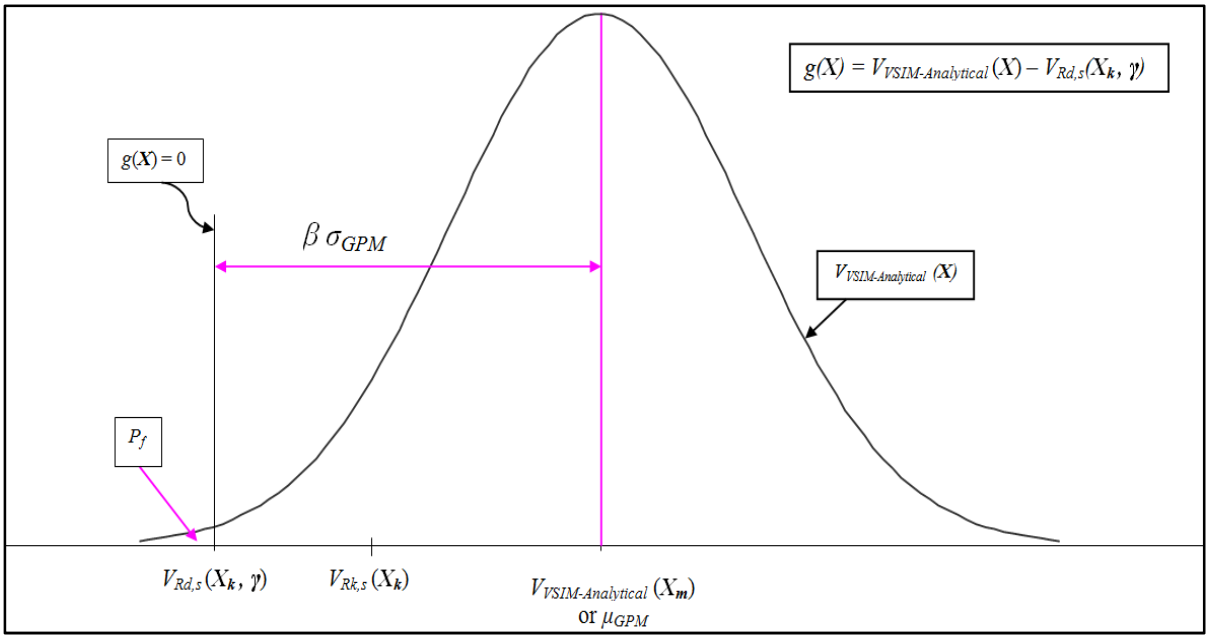

Figure 8.3. Probabilistic representation of the performance function $g(\boldsymbol{X})$ for stirrup resistance

$V_{Rd,s}(\boldsymbol{X_k}, \boldsymbol{\gamma})$, as can be seen from Figure 8.3, is the single deterministic design value for shear resistance determined for a beam section in accordance with EC2. The vector $\boldsymbol{X_k}$ implies the use of characteristic steel (f_{ywk}) and concrete (f_{ck}) strengths, since all other basic variables are treated nominally (bias = 1). $\boldsymbol{\gamma}$ implies the use of partial factors for concrete ($\gamma_C = 1.5$) and steel ($\gamma_S = 1.15$) applied to the respective characteristic strengths, giving:

$$V_{Rd,s}(\boldsymbol{X_k}, \boldsymbol{\gamma}) = \frac{A_{sw}}{s} z \frac{f_{ywk}}{1.15} \cot \theta_{Limited} \qquad [8.2a]$$

and $\theta_{Limited} = \sin^{-1} \sqrt{\frac{A_{sw}(f_{ywk}/1.15)}{b_w s \nu_1 (\alpha_{cck} f_{ck}/1.5)}}$, with $21.8° \leq \theta_{Limited} \leq 45°$ and $z = 0.9d$ [8.2b]

8.1.2 Probability models for the basic random variables of the GPM

Details of the probability models used to represent the basic random variables that formed part of the VSIM-Analytical based GPM (see Equations 8.1a to 8.1c) are given in Table 8.2. The various literature sources from which theoretical probability models were extracted are referenced as appropriate in the Table. Note, however, that the probability model for $MF_{VSIM-Analytical}$ was developed specifically for use in this investigation, and is indicated as such in the Table. The basic variables a and e, both defined in the Table (see Fig. 8.2 as well), were concerned with the area of the stirrups (A_{sw}) and were therefore prescribed a similar probability model to that of A_{sw}. The symbols N, 2P-LN, and 3P-LN refer to the Normal, Two-parameter log-normal, and Three-parameter log-normal probability distributions, respectively.

Table 8.2. Probability models for the basic variables of the GPM

No	Specification of basic variable	Symbol X	Unit	Distribution	Mean μ_X	Std dev σ_X	C.o.V	Source
1	VSIM-Analytical Model Factor	$MF_{VSIM-Analytical}$	-	2P-LN	0.84	0.18	0.21	*Investigated**
2	Stirrup Area (2 legs)	A_{sw}	mm^2	N	nom. A_{sw}	-	0.02	JCSS PMC (2001)
3	Stirrup spacing	s	mm	N	nom. s	-	0.03	Huber (2005)
4	beam height	h	mm	N	nom. h	-	0.01	Holický (2009)
5	Concrete cover	C	mm	2P-LN	-	9	-	Holický et al. (2010)
6	Radius (half-diameter) of tension reinforcement	a	mm	N	nom. a	-	0.02	JCSS PMC (2001)
7	Diameter of stirrups	e	mm	N	nom. e	-	0.02	JCSS PMC (2001)
8	Yield strength of stirrups	f_{yw}	MPa	2P-LN	$f_{ywk} + 1.645\sigma$	30	-	EN 1990
9	Beam width	b_w	mm	N	nom. b_w	-	0.01	Holický (2009)
10	Coefficient for scale/long-term effects	α_{cc}	-	2P-LN	0.85	-	0.1	Holický et al. (2010)
11	Compressive cylinder strength of concrete	f_c	MPa	2P-LN	f_{ck} + 8 MPa	-	-	EC2 / *fib* MC 2010

*Parameter investigated and developed for use as part of reliability/performance assessment

From an inspection of Table 8.1, and in-line with international structural design convention, it is evident that basic variables A_{sw}, s, h, b_w etc. are nominal quantities (Bias = μ_X/X_k = 1). Basic variables f_c and f_{yw} traditionally have differently specified mean (μ_X) and characteristic (X_k) values as shown in the Table i.e. have a characteristic biases. Salient aspects of some of the probability models are discussed in the following Sections.

$MF_{VSIM-Analytical}$

A mean value of $\mu_{MF} = 0.84$ and standard deviation $\sigma_{MF} = 0.18$ were applied for all reliability performance assessments conducted as part of the study i.e. for all Test Cases representing different $\rho_w f_{ywm}$ situations. This action was motivated by results presented in Chapter 7, where Figure 7.8(a) clearly indicates that $MF_{VSIM-Analytical}$ realisations are systematically unconservative, and relatively constant (uniform $\mu_{MF} = 0.84$ at different $\rho_w f_{ywm}$ situations), for the range of beam experiments considered.

The assumption of a constant standard deviation of $\sigma_{MF} = 0.18$ was however more of an approximation, as the scatter of $MF_{VSIM-Analytical}$ realisations about the $\mu_{MF} = 0.84$ line are non-uniform at different $\rho_w f_{ywm}$ i.e. implying non-uniform σ_{MF} at different $\rho_w f_{ywm}$. Slighlty smaller σ_{MF}-values are expected at $\rho_w f_{ywm} < 1.5$ MPa, due to a larger number of more consistent data points. $\sigma_{MF} = 0.18$ can therefore be considered a conservative assumption throughout the parametric range of $\rho_w f_{ywm}$ investigated. Assuming a larger standard deviation for $MF_{VSIM-Analytical}$ has the effect of increasing the overall spread of the GPM for stirrup resistance $V_{VSIM-Analytical}(\boldsymbol{X})$ as can be witnessed from Figure 8.3, hence implying that the derived β-values for the Test Cases reported in all investigations presented in this Chapter were somewhat conservative (only on the basis of σ_{GPM}, there are other factors affecting the accuracy of estimated β-values). The choice of the 2P-LN distribution as a suitable probability model to represent $MF_{VSIM-Analytical}$, which also affects the accuracy of estimated β-values, is discussed in Section 7.4.4.

Yield strength of the stirrups, f_{yw}

The traditional case of the 5 % characteristic value (95 % exceedance probability) was assumed for f_{yw}, hence as shown in Table 8.2:

$$f_{ywm} = \mu_{f_{yw}} = f_{ck} + 1.645\sigma_{f_{yw}} \qquad [8.5]$$

Holický (2009) expresses higher confidence in the European steel production quality standards, suggesting that $1.645\sigma_{f_{yw}}$ from Equation 8.5 be replaced by $2\sigma_{f_{yw}}$ (98 % exceedance probability). The convention of 5 % ($1.645\sigma_{f_{yw}}$) was maintained for use in this

investigation due to lack of evidence of a better quality for South African production standards.

A fixed standard deviation of $\sigma_{f_{yw}} = 30$ MPa was used for both high strength ($f_{ywk} = 450$ MPa; $f_{ywm} = \mu_{f_{yw}} = 500$ MPa) and mild strength ($f_{ywk} = 250$ MPa; $f_{ywm} = \mu_{f_{yw}} = 300$ MPa) steels. The result of the assumption was a higher $C.o.V$ for mild strength steels of 0.10 ($= 30 / 300$), or correspondingly a larger characteristic bias of 1.20 ($= \mu_{f_{yw}}/f_{ywk} = 300/250$) (compared to characteristic bias of 1.11 for high strength steel). A larger $C.o.V$ for mild strength steels was admissible as part of the study due to concerns about its declining use in the local SA industry. It was therefore judged that the aforementioned, coupled with the increased use of recycled materials in the production of mild strength steels (affecting chemical composition and micro-structural parameters), as well as concerns about quality management in its production, could negatively impact on the strength variability of mild strength steels.

The larger characteristic bias associated with mild strength steel had the expected effect of producing larger β-values when compared to estimates of β-values for the same $\rho_w f_{ywm}$ situations established using high strength steel. It is essential to note, with reference to preceding arguments, that only high strength steel was used for the 9 Test Cases used in the performance assessment of EC2's stirrup design procedure. Motivations for using high strength steel for the basic reliability investigations were:

1. It finds itself in common usage for various construction details, is produced with high levels of control, and is increasingly being used for stirrups in construction practice

2. Its lower associated characteristic strength bias ($= \mu_{f_{yw}}/f_{ywk} = 500/450 = 1.11$) resulted in lower (i.e. conservative) estimates of β-values for the Test Cases (compared to equivalent mild strength steel cases in terms of $\rho_w f_{ywm}$,). This fact, coupled with its increasing use as stirrups, warranted that the more stringent case of high strength steels be used in this investigation. Furthermore, for high $\rho_w f_{ywm}$ situations in practice, it is more likely that high strength steel stirrups will be utilised to allow sufficient/practical spacing of the stirrups within the beam (i.e. in situations where use of mild strength steel would result in insufficient spacings to allow proper vibration and compaction of fresh concrete).

The 2P-LN probability distribution assigned to f_{yw} was implemented as a special case of the general 3P-LN distribution, having skewness $s_{k-f_{yw}}$, equal to:

$$s_{k-f_{yw}} = \frac{3\sigma_{f_{yw}}}{\mu_{f_{yw}}} \quad [8.6]$$

Cylinder compressive strength of concrete, f_c

The expression reflecting the characteristic bias for concrete strength f_c in Table 8.2 ($f_{cm} = \mu_{f_{cm}} = f_{ck} + 8$ MPa) is rather straightforward, stated as it is recommended by both EC2 and *fib* MC 2010. Assuming a 5 % characteristic bias for concrete strength ($u_p = -1.645$), a standard deviation of $\sigma_{f_c} = 4.86$ MPa $(= 8/1.645)$ is implied by the 8 MPa difference between f_{ck} and f_{cm}. For $f_{ck} = 25$ MPa (or $f_{cm} = 33$ MPa), this further implied a $C.o.V$ of 0.15 $(= 4.86/33)$, which is a fairly conservative assumption on the basis of Holický (2009) which suggests a range of $0.10 - 0.18$, depending obviously on the level of quality measures. Hence, a $C.o.V$ of 0.15 represents a fairly moderate level of quality management.

The 2P-LN probability distribution assigned to f_c, similar to the case of f_{yw}, was implemented as a special case of the general 3P-LN probability distribution i.e. by applying a skewness Ω_{f_c} which was determined in accordance with Equation 8.6.

8.1.3 Limit State Function for reliability analysis

The Limit State Function (LSF), in general terms, is established when the performance function is set equal to zero i.e. $g(\boldsymbol{X}) = 0$. The Limit State Function was therefore defined as:

$$g(\boldsymbol{X}) =$$

$$MF_{VSIM-Analytical} \cdot \left[\frac{A_{sw}}{s} \cdot 0.9 \cdot (h - C - n_l \cdot a - e) \cdot f_{yw} \cdot \cot\left(\sin^{-1}\sqrt{\frac{A_{sw}f_{yw}}{b_w s \nu_1 \alpha_{cc} f_c}}\right)\right] - V_{Rd,s}(\boldsymbol{X_k}, \boldsymbol{\gamma}) = 0 \quad [8.7]$$

The expressions for the partial derivatives of the LSF in the required standard normal or U-space ($\frac{\partial G}{\partial X} \cdot \sigma_X^N$), as were required when implementing the FORM procedure (see Eqns. 6.14 to 6.18), were evaluated in MATLAB. Cognizance should again be taken of the fact that the EC2 design stirrup resistance $V_{Rd,s}(\boldsymbol{X_k}, \boldsymbol{\gamma})$ from Equation 8.7 is a deterministic quantity, and therefore falls away with differentiation.

MATLAB converted the trigonometric expression from Equation 8.7 $\cot\left(\sin^{-1}\sqrt{\frac{A_{sw}f_{yw}}{b_w s \nu_1 \alpha_{cc} f_c}}\right)$ to the equivalent identity $\frac{\sqrt{1-\frac{A_{sw}f_{yw}}{b_w s \nu_1 \alpha_{cc} f_c}}}{\sqrt{\frac{A_{sw}f_{yw}}{b_w s \nu_1 \alpha_{cc} f_c}}}$ as can be witnessed from Equation 8.8 below. Adequate calculation checks were performed to ensure that the identity and trigonometric expression gave the same result with specified input variables. The partial derivatives of each of the basic random variables at an arbitrary checking point x^* on the limit state (failure) surface were expressed as stated in Equations 8.9a to 8.9k. Hence:

$$g(\boldsymbol{X}) =$$

$$MF_{VSIM-Analytical} \cdot \left[\frac{A_{sw}}{s} \cdot 0.9 \cdot (h - C - n_l \cdot a - e) \cdot f_{yw} \cdot \frac{\sqrt{1-\frac{A_{sw}f_{yw}}{b_w s \nu_1 \alpha_{cc} f_c}}}{\sqrt{\frac{A_{sw}f_{yw}}{b_w s \nu_1 \alpha_{cc} f_c}}}\right] - V_{Rd,s}(\boldsymbol{X_k}, \boldsymbol{\gamma}) = 0 \quad [8.8]$$

$$\left(\frac{\partial g(\boldsymbol{X})}{\partial MF}\right)^{*} = \frac{A_{sw}{}^{*}}{s^{*}} \cdot 0.9 \cdot (h^{*} - C^{*} - n_l \cdot a^{*} - e^{*}) f_{yw}{}^{*} \frac{\sqrt{1 - \frac{A_{sw}{}^{*} f_{yw}{}^{*}}{b_w{}^{*} s^{*} \upsilon_1{}^{*} \alpha_{cc}{}^{*} | f_c{}^{*}}}}{\sqrt{\frac{A_{sw}{}^{*} f_{yw}{}^{*}}{b_w{}^{*} s^{*} \upsilon_1{}^{*} \alpha_{cc}{}^{*} f_c{}^{*}}}} \cdot \sigma_{MF}^{N}{}^{*} \quad [8.9a]$$

$$\left(\frac{\partial g(\boldsymbol{X})}{\partial A_{sw}}\right)^{*} = \frac{\frac{1}{2} MF^{*} \cdot 0.9 \cdot (h^{*} - C^{*} - n_l \cdot a^{*} - e^{*}) f_{yw}{}^{*} (b_w{}^{*} s^{*} \upsilon_1{}^{*} \alpha_{cc}{}^{*} f_c{}^{*} - 2 A_{sw}{}^{*} f_{yw}{}^{*})}{b_w{}^{*} s^{*2} \upsilon_1{}^{*} \alpha_{cc}{}^{*} f_c{}^{*} \sqrt{\frac{A_{sw}{}^{*} f_{yw}{}^{*}}{b_w{}^{*} s^{*} \upsilon_1{}^{*} \alpha_{cc}{}^{*} f_c{}^{*}}} \sqrt{\frac{b_w{}^{*} s^{*} \upsilon_1{}^{*} \alpha_{cc}{}^{*} f_c{}^{*} - A_{sw}{}^{*} f_{yw}{}^{*}}{b_w{}^{*} s^{*} \upsilon_1{}^{*} \alpha_{cc}{}^{*} f_c{}^{*}}}} \cdot \sigma_{A_{sw}}^{N}{}^{*} \quad [8.9b]$$

$$\left(\frac{\partial g(\boldsymbol{X})}{\partial s}\right)^{*} = -\frac{\frac{1}{2} MF^{*} A_{sw}{}^{*} \cdot 0.9 \cdot (h^{*} - C^{*} - n_l \cdot a^{*} - e^{*}) f_{yw}{}^{*} (b_w{}^{*} s^{*} \upsilon_1{}^{*} \alpha_{cc}{}^{*} f_c{}^{*} - 2 A_{sw}{}^{*} f_{yw}{}^{*})}{b_w{}^{*} s^{*3} \upsilon_1{}^{*} \alpha_{cc}{}^{*} f_c{}^{*} \sqrt{\frac{A_{sw}{}^{*} f_{yw}{}^{*}}{b_w{}^{*} s^{*} \upsilon_1{}^{*} \alpha_{cc}{}^{*} f_c{}^{*}}} \sqrt{\frac{b_w{}^{*} s^{*} \upsilon_1{}^{*} \alpha_{cc}{}^{*} f_c{}^{*} - A_{sw}{}^{*} f_{yw}{}^{*}}{b_w{}^{*} s^{*} \upsilon_1{}^{*} \alpha_{cc}{}^{*} f_c{}^{*}}}} \cdot \sigma_{s}^{N*} \quad [8.9c]$$

$$\left(\frac{\partial g(\boldsymbol{X})}{\partial h}\right)^{*} = MF^{*} \frac{A_{sw}{}^{*}}{s^{*}} \cdot 0.9 \cdot f_{yw}{}^{*} \frac{\sqrt{1 - \frac{A_{sw}{}^{*} f_{yw}{}^{*}}{b_w{}^{*} s^{*} \upsilon_1{}^{*} \alpha_{cc}{}^{*} f_c{}^{*}}}}{\sqrt{\frac{A_{sw}{}^{*} f_{yw}{}^{*}}{b_w{}^{*} s^{*} \upsilon_1{}^{*} \alpha_{cc}{}^{*} f_c{}^{*}}}} \cdot \sigma_{h}^{N*} \quad [8.9d]$$

$$\left(\frac{\partial g(\boldsymbol{X})}{\partial C}\right)^{*} = -MF^{*} \frac{A_{sw}{}^{*}}{s^{*}} \cdot 0.9 \cdot f_{yw}{}^{*} \frac{\sqrt{1 - \frac{A_{sw}{}^{*} f_{yw}{}^{*}}{b_w{}^{*} s^{*} \upsilon_1{}^{*} \alpha_{cc}{}^{*} f_c{}^{*}}}}{\sqrt{\frac{A_{sw}{}^{*} f_{yw}{}^{*}}{b_w{}^{*} s^{*} \upsilon_1{}^{*} \alpha_{cc}{}^{*} f_c{}^{*}}}} \cdot \sigma_{C}^{N*} \quad [8.9e]$$

$$\left(\frac{\partial g(\boldsymbol{X})}{\partial a}\right)^{*} = -MF^{*} \frac{A_{sw}{}^{*}}{s^{*}} \cdot 0.9 \cdot n_l \cdot f_{yw}{}^{*} \frac{\sqrt{1 - \frac{A_{sw}{}^{*} f_{yw}{}^{*}}{b_w{}^{*} s^{*} \upsilon_1{}^{*} \alpha_{cc}{}^{*} f_c{}^{*}}}}{\sqrt{\frac{A_{sw}{}^{*} f_{yw}{}^{*}}{b_w{}^{*} s^{*} \upsilon_1{}^{*} \alpha_{cc}{}^{*} f_c{}^{*}}}} \cdot \sigma_{a}^{N*} \quad [8.9f]$$

$$\left(\frac{\partial g(\boldsymbol{X})}{\partial e}\right)^{*} = -MF^{*} \frac{A_{sw}{}^{*}}{s^{*}} \cdot 0.9 \cdot n_l \cdot f_{yw}{}^{*} \frac{\sqrt{1 - \frac{A_{sw}{}^{*} f_{yw}{}^{*}}{b_w{}^{*} s^{*} \upsilon_1{}^{*} \alpha_{cc}{}^{*} f_c{}^{*}}}}{\sqrt{\frac{A_{sw}{}^{*} f_{yw}{}^{*}}{b_w{}^{*} s^{*} \upsilon_1{}^{*} \alpha_{cc}{}^{*} f_c{}^{*}}}} \cdot \sigma_{e}^{N*} \quad [8.9g]$$

$$\left(\frac{\partial g(\boldsymbol{X})}{\partial f_{yw}}\right)^{*} = \frac{\frac{1}{2} MF^{*} A_{sw}{}^{*} \cdot 0.9 \cdot (h^{*} - C^{*} - n_l \cdot a^{*} - e^{*}) (b_w{}^{*} s^{*} \upsilon_1{}^{*} \alpha_{cc}{}^{*} f_c{}^{*} - 2 A_{sw}{}^{*} f_{yw}{}^{*})}{b_w{}^{*} s^{*2} \upsilon_1{}^{*} \alpha_{cc}{}^{*} f_c{}^{*} \sqrt{\frac{A_{sw}{}^{*} f_{yw}{}^{*}}{b_w{}^{*} s^{*} \upsilon_1{}^{*} \alpha_{cc}{}^{*} f_c{}^{*}}} \sqrt{\frac{b_w{}^{*} s^{*} \upsilon_1{}^{*} \alpha_{cc}{}^{*} f_c{}^{*} - A_{sw}{}^{*} f_{yw}{}^{*}}{b_w{}^{*} s^{*} \upsilon_1{}^{*} \alpha_{cc}{}^{*} f_c{}^{*}}}} \cdot \sigma_{f_{yw}}^{N}{}^{*} \quad [8.9h]$$

$$\left(\frac{\partial g(\boldsymbol{X})}{\partial b_w}\right)^{*} = \frac{\frac{1}{2} MF^{*} A_{sw}{}^{*} \cdot 0.9 \cdot (h^{*} - C^{*} - n_l \cdot a^{*} - e^{*}) f_{yw}{}^{*}}{b_w{}^{*} s^{*} \sqrt{\frac{A_{sw}{}^{*} f_{yw}{}^{*}}{b_w{}^{*} s^{*} \upsilon_1{}^{*} \alpha_{cc}{}^{*} f_c{}^{*}}} \sqrt{\frac{b_w{}^{*} s^{*} \upsilon_1{}^{*} \alpha_{cc}{}^{*} f_c{}^{*} - A_{sw}{}^{*} f_{yw}{}^{*}}{b_w{}^{*} s^{*} \upsilon_1{}^{*} \alpha_{cc}{}^{*} f_c{}^{*}}}} \cdot \sigma_{b_w}^{N}{}^{*} \quad [8.9i]$$

$$\left(\frac{\partial g(\boldsymbol{X})}{\partial \alpha_{cc}}\right)^{*} = \frac{\frac{1}{2} MF^{*} A_{sw}{}^{*} \cdot 0.9 \cdot (h^{*} - C^{*} - n_l \cdot a^{*} - e^{*}) f_{yw}{}^{*}}{\alpha_{cc}{}^{*} s^{*} \sqrt{\frac{A_{sw}{}^{*} f_{yw}{}^{*}}{b_w{}^{*} s^{*} \upsilon_1{}^{*} \alpha_{cc}{}^{*} f_c{}^{*}}} \sqrt{\frac{b_w{}^{*} s^{*} \upsilon_1{}^{*} \alpha_{cc}{}^{*} f_c{}^{*} - A_{sw}{}^{*} f_{yw}{}^{*}}{b_w{}^{*} s^{*} \upsilon_1{}^{*} \alpha_{cc}{}^{*} f_c{}^{*}}}} \cdot \sigma_{\alpha_{cc}}^{N}{}^{*} \quad [8.9j]$$

$$\left(\frac{\partial g(\boldsymbol{X})}{\partial f_c}\right)^* = \frac{\frac{1}{2} MF^* \, A_{sw}{}^* \cdot 0.9 \cdot (h^* - C^* - n_l \cdot a^* - e^*) f_{yw}{}^*}{f_c{}^* \, s^* \sqrt{\frac{A_{sw}{}^* f_{yw}{}^*}{b_w{}^* s^* \nu_1{}^* \alpha_{cc}{}^* f_c{}^*}} \sqrt{\frac{b_w{}^* s^* \nu_1{}^* \alpha_{cc}{}^* f_c{}^* - A_{sw}{}^* f_{yw}{}^*}{b_w{}^* s^* \nu_1{}^* \alpha_{cc}{}^* f_c{}^*}}} \cdot \sigma_{f_c}^{N^*} \qquad [8.9k]$$

8.1.4 Reliability analysis of representative design situations

Various parameters that were used to establish the nine (9) basic Test Cases that were designed to investigate the consistency of β-values across the parametric range of $\rho_w f_{ywm}$ are presented in Tables 8.3 and 8.4. Due to the sensitivity of shear resistance to concrete strength (f_{cm}), β-values for the nine basic Test Cases were assessed at three different concrete strengths, namely (1) $f_{cm} = 33$ MPa, (2) $f_{cm} = 40$ MPa, and (3) $f_{cm} = 98$ MPa. In terms of shear reinforcement, the nine Test Cases covered the range of $\rho_w f_{ywm}$ from 0.45 MPa to 1.80 MPa. Derived β-values for the Test Cases were assessed against (1) primarily SA's target resistance reliability of $\beta_{T,RC} = 0.8 \times \beta_{RC}$, where β_{RC} = 3 or 3.5 for RC2 or RC3 structures according to SANS 10160-1, and (2) implications against the more stringent Eurocode RC2 requirements ($\beta_{T,EC} = 0.8 \times 3.8 = 3.04$).

Recall that $\rho_w = A_{sw}/b_w s$. The parametric variation of $\rho_w f_{ywm}$ situations (i.e. the different Test Cases) was achieved by varying the stirrup spacing, s, whilst keeping fixed the values of all other parameters (A_{sw}, b_w and f_{ywm}). Since other factors affecting shear strength (a/d, f_c, ρ_l etc.) did not show any adverse systematic trends in comparing the VSIM-Limitθ procedure to experimental results (discussed in Chapter 7), FORM analyses of $g(\boldsymbol{X})$ applied to a typical section geometry were deemed adequate to provide representative indication of the reliability performance of the EC2 VSIM-based design procedure.

Table 8.3. Mean quantities of basic random variables $\boldsymbol{X}$ common to all Test Cases

h [mm]	C [mm]	a [mm]	e [mm]	α_{cck}	f_{cm} [MPa]
500	30	16	10	0.85	Varied (33; 40; 98)

Table 8.4. Parameters for the Test Cases used for the performance assessment of EC2 design procedure (Elaboration of parameters used to establish different Test Cases)

Test Case No.	$\boldsymbol{A_{sw}}$ **[mm^2]**	$\boldsymbol{f_{ywm}}$ **[MPa]**	$\boldsymbol{b_w}$ **[mm]**	$\boldsymbol{s}$ **[mm]**	$\boldsymbol{\rho_w f_{ywm}}$ $\boldsymbol{(\rho_w f_{ywk})}$ **[MPa]**	$\boldsymbol{MF_{VSIM-Analytical}}$ $\boldsymbol{\{\mu_{MF};\ \sigma_{MF}\}}$
1	157.1	500	350	498	0.45 (0.41)	{0.84; 0.18} for all situations see Fig 7.8(a)
2	157.1	500	350	459	0.49 (0.44)	
3	157.1	500	350	417	0.54 (0.48)	
4	157.1	500	350	300	0.75 (0.67)	
5	157.1	500	350	209	1.07 (0.97)	
6	157.1	500	350	200	1.12 (1.01)	
7	157.1	500	350	175	1.28 (1.15)	
8	157.1	500	350	150	1.49 (1.35)	
9	157.1	500	350	125	1.79 (1.62)	

It must be noted that all Test Cases had Y10 stirrups ($A_{sw} = 157.1\ \text{mm}^2$). This was done to achieve as much as possible stirrup spacings s below EC2's maximum limit of $0.75d$ or 600 mm. For Test Cases 1 to 9, $d = 412$ mm, hence max. spacing $=$ 309 mm. It is immediately evident that Test Cases 1 to 3 had stirrup spacings in excess of EC2's maximum limit. The results obtained for Test Cases 1 to 3 were however valid in so far as the reliability performance of EC2's stirrup design procedure is concerned. The maximum spacing limit can be considered a detailing rule, put in place perhaps for purposes of crack control.

Independent analyses were additionally conducted to determine the effect of using Y12's and Y16's ($A_{sw} = 226.2\ \text{mm}^2$ & 402.1mm^2, respectively) to establish some of the Test Cases reported in Table 8.4. As expected, it was found that estimates of β remained constant for

specific $\rho_w f_{ywm}$ situations established using the different cross-sectional areas (A_{sw}) since stirrup spacings (s) were adjusted accordingly to maintain constant A_{sw}/s ratios (keeping b_w and f_{ywm} fixed, see Equations 8.1 and 8.2 in conjunction with Figure 8.3). The assessment of only the Y10 cases are detailed in this report due to the inconsequential influence of using different cross-sectional areas to achieve the same Test Cases described in Table 8.4. The choice of f_{ywm} (mild or high strength steel), however, does have an affect on the estimate of the β-value for a given Test Case or $\rho_w f_{ywm}$ situation as discussed in Section 8.1.2.

Preliminary sensitivity study and the simplified model for reliability analysis

To cut down on computation time and effort, a simplified reliability function was ultimately developed, and subsequently applied, to all the nine Test Cases presented in Table 8.3. The results of this assessment are presented in Section 8.2 below. Test Cases 1 and 9 (shown shaded in Table 8.4; further illustrated in Figure 8.4) were subjected to preliminary performance assessments based on a full probabilistic representation of $g(\boldsymbol{X})$ as expressed by Equation 8.8 i.e. all basic random variables of $g(\boldsymbol{X})$ having probability models contributing to overall performance uncertainty.

The results of the preliminary, but extensive, performance assessments of Test Cases 1 and 9 indicated that the Model Factor $MF_{VSIM-Analytical}$ had a dominating influence on the probability distribution of $V_{VSIM-Analytical}(\boldsymbol{X})$ from Equation 8.1 (or correspondingly, see Figure 8.3). Hence, a simplified reliability model was developed representing $MF_{VSIM-Analytical}$ as the only random variable of $g(\boldsymbol{X})$, having the benefit of averting the inclusion of any 'ignorance sensitivities' contributing to the probability distribution of $V_{VSIM-Analytical}(\boldsymbol{X})$ as expressed by Melchers (1999). The simplified reliability model is discussed in detail in Section 8.2.

Selection of Test Cases 1 and 9 for the preliminary sensitivity study

Test Cases 1 and 9 were chosen for the preliminary sensitivity study to assess the sensitivity of probability distribution $V_{VSIM-Analytical}(\boldsymbol{X})$ to its basic random variables at low and high

$\rho_w f_{ywm}$, respectively. The choice of the Test Cases was based on the $MF_{VSIM-Limit\theta}$ versus $\rho_w f_{ywm}$ trend derived in Chapter 7 which is repeated here for convenience as Figure 8.4 below.

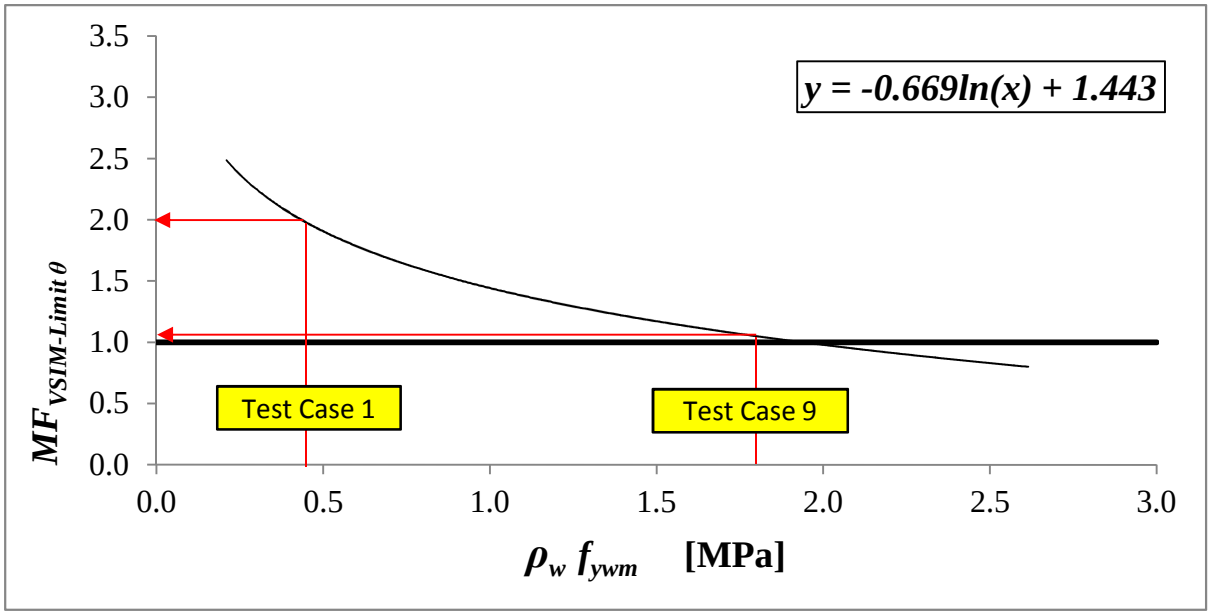

Figure 8.4. Test Cases used for the preliminary sensitivity analysis

8.1.5 Results of the preliminary assessment

The results of the preliminary FORM sensitivity study performed using Test Cases 1 and 9 are presented, respectively, in Tables 8.5 and 8.6 as well as Figures 8.5 and 8.6. Collectively, the Tables and Figures given for each Test Case show:

1. Converged design point β-values
2. Mean input quantities ($\boldsymbol{X_m}$) for $n-1$ basic random variables (except MF)
3. Design point values of the basic random variables $\boldsymbol{x_d}^*$
4. Direction cosines of the basic random variables at the design point $\boldsymbol{\alpha_x}^*$
5. Deterministic design ($V_{Rd,s}(\boldsymbol{X_k}, \boldsymbol{\gamma})$) and characteristic ($V_{Rk,s}(\boldsymbol{X_k})$) quantities of stirrup resistance according to EC2's recommended procedure
6. The mean value $V_{VSIM-Analytical}(\boldsymbol{X_m})$ of the GPM for stirrup resistance, as well as its standard deviation σ_{GPM}

Table 8.5. Converged design point values for Test Case 1 at $f_{cm} = 33$ MPa (Iteration No. 3)

$\beta = 3.45$							
X	**Unit**	X_m	$x_d{}^*$	σ_x	**Distn.**	$\left(\frac{dg}{dx}\right)^*$	α_x^*
MF	-	-	0.41	0.18	2P-LN	23755.6	0.95
A_{sw}	mm^2	157.1	156.1	3.14	N	1105.2	0.04
s	mm	498.1	501.7	3.75	N	-410.5	-0.02
h	mm	500	498.1	5	N	1402.05	0.06
C	mm	30	32.0	9	2P-LN	-2629.82	-0.11
a	mm	16	16.0	0.32	N	-269.19	-0.01
e	mm	10	10.0	0.2	N	-56.1	-0.00
f_{yw}	MPa	500	485.0	30	2P-LN	3296.80	0.13
b_w	mm	350	349.4	3.5	N	596.0	0.02
α_{cc}	-	0.85	0.78	0.085	2P-LN	5935.0	0.24
f_c	MPa	33	26.9	4.86	2P-LN	152.7	0.01
					SRSS	24922.8	1.00

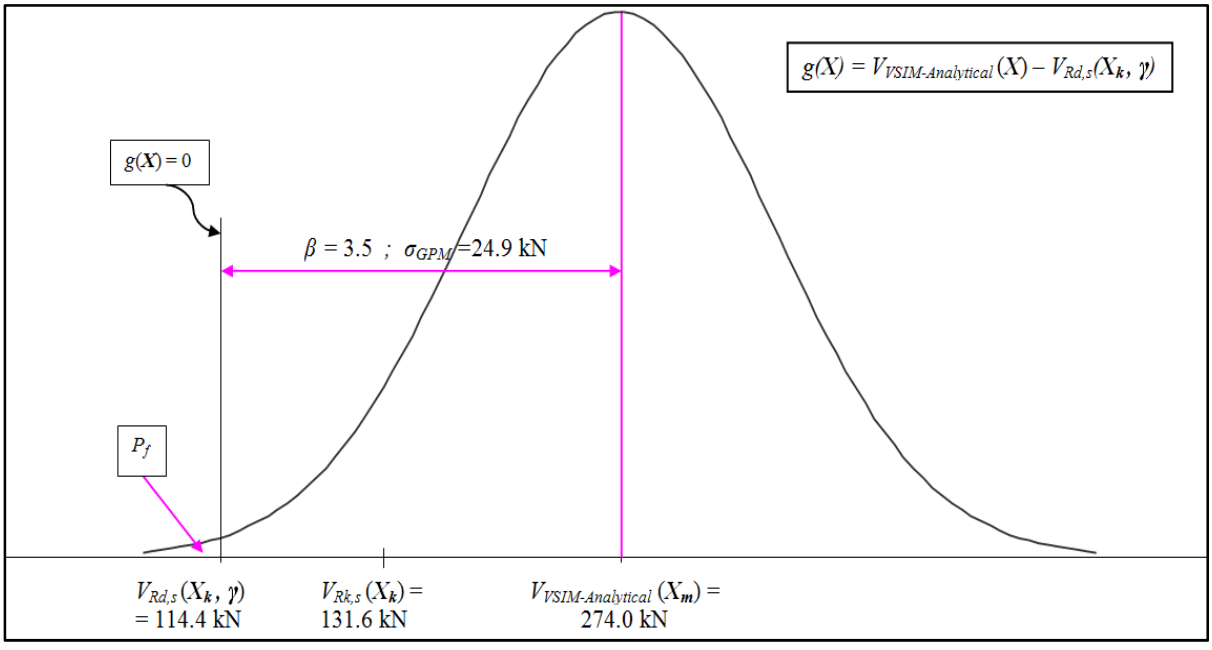

Figure 8.5. Probabilistic representation of $g(X)$ for Test Case 1 at $f_{cm} = 33$ MPa

Table 8.6. Converged design point values for Test Case 9 at $f_{cm} = 33$ MPa (Iteration No. 3)

$\beta = 1.10$							
$\boldsymbol{X}$	**Unit**	$\boldsymbol{X_m}$	$\boldsymbol{x_d}^*$	$\boldsymbol{\sigma_x}$	**Distn.**	$\left(\frac{\boldsymbol{dg}}{\boldsymbol{dx}}\right)^*$	$\boldsymbol{\alpha_x^*}$
MF	-	-	0.68	0.18	2P-LN	79815.8	0.95
A_{sw}	mm^2	157.1	156.9	3.14	N	3258.8	0.04
s	mm	125	125.4	3.75	N	-4861.1	-0.06
h	mm	500	499.50	5	N	4668.7	0.06
C	mm	30	29.48	9	2P-LN	-8127.7	-0.10
a	mm	16	16.00	0.12	N	-896.4	-0.01
e	mm	10	10.00	0.2	N	-186.8	0.00
f_{yw}	MPa	500	495.3	30	2P-LN	9763.8	0.12
b_w	mm	350	349.8	3.5	N	2219.04	0.03
α_{cc}	-	0.85	0.83	0.085	2P-LN	22122.4	0.26
f_c	MPa	33	31.03	4.86	2P-LN	568.5	0.01
					SRSS	84163.5	1.00

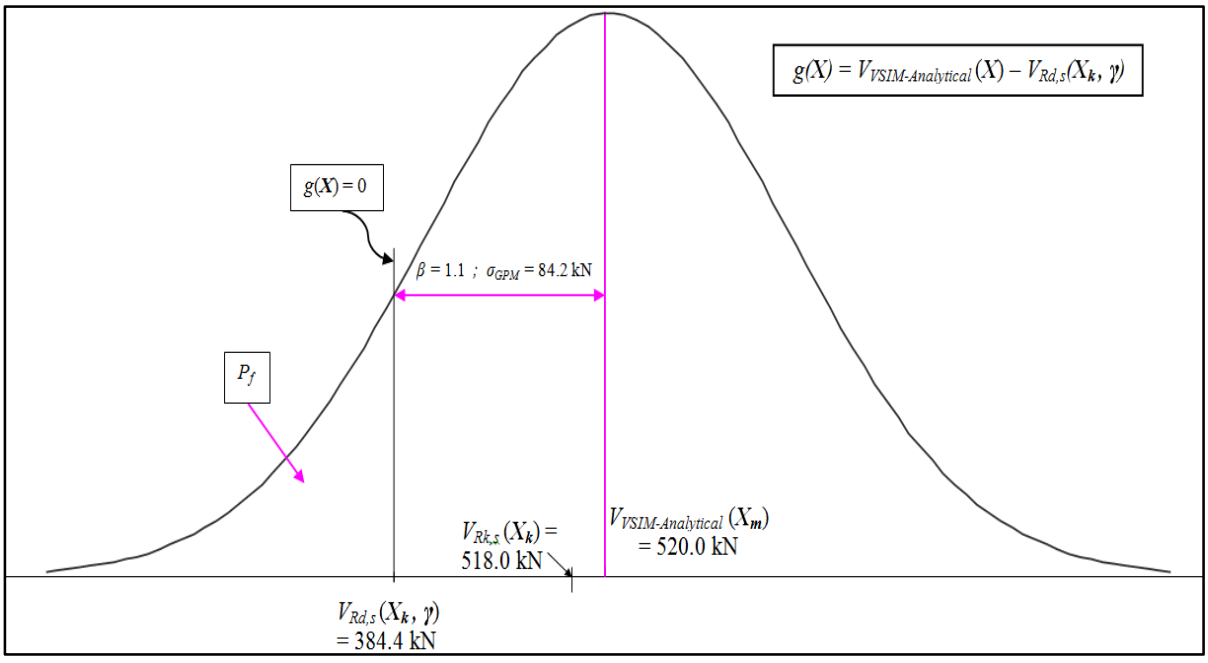

Figure 8.6. Probabilistic representation of $g(\boldsymbol{X})$ for Test Case 9 at $f_{cm} = 33$ MPa

Note that $V_{Rk,s}(\boldsymbol{X_k})$ was determined in essentially the same manner as $V_{Rd,s}$ (Equation 8.2), save for the exclusion of partial factors $\boldsymbol{\gamma}$ in its determination. The characteristic values ($\boldsymbol{X_k}$) of the basic random variables required for the evaluation of $V_{Rk,s}$ were determined in accordance with the transformations presented in Table 8.2. $V_{VSIM-Analytical}(\boldsymbol{X_m})$, which could alternatively be expressed as μ_{GPM}, was determined by inserting the vector of mean values of the basic variables $\boldsymbol{X_m}$ into the GPM expression in Equation 8.8.

Assessment of preliminary results

β-values: Test Case 1, with an estimated β-value of 3.5, satisfied performance requirements according to both SANS 10160-1 and EC0 ($\beta_{T,RC}$ for SANS 10160-1 $= 2.8$ and $\beta_{T,EC} = 3.04$). Conversely, Test Case 9, with an estimated β-value of 1.1, failed to meet both SANS 10160-1 and EC0 requirements for resistance.

These results confirmed initial concerns, stimulated by the trend shown in Figure 8.4, that β varies with $\rho_w f_{ywm}$. More importantly, the performance of EC2's design procedure is insufficient at high $\rho_w f_{ywm}$. A further concern, in addition to the failure to meet basic performance requirements for ductile failure modes, is the increased possibility of brittle failures in highly stirrup-reinforced concrete members. It is generally accepted in the fraternity (Melchers, 1999; Thoft-Christensen & Baker, 1982) that higher target levels of β_T be assigned to situations where brittle failure dominates, owing to the sudden occurrence of such failures. This is an issue requiring further investigation.

α_X values: It is clear from Table 8.5 and Table 8.6 that $MF_{VSIM-Analytical}$ dominates the uncertainty associated with probability distribution $V_{VSIM-Analytical}(\boldsymbol{X_m})$, achieving for both Test Cases 1 and 9 a value of α_X of 0.95 (Note: SRSS $\alpha_X = 1$). A simplified reliability model reflecting only $MF_{VSIM-Analytical}$ as a random variable would surely provide good indication of actual performance levels, as confirmed by the results of Section 8.2. Figure 8.7 depicts the dominating influence of $MF_{VSIM-Analytical}$ for the range of $\rho_w f_{ywm}$ of 0.5 to 2.3 MPa. To avoid a clustered presentation, α_X values are shown in Figure 8.7 only for the four most influential basic random variables found to affect probability distribution $V_{VSIM-Analytical}(\boldsymbol{X})$. Note that the vertical axis in Figure 8.7 is in log-scale.

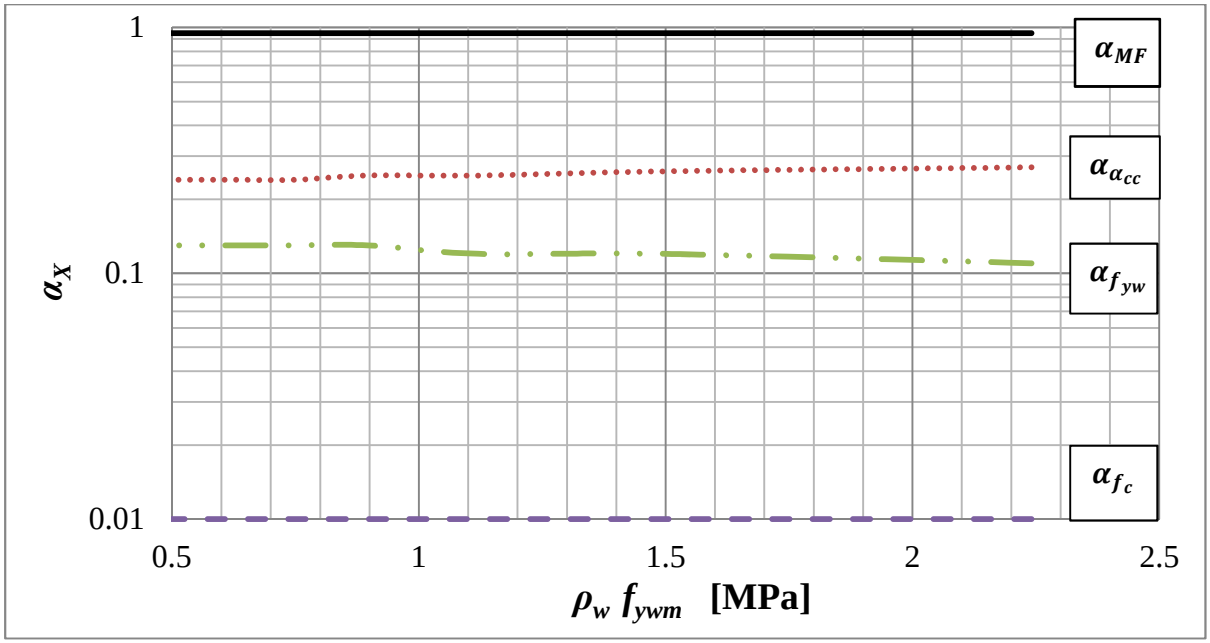

Figure 8.7. Direction cosines α_X for $MF_{VSIM-Analytical}$, α_{cc}, m, and f_{yw} at $f_{cm} = 33$ MPa

$V_{Rd,s}(\boldsymbol{X_k}, \boldsymbol{\gamma})$, $V_{Rk}(\boldsymbol{X_k})$, and $V_{VSIM-Analytical}(\boldsymbol{X_m})$: For Test Case 1, Figure 8.5 shows vividly that $V_{Rk,s}(\boldsymbol{X_k})$ lies between $V_{Rd,s}(\boldsymbol{X_k}, \boldsymbol{\gamma})$ and $V_{VSIM-Analytical}(\boldsymbol{X_m})$. This should generally be the case for properly calibrated models (in all situations), where the characteristic bias introduces sufficient conservatism into the process of establishing design resistance V_{Rd}.

Figure 8.6, on the other hand, demonstrates the absence of a thorough calibration of EC2's stirrup design procedure, particularly at high $\rho_w f_{ywm}$. The inspection of Figures 8.5 and 8.6 makes it clear that the margin of safety between $V_{Rk,s}(\boldsymbol{X_k})$ and $V_{VSIM-Analytical}(\boldsymbol{X_m})$ decreases as $\rho_w f_{ywm}$ increases. This implies that the characteristic bias fails to introduce sufficient conservatism into the procedures at all $\rho_w f_{ywm}$ situations. This is obviously not functionally correct for the characteristic bias of a resistance model.

8.2 SIMPLIFIED TOOL FOR RELIABILITY ANALYSIS

The main reliability performance assessments of the EC2 stirrup design procedure ($V_{Rd,s}$), from which conclusive views were ultimately drawn, were based on a simplified version of the performance function $g(\boldsymbol{X})$, newly denoted $g(\boldsymbol{X})_s$. $g(\boldsymbol{X})_s$ treated $MF_{VSIM-Analytical}$ as the only random variable of $V_{VSIM-Analytical}(\boldsymbol{X})$ due to its dominating influence on the probability distribution of the GPM (or $V_{VSIM-Analytical}(\boldsymbol{X})$) as discussed in Section 8.1.4. The determination of the estimated β-value for this set (simplified set) of analyses was therefore a straightforward process requiring a single and direct evaluation (a single run of the FORM procedure as expressed in Section 6.2). This was because the space of basic random variables reduced to a one-dimensional space.

The simplified limit state function was established as:

$$g(\boldsymbol{X})_s = MF_{VSIM-Analytical} \cdot \left[\frac{A^*_{sw1}}{s^*_1} m^*_1 (h^*_1 - C^*_1 - n_l \cdot a^*_1 - e^*_1) f^*_{yw1} \cdot K\right] - V_{Rd,s}(\boldsymbol{X_k}, \boldsymbol{\gamma}) = 0 \quad [8.10]$$

Where K is a once-off calculated quantity defined as:

$$K = \cot\left(\sin^{-1}\sqrt{\frac{A^*_{sw1} f^*_{yw1}}{b^*_{w1} s^*_1 \nu^*_1 \alpha^*_{cc1} f^*_{c1}}}\right) \quad [8.11]$$

$A^*_{sw1}, s^*_1, m^*_1, f^*_{yw1}, h^*_1, C^*_1, a^*_1, e^*_1, b^*_{w1}, s^*_1, \nu^*_1, \alpha^*_{cc1}, f^*_{c1}$ represent the checking point values of the basic variables established for the first iteration of FORM analysis, which were set equal to their respective mean values. $MF_{VSIM-Analytical}$ was the only random variable in Equation 8.10 and thus only $\left(\frac{\partial g(\boldsymbol{X})}{\partial MF}\right)^*$ was evaluated as follows:

$$\left(\frac{\partial g(\boldsymbol{X})}{\partial MF}\right)^* = \frac{A^*_{sw,1}}{s^*_1} m^*_1 (h^*_1 - C^*_1 - n_l \cdot a^*_1 - e^*_1)\, f^*_{yw,1} \cdot K \cdot \sigma^N_{MF} \quad [8.12]$$

8.2.1 Assessment of $V_{Rd,s}(X_k, \gamma)$, $V_{Rk,s}(X_k)$, and $V_{R2k}(X_m)$ trends, and other performance indicators, at different $\rho_w f_{ywm}$ and f_{cm} situations

The occurrence of the EC2's deterministic design ($V_{Rd,s}(\boldsymbol{X_k}, \boldsymbol{\gamma})$), and characteristic ($V_{Rk,s}(\boldsymbol{X_k})$) values for stirrup resistance, as well as the mean value of the VSIM-Analytical based GPM $V_{VSIM-Analytical}(\boldsymbol{X_m})$, are shown for different concrete strengths ($f_{cm} = 33$ MPa & $f_{cm} = 98$ MPa) in Figures 8.8 and 8.9, respectively, for the parametric range of $\rho_w f_{ywm}$ from 0.45 MPa to 1.8 MPa. It should be noted that the general sequence in which $V_{Rd,s}(\boldsymbol{X_k}, \boldsymbol{\gamma})$, $V_{Rk,s}(\boldsymbol{X_k})$, and $V_{VSIM-Analytical}(\boldsymbol{X_m})$ occur throughout the parametric range of $\rho_w f_{ywm}$ is fundamentally the same as that portrayed in Figure 8.3 above. However, specific trends and relative proportions of the aforementioned performance indicators (($V_{VSIM-Analytical}(\boldsymbol{X_m})$, $V_{Rd,s}(\boldsymbol{X_k}, \boldsymbol{\gamma})$, σ_{GPM}, and β), differ both with $\rho_w f_{ywm}$ and f_{cm}, as discussed below. Tables 8.7 and 8.8 correspond, respectively, to Figures 8.8 and 8.9. For each Test Case, the Tables:

1. Report numerical values of the performance indicators shown in the Figures.

2. Give design point values for the basic variable $MF_{VSIM-Analytical}$ (denoted $\boldsymbol{MF_d}^*$ in the Tables). Recall that $MF_{VSIM-Analytical}$ was the only random variable of $g(\boldsymbol{X})_s$.

3. Give the estimated measure of dispersion (standard deviation) σ_{GPM} of the GPM for stirrup resistance $V_{VSIM-Analytical}(\boldsymbol{X})$. σ_{GPM} was estimated as the Square Root of the Sum of Sqaures (SRSS) of the differential $\frac{\partial g(X)}{\partial MF}$ at the FORM design point.

4. Present estimated β-values as influenced by the different proportions of the various performance indicators (i.e. $V_{VSIM-Analytical}(\boldsymbol{X_m})$, $V_{Rd,s}(\boldsymbol{X_k}, \boldsymbol{\gamma})$, and σ_{GPM}).

To aid with discussions that immediately follow, cognizance must be taken of the fact that the difference $V_{VSIM-Analytical}(\boldsymbol{X_m}) - V_{Rd,s}(\boldsymbol{X_k}, \boldsymbol{\gamma})$ represents the distance '$\beta \cdot \sigma_{GPM}$' as shown in Figure 8.3. This directly implies that estimated β-values are sensitive to the relative proportions of $V_{VSIM-Analytical}(\boldsymbol{X_m})$, $V_{Rd,s}(\boldsymbol{X_k}, \boldsymbol{\gamma})$, and σ_{GPM} (see the results of Tables 8.7 and 8.8).

Table 8.7. Performance indicators derived from the simplified reliability model applied to the 9 Test Cases at MPa

Test Case No.		) [kN]	[kN]	[kN]	[kN]	β
1	0.35	114.4	131.6	274.0	23.8	4.1
2	0.36	124.1	142.7	284.9	25.8	3.9
3	0.38	136.7	157.2	298.5	28.4	3.7
4	0.45	190.0	218.5	349.3	39.4	2.8
5	0.55	273.3	314.3	414.0	56.8	1.9
6	0.56	285.0	327.7	422.0	59.2	1.8
7	0.61	325.7	374.5	448.4	67.6	1.4
8	0.62	357.5	436.9	480.5	74.2	1.3
9	0.62	384.4	518.0	520.3	79.8	1.3

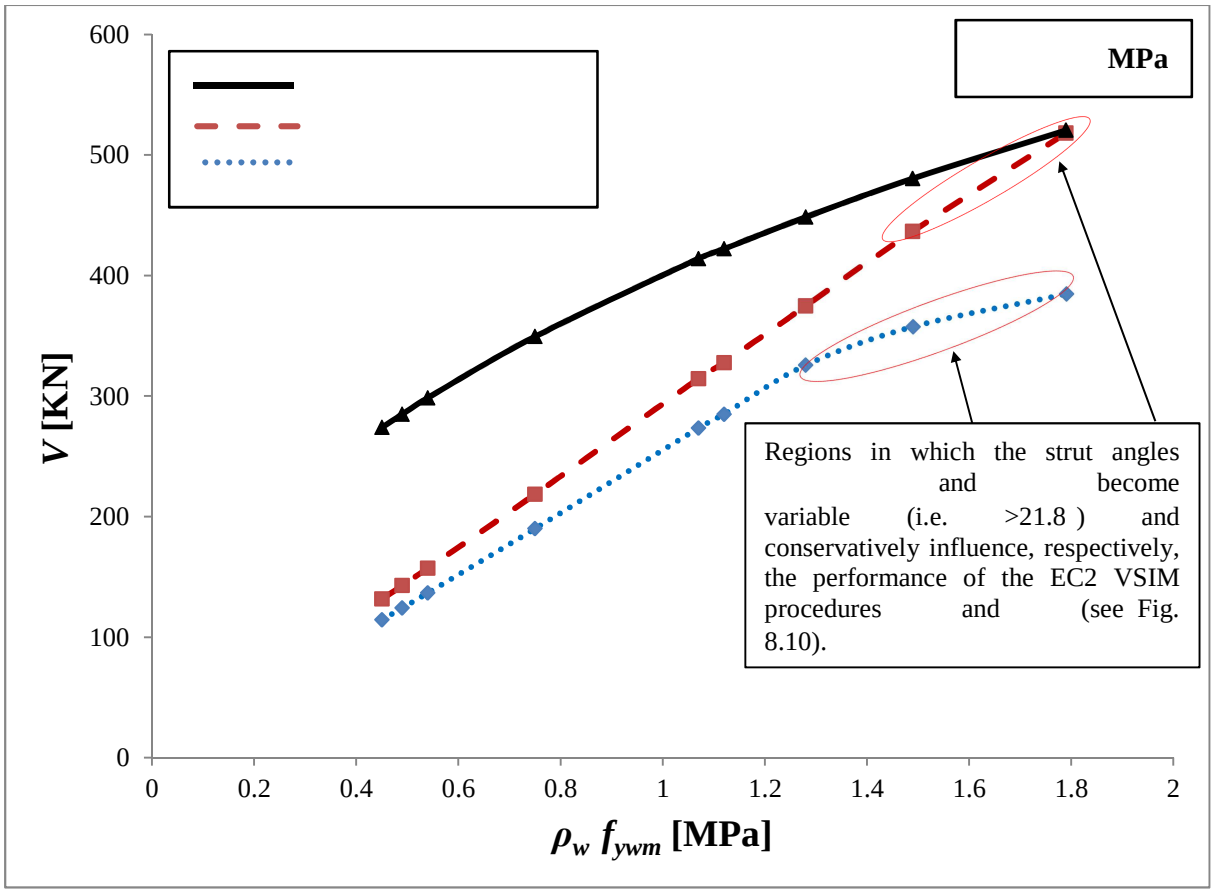

Figure 8.8. Graph of , , and versus at MPa

Table 8.8. Performance indicators derived from the simplified reliability model $g(\boldsymbol{X})_s$ applied to the 9 Test Cases at $f_{cm} = 98$ MPa

Test Case No.	$MF_d{}^*$	$V_{Rd,s}(\boldsymbol{X_k}, \boldsymbol{\gamma})$ [kN]	$V_{Rk,s}(\boldsymbol{X_k})$ [kN]	$V_{VSIM-Analytical}(\boldsymbol{X_m})$ [kN]	σ_X [kN]	β
1	0.24	114.4	131.6	398.4	23.8	5.9
2	0.25	124.1	142.7	414.6	25.8	5.7
3	0.26	136.7	157.2	434.8	28.4	5.5
4	0.31	190.0	218.5	510.8	39.4	4.7
5	0.38	273.3	314.3	609.3	56.8	3.8
6	0.38	285.0	327.7	621.6	59.2	3.7
7	0.41	325.7	374.5	662.7	67.6	3.3
8	0.45	379.9	436.9	713.2	78.9	2.9
9	0.49	455.9	524.3	777.2	94.7	2.5

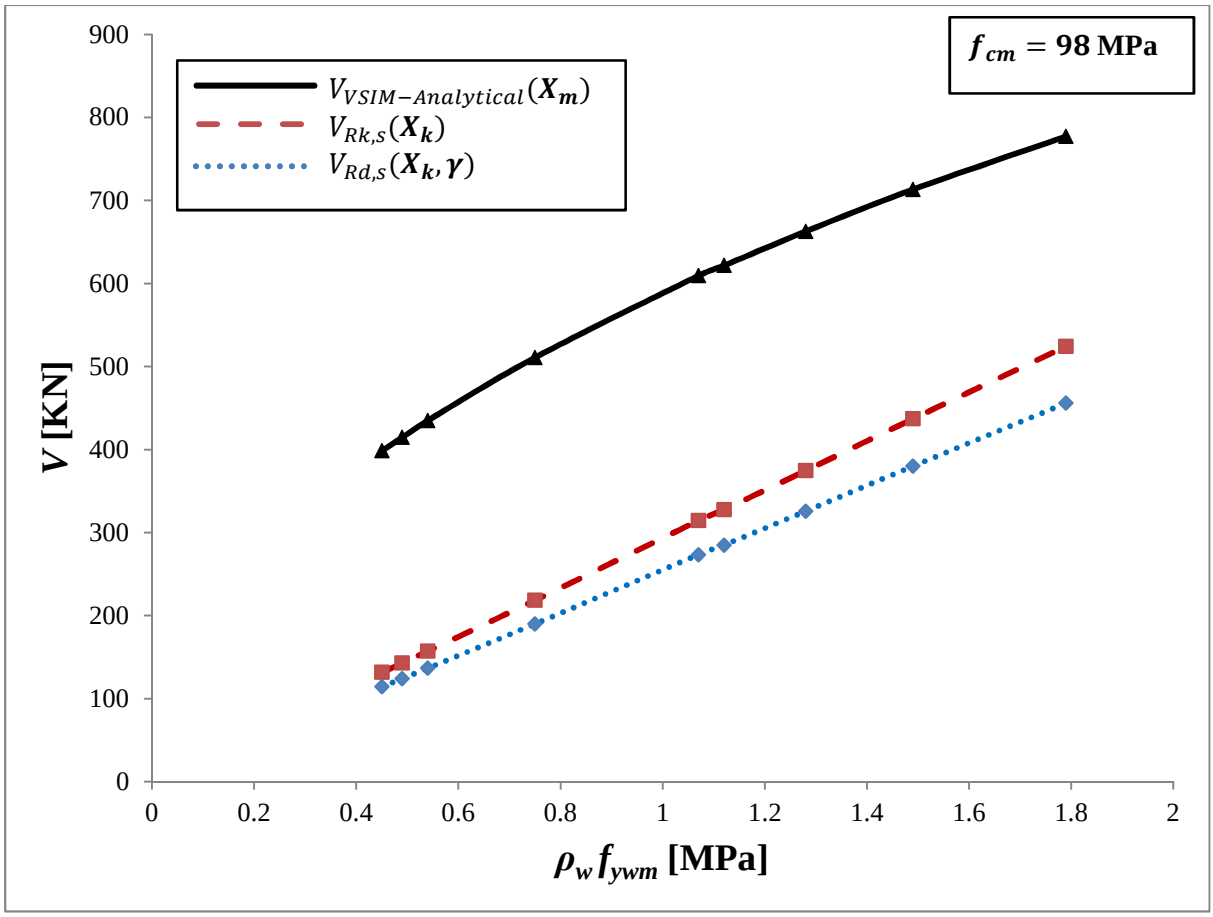

Figure 8.9. Graph of $V_{Rd,s}(\boldsymbol{X_k}, \boldsymbol{\gamma})$, $V_{Rk,s}(\boldsymbol{X_k})$, and $V_{VSIM-Analytical}(\boldsymbol{X_m})$ versus $\rho_w f_{ywm}$ at $f_{cm} = 98$ MPa

Assessment of estimated β- and σ_{GPM}-values as $\rho_w f_{ywm}$ varies

The inspection of Figure 8.8 ($f_{cm} = 33$ MPa) reveals that a conservative characteristic bias ($V_{VSIM-Analytical}(\boldsymbol{X_m}) > V_{Rk,s}(\boldsymbol{X_k})$ or $\frac{V_{VSIM-Analytical}(\boldsymbol{X_m})}{V_{Rk,s}(\boldsymbol{X_k})} > 1$) is maintained for the parametric range of $\rho_w f_{ywm}$ investigated. The Figure further illustrates that the difference $V_{VSIM-Analytical}(\boldsymbol{X_m}) - V_{Rd,s}(\boldsymbol{X_k}, \boldsymbol{\gamma})$ (or correspondingly, the $\beta \cdot \sigma_{GPM}$ distance) does not change significantly for the range of $\rho_w f_{ywm}$ considered (approx. 160 kN at 0.45 MPa; 123 kN at 1.3 MPa; 136 kN at 1.8 MPa). Table 8.7, on the other hand, indicates an increase in the uncertainty of the GPM σ_{GPM} with an increase in $\rho_w f_{ywm}$ (from Test Case 1 to 9), hence the reducing β-values with increasing $\rho_w f_{ywm}$ as shown in the Table. Similar observations can be made from Figure 8.9 and corresponding Table 8.8 for the situation when $f_{cm} = 98$ MPa.

The estimated β-values for the nine different $\rho_w f_{ywm}$ situations as described in Table 8.4, evaluated at three different concrete strengths ($f_{cm} = 33$ MPa, 40 MPa & 98 MPa), are shown graphically in Figure 8.10 in Section 8.2.2, where the trends of β-values at different $\rho_w f_{ywm}$ and f_{cm} situations are further discussed.

Influence of concrete strength f_{cm} on the predictions of $V_{Rd,s}(\boldsymbol{X_k}, \boldsymbol{\gamma})$, $V_{Rk,s}(\boldsymbol{X_k})$, σ_{GPM}, and $V_{VSIM-Analytical}(\boldsymbol{X_m})$

By primarily comparing Figure 8.9 ($f_{cm} = 33$ MPa) to Figure 8.8 ($f_{cm} = 98$ MPa), the following features are evident about the performance of the EC2 VSIM procedures due to a change in concrete strength (f_{cm}):

1. Firstly, it should be realised that the values of $V_{Rd,s}(\boldsymbol{X_k}, \boldsymbol{\gamma})$ and $V_{Rk,s}(\boldsymbol{X_k})$ are largely the same for the two Figures at the different $\rho_w f_{ywm}$ situations (i.e. they remain mostly unaltered by changes in concrete strength). The only differences in $V_{Rd,s}$ and $V_{Rk,s}$-values shown by the two Figures occur at a combination of (1) low concrete strengths (f_{cm}), and (2) high $\rho_w f_{ywm}$ situations; where both $V_{Rd,s}$ and $V_{Rk,s}$ predictions start to become non-linear as clearly indicated in Figure 8.8. The initial linearity portrayed by $V_{Rk,s}$ and $V_{Rd,s}$ predictions with increasing $\rho_w f_{ywm}$ situations in Figure 8.8 is caused by the 21.8° limit imposed on the concrete strut angle $\theta_{Limited}$ to prevent flatter angles and achieve operational VSIM procedures as discussed in

Sections 8.1.1 and 7.3.4. Flatter angles would imply higher (less conservative) $V_{Rk,s}$ and $V_{Rd,s}$ predictions. Naturally, the VSIM predicts flatter angles (< 21.8°) of the virtual concrete strut according to Equation 8.1. The concrete strut angle $\theta_{Analytical}$ for the VSIM-based GPM function $V_{VSIM-Analytical}(\boldsymbol{X})$ was allowed to freely assume calculated values according to Equation 8.1 (with no restriction), hence the greater and non-linear performance of $V_{VSIM-Analytical}(\boldsymbol{X_m})$ predictions at various $\rho_w f_{ywm}$ situations. Figure 8.8 (in contrast to Figure 8.9) clearly shows the region in which the concrete strut angle $\theta_{Limited}$ becomes variable (i.e. >21.8°; at low f_{cm} and high $\rho_w f_{ywm}$ situations) and begins to conservatively impact on the performance of $V_{Rd,s}$ procedures by affecting the $V_{VSIM-Analytical}(\boldsymbol{X_m}) - V_{Rd,s}(\boldsymbol{X_k}, \boldsymbol{\gamma})$ distance ($= \beta \cdot \sigma_{GPM}$ distance) for the limited range shown in the Figure.

2. Secondly, it should be noted that Figure 8.9 ($f_{cm} = 98\,MPa$) shows a larger $V_{VSIM-Analytical}(\boldsymbol{X_m}) - V_{Rd,s}(\boldsymbol{X_k}, \boldsymbol{\gamma})$ difference ($= \beta \cdot \sigma_{GPM}$ distance) than Figure 8.8 ($f_{cm} = 33\,MPa$) at all comparable $\rho_w f_{ywm}$ situations. Recall from point (1) above that $V_{Rd,s}$-values are largely the same for both Figures; hence implying that the change in the $V_{VSIM-Analytical}(\boldsymbol{X_m}) - V_{Rd,s}(\boldsymbol{X_k}, \boldsymbol{\gamma})$ difference is predominantly caused by $V_{VSIM-Analytical}(\boldsymbol{X_m})$ predictions being sensitive to concrete strength (f_{cm}). The sensitivity of $V_{VSIM-Analytical}(\boldsymbol{X_m})$ to f_{cm} is explained by the absence of a restriction on its associated concrete strut angle $\theta_{Analytical}$, which freely assumes any calculated value as discussed in Section 8.1.1. Most of the calculated $\theta_{Analytical}$-values for the various Test Cases were below 21.8°, save for a select few cases that were representative of a combination of low f_{cm}.and high $\rho_w f_{ywm}$ situations.

3. Cognizance must also be taken from Tables 8.7 ($f_{cm} = 33\,MPa$) and 8.8 ($f_{cm} = 98\,MPa$) that σ_{GPM}-values are predominantly the same for comparable Test Cases; with only marginal differences in σ_{GPM}-values for Test Cases 8 and 9 shown between the Tables. σ_{GPM}-values are therefore not sensitive to concrete strength f_{cm}.

4. Hence considering comments from points (1), (2), and (3) above, structural performance at different concrete strengths (f_{cm}) is influenced predominantly by the sensitivity of $V_{VSIM-Analytical}(\boldsymbol{X_m})$ predictions to concrete strength. The sensitivity

of $V_{Rk,s}$ and $V_{Rd,s}$ to concrete strength f_{cm} is inhibited predominantly by the enforcement of the 21.8° concrete strut angle lower limit. Recall that concrete strength is reflected only through its influence on the strut angle in VSIM procedures (see Equation 8.2); bearing no direct contribution to shear resistance (operational resistance of VSIM procedures provided by stirrups only).

Trends of estimated β-values with f_{cm} and $\rho_w f_{ywm}$ are reported and discussed in Section 8.3.

8.3 β-VALUES AT DIFFERENT $\rho_w f_{ywm}$ AND f_{cm} SITUATIONS

The estimated β-values obtained for the 27 Test Cases (9 $\rho_w f_{ywm}$ situations investigated at 3 different concrete strengths, see Section 8.1.4), determined from FORM analyses of $g(\boldsymbol{X})_s$, are presented in Figure 8.8. The resistance performance requirements for SANS 10160-1 RC2 ($\beta_{Rt} = 2.4$) and RC3 ($\beta_{Rt} = 2.8$), and EC0 RC2 ($\beta_{Rt} = 3.04$) are also shown in the Figure. The estimated β-values associated with an additional situation at $f_{cm} = 40$ MPa is presented in the Figure, to properly capture the variation of β-values with changing concrete strength (f_{cm}). The $f_{cm} = 40$ MPa situation was omitted from preceding discussions as the results of situations $f_{cm} = 33$ MPa versus those of $f_{cm} = 98$ MPa (i.e. the extremes) were adequate in making pertinent points about the performance of VSIM procedures.

As expected, Figure 8.10 shows:

1. A decrease in estimated β-values as $\rho_w f_{ywm}$ increases, and
2. A general increase in β-values with increasing concrete strength f_{cm}

Reasons for the specific trends of β-values with varying $\rho_w f_{ywm}$ and f_{cm} situations are detailed below.

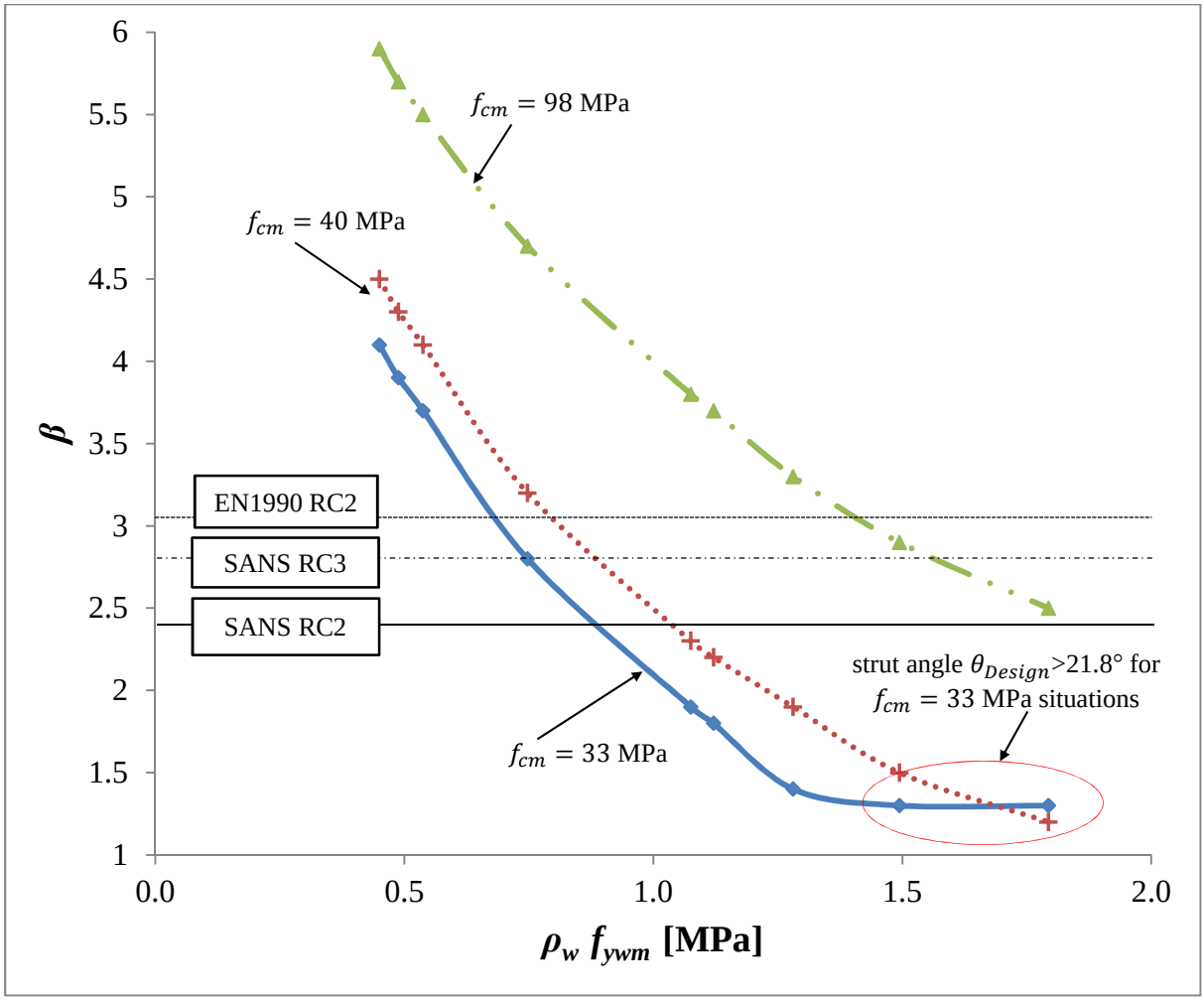

Figure 8.10. Reliability performance β versus the amount of stirrup reinforcement $\rho_w f_{ywm}$ at different concrete strengths (f_{cm})

8.3.1 Reason for non-linear (parabolic) trend of β-values with $\rho_w f_{ywm}$

The non-linear trend of β-values with increasing $\rho_w f_{ywm}$ situations is expected, due predominantly to the inherent non-linearity of GPM predictions $V_{VSIM-Analytical}(\boldsymbol{X_m})$ in such situations as can be witnessed from Figures 8.8 (f_{cm} = 33 MPa) and 8.9 (f_{cm} = 98 MPa). The non-linear performance of $V_{VSIM-Analytical}(\boldsymbol{X_m})$ predictions shown in the Figures is caused by its dependence on the variable concrete strut angle $\theta_{Analytical}$, which is a non-linear trigonometric function that typically predicts strut angles flatter than 21.8° as previously discussed.

8.3.2 Reason for the decrease in β-values with increasing $\rho_w f_{ywm}$

For a given case of concrete strength (either of $f_{cm} = 33$ MPa, or 98 MPa etc.), the distance $V_{VSIM-Analytical}(\boldsymbol{X_m}) - V_{Rd,s}(\boldsymbol{X_k}, \boldsymbol{\gamma})$ remains relatively constant at the various $\rho_w f_{ywm}$ situations considered as can be observed from Figure 8.8 or Figure 8.9. However, there is increasing uncertainty about the GPM as $\rho_w f_{ywm}$ increases (i.e. σ_{GPM} increases also), hence the decreasing β-values with increasing $\rho_w f_{ywm}$ situations.

8.3.3 Reason for the sensitivity of estimated β-values to concrete strength f_{cm}

The inspection of Figures 8.8 ($f_{cm} = 33$ MPa) and Figure 8.9 ($f_{cm} = 98$ MPa) and associated Tables show

1. $V_{Rd,s}$ and $V_{Rk,s}$ predictions are generally not sensitive to changes in concrete strength f_{cm}, except for the limited range shown in Figure 8.8 at a combination of high $\rho_w f_{ywm}$ (> 1.3 MPa) and low f_{cm},
2. σ_{GPM}-values are also generally not sensitive to concrete strength f_{cm}, except for the same region distinguished in (1) above (based on the comparison of σ_{GPM}-values from Tables 8.7 and 8.8)
3. $V_{VSIM-Analytical}(\boldsymbol{X_m})$ predictions are, however, sensitive to concrete strength f_{cm} since the magnitude of its predicted values differ between the two Figures.

Sensitivity of β to f_{cm} is clearly influenced to some degree by the sensitivity of $V_{VSIM-Analytical}(\boldsymbol{X_m})$ predictions to f_{cm}. Furthermore, as a consequence of point (1) above, $V_{Rd,s}$ generally does not give credit for increasing f_{cm}. In the light of that, sensitivity of β to f_{cm} evolves from (1) under-prediction by $V_{Rd,s}$ of the extra design capacity achieved by increased concrete strength, and (2) sensitivity of $V_{VSIM-Analytical}(\boldsymbol{X_m})$ predictions to f_{cm}.

The general trend of β-values as concrete strength increases is not upheld in the combined region of low f_{cm} and high $\rho_w f_{ywm}$ situations as highlighted in Figure 8.10. This behaviour is caused by the fact that at a combination of low f_{cm} and high $\rho_w f_{ywm}$ situations ($f_{cm} = 33$ MPa & $\rho_w f_{ywm} > 1.5$ MPa approx.), the strut angle $\theta_{Limited}$ from Equation 8.2 ($V_{Rd,s}$

function) becomes greater than 21.8°, after which it can assume any calculated value below 45°. This induces non-linearity to the performance of $V_{Rd,s}$ procedures and reduces the rate of increase of $V_{Rd,s}$ predictions as $\rho_w f_{ywm}$ further increases as shown in Figure 8.8. This implies at high $\rho_w f_{ywm}$ and low f_{cm} a slightly increased distance $V_{VSIM-Analytical}(\boldsymbol{X_m}) - V_{Rd,s}(\boldsymbol{X_k}, \boldsymbol{\gamma})$ ($= \beta \cdot \sigma_{GPM}$ distance), thereby producing the 'levelling off' or 'plateau' effect highlighted in Figure 8.10; to the extent that β-values at $f_{cm} = 33$ MPa exceed those at the higher strength $f_{cm} = 40$ MPa for the region indicated in the Figure.

8.3.4 Assessment of β-values versus performance requirements for shear resistance

For all f_{cm} situations considered, the β-values presented in Figure 8.10 generally decline with increasing $\rho_w f_{ywm}$ until they eventually cease to satisfy the performance requirements for shear resistance recommended by basis of design standards SANS 10160-1 and EC0.

The most critical performance is, of course, the case of low concrete strength at $f_{cm} = 33$ MPa, exceeding limits of safe application according to EC0 RC2, SANS 10160-1 RC3 and RC2, respectively, at approximately 0.7 MPa, 0.75 MPa, and 0.9 MPa. For slightly higher concrete strengths at $f_{cm} = 40$ MPa, the same sequence of performance limits are exceeded at approximately 0.8 MPa, 0.9 MPa, and 1 MPa. At $f_{cm} = 98$ MPa, same sequence occurs at approximately 1.4 MPa, 1.6 MPa, and ≈ 1.9 MPa (a bit of an extrapolation, see Figure 8.10).

8.3.5 Implications for the application of EC2's VSIM design procedure

Based on the results from the previous Section, the following conclusive statements can be made about the application/performance of the EC2 VSIM design procedure:

1. Higher concrete grades/strengths can be used to improve the safety and reliability performance of the procedures for a specific $\rho_w f_{ywm}$ situation

2. Based on the results of the estimated β-values presented in Figure 8.10, it is advisable to use high strength concretes (> 50 MPa) at $\rho_w f_{ywm}$ of approx. 0.8 MPa (to satisfy EC0 RC2 requirements); 0.9 MPa (to satisfy SANS 10160-1 RC3); and approx. 1.0 MPa (to satisfy SANS 10160-1 RC2)

3. Expressly stated, based on (1) and (2) above, high strength concrete should be used both in situations where shear is critical (heavy loads in shear) viz. situations where large quantities of stirrups are utilised (high $\rho_w f_{ywm}$)

8.4 COMPARISON OF β-VALUES OBTAINED FROM $g(X)$ AND $g(X)_s$

Table 8.9 below provides a comparison of the estimated β-values for Test Cases 1 and 9 (evaluated at concrete strength $f_{cm} = 33\ MPa$) obtained from the full probabilistic model $g(\boldsymbol{X})$, versus those obtained from the simplified performance function $g(\boldsymbol{X})_s$.

Table 8.9. Estimated β-values for Test Cases 1 and 9 at $f_{cm} = 33$ MPa compared

Test Case No.	**β from $g(X)$**	**β from $g(X)_s$**
1	3.5	4.1
9	1.1	1.3

The results from Table 8.9 indicate that estimates of β obtained from $g(\boldsymbol{X})_s$ were of magnitude 0.2 to 0.6 greater than β-values obtained from $g(\boldsymbol{X})$. Estimates of β generated from $g(\boldsymbol{X})_s$ were expected to be greater, since for the simplified reliability model σ_{GPM} is smaller (as compared to σ_{GPM} from $g(\boldsymbol{X})$). The smaller σ_{GPM}-values associated with $g(\boldsymbol{X})_s$ are caused by the underestimation of the dispersion of $g(\boldsymbol{X})$ due to neglecting the contributions of other basic variables in the simplified version of the performance function (since it is dependent only on the uncertainty associated with $MF_{VSIM-Analytical}$, hence larger β-values to satisfy a fixed '$\beta \cdot \sigma_{GPM}$' distance).

8.5 VALIDATION OF MS EXCEL ANALYSIS TOOLS USING VaP 1.6

VaP 1.6 was used to ensure the correctness of all FORM-related calculations conducted using programmed Excel tools developed for this study. VaP validations were set up to allow full probabilistic representation of $g(\boldsymbol{X})$ hence the results from Figures 8.11 and 8.12 below can be compared to the results of Test Cases 1 and 9 given, respectively, in Tables 8.5 and 8.6. It should be noted that a concrete mean value strength of $f_{cm} = 33$ MPa was employed during all assessments in this Section. Two kinds of checks were performed using VaP 1.6, namely:

1. A check of converged β-values (or HL-Index in Figures below) for Test cases 1 and 9
2. A check of the expected value of the performance function $g(\boldsymbol{X})$ for Test Cases 1 and 9 (or G[E{**X**}]) in the Figures below, where:

$$\mathrm{G[E\{\mathbf{X}\}]} = V_{VSIM-Analytical}(\boldsymbol{X_m}) - V_{Rd,s}(\boldsymbol{X_k}, \boldsymbol{\gamma}) \qquad [8.13]$$

Notice that G[E{**X**}] is equivalent to the $\beta \cdot \sigma_{GPM}$ distance shown in Figures 8.5 and 8.6.

```
Limit State Function G :

    G = (M*(A/s)*0.9*(h-C-3*a-e)*f*SQRT(1-((A*f)/(b*s*v*d*z)))/SQRT((A*f)/(b*s*v*d*z)))-114420.14

FORM Analysis of G:

    HL - Index = 3.65          P(G<0) = 0.000131

    Name          Alpha        Design Value
    A            -0.042         156.624
    C             0.099          31.947
    M            -0.899           0.413
    a             0.010          16.012
    b            -0.022         349.713
    d            -0.224           0.780
    e             0.002          10.002
    f            -0.124         485.061
    h            -0.053         499.037
    s             0.062         501.444
    z            -0.329          27.383


G(E[X]) for G:

    G(E[X]) = 159440
```

$V_{Rd,s}(\boldsymbol{X_k}, \boldsymbol{\gamma})$ in N

Figure 8.11. Results of VaP 1.6 FORM analysis of Test Case 1 at $f_{cm} = 33$ MPa

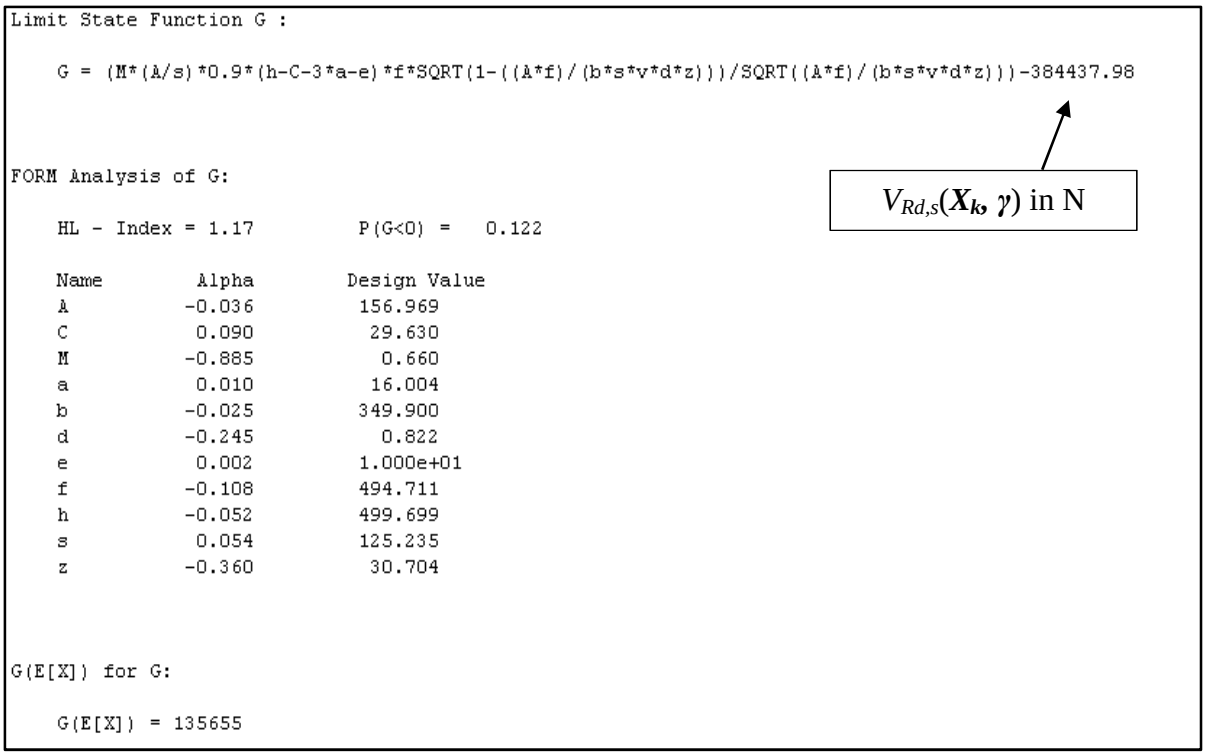

Figure 8.12. Results of VaP 1.6 FORM analysis of Test Case 9 at $f_{cm} = 33$ MPa

VaP only allows the use of a limited number of symbols, creating the need for alternative symbols to be used when defining $g(\boldsymbol{X})$. The symbol 'd' from the Figures 8.11 and 8.12 was used to represent the scale effects coefficient α_{cc}, and z for concrete strength f_c.

8.5.1 Comparison of β-values and other performance indicators between Excel calculations and VaP results

A comparison of the results of Figures 8.11 and 8.12, respectively, to the results of Tables 8.5 and 8.6 reveals the following:

1. That estimated β-values determined from VaP analysis and Excel calculations are closely comparable; a maximum difference in the estimated β-value of 0.2 is observed for Test Case 9 ($\beta_{VaP} = 3.65$; $\beta_{Excel\ calc} = 3.45$)
2. That the uncertainty of the VSIM based GPM function $V_{VSIM-Analytical}(\boldsymbol{X})$ is indeed almost completely dominated by $MF_{VSIM-Analytical}$ (average sensitivity factor for

$MF_{VSIM-Analytical}$ $\alpha_{MF} = 0.9$ from VaP results; average $\alpha_{MF} = 0.95$ from Excel calculations)

Further comparison of the expected values of the performance function $g(\boldsymbol{X})$ (or G[E{**X**}]) showed that the $\beta \cdot \sigma_{GPM}$ distances evaluated from the developed Excel tools were almost identical to those evaluated corresponding VaP analyses. For Test Case 1, G[E{**X**}] = 159.6 kN from the Excel tool (see Figure 8.5), versus G[E{**X**}] = 159.4 kN from VaP analysis (shown in Figure 8.11). For Test Case 9, G[E{**X**}] = 135.9 kN from the Excel tool (see Figure 8.6), versus G[E{**X**}] = 135.7 kN from VaP analysis (as shown in Figure 8.12).

The estimated β-values from VaP analyses were consistently greater than those determined from equivalent Excel calculations. Given the fact that $\beta \cdot \sigma_{GPM}$ distances were almost identical from both assessments, the greater β-values from the VaP analyses were obviously caused by a lower estimate of the dispersion of the GPM function σ_{GPM} during VaP analyses compared to equivalent assessments performed using the developed Excel tools. This could be attributed to the fact that VaP predicted a slightly lower influence of the highly uncertain parameter $MF_{VSIM-Analytical}$ (relatively high C.O.V = 0.18 / 0.84 = 0.21, see Table 8.2) on the distribution of the GPM function $V_{VSIM-Analytical}(\boldsymbol{X})$ ($\alpha_{MF} \approx 0.9$). Excel calculations, on the other hand, predicted a slightly greater influence of $MF_{VSIM-Analytical}$ on $V_{VSIM-Analytical}(\boldsymbol{X})$ ($\alpha_{MF} \approx 0.95$), resulting in larger uncertainty associated with the GPM function (higher σ_{GPM}-values).

Nonetheless, the comparability of obtained β-values, direction cosines (α_X), and G(E{**X**}) values provided sufficient indication that spreadsheet operations programmed for this study were in proper working order.

CHAPTER 9

RELIABILITY ANALYSIS USING R2k CAPCITY PREDICTIONS TO GENERATE THE GPM FOR STIRRUP RESISTANCE

This Chapter presents an alternative approach to the reliability performance assessment of the EC2 stirrup design procedure. For the case of the performance function $g(\boldsymbol{X})$ presented here, the GPM for stirrup resistance is established on the basis of the probabilistic representation of unbiased R2k shear capacity predictions. The reliability performance assessment presented here was commissioned to validate the results obtained from the basic reliability investigations presented in Chapter 8 i.e. where the GPM is based on the VSIM-Analytical calculation procedure.

R2k unbiased capacity predictions were admitted as an alternative for GPM representation for two reasons (based on results presented from Chapter 7):

1. Slightly improved accuracy of MF_{R2k} realisations ($\mu_{MF} = 1.14$, 14 % over-conservative) compared to $MF_{VSIM-Analytical}$ realisations ($\mu_{MF} = 0.84$, 16 % under-conservative)
2. More importantly, MF_{R2k} realisations were associated with a standard deviation $\sigma_{MF} = 0.20$ comparable to that of $MF_{VSIM-Analytical}$ realisations ($\sigma_{MF} = 0.18$). The VSIM-Analytical calculation procedure was used as the primary means of establishing the GPM for stirrup resistance due to the lower standard deviation σ_{MF} associated with $MF_{VSIM-Analytical}$ realisations.
3. In comparison to $MF_{VSIM-Analytical}$ realisations, MF_{R2k} realisations showed milder trends to important design parameters affecting shear strength, especially $\rho_w f_{yw}$ (see Figures 7.8 and 7.9). Furthermore, the trend of normalised resistance predictions from R2k provided a closer match to equivalent experimental results, compared to VSIM-Analytical (see Figure 7.10).
4. R2k capacity predictions can be classified as LoA IV estimates of shear resistance (highest level of approximation) according to the *fib* MC 2010 classification system.

This Chapter is structured in essentially the same manner as Chapter 8, bearing very much the outline presented in Figure 8.1, but is presented in a concise manner.

9.1 R2K BASED PERFORMANCE FUNCTION FOR RELIABILITY ANALYSIS

For reliability assessments conducted using R2k predictions, the performance function $g(\boldsymbol{X})$ and Limit State Function $g(\boldsymbol{X}) = 0$ for stirrup resistance were described by:

$$g(\boldsymbol{X}) = V_{R2k}(\boldsymbol{X}) - V_{Rd,s}(\boldsymbol{X_k}, \boldsymbol{\gamma}) \quad [9.1]$$

$$\therefore\ g(\boldsymbol{X}) = MF_{R2k} \cdot V_{R2k}(\boldsymbol{x}) - V_{Rd,s}(\boldsymbol{X_k}, \boldsymbol{\gamma}) = 0 \quad [9.2]$$

where $V_{R2k}(\boldsymbol{X})$ from Equation 9.1 represents the probability distribution of stirrup resistance based on sectional analysis program R2k. $V_{R2k}(\boldsymbol{x})$ in Equation 9.2 is therefore the unbiased shear capacity of a stirrup reinforced concrete beam offered by R2k, based on input quantities of its basic variables $\boldsymbol{x}$. The basic input variables required to enable R2k capacity predictions are discussed in Section 9.1.1. Due to the non-analytical manner in which R2k is used in the investigation, a laborious numerical differentiation procedure was used to obtain the reliability model as discussed in Section 9.1.2; save for the exception of MF_{R2k} whose checking point partial derivative $\left(\frac{\partial g(\boldsymbol{X})}{\partial MF_{R2k}}\right)^*$ could be determined analytically as can be witnessed from Equation 9.2.

9.1.1 Additionally required parameters for the probability model $g(\boldsymbol{X})$

$V_{R2k}(\boldsymbol{X})$, as a direct consequence of being based on R2k, was comprised of essentially the same basic variables given in Table 8.2 (with the exception of a, e, α_{cc}, and obviously $MF_{VSIM-Analytical}$ which is replaced by MF_{R2k}). Furthermore, additionally required random variables that were initially required to establish $V_{R2k}(\boldsymbol{X})$ (only during the preliminary sensitivity study) were (1) the yield strength of longitudinal tension reinforcement f_{yl}, and (2) the total cross-section area of the longitudinal tension reinforcement $A_{s,tot}$.

Parameters for the longitudinal geometry were also required since R2k provides capacity predictions based on beam behaviour (shear-flexure interactions) and not simply on the definition of beam cross-section parameters. As such, other deterministic parameters (shear span-to-depth ratio a/d and aggregate size d_{agg}) had to be specified to enable the use of R2k

in establishing $V_{R2k}(\boldsymbol{X})$. Table 9.1 below gives the quantities of the additional parameters (common to all Test Cases used for the performance assessment) that were specified to enable R2k predictions.

Table 9.1. Characteristic quantities of some parameters common to all Test Cases required by R2k

*† $A_{s,tot}$ [mm^2]	† f_{yl} [MPa]	d_{agg} [mm]	a/d	**Beam Longitudinal geometry**
4825.5	450	19	2.5	Simply supported, with central point load

*6 Y32 bars (A_s 1 bar = 804.25 mm^2), see Figure 8.2.

†Same probability models as A_{sw} (for $A_{s,tot}$) and f_{yw} (for f_{yl}) from Table 8.2.

As discussed in Section 5.3, the value of a/d of 2.5 was selected for R2k analyses to represent the shear-critical performance of RC structures. The value of a/d of 2.5 represents a regime where diagonal-tension stresses are prominent and shear strength therefore becomes critical.

9.1.2 Procedure for numerical differentiation

To generate the distribution of the GPM $V_{R2k}(\boldsymbol{X})$ for the reliability analysis by checking point iterations, a prediction was first made using an original value of the basic random variable X, denoted X_{orig}. A repeat prediction was thereafter made using a 2 % increment in X ($X_{2\%\,inc}$) – all other variables kept fixed. The change in the ultimate shear strength prediction associated with the increment of parameter X was noted. It then followed that:

$$\left(\frac{\partial g(\boldsymbol{X})}{\partial \boldsymbol{X}}\right)^{*} = \left(\frac{V^{*}_{R2k,2\%\,inc} - V^{*}_{R2k,orig}}{X^{*}_{2\%,inc} - X^{*}_{orig}}\right) \cdot \sigma^{N}_{X} \qquad [9.3]$$

where Equation 9.3 was applied initially in the assessment of the partial derivatives for all basic random variables (during preliminary sensitivity study) such as A_{sw}, s, h, f_{yw}, f_c, etc.

A simplified performance function $g(\boldsymbol{X})_s$ was ultimately developed, maintaining only the basic variables MF_{R2k}, f_{yw}, and f_c as random quantities as discussed in Section 9.1.4. The partial derivative of the MF was determined analytically from Equation 9.2 as:

$$\left(\frac{\partial g(\boldsymbol{X})}{\partial MF_{R2k}}\right)^* = V_{R2k}(\boldsymbol{x}^*) \cdot \sigma_{MF}^N \quad [9.4]$$

where $V_{R2k}(\boldsymbol{x}^*)$ represents the value of unbiased shear resistance determined by feeding the unbiased checking point values x^* of selected basic variables at each iteration into the sectional analysis program R2k.

9.1.3 Reliability analysis of the representative design situations

Parameters for the nine (9) basic Test Cases that were established to investigate the consistency of β-values across the parametric range of $\rho_w f_{ywm}$ are presented in Tables 9.2. As established in Chapter 8, the sensitivity of shear resistance to concrete strength (f_{cm}) further warranted the inspection of the nine basic Test Cases at three different concrete strengths; namely (1) $f_{cm} = 33$ MPa, (2) $f_{cm} = 40$ MPa, and (3) $f_{cm} = 98$ MPa. In terms of shear reinforcement, the nine Test Cases covered the range of $\rho_w f_{ywm}$ from 0.64 MPa to 2 MPa.

The results obtained in this Chapter (β-values) were not compared against the basis of design requirements set by the standards SANS 10160-1 and EC0, as was done in Chapter 8. This was primarily due to the fact that performance investigations conducted using R2k were incorporated simply to validate results obtained from the conventional reliability model (Chapter 8). However, some important insights were gained from the use R2k as part of an alternative procedure as discussed in Chapter 10.

Table 9.2. Parameters for the Test Cases used for the performance assessment of EC2 stirrup design procedure (Elaboration of parameters used to establish different Test Cases)

Test Case No.	A_{sw} **[mm^2]**	f_{ywm} **[MPa]**	b_w **[mm]**	s **[mm]**	$\rho_w f_{ywm}$ $(\rho_w f_{ywk})$ **[MPa]**	MF_{R2k} $(\mu_{MF};\ \sigma_{MF}{}^{\dagger})$
1	157.1	500	350	350	0.64 (0.58)	1.16
2	157.1	500	350	300	0.75 (0.67)	1.15
3	157.1	500	350	250	0.90 (0.81)	1.14
4	157.1	500	350	225	1.00 (0.90)	1.13
5	157.1	500	350	200	1.12 (1.01)	1.11
6	157.1	500	350	180	1.25 (1.12)	1.10
7	157.1	500	350	150	1.49 (1.35)	1.08
8	157.1	500	350	125	1.79 (1.62)	1.04
9	157.1	500	350	110	2.04 (1.84)	1.02

† Constant standard deviation $\sigma_{MF} = 0.20$ applied for all Test cases

It must be noted from Table 9.2 that the mean value μ_{MF} of MF_{R2k} was considered sensitive to $\rho_w f_{ywm}$; this action was motivated by the trend of MF_{R2k} versus $\rho_w f_{ywm}$ shown in Figure 7.9(a). Based on observations of the aforementioned Figure, the mean value of MF_{R2k} was defined by the relation:

$$\mu_{MF} = -0.102\left(\rho_w f_{ywm}\right) + 1.228 \qquad [9.5]$$

The standard deviation of MF_{R2k}, on the other hand, was taken as the constant value of $\sigma_{MF} = 0.20$ as noted in Table 7.4.

9.1.4 Preliminary sensitivity study and the simplified model $g(X)_s$ for reliability analysis

In similar fashion to Chapter 8, a simplified performance function $g(\boldsymbol{X})_s$ was developed to conduct the main reliability (β-value) assessments of the EC2 design function $V_{Rd,s}(\boldsymbol{X_k}, \boldsymbol{\gamma})$. However, Test Case 8 (shown shaded in Table 9.2, equivalent also to Test Case 9 shown in Figure 8.4) was used as part of a preliminary sensitivity study used to determine the basic random variables relevant for the effective representation of the R2k-based GPM for shear resistance $V_{R2k}(\boldsymbol{X})$.

Due to the laborious nature of implementing R2k to represent $V_{R2k}(\boldsymbol{X})$ (as a consequence of the number of input parameters required for R2k predictions discussed in 9.1.1, in addition to numerical process of obtaining partial derivatives $\left(\frac{\partial g(\boldsymbol{X})}{\partial \boldsymbol{X}}\right)^*$ described in Section 9.1.2) the preliminary sensitivity Test Case was not solved until convergence at the FORM design point i.e. convergence of estimated β-value at the design point $\boldsymbol{x_d}^*$. Instead, the results of the 1st iteration of the FORM procedure were used for the assessment of the various direction cosines α_X. Preliminary indications showed clearly that MF_{R2k} is also a prominent source of uncertainty affecting the probability distribution $V_{R2k}(\boldsymbol{X})$ (similar to $V_{VSIM-Analytical}(\boldsymbol{X})$ which is completely dominated by $MF_{VSIM-Analytical}$). However, unlike $V_{VSIM-Analytical}(\boldsymbol{X})$, the simplified performance function $g(\boldsymbol{X})_s$ also considered the influences of stirrup yield strength, f_{yw}, and concrete strength, f_c, as part of the representation of $V_{R2k}(\boldsymbol{X})$. The results of the preliminary sensitivity study are presented in the next Section.

It is worth noting at this point that due to some numerical difficulties experienced with the application of R2k during reliability modelling, only a limited set of verifications were conducted using GPM representation $V_{R2k}(\boldsymbol{X})$ to verify main trends of shear performance from Chapter 8 (where VSIM-Analytical forms the basis of the GPM). The application of R2k during reliability modelling, including instabilities experienced, is given specific attention in Section 9.1.6.

9.1.5 Results of the preliminary sensitivity assessment

The results of the 1st iteration of the FORM sensitivity study for Test Case 8 ($\rho_w f_{ywm} = 1.8$ MPa), considered at $f_{cm} = 33$ MPa, are presented in Table 9.3 below. The Table provides indication of the dominating influence of MF_{R2k} with $\alpha_{MF} = 0.86$. Since only the 1st iteration FORM analysis was considered, other less considerable influences with $\alpha_X \approx |0.2|$ and above were admitted as part of the simplified GPM model. Hence, basic variables f_{yw} and f_c were maintained as random quantities in the simplified performance function $g(\boldsymbol{X})_s$.

Table 9.3. Results of the 1st Iteration of the FORM analysis for Test Case 8 at $f_{cm} = 33$ MPa

$\boldsymbol{X}$	**Unit**	$\boldsymbol{X_k}$	$\boldsymbol{x^*}$	$\boldsymbol{\sigma_x}$	**Distn.**	$\left(\frac{\boldsymbol{dg}}{\boldsymbol{dx}}\right)^*$	$\boldsymbol{\alpha_x^*}$
MF_{R2k}	-	-	0.67	0.20	2P-LN	74069.4	0.86
A_{sw}	mm^2	157.1	157.1	3.14	N	3900	0.05
s	mm	125	125	3.75	N	-8400	-0.1
h	mm	500	500	5	N	-7200	0.08
C	mm	30	30	9	2P-LN	-23484.3	-0.27
f_{yw}	MPa	450	500	30	2P-LN	15606.3	0.18
f_{yl}	MPa	450	500	30	2P-LN	0	0
b_w	mm	350	350	3.5	N	2300	0.03
f_c	MPa	25	33	4.86	2P-LN	32228.8	0.37
$A_{s,tot}$	mm^2	4825.5	4825.5	96.5	N	600	0.01
					SRSS	86390.5	1.00

Notice from Table 9.3 that concrete cover C as a random variable initially showed a contribution of $\alpha_X > |0.2|$ i.e. $\alpha_C = -0.27$. However, independent (initial stage) analyses provided sufficient indication that C could be treated Deterministically (DET) during the performance assessment of the simplified function $g(\boldsymbol{X})_s$. Estimated β-values were compared at the FORM design point for Test Cases 4 (1.0 MPa) and 5 (1.1 MPa) from Table 9.2, both having a mean concrete strength of $f_{cm} = 33$ MPa. Separate situations for each Test Case were considered where (1) C was treated deterministically at 30 mm, versus (2)

situations where C was allowed to assume the probability described in Table 9.3. The influence of treating C deterministically had an inconsequential influence on the estimated β-value for the Test Cases. Thus, to save on computation time and effort (without losing design point accuracy), C was subsequently treated deterministically at 30 mm for all basic investigations.

9.1.6 The stability of R2k best-estimate predictions during the process of numerical differentiation

Recall that the good accuracy ($\mu_{MF_{R2k}} = 1.14$) and reasonable spread ($\sigma_{MF_{R2k}} = 0.20$) associated with R2k capacity predictions warranted the consideration of $V_{R2k}(\boldsymbol{X})$ as an alternative GPM representation to validate results obtained from the primary function $V_{VSIM-Analytical}(\boldsymbol{X})$.

However, R2k did not portray absolute stability with respect to the variables necessary for the representation of $V_{R2k}(\boldsymbol{X})$ (i.e. f_{yw} & f_c) when the numerical differentiation procedure described in Section 9.1.2 was applied during reliability analysis. This was particularly the case for the set of $\rho_w f_{ywm}$ Test Cases (shown in Table 9.2) assessed at $f_{cm} = 40$ MPa and $f_{cm} = 98$ MPa. The lack of stability of R2k capacity predictions with respect to f_{yw} and f_c did not pose a problem for the set of $\rho_w f_{ywm}$ Test Cases assessed at $f_{cm} = 33$ MPa..

Intuitively, ultimate resistance in shear V should increase proportionally with either of f_{yw} or f_c. This, however, was not always the case with R2k predictions with respect to both f_c (at $f_{cm} = 40$ MPa & 98 MPa situations) and f_{yw} when 2 % increments were applied to either variable to obtain the respective checking point derivatives $\left(\frac{\partial g(\boldsymbol{X})}{\partial \boldsymbol{X}}\right)^*$ (see Equation 9.3). Signs for $\left(\frac{\partial g(\boldsymbol{X})}{\partial \boldsymbol{X}}\right)^*$ would fluctuate between negative $(-)$ and positive $(+)$, implying increments in f_c or f_{yw} did not always result in the expected increments in ultimate resistance V. This anomaly made it impossible to converge to an estimate of β for situations in which it occurred. Hence, the estimated β-values reported in Figure 9.4 pertain exclusively to

situations where convergence was achieved (situations where convergence was not achieved are not reported).

Figures 9.1 and 9.2 below show the results of a simple study, illustrating the fluctuation of R2k's capacity predictions V_{R2k} against basic variables f_c and f_{yw}, respectively, for a Test Case for which design point convergence could not be achieved; Test Case 1 from Table 9.2 ($\rho_w f_{ywm} = 0.64$ MPa) assessed at $f_{cm} = 40$ MPa. Similar inconsistent behaviour was observed at the higher concrete strength situation $f_{cm} = 98$ MPa. Increments in either of f_c or f_{yw} in the Figures were considered at 1 % intervals, using the finer grid (reduced from 2 %) to better capture sensitivities of V_{R2k} with respect to the variables.

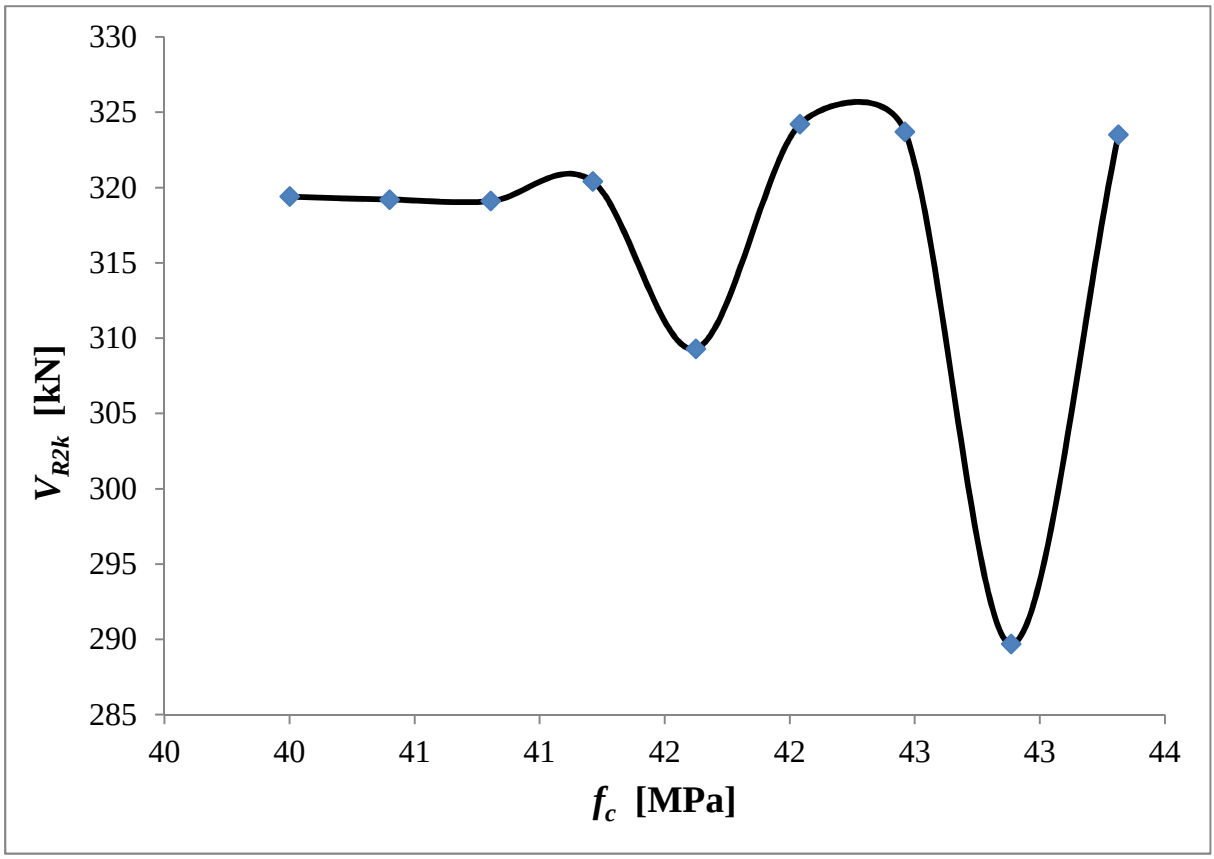

Figure 9.1. The stability of R2k capacity predictions with respect to f_c

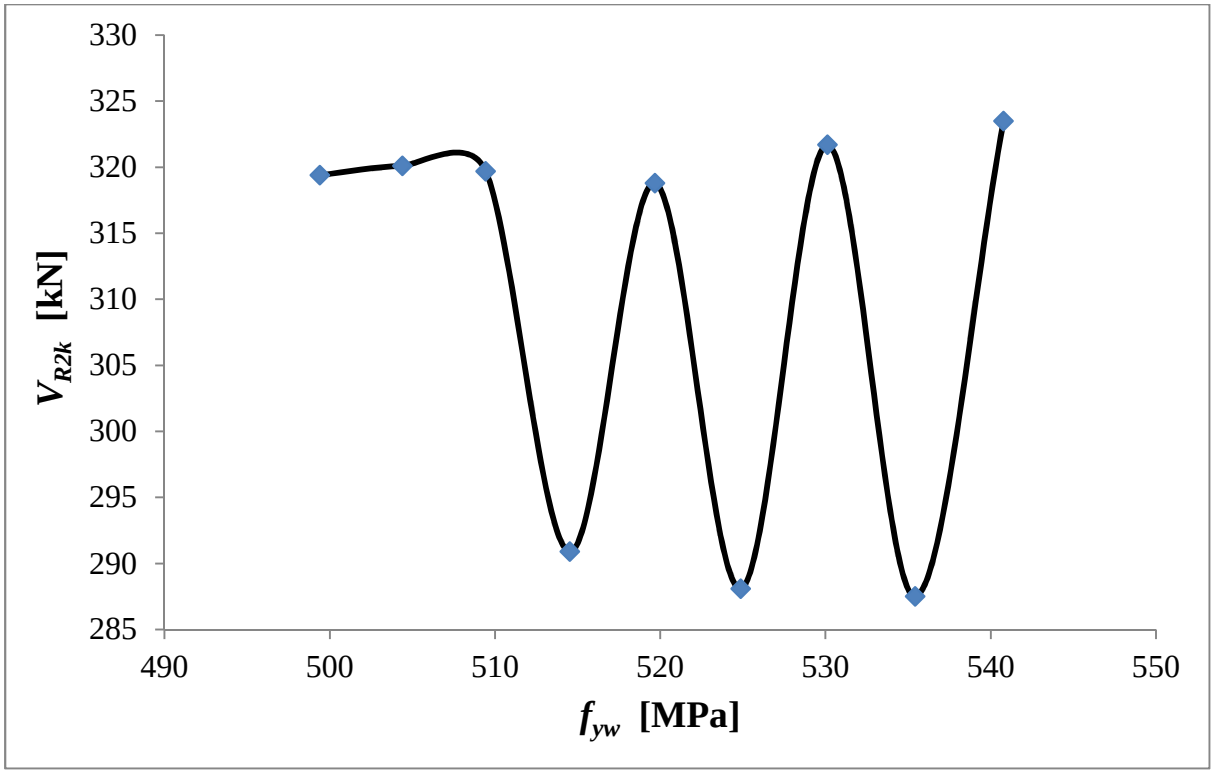

Figure 9.2. The stability of R2k capacity predictions with respect to f_{yw}

Figure 9.1 and Figure 9.2 clearly demonstrate the lack of stability of R2k predictions with respect to the shown variables (for the situation considered).

Although R2k predictions occasionally mal-performed during iterative calculations, its once-off predictions of shear resistance are credible, proven by (1) good accuracy of its Model Factor, (2) reasonable spread (closely comparable to that of VSIM-Analytical), and (3) close match of the trend of normalised resistance predictions to the trend of experimental results as shown in Figure 7.10. The commissioning of R2k capacity predictions to obtain the alternative GPM representation $V_{R2k}(\boldsymbol{X})$ was therefore considered to be valid.

Nevertheless, a sufficient number of Test Cases (not all, but 15 out of a possible 27 Cases) considered achieved design point convergence, providing trends of results that were sufficient to validate basic results from Chapter 8. This issue is further discussed in Section 9.3.

9.2 RESULTS OF THE SIMPLIFIED RELIABILITY ANALYSIS

9.2.1 Design point values x_d^* and direction cosines α_X for the random variables of $g(X)_s$

The design point quantities x_d^* for the basic random variables MF_{R2k}, f_{yw}, and f_c are reported in Table 9.4 across the nine $\rho_w f_{ywm}$ Test Cases for the example situation when mean concrete strength $f_{cm} = 33$ MPa. The number of iterations of the FORM procedure, described in Section 6.2, required to reach the design point for the example Cases are also reported in the Table. The direction cosines α_X at the converged design point are shown parametrically against $\rho_w f_{ywm}$ for the situation when $f_{cm} = 33$ MPa in Figure 9.3. Similar trends of results (the orders of α_{MF}, α_{f_c}, and $\alpha_{f_{yw}}$) were obtained for the higher concrete strength situations at $f_{cm} = 40$ MPa and $f_{cm} = 98$ MPa.

Table 9.4. Design point values for MF_{R2k}, C, f_{yw}, and f_c (with no. of iterations until convergence for example situation $f_{cm} = 33$ MPa)

Test Case No.	MF_d^*	$f_{yw_d}{}^*$ [MPa]	$f_{c_d}{}^*$ [MPa]	No. of iterations to design point x_d^*
1	0.58	474.0	25.2	4
2	0.61	476.4	26.1	7
3	0.65	479.8	27.1	6
4	0.68	482.0	27.6	5
5	0.70	485.0	28.0	4
6	0.72	487.4	28.9	5
7	0.72	487.6	29.9	7
8	0.71	487.3	29.9	6
9	0.70	487.7	29.7	6

An inspection of Figure 9.3 provides clear indication of the dominating influence of MF_{R2k} (by way of α_{MF}) on the uncertainty associated with $V_{R2k}(\boldsymbol{X})$ for the parametric range of $\rho_w f_{ywm}$ considered. Cognizance should also be taken of the fact that the relative order of influence of α_{MF}, α_{f_c}, and $\alpha_{f_{yw}}$ as suggested by the preliminary sensitivity study (Table 9.3) were maintained throughout the parametric range of $\rho_w f_{ywm}$ shown in Figure 9.3. This

provides some confirmation on the adequacy of the simplified representation of $V_{R2k}(\boldsymbol{X})$ adopted during the performance assessment of $g(\boldsymbol{X})_s$.

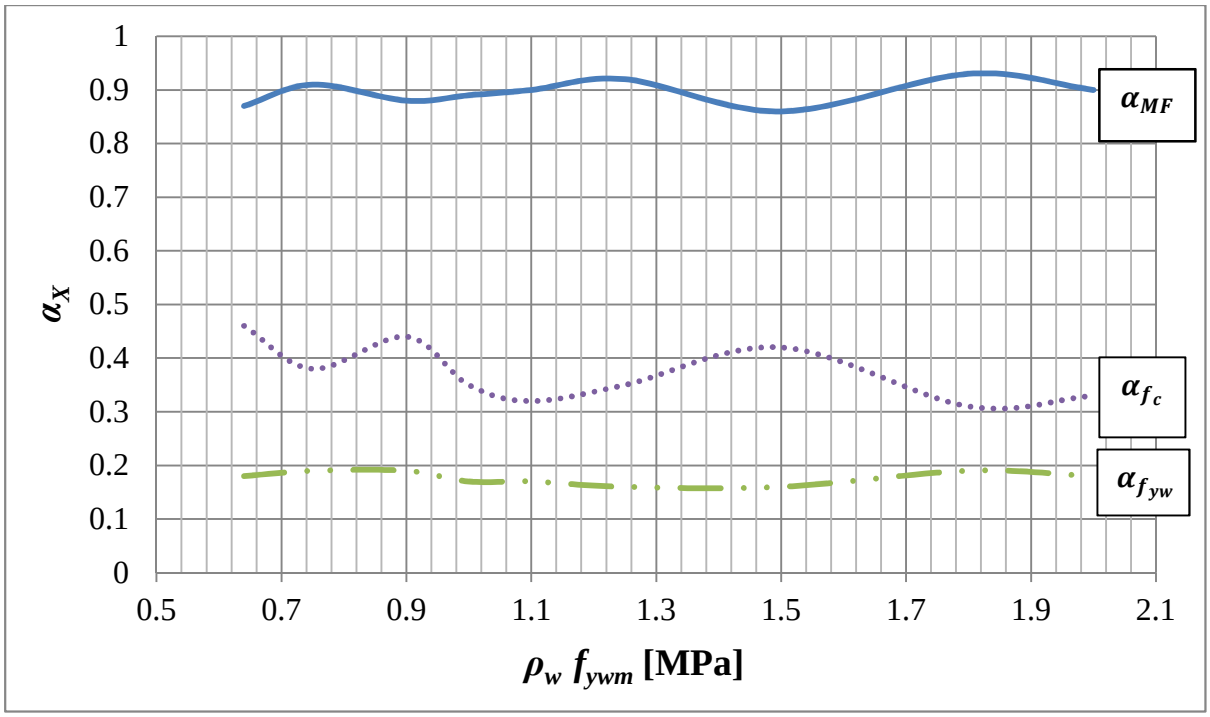

Figure 9.3. Graph of direction cosines α_X at the design point for the parametric range $\rho_w f_{ywm}$ from 0.64 MPa to 2 MPa at $f_{cm} = 33$ MPa

9.2.2 β-values from the two GPM models compared

Figure 9.4 provides a comparison of the estimated β-values (versus $\rho_w f_{ywm}$ and f_{cm} situations) at the FORM design point obtained from:

1. The alternative performance function $g(\boldsymbol{X})_s$ based on the simplified representation of the R2k-based GPM $V_{R2k}(\boldsymbol{X})$, denoted β_{R2k}-values for ease of reference, and
2. The conventional performance function $g(\boldsymbol{X})_s$ based on the simplified representation of the VSIM-based GPM $V_{VSIM-Analytical}(\boldsymbol{X})$ shown in Figure 8.10, denoted β_{VSIM}-values.

Notice that the β_{R2k}-values at $f_{cm} = 40$ MPa and $f_{cm} = 98$ MPa situations are characterised only for the limited $\rho_w f_{ywm}$ ranges shown in the Figure. Converged design point β-values

were not achieved at lower ranges of $\rho_w f_{ywm}$ due to the lack of stability of R2k best-estimate predictions in such situations as detailed in Section 9.1.6. Nonetheless, the converged β_{R2k}-values obtained were sufficient to enable basic validation of the trends of β_{VSIM}-values reported in Chapter 8.

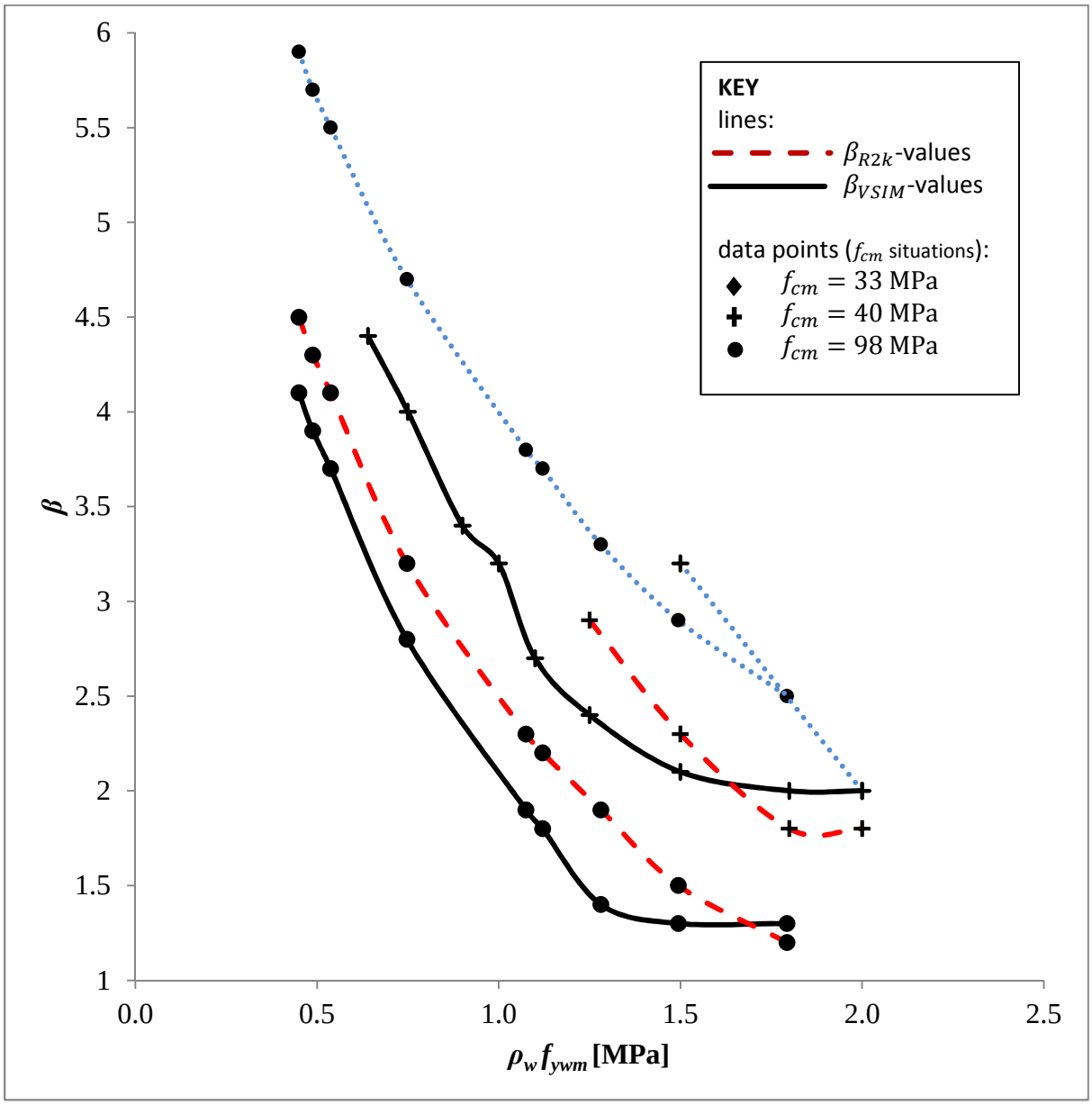

Figure 9.4. β_{VSIM} and β_{R2k}-values compared parametrically against $\rho_w f_{ywm}$ and f_{cm}

The inspection of corresponding β_{R2k} and β_{VSIM} curves from Figure 9.4 revealed the following:

1. Firstly, it should be noted that for a specified combination of $\rho_w f_{ywm}$ and f_{cm} situations, β_{R2k}-values are generally greater than corresponding β_{VSIM}-values.

2. For a specified f_{cm} situation (e.g. $f_{cm} = 33$ MPa, or 40 MPa, etc.), both β_{VSIM} and β_{R2k}-values decrease with an increase in $\rho_w f_{ywm}$, with the more critical decline in β shown for the β_{VSIM}-values. Expressly stated, the β_{R2k}-values were consistently higher than β_{VSIM}-values for the parametric range of $\rho_w f_{ywm}$ considered, although the declining trends of β-values with increasing $\rho_w f_{ywm}$ were somewhat similar for the two cases (with the exception of the $f_{cm} = 98$ MPa situation, see the Figure).

3. At $f_{cm} = 98$ MPa, there seems (i) less agreement between the declining trends of β_{R2k} and β_{VSIM}-values, and (ii) the β_{R2k}-values appear not to be consistently greater than corresponding β_{VSIM}-values (compared to other f_{cm} situations). However, judging from the fact that the β_{R2k}-value trend at $f_{cm} = 98$ MPa was based on only 2 Test Cases, no strong inferences can be drawn from this situation.

4. The cross-over point of the β_{VSIM}-curves at $f_{cm} = 33$ MPa and $f_{cm} = 40$ MPa which occurs at $\rho_w f_{ywm}$ of 1.67 MPa similarly occurs for the corresponding β_{R2k}-curves at approximately the same $\rho_w f_{ywm}$ situation (≈ 1.65 MPa). The β_{R2k}-curves cross-point is, of course, above that of the β_{VSIM}-curves (see the Figure). This similarity, in addition to that from (2) above, gave credibility to β_{R2k}-values presented in the Figure (particularly at $f_{cm} = 33$ MPa and $f_{cm} = 40$ MPa situations).

5. As f_{cm} increases, the general β_{R2k}/β_{VSIM} ratio tends to decrease. Consider, for example, the situation when $\rho_w f_{ywm} = 1.5$ MPa:

   a. $\beta_{R2k}/\beta_{VSIM} = \frac{2.1}{1.3} = 1.62$ at $f_{cm} = 33$ MPa
   b. $\beta_{R2k}/\beta_{VSIM} = \frac{2.3}{1.5} = 1.53$ at $f_{cm} = 40$ MPa
   c. $\beta_{R2k}/\beta_{VSIM} = \frac{3.2}{2.9} = 1.1$ at $f_{cm} = 98$ MPa

From points (1) and (2) above, β_{R2k}-values generally confirm that indeed shear performance (β) is sensitive to the amount of shear reinforcement $\rho_w f_{ywm}$; with declining performance as the amount of stirrups increase. β_{R2k}-values further affirm that shear performance (β) is also sensitive to concrete strength f_{cm}; with increasing performance as concrete strength increases.

β_{R2k}-values are, however, consistently greater than corresponding β_{VSIM}-values. The reason for the disparity between β_{R2k} and β_{VSIM} is explored in Section 9.3.

9.3. DISCUSSION OF THE DIFFERENCES BETWEEN $\boldsymbol{\beta_{VSIM}}$ AND $\boldsymbol{\beta_{R2k}}$-VALUES

Figure 9.5 shows for the situation when $f_{cm} = 33$ MPa the occurrence of (1) the mean values of the GPM functions $V_{R2k}(\boldsymbol{X_m})$ and $V_{VSIM-Analytical}(\boldsymbol{X_m})$, as well as (2) the occurrence of EC2's VSIM deterministic design value function $V_{Rd,s}(\boldsymbol{X_k}, \boldsymbol{\gamma})$ parametrically against $\rho_w f_{ywm}$. Table 9.5 establishes the performance indicators ($V_{Rd,s}(\boldsymbol{X_k}, \boldsymbol{\gamma})$; $V_{R2k}(\boldsymbol{X_m})$; σ_{GPM}; and β) for the R2k-based Limit State Function (LSF) for the situation when $f_{cm} = 33$ MPa. The Table bears similar attributes as Table 8.7 for the VSIM-based LSF as described in Section 8.2.1.

The results of the FORM assessment of Test Case 8 ($\rho_w f_{ywm} = 1.8$ MPa, Test Case 9 from Table 8.7) at $f_{cm} = 33$ MPa according to GPM functions $V_{R2k}(\boldsymbol{X})$ and $V_{VSIM-Analytical}(\boldsymbol{X})$ are used in following discussions to explain the general difference between β_{R2k} and β_{VSIM}-values at specific $\rho_w f_{ywm}$ and f_{cm} situations.

Cognizance must be taken of the following:

1. That the difference $V_{GPM}(\boldsymbol{X}) - V_{Rd,s}(\boldsymbol{X_k}, \boldsymbol{\gamma})$ shown in Figure 8.3 represents the distance '$\beta \cdot \sigma_{GPM}$'.
2. Ideally, for a specified combination $\rho_w f_{ywm}$ and f_{cm}, both the expected values of true shear resistance predicted by the GPMs ($V_{VSIM-Analytical}(\boldsymbol{X_m})$ and $V_{R2k}(\boldsymbol{X_m})$) should

produce approximately equal values; implying that the GPM models similarly predict the point of true shear resistance V_{true}.

Table 9.5. Performance indicators for the simplified reliability model $g(\boldsymbol{X})_s$ applied to the Test Cases at $f_{cm} = 33$ MPa

Test Case No.	$\boldsymbol{V_{Rd,s}(X_k, \gamma)}$ **[kN]**	$\boldsymbol{V_{R2k}(X_m)}$ **[kN]**	$\boldsymbol{\sigma_{GPM}}$ **[kN]**	**β**
1	162.8	330.4	31.6	4.4
2	190.0	400.0`	37.5	4.0
3	228.0	443.9	46.3	3.4
4	253.3	469.4	50.8	3.2
5	285.0	493.8	57.5	2.7
6	316.6	519.8	62.6	2.4
7	357.5	563.5	76.9	2.1
8	384.4	594.9	79.6	2
9	403.5	621.0	87.9	2

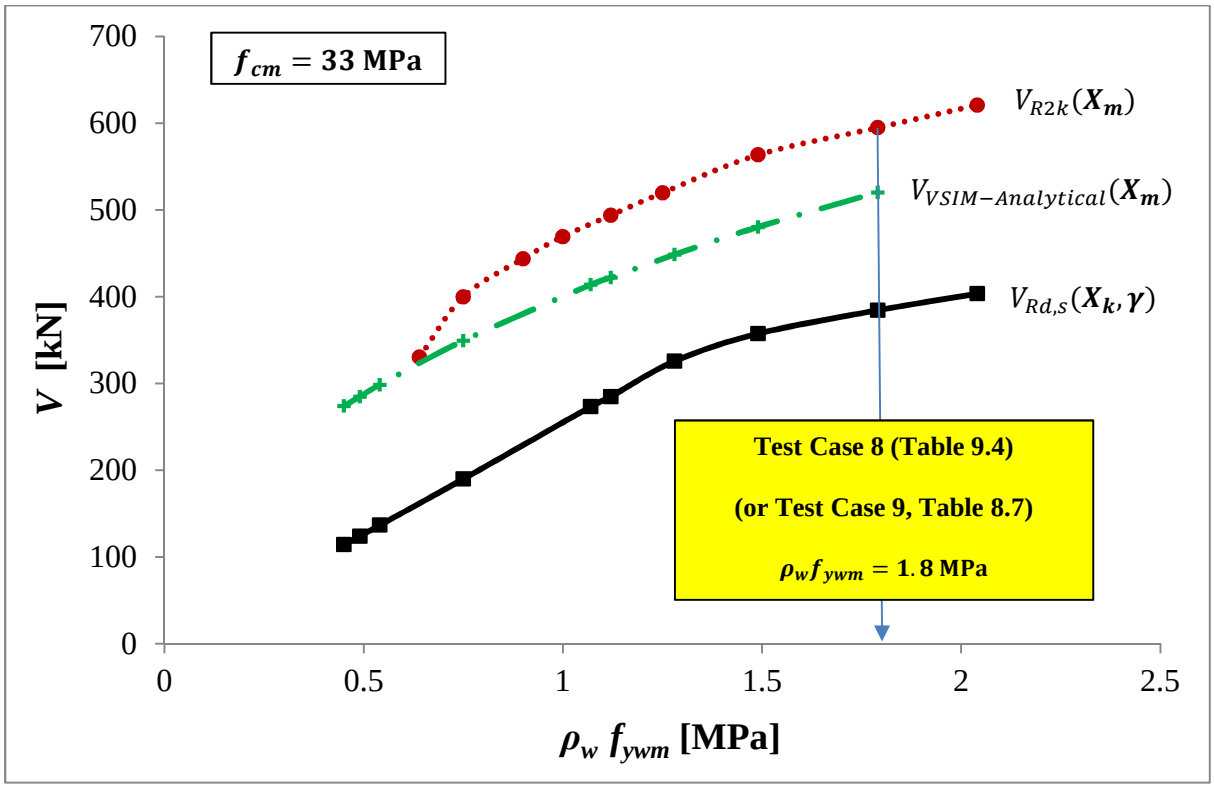

Figure 9.5. Graph of $V_{R2k}(\boldsymbol{X_m})$, $V_{VSIM-Analytical}(\boldsymbol{X_m})$, and $V_{Rd,s}(\boldsymbol{X_k}, \boldsymbol{\gamma})$ against $\rho_w f_{ywm}$ at $f_{cm} = 33$ MPa

3. The fact that $V_{Rd,s}(\boldsymbol{X_k}, \boldsymbol{\gamma})$ has a fixed value for specific $\rho_w f_{ywm}$ and f_{cm} situations or Test Cases (hence, Test Case 8 (Table 9.5) and Test Case 9 (Table 8.7), both have the same $V_{Rd,s}(\boldsymbol{X_k}, \boldsymbol{\gamma})$-value of 384.4 kN).
4. In light of points 1 to 3 above, $V_{true} - V_{Rd,s}(\boldsymbol{X_k}, \boldsymbol{\gamma})$ should be a fixed distance for given $\rho_w f_{ywm}$ and f_{cm} situations, hence implying that β is reliant on the dispersion of the GPM σ_{GPM} (assuming that there is no disparity in the estimated value of V_{true} by $V_{VSIM-Analytical}(\boldsymbol{X_m})$ and $V_{R2k}(\boldsymbol{X_m})$)
5. However, further inspection of the Tables 8.7 and 9.5, respectively, showed that the probability models $V_{VSIM-Analytical}(\boldsymbol{X})$ and $V_{R2k}(\boldsymbol{X})$ had similar dispersions of $\sigma_{GPM} = 79.8$ kN and $\sigma_{GPM} = 79.6$ kN at $\rho_w f_{ywm} = 1.8$ MPa and $f_{cm} = 33$ MPa. This closeness of σ_{GPM} was expected since both $MF_{VSIM-Analytical}$ and MF_{R2k} dominate the uncertainty probability distributions $V_{VSIM-Analytical}(\boldsymbol{X})$ and $V_{R2k}(\boldsymbol{X})$, with similar standard deviations σ_{MF} of 0.18 and 0.20, respectively.

Thus, the disparity between the β_{VSIM}-value ($\beta = 1.1$) and β_{R2k}-values ($\beta = 2.0$) for Test Case 8 was due to a systematic difference of the estimated V_{true} value by GPM functions $V_{VSIM-Analytical}(\boldsymbol{X_m})$ and $V_{R2k}(\boldsymbol{X_m})$. The estimated β_{R2k}-value was larger than the equivalent β_{VSIM}-value since $V_{R2k}(\boldsymbol{X_m})$ was larger (= 594.9 kN) than $V_{VSIM-Analytical}(\boldsymbol{X_m})$ (= 520.3 kN) as can be clearly witnessed from Figure 9.5.

Figure 9.5 clearly indicates that the '$\beta \cdot \sigma_{GPM}$' distance between $V_{R2k}(\boldsymbol{X_m})$ and $V_{Rd,s}(\boldsymbol{X_k}, \boldsymbol{\gamma})$ is consistently greater than the distance between $V_{VSIM-Analytical}(\boldsymbol{X_m})$ and $V_{Rd,s}(\boldsymbol{X_k}, \boldsymbol{\gamma})$ for the range shown. Hence, assuming similar standard deviations σ_{GPM} for both GPM models at different $\rho_w f_{ywm}$ as suggested by Tables 8.7 and 9.4 (discussed in bullet 5 above), β_{R2k} values should be larger than comparable β_{VSIM}-values, as reported in Figure 9.5.

9.3.1 Reason for the difference between expected values $V_{VSIM-Analytical}(\boldsymbol{X_m})$ and $V_{R2k}(\boldsymbol{X_m})$

The comparable dispersion of the two alternative GPM's (VSIM-Analytical & R2k) based on the two respective MF statistics and dominance of MF in comparison to other basic variables indicate that σ_{GPM} for the respective GPM's are comparable. However, the estimates of V_{true} for the two methods are parameter dependent (ρ_l, b_w, d; $\rho_w f_{ywm}$, etc.) in different ways (see

Figures 7.8 and 7.9). The single 'bias adjustment' according to only $\rho_w f_{ywm}$ done for each method evidently does not engineer normalisations for each and every set of parameter values (since $V_{R2k}(\boldsymbol{X_m}) \neq V_{VSIM-Analytical}(\boldsymbol{X_m})$ from Figure 9.5).

As a result, differences between corresponding β_{VSIM} and β_{R2k}-values derive directly from differences in the estimates of the *true mean of shear resistance*! The proper estimate of β depends directly on the estimate of the mean, with best estimates of the dispersion (σ) from the experimental database presently showing good agreement across the parametric range of the database.

CHAPTER 10

INSIGHTS AND OUTLOOKS FOR EFFECTIVE RELIABILITY MANAGEMENT DURING STIRRUP DESIGN

This Chapter tasks itself with the important duty of providing a critical appraisal of the various topics presented in Chapters 2 to 9. Key outcomes from the various Sections are employed as part of a general discussion on the management of reliability performance for stirrup design. The main issues reflected upon in forthcoming discussions include:

1. The critical appraisal of the reliability framework for structural design, focusing on structural concrete resistance, particularly model uncertainty representation during reliability analysis. Model uncertainties are considered a critical issue for shear performance in general, stirrup design included, since a general survey of the internationally available procedures revealed the lack of a unified basis to the analysis and design of structures subjected to shear.

2. An assessment of the various design analogies available for stirrup design, discussing the suitability of simplified methods like the EC2 VSIM procedure for routine design. Views are also shared on the effective representation of General Probabilistic Models (GPMs) for shear resistance.

3. A brief assessment of the performance requirements for stirrup design, discussing the requirements for the ductile mode of stirrup yielding versus those for the possible brittle mode of web-crushing

The following discussions are structured in such a manner that important points are briefly re-capped then integrated into current discussions to provide full appreciation of all interactions and interrelations of the reliability chain.

10.1 PARTIAL FACTOR LIMIT STATES DESIGN

Partial Factor Limit States Design is the conventionally accepted approach to achieving operational designs in practice. It should be based on the design values concept of the FORM procedure. Limit states are satisfied if the inequality $E_d < R_d$ holds true, where E_d represents the design value of the load effects and R_d represents the design resistance. Since the focus is on concrete resistance, only the general form of R_d is further assessed.

R_d is symbolically expressed in terms of the design values of the material properties (X_d), geometry (a_d) and model uncertainty (θ_d), as:

$$R_d = R\{X_{d1}, X_{d2}, \dots\ a_{d1}, a_{d2}, \dots\ \theta_{d1}, \theta_{d2}, \dots\} \qquad [10.1]$$

$$R_d = \frac{1}{\gamma_{Rd}} R\{X_{d,i}; a_d\} = \frac{1}{\gamma_{Rd}} R\left\{\eta_i \frac{X_{k,i}}{\gamma_{m,i}};\ a_d\right\} \quad i \geq 1 \qquad [10.2]$$

η_i takes scale and other effects into account. The following key observations should be made in relation to Equation 10.2:

1. That due to associated uncertainties, partial factors are applicable to characteristic material properties $X_{k,i}$ (partial factor $\gamma_{m,i}$) as well as to the overall resistance or structural mechanics model R (partial factor γ_{Rd})

2. That the characteristic bias for structural concrete design is classically expressed through characteristic concrete (f_{ck}) and steel yield (f_{ywk}, in this instance stirrup-yield) strengths, with all other variables usually receiving nominal treatment (geometrical properties a_d).

It is worth noting that quality control is an important part of the design process, particularly for structural resistance and integrity, where production control has a direct influence on the practically achieved values (and associated variability) of both material and geometrical

properties. A closer look at the interaction between (1) partial factors, (2) quality control, (3) prediction uncertainty, and (4) reference reliability β is presented in Section 10.1.1 below.

10.1.1 Probabilistic basis of the partial factors for structural resistance

Assuming first a Lognormal (with 0-value lower bound), followed by a Normal distribution for resistance properties, applicable to both structural model predictions R and their associated material properties X, the following Equations for partial factors γ_{Rd} and γ_m apply:

$$\gamma_{Rd} = \frac{R_k}{R_d} = \frac{\exp(-1.645\cdot(C.o.V_R))}{\exp(-\alpha_R\beta\cdot(C.o.V_R))} \quad or \quad \gamma_m = \frac{X_k}{X_d} = \frac{\exp(-1.645\cdot(C.o.V_X))}{\exp(-\alpha_R\beta(C.o.V_X))} \qquad [10.3]$$

$$\gamma_{Rd} = \frac{R_k}{R_d} = \frac{1-1.645\cdot(C.o.V_R)}{1-\alpha_R\beta\cdot(C.o.V_R)} \quad or \quad \gamma_m = \frac{X_k}{X_d} = \frac{1-1.645\cdot(C.o.V_X)}{1-\alpha_R\beta\cdot(C.o.V_X)} \qquad [10.4]$$

where $C.o.V_{X,R}$ is the coefficient of variation $\left(\sigma_{X,R}/\mu_{X,R}\right)$ of general resistance property X or R. As discussed in Chapter 2, an inspection of Equations 10.3 and 10.4 indicates that partial factors are dependent on the control of the production process for various materials (modelled by $C.o.V_X$) as well as uncertainties associated with the prediction model (modelled by $C.o.V_R$). Furthermore, γ_m and γ_{Rd} depend on:

1. The FORM sensitivity factors or direction cosines α_X, a property which is sensitive to the limit state under consideration (shear, bending, axial deformations etc.), sensitive also to the choice of General Probabilistic Model (GPM) used for the performance assessment as can be witnessed from the comparison of the results of Chapters 8 and 9. It is usually approximated as $\alpha_R = 0.8$ for resistance properties,

2. The reference level of reliability β, which in itself is (a) national specific, (b) then failure mode specific, then (c) differentiated accordingly for different Reliability Classes (structural importance classes tied to socio-economic principles of risk), leading to different performance requirements (different target β-values) for each class.

The interplay between the various elements of Equations 10.3 and 10.4, with a specific view on the reliability performance of stirrup design procedures is discussed in the following Sections.

10.1.2 Characteristic bias

The characteristic bias is an influential part of the process of achieving operational design values (i.e. $X_d = X_k/\gamma_m$) used in limit state assessments. It is however a property based on production quality, for which the 5 % characteristic fractile is generally accepted for resistance models. However, lack of South African (SA) data on probability models for common basic variables affecting structural resistance impedes a performance assessment that is fully representative of local conditions and practice, since conventional European models are utilised for the assessment. Consequently, expert judgement treads conservatively in such situations, due to the general perception that South African quality levels of standard practice are generally lower than those of equivalent European practice. The question of how conservative is based on the sensitivity of the basic variable to the design problem. Such sensitivities can be assessed from the direction cosines α_X of the GPM implemented for the performance assessment.

Chapters 8 and 9 implement different GPMs for shear resistance ($V_{VSIM-Analytical}(\boldsymbol{X})$ and $V_{R2k}(\boldsymbol{X})$, respectively), both of which indicate that the reliability performance of the EC2 stirrup design procedure is not alarmingly sensitive to material parameters (whose variability can be controlled by the production process), particularly f_c and f_{yw} which are conventionally expressed as characteristic quantities in the design process. The following results were reported:

1. From Chapter 8, based on the VSIM-Analytical representation of the GPM for stirrup resistance $V_{VSIM-Analytical}(\boldsymbol{X})$, basic variables f_c and f_{yw} (and other material properties) all had direction cosines $\alpha_X < 0.3$, see Figure 8.7.
2. From Chapter 9, based on R2k generated GPM for shear resistance $V_{R2k}(\boldsymbol{X})$, the direction cosine reported for concrete strength α_{f_c} was generally less than 0.4,

whereas $\alpha_X < |0.2|$ for all other basic random variables including stirrup yield strength f_{yw} (see Figure 9.3).

Both GPM representations, however, showed significant sensitivity to model uncertainty, the implications of which are discussed in the next Section.

Based on the discussed results, the lack of South African data on theoretical distributions for common variables (particularly f_c and f_{yw}) was judged to have negligible effect on the estimated β-values for the various design situations used in this investigation. It would nonetheless be interesting to incorporate SA data into the performance assessment of EC2's stirrup design procedure as it becomes available. However, it should be noted that new data would be inconsequential if a local investigation confirms the classic convention of the 5 % characteristic bias as appropriate for SA conditions and practice.

10.1.3 Model uncertainty

Model uncertainty is a critical issue affecting the reliability performance assessments (therefore calibration as well) of structures in practice. Model uncertainties for reliability analysis are selected based predominantly on expert guidance, thereby usually lacking a critical assessment of its statistical properties. Model uncertainties should ideally be characterised against a database of tests representative of the failure mode under investigation. The model uncertainty should additionally be investigated parametrically for the relevant design situations in order to pick up any underlying sensitivities which could be remedied during calibration.

For the case of shear performance considered in this investigation, the model uncertainty was found sensitive to the amount of stirrup reinforcement $\rho_w f_{ywm}$, with more serious concerns at high $\rho_w f_{ywm}$ where predictions are potentially unsafe. This result followed from correlation and regression assessment which yielded no severe trends to other important shear parameters such as the shear span to depth ratio (a/d), the amount of longitudinal reinforcement (ρ_l), the concrete strength (f_c), etc. Reliability performance investigations, based on the FORM procedure, were therefore commissioned to assess the consistency of β-values parametrically against $\rho_w f_{ywm}$.

Model uncertainty representation could have alternatively been based on the JCSS PMC (2001) recommendation, which describes the Model Factor MF for shear performance as Lognormally distributed with first and second moments $\mu_{MF} = 1.0$ and $\sigma_{MF} = 0.1$. Table 10.1 provides a qualitative comparison which describes the influence the JCSS MF recommendation would have on the results of the reliability performance assessments conducted in Chapters 8 and 9.

Table 10.1 Comparison of nominally applied MF values versus rationally determined values

Model Factor	**Comparison to JCSS MF recommendation** ($\mu_{MF} = 1.0$; $\sigma_{MF} = 0.1$)
$MF_{VSIM-Analytical}$ ($\mu_{MF} = 0.84$; $\sigma_{MF} = 0.18$)	Compared to $MF_{VSIM-Analytical}$, the JCSS assumption of MF would: 1. Over-estimate β on the basis of its reduced spread 2. Over-estimate β on the basis of its larger mean value The JCSS assumption would thus lead to unconservative estimates of β.
MF_{R2k} ($\mu_{MF} = 1.14$; $\sigma_{MF} = 0.20$)	Compared to MF_{R2k}, the JCSS assumption of MF would: 1. Over-estimate β on the basis of its reduced spread 2. Under-estimate β on the basis of its smaller mean value The net effect of the JCSS assumption should still be unconservative, since β is more sensitive to σ_{MF}

It should be noted that the term unconservative from Table 10.1 implies that the estimated β-values are higher than should be. In reliability terms, this implies that more safety is estimated than there actually is! According to Figure 8.10, this would unjustifiably result in higher maximum limits of application of the EC2 stirrup design procedure according to both SANS 10160-1 and EC0 requirements. This is certainly undesirable, particularly at high $\rho_w f_{ywm}$ where marginal to insufficient performance is experienced, and stringent measures should rather be enforced as discussed in Section 10.3.

Due to the relatively large uncertainties associated with VSIM-Analytical and R2k predictions ($C.o.V > 0.15$, generally), the Model Factor dominated the uncertainty associated with both the GPMs $V_{VSIM-Analytical}(\boldsymbol{X})$ ($\alpha_{MF} \approx 0.95$, see Tables 8.5 and 8.6) and $V_{R2k}(\boldsymbol{X})$ ($\alpha_{MF} \approx 0.86$, see Table 9.3). Accurate representation of MF is therefore

essential for a meaningful performance assessment, an influence which may have been underestimated due to the smaller $C.o.V$ of the JCSS recommendation for MF.

Performance control in terms of achieving uniform reliability (β-values) across the various design situations is best achieved by the basic variable with the most significant direction cosine or sensitivity factor; hence for stirrup design, this implies incorporating γ_{Rd} covering model uncertainties into the procedures, which would be most effective in achieving uniform performance across the different situations, particularly $\rho_w f_{ywm}$.

Due to a general deficiency in implementation of the structural reliability framework for resistance, it is the author's opinion that for concrete structures, operational design models are predominantly achieved by a combination of:

1. 'Safe side' adjustment, against representative tests, of the expected value predictions of resistance provided by the model. This is done to build inherent conservative bias into the procedures.

2. Implementing characteristic values, vector $\boldsymbol{X_k}$, for material properties, typically expressed through concrete (f_c) and steel yield (f_{yw}) strengths, and

3. Introducing conventional partial factors for concrete $\gamma_C = 1.5$ and $\gamma_S = 1.15$ which have only been verified by a limited number of calibration studies, mostly performed against relatively well understood limit states such as flexure and axial compression. Due to the substantially improved prediction accuracy of the aforementioned modes of resistance, model uncertainty has a less dominating influence, with influences from concrete and steel strengths more prevalent. For such situations, conventionally assumed $\gamma_C = 1.5$ and $\gamma_S = 1.15$ are effective in maintaining a more consistent reliability performance across the relevant situations. They however fail to do so for the case of shear performance as can be witnessed from an inspection of Figure 9.4, where β-values decrease quite rapidly as $\rho_w f_{ywm}$ increases (for which $\gamma_C = 1.5$ and $\gamma_S = 1.15$ were implemented when determining $V_{Rd,s}(\boldsymbol{X_k}, \boldsymbol{\gamma})$).

The parametric assessment of the alternative Model Factors ($MF_{VSIM-Limit\theta}$, $MF_{VSIM-Analytical}$, and MF_{R2k}) used for this investigation revealed two key sensitivities that guided basic reliability investigations, described briefly as:

1. Trend of decreasing safety bias of the operational VSIM-Limitθ predictions with increasing $\rho_w f_{ywm}$ as shown in Figure 7.7(a), thus warranting the assessment of the consistency of estimated β-values parametrically against $\rho_w f_{ywm}$.
2. MF_{R2k} also portrayed a trend of decreasing safety bias with an increase in $\rho_w f_{ywm}$ as shown in Figure 7.9(a), although less severe than that of (1) above. Nonetheless, it was significant enough to warrant the parametric adjustment of MF_{R2k}-values during the performance assessment of different $\rho_w f_{ywm}$ situations, hence accounting for the trend.

Shear performance (estimated β-values) was also assessed across a range of concrete strengths f_{cm}. However, this sensitivity of estimated β-values to concrete strength was not exposed by characteristics of the Model Factor. Recall that the Model Factor (MF) consists of the comparison of the resistance from an experimental beam to the equivalent prediction offered by a resistance model i.e. the inherent uncertainty of the prediction model is sought, and not the sensitivity of the prediction model to its component parameters. Cognizance must be taken of the fact that, in general, shear resistance predictions V are proportionally sensitive to changes in concrete strength. That is, the higher the concrete strength, the greater the resistance predictions, and vice versa holds true.

10.2 SIMPLIFIED VERSUS ADVANCED MODELS FOR SHEAR RESISTANCE

A plethora of approaches exist for the analysis and design of stirrup-reinforced concrete structures. They generally vary in terms of complexity, effort, and level of detail. Results from this investigation indicate that the more accurate R2k predictions, which are also computationally more expensive and require more effort, could be best-suited for GPM

representation. However, some instabilities experienced whilst using R2k during reliability modelling (detailed in Section 9.1.6) inhibited its application as the primary means of establishing the GPM for shear resistance.

Simplified methods, on the other hand, are best used for analysis and design of routine structures. Brief discussions of the findings obtained from this investigation are presented below.

10.2.1 Effective GPM representation for shear resistance

In spite of the fact that the VSIM-Analytical calculation procedure was adopted as the primary means of generating the GPM for performance assessments ($V_{VSIM-Analytical}(\boldsymbol{X})$ in Chapter 8), a thorough assessment of the results provided initial indication that the alternatively applied R2k-based GPM ($V_{R2k}(\boldsymbol{X})$) was perhaps better suited for GPM representation for the following reasons:

1. R2k is comparable to VSIM-Analytical in terms of accuracy and spread, although it tends to be systematically conservative ($\mu_{MF_{R2k}} = 1.14$) compared to VSIM-Analytical which tends to be systematically unconservative ($\mu_{MF_{VSIM-Analytical}} = 0.84$)
2. Moderate to mild trends, if any, with important design parameters affecting shear ($\rho_w f_{ywm}$, f_c, ρ_l, etc.), as well as predominantly a systematic conservative bias for the ranges of parameters considered as shown in Figure 7.9
3. A closer match between the trend of normalised R2k shear resistance predictions ($V_{R2k}/b_w d$ *vs.* $\rho_w f_{ywm}$) and the trend of equivalent experimental results, compared to VSIM-Analytical predictions as shown in Figure 7.10.

Due to instabilities encountered with R2k, it was applied in an alternative assessment conducted to validate the results of basic investigations presented in Chapter 8. Furthermore, exploratory assessment by R2k indicated that its mean predictions are sensitive to a number of factors (ρ_l, a/d, etc.). Investigation of some of the parameters of R2k, which are not provided for in the general VSIM procedures, fell outside the scope of basic performance investigations on EC2's VSIM design procedure. Nevertheless, use of an alternative GPM representation shed light on some useful insights, as discussed below.

10.2.2 Systematic effects in predicting true shear resistance V_{true}

The implementation of two different prediction models (VSIM-Analytical and R2k) to establish the two separate GPM functions for shear resistance ($V_{VSIM-Analytical}(\boldsymbol{X})$ and $V_{R2k}(\boldsymbol{X})$) indicated the following:

1. That each prediction method is uniquely parametrically sensitive to different design parameters (see Figures 7.8 and 7.9)
2. As a consequence of (1), the single factor adjustments according to $\rho_{w}f_{ywm}$, applied to of the mean values of the respective Model Factors ($\mu_{MF_{VSIM-Analytical}}$ & $\mu_{MF_{R2k}}$) during reliability analysis were inadequate in equating best-estimate predictions $V_{VSIM-Analytical}(\boldsymbol{X_m})$ and $V_{R2k}(\boldsymbol{X_m})$ for the range considered (see Figure 9.5)
3. Hence, the incompatibility from (2) above ($V_{VSIM-Analytical}(\boldsymbol{X_m}) \neq V_{R2k}(\boldsymbol{X_m})$) indicates both methods have systematic influences affecting their prediction of true shear strength V_{true}.

It is anticipated that refinements through multi-factor adjustment of both $\mu_{MF_{VSIM-Analytical}}$ & $\mu_{MF_{R2k}}$ would improve the similarity between $V_{VSIM-Analytical}(\boldsymbol{X_m})$ and $V_{R2k}(\boldsymbol{X_m})$ shown in Figure 9.5; this would, in effect, also improve both their estimates of true shear resistance V_{true}.

10.2.3 Simplified methods for stirrup design

The shear resistance predictions of three alternative stirrup design approaches (varying in complexity, effort, and level of detail) were compared to predictions from EC2's stirrup design procedure. The comparison was conducted for a beam of representative geometry, which was varied parametrically with the amount of stirrup reinforcement $\rho_w f_{ywm}$. The alternative procedures considered were (1) the SANS 10100-1 semi-empirical design procedure, (2) the *fib* MC 2010 MCFT-based LoA I procedure, and (3) the more elaborate and computationally expensive *fib* MC 2010 MCFT-based LoA III procedure.

Results from the comparative analysis, which are presented in Figure 5.3, showed that the design value predictions for shear resistance (V_{Rd}) offered by the different approaches were similar in the ranges of $\rho_w f_{ywm} < 1$ MPa and $\rho_w f_{ywm} > 2$ MPa. The EC2 stirrup design procedure, however, offered quite substantially larger resistance predictions in the range of $1 \text{ MPa} < \rho_w f_{ywm} < 2$ MPa.

Recall that unbiased VSIM-Limitθ predictions (analogy on which EC2 design procedure derives directly from) are potentially unsafe in the vicinity of $\rho_w f_{ywm}$ of 2 MPa (see Figure 7.8(a)). Furthermore, the results of FORM assessments show, from Figure 8.10, deficient reliability performance of the EC2 design procedure in this range according to both SANS and EN requirements. Hence, similarity of design value predictions in this range of $\rho_w f_{ywm}$ provides early indication of a lack of rational reliability calibration for alternative methods, with the potential for deficient reliability performance at high $\rho_w f_{ywm}$ as well!

Simpler methods are therefore recommended for purposes of routine stirrup design, since they are quick to use and relatively easy to understand, thereby reducing the possibility of conceptual design errors. A common attribute of simplified models is that they are usually achieved through the neglect of the influence some variables, leading to design sensitivities as that shown against $\rho_w f_{ywm}$ in this investigation. The resolve to adopting simpler models can therefore only be a reliability calibration to mitigate performance uncertainties introduced into the process by intentional simplifications. The outcome of a reliability assessment could be either, or a combination, of:

1. Maximum limits for application of the procedures.
2. Following from (1), could be further extended to derive a suitable partial factor set $\boldsymbol{\gamma}$ to achieve consistent performance across the different situations. For the EC2 stirrup design procedure, resistance factor γ_{Rd} will be most effective in achieving uniform reliability.
3. Reliability based constants or coefficients implemented for some purpose of performance control

10.2.4 Suggested modifications to improve the reliability performance of the EC2 VSIM design procedure

Based on the results from Chapter 8, specific adjustments that could be applied to improve the performance of the EC2 VSIM design procedures include:

1. *Increase the lower limit of the concrete strut angle $\theta_{Limited}$:* $\theta_{Limited}$ could be increased from 21.8° to a larger angle. A suitable value for the increased strut angle could be determined from reliability calibration. With reference to Figure 8.8, an increased strut angle $\theta_{Limited}$ would increase the $V_{VSIM-Analytical}(\boldsymbol{X_m}) - V_{Rd,s}(\boldsymbol{X_k}, \boldsymbol{\gamma})$ distance (or $\beta \cdot \sigma_{GPM}$ distance) for the range considered. The increased $\beta \cdot \sigma_{GPM}$ distance would be caused solely by lower $V_{Rd,s}(\boldsymbol{X_k}, \boldsymbol{\gamma})$ predictions (i.e $\cot\theta_{Limited}$ reduces as $\theta_{Limited}$ increases, see Equation 8.2). Note that $V_{VSIM-Analytical}(\boldsymbol{X_m})$ and σ_{GPM} are not affected by strut angle limits, since the VSIM-Analytical calculation procedure allows associated strut angle $\theta_{Analytical}$ to freely assume its calculated value (see Section 8.1.1). Therefore, an increased $\beta \cdot \sigma_{GPM}$ distance due to increasing $\theta_{Limited}$ directly implies larger estimates of β. This further implies that $\theta_{Limited}$ can be adjusted and corresponding FORM analyses conducted (as done in Chapter 8) to achieve desired levels of performance.

2. *Resistance factor adjustment to VSIM-Analytical:* Alternatively, the EC2 $V_{Rd,s}(\boldsymbol{X_k}, \boldsymbol{\gamma})$ design function could be derived from a simple factor adjustment (reduction) of the VSIM-Analytical calculation procedure; this would imply that no limiting concrete strut angle is applied to operational $V_{Rd,s}(\boldsymbol{X_k}, \boldsymbol{\gamma})$ procedures. With reference to Figure 8.8, a resistance factor could be applied to $V_{VSIM-Analytical}(\boldsymbol{X_m})$ predictions to achieve operational $V_{Rd,s}(\boldsymbol{X_k}, \boldsymbol{\gamma})$-values. A suitable resistance factor could then be calibrated from corresponding FORM analyses following a similar procedure as described in (1) above.

10.3 PERFORMANCE REQUIREMENTS FOR STIRRUP DESIGN

Stirrups are provided to reinforced concrete beams to avert sudden brittle shear (diagonal-tension) failures, and promote the ductile response of the structure. The EC2 stirrup design procedure comprises dual design functions for such situations. The primary function describes stirrup yielding ($V_{Rd,s}(\boldsymbol{X_k}, \boldsymbol{\gamma})$), accompanied by a maximum limit for shear resistance set to prevent premature occurrence of web-crushing failures ($V_{Rd,max}(\boldsymbol{X_k}, \boldsymbol{\gamma})$). The design inequality $V_{Rd,s} < V_{Rd,max}$ must therefore be satisfied, as was done for all investigations reported in Chapters 7, 8, and 9.

Stirrup yielding was considered as the dominant failure mechanism of the VSIM procedure. This was confirmed by an inspection of the calculated theoretical strut angles $\theta_{Analytical}$ for all beams used in this investigation (beams from experimental database & Test Cases for parametric studies), which fell predominantly below the EN 1992-1-1 limiting value of 21.8°.

Cognizance must be taken of the fact that this investigation was limited to Model Factor effects for stirrup failure. The $V_{Rd,s}(\boldsymbol{X_k}, \boldsymbol{\gamma})$) function of the EC2 stirrup design procedure was therefore assessed against basic ductility requirements, which are embedded in the reference β-values for the different Reliability Classes (RC1, RC2, etc.) of SANS 10160-1 and EC0 used in Chapters 8 and 9.

However, there are concerns about the increased possibility of brittle web-crushing failures at high $\rho_w f_{ywm}$, typically in the range > 2 MPa according to an assessment by Prinsloo (2012) (considered range of $\rho_w f_{ywm}$ from approx. 3 to 13.5 MPa). The increased presence of stirrups at high $\rho_w f_{ywm}$ increases the possibility of the ultimate web strength being reached before stirrup yielding occurs. For such situations, SANS 10160-1 recommends that the minimum level of reliability is $\beta_t = 4.0$ (hence for resistance models, $\beta_{Rt} = 3.2$). A reliability performance assessment for web-crushing failures would (1) require the determination of its modelling effects from a database of representative tests (as was done for stirrup yielding in Chapter 7), then (2) subsequently applied in reliability performance assessments as performed in Chapters 8 and 9, whilst (3) taking into account increased requirements due to brittle nature of the failure mode. Therefore to achieve full reliability calibration of EC2's stirrup design procedure, extensive reliability investigations of both the

$V_{Rd,s}$ and $V_{Rd,max}$ design functions must be considered, using appropriately derived Model Factors for each case, as well as accounting for any correlations between the failure modes.

CHAPTER 11

CONCLUSIONS AND RECOMMENDATIONS

Structural design is a practice fraught with uncertainties. Uncertainties are inherent in the entire life-cycle of a project; ranging from issues in design and detailing, to issues of construction, even extending to maintenance and demolition in modern and more advanced design recommendations. The reasonable action thus suffices to carry out the project process ensuring some rational safety verification of the process. This is a natural requirement, considering that structures, in their failure:

1. Pose obvious and serious risks to human life (injuries, deaths)
2. Potentially represent loss of considerable economic investment
3. Lead to a disruption of services associated with the constructed facility (loss of function, possibly also to other structures in the vicinity; general public nuisance)
4. Could potentially cause adverse environmental effects and pollution

In order to reflect the need of safe and dependable structures, modern international trends for the codified design of structures have chosen to adopt reliability-based formats to verify acceptable levels of structural performance. In this format, actions and resistances are expressed as random variables, by way of mathematical statistics, to reflect (1) their randomness in nature, as well as to (2) enable a probabilistic assessment of the modelled physical processes at large. Probability statements about load and resistance are then used to quantify the probability or likelihood that the structural load will exceed the structural resistance; an event affectionately referred to in the fraternity as the probability of failure, denoted as P_f.

Considering the uncertainties in loads and actions, as well as the large effort, material and financial resource required to fully account for the uncertainties and prevent failure, the probability of failure P_f cannot be considered as zero. This would be too unrealistic an assumption as in reality structural failures do occur. Structural failures can be attributed to either or a combination of (1) inadequate modelling of the physical process showing incomplete understanding of the structure and/or its loading conditions, or (2) construction error, or (3) design error; all of which affect the performance of the constructed facility.

The reliability index, β, has therefore been introduced as an integral part of the First Order Reliability Method (FORM). FORM is a Level II safety assessment format (of a 3-tier system) that can be applied to characterise and calibrate the reliability performance of models used for structural design. β is an indirect measure of the probability of failure, P_f. β is incorporated in the performance assessment or calibration process to reflect some acceptably low failure occurrence of structures based on socio-economic principles of risk. Calibration against β therefore implies that cognizance of the possibility of structural failure is duly accounted for in the process of specifying guidelines for structural design. The intention is to encourage conscious and cautious treatment of structural safety and reliability performance when drafting guidelines for structural design.

11.1 PARTIAL FACTOR LIMIT STATES DESIGN, STRUCTURAL EUROCODES AND STRUCTURAL RELIABILITY

Modern and technologically advanced design codes recommend the application of the principles of structural reliability as the theoretical basis for the Partial Factor Limit States Design method. The method applies partial factors, the vector $\{\boldsymbol{\gamma}\}$, to increase action values as well as reduce material property and resistance values to generate their design values for use in a limit state assessment. Characteristic values, the vector $\{\boldsymbol{X_k}\}$, are also introduced into limit state functions where partial factors are applied to make an economically but safe assessment of structural performance. The governing condition of a limit state assessment is that the action effects E should be less than the available resistance R (i.e. $E < R$). In this method, dimensions are generally implemented at nominal values, but in some cases (second-order effects, geometrical imperfections, buckling) can assume design values by applying some tolerance limit

The suite of structural Eurocodes represents arguably the most advanced application of reliability principles in deriving design provisions for routine structural design. The Eurocodes are based on a general set of conditions that aim to cater for the diverse conditions shared amongst EU member states. These varying conditions could emanate from

differences in climates, soils, levels of workmanship, as well as different economic and legal requirements for structures in the different member states. Therefore, before the Eurocodes are made operational in any member state, they should be supported by relevant annexures that provide country-specific guidance on the Nationally Determined Parameters (NDPs); the same applying for non-EU member states wishing to adopt the standard.

The structural Eurocodes comprise of a material independent *Basis of Design* standard EN 1990 which contains the principles and requirements to consider when specifying provisions for structural design. The design provisions and guidelines for materials-specific standards, including the concrete design standard EN 1992-1-1 *Eurocode 2: Design of concrete structures – Part 1-1: General rules and rules for buildings,* standard should then be established based on the principles of EN 1990.

11.2 SOUTH AFRICA'S CONCRETE CODE REVIEW AND ITS RELATIONSHIP WITH THE EUROCODES

South Africa (SA) is currently in the process of a general review and reliability updating of its local concrete design standard SANS 10100-1 *The Structural Use of Concrete*. This action was stimulated by the SA concrete code committee's decision to recommend the adoption of the European standard EN 1992-1-1 as the local standard for structural concrete design. The review process has been motivated by (1) the old British standard for concrete design standard BS8110-1, on which the currently operational local standard SANS 10100-1 is based, is now defunct and has been replaced by EN 1992-1-1, (2) South Africa has chosen to follow the reliability-based approach to specifying structural design provisions, and (3) SA's currently operational standard SANS 10160-1 *Basis of Design* is derived to a large extent from the Eurocode equivalent head standard EN 1990

Although SANS 10160-1 can largely be perceived as fully compatible with EN 1990, it contains some SA specific modifications which are warranted/justified within the framework of structural reliability. The point of departure for reliability-based investigations most often lies in the reference level of reliability, β, set for local practice by different states adopting

the Eurocodes. SA adopts a four tier classification of reliability performance classes (RC1 – RC4), whereas EN 1990 specifies three Classes (RC1 – RC3). Furthermore, the different Reliability Classes (RCs) from the different standards are associated with different levels of target / reference reliability β_T. SANS 10160-1 offers reliability classes RC2 ($\beta_{RC2} = 3.5$) and RC3 ($\beta_{RC3} = 3.5$) which mostly apply to the design of conventional buildings and routine structures. These two Reliability Classes correspond to RC2 for Eurocode ($\beta_{RC2} =$ 3.8 in EN 1990).

11.3 APPLICATION OF THE RELIABILITY FRAMEWORK IN ESTABLISHING DESIGN PROVISIONS FOR STRUCTURAL RESISTANCE

In the process of converting the principles of structural reliability into deterministic design rules through a method of calibration, the emphasis is placed to a large extent on actions whilst systematic calibration of the materials standards is limited. Although a reliability framework is developed also for structural resistance in the form of partial factors, model and resistance factors for respective classes of failure modes, systematic calibration of materials standards is limited.

Basis of Design standards EN 1990 and SANS 10160-1 both present an elaborate scheme of action partial safety factors to be applied to various design situations and the associated limit states. For structural concrete resistance, on the other hand, a simple scheme of partial factors is employed to cover a very broad scope of design procedures for concrete resistance (evident from limited set of partial factors allocated to cater for wide range of structural details, concepts, configurations, resistance modes etc.). For conventional reinforced concrete, the partial material factors $\gamma_C = 1.5$ for concrete and $\gamma_S = 1.15$ for steel can be seen to prevail during ultimate limit state verifications across all modes of resistance (limit states) and design situations.

11.4 THRUST OF THE DISSERTATION

This investigation treats the adoption of EN 1992-1-1 as a local standard from the viewpoint of reliability performance implications of the adapted standard versus local conditions and practice. The reliability assessment of a future South African concrete standard should consist firstly of reviewing the degree to which EN 1992 complies with and applies reliability principles as set out in EN 1990; and secondly to calibrate it in accordance with SANS 10160-1 requirements, including required levels and classes of reliability for the restricted scope of building structures. A broad survey of the principles of structural reliability as basis for the implementation for Partial Factor Limit States Design procedures was therefore commissioned to:

1. Trace requirements from the reliability framework for structural resistance models, performed using principally SANS 10160-1 and EN 1990.
2. Trace the extent in which principles from (1) have been applied in specifying provisions for resistance in EN 1992-1-1, identifying generic investigations to be perform against SA conditions and practice. More importantly, the goal was to identify general deficiencies in the current application of the reliability framework to structural resistance. The findings of the survey are chronicled below.

11.4.1 Survey of the reliability framework for structural concrete resistance

The findings from various surveys conducted as part of the effort to determine the level of application of reliability principles in establishing provisions for structural concrete resistance are detailed below.

Comparison of SANS target levels of performance to those of EN, JCSS, and ISO: The SANS 10160-1 prescriptive levels of performance (target reliabilities β_t) for its various Reliability Classes are across board lower than those from equivalent European standard EN 1990. SANS levels of performance are however more closely defendable from the viewpoints of the JCSS Probabilistic Model Code (JCSS PMC) and ISO 2394 *General Principles on Reliability for Structures*. The general conclusion is that SANS performance levels are acceptable, with

EN performance requirements clearly selected on a conservative basis to influence conservative designs. SA performance levels are fully acceptable (from viewpoint of ISO 2394 & JCSS PMC) but economical (compared to EN values).

Initial calibration of resistance models from EN 1992-1-1 against SANS 10160-1 performance requirements: Holický et al. (2010) conducted limited calibration for flexural and compressive models for resistance from EN 1992-1-1 against SANS 10160-1 performance requirements. Key insights were gained from this investigation, including:

1. A number of factors influence structural concrete performance, besides concrete strength and steel strength which are conventionally catered for explicitly by partial factors γ_C and γ_S respectively
2. Although model uncertainty statistics associated with the prediction models were selected based on expert judgement, a significant influence was shown for model uncertainty affecting particularly compressive resistance. Hence, the results indicated that (a) model uncertainty representation could be improved by characteristaion against representative tests – for a more representative analysis, and (b) model uncertainties could be more influential on structural performance for modes of resistance where prediction accuracy is less consistent or accurate, as has classically been the case with shear resistance (with or without stirrups).
3. Given the above arguments, reduced partial factors of $\gamma_S = 1.10$ & $\gamma_C = 1.40$ were found applicable for these conventional modes of resistance (flexure and compression); but more studies were suggested to assess the partial factor set for (a) other modes of resistance, and (b) more representative use of Model Factor statistics.

Structural performance and reliability calibration of EN 1992-1-1 models for shear resistance: A survey of background publication Eurocode 2 Commentary (European Concrete Platform, 2008a) showed evidence of the calibration of EC2's shear design model for members without stirrups (reliability-based coefficient is applied to the empirically determined design formula). A similar calibration/assessment for the design model for members with stirrups has been lacking. This is surprising considering the fact that the provision of stirrups or vertical reinforcement in design signifies an important and highly

routine design situation that frequently occurs in practice to prevent sudden brittle failures. EC2 applies the Variable Strut Inclination Method (VSIM) as the analogy for stirrup design. The assessment of the general performance of the VSIM as presented by EN 1992-1-1 therefore becomes one of the essential activities of SA's adoption process.

Furthermore, investigations by Cladera and Mari (2007) provided initial indication of the uncertainties associated with the VSIM prediction model; indicating them to be systematically sensitive to the amount of stirrups $\rho_w f_{yw}$ provided in design. Investigations presented in chapter 7 of this report confirmed findings by Cladera and Mari (2007), showing unbiased VSIM capacity predictions to generally give excessively conservative capacity predictions at low $\rho_w f_{yw}$, progressing to become marginally conservative and eventually unconservative as $\rho_w f_{yw}$ increases (the Model Factor $MF < 1$ at approx. $\rho_w f_{yw}$ of 1.9 MPa, see Figure 7.7(a)).

The main thrust of this investigation stemmed around the performance of VSIM procedures for stirrup design; particularly the performance of the procedures parametrically against $\rho_w f_{yw}$. The various investigations undertaken to characterise the performance of EC2's VSIM design procedure are summarised in Section 11.5 below.

11.5 THE VARIABLE STRUT INCLINATION METHOD AND ITS RELIABILITY PERFORMANCE

The EC2 VSIM comprises dual design functions. The primary function pertains to the contribution of the stirrups, $V_{Rd,s}$ – which is considered the ultimate shear resistance a stirrup reinforced section, hence neglecting the concrete contribution to shear resistance. $V_{Rd,s}$ is, however, only valid provided that the design inequality $V_{Rd,s} \leq V_{Rd,max}$ is satisfied; where $V_{Rd,max}$ is a function representing the upper limit of design shear resistance set to avoid premature web-crushing failures. An important feature of $V_{Rd,s}$ and $V_{Rd,max}$ to take note of is the fact that both functions limit the virtual concrete compressive strut conventionally used for shear design to occur in the confines $21.8° \leq \theta_{Limited} \leq 45°$ (or alternatively

$1 \leq \cot\theta_{Limited} \leq 2.5$). It was concluded that the VSIM method (unbiased $V_{Rd,s}$ predictions; $V_{Rd,max}$ merely a constraint set) is highly conservative for slightly shear reinforced concrete members. This is ascribed to the effect of neglecting concrete shear resistance, which is significant with limited steel shear resistance. However the method is slightly unconservative for high shear reinforcement. This is ascribed to the fact that the strut inclination angle is assumed to be as low as $\cot^{-1}2.5$.

11.5.1 Comparison of VSIM to alternative methods

The sensitivity of VSIM procedures to the amount of shear reinforcement $\rho_w f_{yw}$, plus the lack of a transparent calibration of VSIM procedures accounting for the trend, warranted a comparison of EC2's VSIM mean and design value predictions against the following available alternative procedures:

1. Semi-empirical 45° constant angle truss model with empirically derived concrete contribution term as implemented in the currently operational local SA standard SANS 10100-1
2. The *fib* Model Code 2010 Modified Compression Field Theory (MCFT)-based design analogies (Levels of Approximation I & III)
3. MCFT-based predictions from sectional analysis program Response-2000 (R2k) serving as best-estimate predictions representative of test results. R2k capacity predictions can also be considered as Level IV method of Approximation according to the *fib* system of classification.

The assessment confirmed the potentially unconservative nature of VSIM for high $\rho_w f_{yw}$, thereby affirming the need to assess β parametrically against $\rho_w f_{yw}$. However, the other design methods (excluding best-estimate R2k predictions, since R2k is not a design procedure) showed similarity to VSIM design value predictions at $\rho_w f_{yw}$ of approximately 2 MPa; recall that this is the vicinity where unbiased VSIM predictions are unconservative (see Section 11.4.1).

The aforementioned behaviour led to concerns as to whether the conventionally applied partial factors for concrete γ_C (= 1.5) and steel γ_S (= 1.15) were appropriately calibrated to cater for VSIM model uncertainties and build sufficient conservatism into the procedures.

Investigations were therefore commissioned to assess predominantly the reliability performance (estimated β-values) of the VSIM procedures ($V_{Rd,s}(\boldsymbol{X_k}, \boldsymbol{\gamma})$ design function) parametrically against $\rho_w f_{yw}$. Furthermore, shear strength is proportionally sensitive to concrete strength f_c; hence β was assessed parametrically against concrete strength f_c as well.

The reliability performance investigations conducted confirmed initial concerns about declining levels of performance as $\rho_w f_{yw}$ increases; further confirming the intuitive trend of increasing β as f_c increases. The results of the reliability performance assessment are reviewed in more detail in the following Section.

11.5.2 Reliability assessment of EC2's VSIM design function $V_{Rd,s}(X_k, \gamma)$

The FORM method was implemented for the performance analysis of VSIM procedures. Model Factor (MF) statistics were investigated in detail to incorporate its effective representation as part of the assessment, since:

1 Model uncertainty has historically been shown to be treated in an approximate manner, choosing values based on expert judgement, and
2 Model uncertainty has been shown to potentially have severe influence on reliability performance; the situation can be compounded by the application of judgement based factors which have the potential of not picking up important trends, worsening the situation!

In an attempt to circumvent these shortcomings, a number of Model Factor statistics were determined according to a database of representative tests to enable the meaningful performance assessment of operational VSIM procedures. Some revealing conclusions and insights were gained with reference to both shear reliability performance and the convention of reliability modelling itself, as a result of the various Model Factor statistics included in the study. Model Factor statistics were derived for three different prediction models (VSIM-Limitθ, VSIM-Analytical & R2k) used as part of the performance assessment of EC2 VSIM procedures. Key MF statistics were its mean μ_{MF} and standard deviation σ_{MF}. Each MF was assessed, by means of correlation and regression analyses, against common factors affecting

shear strength, namely the amount of stirrup-reinforcement $\rho_w f_{yw}$; shear span to depth ratio a/d; amount of longitudinal tension reinforcement ρ_l; effective depth d; concrete strength f_c; and beam width b_w. The significance of the various Model Factors derived for the performance assessment of VSIM procedures are discussed below.

11.5.3 Significance of the three Model Factors

The Model Factor $MF_{VSIM-Limit\theta}$ was associated with the VSIM-Limitθ calculation procedure. It is essential to note that VSIM-Limitθ predictions represent the unbiased behaviour of the EC2 VSIM design function $V_{Rd,s}(\boldsymbol{X_k}, \boldsymbol{\gamma})$; however, note that the VSIM-Limitθ procedure still limits the virtual concrete compressive strut angle to occur between confines $21.8° \leq \theta_{Limited} \leq 45°$. An assessment of VSIM-Limitθ predictions therefore directly revealed sensitivities and uncertainties that design function $V_{Rd,s}(\boldsymbol{X_k}, \boldsymbol{\gamma})$ ought to have been calibrated against.

Correlation and regression analyses of the parameter plots revealed that VSIM-Limitθ predictions are parametrically very sensitive to $\rho_w f_{yw}$; more importantly, its performance declines to marginally conservative and eventually unconservative as $\rho_w f_{yw}$ increases. The lack of the transparent calibration of the EC2 VSIM procedures directed concern as to whether characteristic values $\boldsymbol{X_k}$ and partial factor set $\boldsymbol{\gamma}$ were adequate to (1) control mainly the sensitivity to $\rho_w f_{yw}$ to net safe predictions, and (2) incorporate sufficient safety/conservatism across the different design situations as required by the modern of basis of design standards EN 1990 and SANS 10160-1, particularly against $\rho_w f_{yw}$.

$MF_{VSIM-Limit\theta}$ was therefore the prompt to assess consistency of β parametrically against $\rho_w f_{yw}$; the assessment of β against concrete strength f_c , on the other hand, was automatic, since shear strength is classically (and should be) sensitive to f_c.

The trend of $MF_{VSIM-Limit\theta}$ predictions against $\rho_w f_{yw}$, in addition to (1) its large bias and high uncertainty ($\mu_{MF} = 1.65$, $\sigma_{MF} = 0.50$), and (2) the fact that the limited strut angle $\theta_{Limited}$ is not a natural part of the VSIM procedure, resulted in the assessment of alternative functions better suited for best-estimate predictions of shear resistance.

Alternative best-estimate options, better suited for General Probabilistic Model (GPM) representation during reliability analysis, considered were:

1. The original version of the VSIM procedure, termed VSIM-Analytical – allowing flatter angles of virtual concrete strut, denoted $\theta_{Analytical}$
2. MCFT-based Response-2000 (R2k) capacity predictions

Both VSIM-Analytical and R2k prediction models achieved better representation of model uncertainty associated with shear resistance of members with stirrups both in terms of bias and spread ($\mu_{MF_{VSIM-Limit\theta}} = 1.65$, $\sigma_{MF_{VSIM-Limit\theta}} = 0.50$); ($\mu_{MF_{VSIM-Analytical}} = 0.84$, $\sigma_{MF_{VSIM-Analytical}} = 0.18$); ($\mu_{MF_{R2k}} = 1.14$, $\sigma_{MF_{R2k}} = 0.20$). Furthermore, both prediction models showed much improved sensitivity to the amount of stirrups $\rho_w f_{yw}$. The Model Factor trends to $\rho_w f_{yw}$ were nonetheless taken into account in the reliability analysis, particularly that associated with R2k predictions or MF_{R2k}. Although R2k was in principle the more accurate predictor of shear resistance ($\mu_{MF_{R2k}} = 1.14$; $\mu_{MF_{VSIM-Analytical}} = 0.84$), VSIM-Analytical predictions were implemented as the primary means of establishing the GPM for shear resistance. R2k was seconded to a validation procedure for the following reasons:

1. Although comparable, VSIM-Analytical had more precise predictions associated with it ($\sigma_{MF_{VSIM-Analytical}} = 0.18$; $\sigma_{MF_{R2k}} = 0.20$)
2. R2k showed some instabilities against some important variables affecting shear when applied numerically during FORM analysis, consequently enabling the assessment of a limited number of design situations compared to VSIM-A (more extensive range covered by VSIM-A, in terms of both $\rho_w f_{yw}$ and f_c). It was confirmed that R2k once-off predictions of model uncertainty used to obtain MF_{R2k} statistics were credible and not subject to numerical instabilities.
3. The use of VSIM-Analytical as the primary GPM was somewhat also guided by convention i.e. the conventional process of converting the design function under investigation to its unbiased best-estimate form and implementing it as GPM.

Use of R2k to validate the limited range of results however provided powerful and useful insights, both in terms of:

- Validating important trends of results about shear reliability performance obtained from basic investigations using VSIM-A. Estimated β-values from the R2k-based performance function (β_{R2k}-values) confirmed main trends of results obtained using the VSIM-Analytical based performance function (β_{VSIM}-values). β_{R2k}-values were, however, consistently greater than corresponding β_{VSIM}-values for the parametric range considered. Values of dispersion of the VSIM-Analytical and R2k GPM functions were comparable, as expected, since both GPM functions were dominated by model uncertainty and the Model Factor dispersions are similar (see point (1) above). Since the dispersions were comparable, the difference in the estimated structural performance (β_{VSIM} versus β_{R2k}-values) between VSIM-Analytical and R2k GPM functions led to the conclusion that the differences in performance were due to systematic effects of either model affecting their prediction of the expected value of true shear resistance V_{true}

- Systematic differences of the expected value V_{true} from the two GPM models (VSIM-Analytical and R2k), depending on design parameters (specifically concrete strength f_c) results in different predictions of β for the VSIM design method. Although the β_{R2k}-values from Figure 9.4 were generally greater than corresponding β_{VSIM}-values, the difference between the two trends ($\beta_{VSIM} - \beta_{R2k}$) noticeably reduced with increasing f_c. An improvement on the representation of β would therefore primarily require further investigation of the differences of sensitivities of R2k and VSIM-Analytical to f_c; done with the intention to make appropriate adjustments for f_c during reliability analysis. Other neglected parameters (b_w, d, etc.) may have an influence on the prediction of V_{true}, and could be investigated once the sensitivity of predictions to f_c is brought under control.

11.5.4 Main conclusions on the reliability performance of VSIM

In addition to R2k being used to validate basic investigations using VSIM-Analytical, it certainly also served in a regulatory capacity, revealing that:

- Performance results obtained using VSIM-Analytical as GPM are subject to systematic effects and should be taken as indicative of the real situation, rather than conclusive. It is for this reason that the limits of application of VSIM procedures

according to SANS 10160-1 and EN 1990 requirements for resistance models, shown in Figure 8.10 and discussed in Section 8.3.4, are not taken as strict restrictions. However, based on the trend of results presented in Figure 9.4, β_{VSIM}-values can in the interim be treated as lower bound estimates of the performance of VSIM design procedures, with corresponding β_{R2k}-values serving as upper bound estimates.

- For a more accurate representation of the reliability performance of EC2 VSIM procedures, concrete strength f_c and its influence on VSIM-Analytical and R2k predictions is a significant issue warranting urgent investigation (following from the amount of stirrup reinforcement $\rho_w f_{yw}$).

Although the results obtained are indicative of the real situation (since systematic effects exist in predicting V_{true}), certain aspects about shear reliability performance are nonetheless confirmed by the trends of both β_{VSIM} and β_{R2k}-values, particularly:

1. Shear reliability performance (estimated β-values) decreases as the amount of stirrup reinforcement $\rho_w f_{yw}$ increases; confirming initial suspicions about the sensitivity of EC2's VSIM procedure against $\rho_w f_{yw}$.
2. Shear reliability performance (estimated β-values) increases as concrete strength f_c increases.
3. Shear reliability performance is dominated by the model uncertainty (Important finding warranting structural mechanic model improvement).

A strong observation from the conclusions above certainly holds that in situations where shear is critical (high $\rho_w f_{yw}$) high concrete grades f_c should be provided for design ($f_c > 50$ MPa)

11.6 RECOMMENDATIONS FOR FURTHER RESEARCH

Some recommendations for further study, based on results and reflections from this investigation, are shared in the list below.

1. In order to make a more definitive performance assessment of the EC2 VSIM design procedure against the requirements of SANS 10160-1 and EN 1990, systematic effects in predicting V_{true} needs to be brought under control. The investigation of f_c and its proper representation during reliability analysis are therefore recommended as immediate refinements to the performance assessment of EC2 VSIM procedures.

2. Once issue no. (1) is brought under control, it might be feasible to modify VSIM procedures. This could be achieved either by adding a concrete contribution term or revising the strut angle lower limit of 21.8° to a reasonably higher value, or both. Such an adjustment should be sought to (i) alleviate the trend of the VSIM-Limitθ unbiased procedure to $\rho_w f_{yw}$, in tandem with (ii) improving the reliability performance of the VSIM design procedure against $\rho_w f_{yw}$ (as well as other parameters affecting shear strength) to desired levels of performance. Insights as to how this can be achieved are shared in Chapter 10.

3. Both VSIM-Analytical and R2k GPM representations showed significant sensitivity to model uncertainty as shown in Figures 8.7 and 9.3, respectively. This provides clear indication that shear reliability performance is heavily influenced by uncertainties associated with the prediction models (i.e. and not the basic variables of the prediction models such as f_{yw}, f_c, b_w, etc.). The uncertainties (mean μ and spread σ) associated with existing prediction models for shear resistance can be controlled by incorporating adjustments into the procedures to suit experimental results. Such models would improve not only problems associated with accurate predictions and analysis, but very much improve those of calibration and performance control as well.

4. A more thorough treatment of model uncertainties should be afforded during reliability analysis. This applies not only to the skilled analyst, but should be reflected in professional documents that give guidelines for reliability analysis as well. Based on the steps taken in this investigation, and the useful results and insights gained, the following progressive guidelines are recommended:

    a. Derive a Model Factor MF probability model from the statistics of the comparison of experimental results and predictions for the model under investigation.
    b. Check for systematic effects of MF through the trend correlation and regression analysis
    c. If trends are picked up, modify the model to improve the MF probability model and get rid of systematic trends (possibly with the intention to also improve the fit (bias & dispersion))
    d. Following steps (a) to (c) above, investigate the application of an independent model based on a more advanced Level of Approximation (LoA) to serve as basis for a GPM (possibly against which the basic function can be compared).

5. Basic reliability analysis and calibration of the upper limit to prevent web-crushing failure $V_{Rd,max}$ is an important issue which needs attention. Preliminary indications reported by Prinsloo (2012) are that the procedures are alarmingly sensitive to b_w and d. However, the number of experiments from which inferences are drawn is limited, but can nonetheless be taken as indicative in the interim. Correlation between the two failure modes (ductile stirrup yield vs. premature web-crushing & transition zones between the two) should also be investigated. Cognizance must be taken of the fact that $V_{Rd,max}$ should to be calibrated to increased level of performance, since web-crushing is a brittle mode of failure.

6. This report confirms potentially inadequate reliability performance of EC2's VSIM design function at high $\rho_w f_{yw}$. The alternative stirrup design methods compared in Chapter 5 showed similar design value predictions to VSIM at high $\rho_w f_{yw}$. There is therefore some concern about the reliability performance of the alternative design methods, particularly at high $\rho_w f_{yw}$. Reliability analyses and calibrations are

therefore recommended to investigate and regulate the performance of the alternative procedures.

REFERENCES

Main references (All references cited in-text)

ACI-ASCE Committee 445 Report on Shear and Torsion. (2009). Recent Approaches to Shear Design of Structural Concrete. *ACI Structural Journal*, 124, 1375-1416.

Aïtcin, P-C., Miao, B., Cook, W.D., & Mitchell D. (1994). Effects of Size and Curing on Cylinder Compressive Strength and Normal and High-Strength Concretes. *ACI Materials Journal*, 91 (4), 349-354.

Ang, A.H-S., & Tang, W.H. (1975). *Probability Concepts in Engineering and Planning Design, Volume I: Basic Principles*. John Wiley and Sons, New York.

Ang, A.H-S., & Tang, W.H. (1984). *Probability Concepts in Engineering Planning and design. Volume II - Decision, Risk and Reliability*. Wiley, New York.

Ashour, A., & Yang, K.H. (2007). *Application of the Plasticity Theory to Reinforced Concrete Deep Beams*. Morley symposium on concrete plasticity and its application at the University of Cambridge. Retrieved June 11, 2011, from http://www-civ.eng.cam.ac.uk/cjb/concplas/02ashraf.pdf

Balázs, G.L. (2010). A historical review of shear. *Technical report, fib bulletin 57: Shear and punching shear in RC and FRC elements*. fédération international du béton (*fib*), Switzerland.

Bentz, E.C. (2000). *Sectional analysis of Reinforced Concrete Members*. PhD Thesis, Department of Civil Engineering, University of Toronto, Canada, 210 pp. Retrieved May 27, 2011, from http://www.ecf.utoronto.ca/~bentz

Bentz, E.C. (2010). MC2010: Shear strength of beams and implications of the new approaches. *Technical report, fib bulletin 57: Shear and punching shear in RC and FRC elements*. fédération international du béton (*fib*), Switzerland.

Bentz, E.C. & Collins, M.P. (2006). Development of the 2004 Canadian Standards Association (CSA) A23.3 shear provisions for reinforced concrete. *Canadian J. Civ. Eng* 33: 521-534.

Bræstrup, M.W., Nielsen, M.P., & Bach, F. (1976). *Rational Analysis and Design of Stirrups in Reinforced Concrete Beams*. Report no. R 79, Structural Research Laboratory, Technical University of Denmark.

Bresler, B., & Scordelis, A.C. (1963). Shear Strength of Reinforced Concrete Beams. *ACI Structural Journal*, 86, 51-74.

BS 8110-1. (1997). *Structural use of concrete - Part 1: Code of practice for design and construction*. British Standards Institution, UK.

Carrasquillo, P.M., & Carrasquillo, R.L. (1998). Evaluation of the Use of Current Concrete Practice in the Production of High-Strength Concrete. *ACI Materials Journal*, 85 (1), 49-54.

Cladera A., & Mari A.R. (2007). Shear strength in the new Eurocode 2: A step forward?. *Structural concrete*, 8 (2), 57-66.

Collins, M.P., Bentz, E.C., Sherwood, E.G., & Xie, L. (2007). *An Adequate Theory for the Shear Strength of Reinforced Concrete Structures*. Morley symposium on concrete plasticity and its application at the University of Cambridge. Retrieved June 11, 2011, from http://www-civ.eng.cam.ac.uk/cjb/concplas/07collins.pdf

Comité Euro-International du Béton (CEB) & Fédération International de la Precontrainte (FIP). (1978(a)). *Interantional System of Unified Standard Codes of Practice for Structures, Volume I: Common Unified Rules for Different Types of Construction and Material. (3rd ed.).* CEB, Lausanne, Switzerland.

Comité Euro-International du Béton (CEB) & Fédération International de la Precontrainte (FIP). (1978(b)). *Interantional System of Unified Standard Codes of Practice for Structures, Volume II: CEB-FIP Model Code for Concrete Structures. (3rd ed.).* CEB, Lausanne, Switzerland.

Comité Euro-International du Béton (CEB) & Fédération International de la Precontrainte (FIP). (1993). *CEB-FIP Model Code 1990*. Thomas Telford, London.

Dithinde, M. (2007). Characterisation of Model Uncertainties for Reliaility Based Design of Pile Foundations. PhD Thesis, Department of Civil Engineering, 327 pp.

Ellingwood, B.R. (1994). Probability-based codified design: past accomplishments and future challenges. *Structural safety*, 13, 159-176.

EN 1990. (2002). *Eurocode – Basis of structural design*. European Committee for Standardisation (CEN), Brussels.

EN 1992-1-1. (2004). *Eurocode 2: Design of concrete structures – Part 1-1: General rules and rules for buildings.* European Committee for Standardisation (CEN), Brussels.

European Concrete Platform. (2008a). *Eurocode 2 Commentary*. Retrieved Dec 2008, from: http://www.ding.unisannio.it/ricerca/gruppi/ingciv/ceroni/commentario_EC2_2004.pdf

European Concrete Platform. (2008b). *Eurocode 2 Worked Examples*. Retrieved Dec 2008, from: http://www.europeanconcrete.eu/index.php?option=com_docman&task=doc_view&gid=28

fédération internationale du béton (*fib*). (2010a). *fib bulletin 56, Model Code 2010 – First complete draft, Volume 1. fib, Lausanne, Switzerland.*

fédération internationale du béton (*fib*). (2010b). *fib bulletin 56, Model Code 2010 – First complete draft, Volume 2. fib,Lausanne, Switzerland.*

French, C.W., & Mokhtarzadeh A. (1993). High Strength Concrete: Effects of Materials, Curing and Test Procedure on Short-Term Compressive strength. *PCI Journal*, 38 (3), 76-87.

Holický, M. (2009). Reliability analysis for structural design. ISBN 978-1-920338-11-4, SUN MeDIA, Stellenbosch, South Africa.

Holický, M. (2013). *Advanced Seminar on the Reliability Basis of structural design* (presentation slides), held at the University of Stellenbosch.

Holický, M., & Diamantidis, D. (2010). *Reliability differentiation in the Eurocodes*. Proceedings of the SEMC conference, Cape Town.

Holický, M., & Marková, J. (2007). *Reliability differentiation and production quality in structural design*. Proceedings of the European Safety and Reliability Conference "Risk, Reliability and Social Safety". London, England.

Holický, M., & Retief, J.V. (2010). *Probabilistic Basis of Present Codes of Practice*. Proceedings of the SEMC conference, Cape Town.

Holický, M., Retief, J.V., & Dunaiski, P.E. (2007). *The reliability basis of design for structural resistance*. Proceedings of the SEMC conference, Cape Town.

Holický, M., Retief, J.V., & Wium, J.A. (2010). Partial factors for selected reinforced concrete members: Background to a revision of SANS 10100-1. *SAICE Journal*, 52 (1), 36-44.

Hsu, T.T.C., & Mo, Y.L. (2010). *Unified Theory of Concrete Structures*. John Wiley & Sons Ltd, West Sussex, UK.

Huber, U.A. (2005). *Reliability of Reinforced Concrete Shear Resistance*. Masters Thesis, Department of Civil Engineering, University of Stellenbosch, 188 pp.

ISO 2394. (1998). *General principles on reliability for structures*. International Organisation for Standardisation, Geneva.

ISO Workshop. (2011). *Harmonised Structural Standards Workshop*, held at the University of Stellenbosch.

Jackson, P., & Salim, W.S. (2006). Web Crushing in EN 1992. *The Structural Engineer*, 84 (23), 50-57.

JCSS. (2001). *Probabilistic Model Code, Part 1 to 4, Basis of design, Load and resistance models, Examples*. Joint Committee on Structural Safety. http://www.jcss.byg.dtu.dk/Publications/Probabilistic_Model_Code.aspx

Jensen, B.C., & Lapko, A. (2009). On Shear Reinforcement Design of Structural Concrete Beams on the Basis of the Theory of Plasticity. *Journal of Civil Engineering and Management*, 15 (4), 395-403.

Joint Research Centre (JRC). (2008). *Eurocodes Background and Applications: "Dissemination of information for training" workshop*. Retrieved April 5, 2011, from http://eurocodes.jrc.ec.europa.eu

König, G., Hosser, D., & Wittke, B. (1985). Basic Notes on Model Uncertainties. *CEB Bulletin no. 170*. Comité Euro-International du Béton (CEB), Switzerland.

Kuchma, D.A., Hawkins, N.M., Sang-Ho, K., Shaoyun, S. & Kang, S.K. (2008). Simplified shear provisions of the AASHTO LRFD Bridge Design specifications. *PCI Journal*.

Melchers, R.E. *Structural Reliability Analysis and Prediction (2nd ed.)*. John Wiley & Sons, West Sussex, England.

Mensah, K.K., Retief J.V., & Barnardo C. (2010). *Structural Reliability and the Basis of Design for Concrete Structures*. Proceedings of the SEMC conference, Cape Town.

Milford, R.V. (1988). Target safety and SABS 0160 load factors. *The Civil Engineer in South Africa*, Oct '88, 475-478.

Montgomery, D.C., & Runger, G.C. (2007). *Applied Statistics and Probability for Engineers (4th Ed.).* John Wiley & Sons, USA.

Mosley, B., Bungey, J., & Hulse, R. (2007). *Reinforced Concrete Design to Eurocode 2 (6th ed.).* Palgrave Macmillan, New York, USA.

Mphonde, A.G, & Frantz, G.C. (1985). *SP-87: Shear Tests of High- and Low-Strength Concrete Beams with Stirrups*. American Concrete Institute (ACI), Michigan, USA.

Narayanan R.S., & Beeby A. (2005). *Designers 'Guide to EN 1992-1-1 and EN 1992-1-2. Eurocode 2: Design of concrete structures. General rules and rules for buildings and structural fire design*. Thomas Telford Ltd, London, UK.

O'Brien, E.J., Dixon, A.S. (1995). *Reinforced and Prestressed Concrete Design: The Complete Process*. Longman Scientific & Technical, Essex, England.

O'Brien, E.J., Dixon, A.S. & Sheils, E. (2012). *Reinforced and Prestressed Concrete Design: The Complete Process (2nd ed.).* Oxon, UK: Spon Press, England.

Prinsloo, J.P. (2012). *Assessment and Reliability Implications of Web-Crushing of Beams According to Eurocode 2.* BEng(Civil) final year project, Dept. of Civ. Eng., Univ. of Stellenbosch, Stellenbosch, South Africa.

Retief, J.V., & Dunaiski P.E. (2009). *The limit states basis of structural design for SANS 10160-1*. In Retief, J.V., & Dunaiski, P.E. (Editors) Background to SANS 10160. SUN MeDIA, ISBN 978-1920338-10-7.

SANS 10100-1. (2000). *The structural use of concrete – Part 1: Design.* South African Bureau of Standards, Pretoria.

SANS 51992-1-1 (*Draft*). South African Bureau of Standards, Pretoria

SAKO. (1999). *Basis of Design of Structures: Proposals for Modification of Partial Safety factors in Eurocodes*. Nordic Committee on Building Regulations (NKB) and Nordic standardisation in the Construction Field (INSTA-B), Oslo.

SANS 10160-1. (2011). *Basis of structural design and actions for buildings and industrial structures. Part 1: Basis of structural design*. South African Bureau of Standards, Pretoria.

Schneider, J. (2006). Introduction to the Safety and Reliability of Structures. *Structural Engineering Documents 5*. International Association for Bridge and Structural Engineering (IABSE) - Association Internationale des Ponts et Charpentes (AIPC) – Internationale Vereinigung für Brückenbau und Hochbau (IVBH), Switzerland.

Taerwe, L. (1993). Towards a Consistent Treatment of model uncertainties in reliability formats for concrete structures. *CEB Bulletin no. 219: Safety and Performance Concepts*. Comité Euro-International du Béton (CEB), Switzerland.

Thoft-Christensen, P., & Baker, M.J. (1982). *Structural Reliability Theory and its Applications*. Springer-Verlag, Berlin, Germany.

UK National Annex to Eurocode 2: Design of concrete structures – Part 1-1: General rules and rules for buildings. (2005). British standards institute, UK.

Vecchio, F.J., Collins, M.P. (1986). The Modified Compression-Field Theory for Reinforced Concrete Elements Subjected to Shear. *ACI Journal*, 83 (22), 219-231.

Walraven, J. (2005). Toward a New Model Code For Concrete Structures. African Concrete Code Symposium. Retrieved March 29, 2009, from http://www.acmc-ngo.org/pdf/paper%203.pdf

Experimental Database references (not cited in-text)

Adebar, P., & Collins, M.P. (1996). Shear Strength of Members Without Transverse Reinforcement. *Canadian Journal of Civil Engineering*, 23, 30-41.

Anderson, N.S., & Ramirez, J.A. (1989). Detailing of Stirrup Reinforcement. *ACI Structural Journal*, 86 (5), 507-515.

Angelakos, D., Bentz, E.C., & Collins, M.P. (2001). Effect of Concrete Strength and Minimum Stirrups on Shear Strength of Large Members. *ACI Structural Journal*, 98 (3), 290-300.

Bresler, B., & Scordelis, A.C. (1963). Shear Strength of Reinforced Concrete Beams. *ACI Structural Journal*, 86, 51-74.

Cladera, A., & Mari, A.R. (2005). Experimental Study on High-Strength Concrete Beams Failing in Shear. *Engineering Structures*, 27, 1519-1527.

Collins, M.P., & Kuchma, D. (1999). How Safe Are Our Large, Lightly Reinforced Concrete Beams, Slabs, and Footings?. *ACI Structural Journal*, 96 (4), 482-490.

Elzanaty, A.H., Nilson, A.H., & Slate, F.O. (1985). Shear Capacity of Reinforced Concrete Beams using High Strength Concrete. *ACI Journal*, 83, 290-296.

Johnson, M.K., & Ramirez, J.A. (1989). Minimum Shear Reinforcement in Beams with Higher Strength Concrete. *ACI Structural Journal*, 86 (4), 376-382.

Kong, P.Y.L., & Rangan, B.V. (1998). Shear Strength of High-Performance Concrete Beams. *ACI Structural Journal*, 95 (6), 677-688.

McGormley, J.C., Cleary, D.B., & Ramirez, J.A. (1996). The Performance of Epoxy-Coated Shear Reinforcement. *ACI Structural Journal*, 93 (5), 531-537.

Mphonde, A.G, & Frantz, G.C. (1985). *SP-87: Shear Tests of High- and Low-Strength Concrete Beams with Stirrups*. American Concrete Institute (ACI), Michigan, USA.

Ozcebe, G., Ersoy, U., & Tankut, T. (1999). Evaluation of Minimum Shear Reinforcement Requirements for Higher Strength Concrete. *ACI Structural Journal*, 96 (3), 361-369.

Placas, A., & Regan, P.E. (1971). Shear Failure of Reinforced Concrete Beams. *ACI Journal*, 68, 763-773.

Roller, J.J., & Russell, H.G. (1990). Shear Strength of High-Strength Concrete Beams with Web Reinforcement. *ACI Structural Journal*, 87 (2), 191-198.

Sarsam, K.F., & Al-Musawi, M.S. (1992). Shear Design of High- and Normal Strength Concrete Beams with Web Reinforcement. *ACI Structural Journal*, 89 (6), 658-664.

Swamy, R.N., & Andriopoulos, A.D. (1974). *SP-42: Contribution of Aggregate Interlock and Dowel Forces to the Shear Resistance of Reinforced Beams with Web Reinforcement*. American Concrete Institute (ACI), Michigan, USA.

Tompos, E.J., & Frosch, R.J. Influence of Beam Size, Longitudinal Reinforcement, and Stirrup Effectiveness on Concrete Shear Strength. *ACI Structural Journal*, 99 (5), 559-567.

Xie, Y., Ahmad, S.H., Yu, T., Hino, S., & Chung, W. (1994). Shear Ductility of Reinforced Concrete Beams of Normal and High-Strength Concrete. *ACI Structural Journal*, 91 (2), 140-147.

Yoon, Y-S., Cook, W.D., & Mitchell, D. (1996). Minimum Shear Reinforcement in Normal, Medium and High-Strength Concrete Beams. *ACI Structural Journal*, 93 (5), 576-584.

Zararis, P.D. (2003). Shear Strength and Minimum Shear Reinforcement of Reinforced Concrete Slender Beams. *ACI Structural Journal*, 100 (2), 203-214.

APPENDIX A

Test No.	Author [Source]	Beam name	b_w [mm]	d [mm]	f_{cm} [MPa]	ρ_l [%]	ρ_w [%]	f_{ywm} [MPa]	$\rho_w f_{ywm}$ [MPa]	a/d	$V_{experiment}$ [kN]	$V_{VSIM\text{-}Limit0}$ [kN]	$MF_{VSIM\text{-}Limit0}$	$\theta_{VSIM\text{-}Analytical}$ [°]	$V_{VSIM\text{-}Analytical}$ [kN]	$MF_{VSIM\text{-}Analytical}$	V_{R2k} [kN]	MF_{R2k}
1	1. Bressler & Scordelis	A-1	307	466	24.1	1.8	0.10	325.4	0.33	3.92	233.2	104.8	2.23	9.9	241.2	0.97	177.8	1.31
2		A-2	305	464	24.3	2.3	0.10	325.4	0.33	4.93	244.8	103.6	2.36	9.8	239.5	1.02	170.7	1.43
3		B-1	231	461	24.8	2.4	0.15	325.4	0.49	3.95	222.5	117.0	1.90	11.9	221.1	1.01	166.5	1.34
4		B-2	229	466	23.2	2.4	0.15	325.4	0.49	4.91	200.2	117.2	1.71	12.3	214.8	0.93	156.3	1.28
5		C-1	155	464	29.6	1.8	0.20	325.4	0.65	3.95	156.1	105.3	1.48	12.8	185.8	0.84	144	1.08
6		C-2	152	464	23.8	3.7	0.20	325.4	0.65	4.93	161.5	103.3	1.56	14.1	164.6	0.98	131	1.23
7		CRA-1	305	460	25.1	1.7	0.10	350.0	0.35	3.98	168.4	110.5	1.52	10.0	249.6	0.67		
8		CRB-1	229	457	23.6	2.3	0.15	340.0	0.51	4.01	172.7	120.1	1.44	12.5	216.8	0.80		
9		CRC-1	155	458	24.4	1.7	0.20	345.0	0.69	4.00	118.6	110.2	1.08	14.4	172.3	0.69		
10		1WCRA-1	305	457	26.3	1.7	0.10	350.0	0.35	4.01	214.6	109.8	1.95	9.8	253.3	0.85		
11		1WCRB-1	229	459	23.2	2.3	0.15	340.0	0.51	3.99	203.9	120.6	1.69	12.6	216.0	0.94		
12		1WCRC-1	152	460	26.7	1.7	0.20	350.0	0.70	3.96	143.3	110.1	1.30	13.9	178.3	0.80		
13		1WCA-1	305	462	25.2	1.8	0.10	350.0	0.35	3.95	219.8	111.0	1.98	10.0	251.2	0.88		
14		1WCB-1	231	460	26.5	2.3	0.15	340.0	0.51	3.97	201.9	121.9	1.66	11.9	232.3	0.87		
15		1WCC-1	155	460	24.9	1.8	0.20	345.0	0.69	3.97	142.6	110.7	1.29	14.2	174.7	0.82		
16		2WCA-1	305	461	26.3	1.8	0.10	350.0	0.35	3.96	241.8	110.7	2.18	9.8	255.6	0.95		
17		3WCA-1	305	460	26.3	1.8	0.10	350.0	0.35	3.97	207.6	110.5	1.88	9.8	255.0	0.81		
18	2. Bahl	B15	240	300	26.8	1.3	0.15	440.0	0.66	3.00	130.0	106.9	1.22	13.4	178.9	0.73		
19		B25	240	600	25.1	1.3	0.15	440.0	0.66	3.00	252.5	213.9	1.18	13.9	346.9	0.73		
20		B35	240	900	26.3	1.3	0.15	440.0	0.66	3.00	372.5	320.8	1.16	13.6	531.9	0.70		
21		B45	240	1200	25.4	1.3	0.15	440.0	0.66	3.00	468.0	427.7	1.09	13.8	697.7	0.67		
22	3. Placas and Regan	R8	152	272	26.7	1.5	0.21	276.2	0.58	3.36	79.6	54.0	1.48	12.6	96.4	0.83		
23		R9	152	272	29.6	1.5	0.43	267.4	1.15	3.36	104.5	107.0	0.98	17.1	139.1	0.75		
24		R10	152	272	29.6	1.0	0.21	276.2	0.58	3.36	75.5	54.1	1.40	12.0	101.4	0.74		
25		R11	152	272	26.2	1.0	0.21	276.2	0.58	3.36	89.5	54.1	1.65	12.7	95.9	0.93		
26		R12	152	272	33.9	4.2	0.21	276.2	0.58	3.60	117.3	54.1	2.17	11.4	107.7	1.09		
27		R13	152	272	32.3	4.2	0.43	267.4	1.15	3.60	160.0	107.2	1.49	16.4	145.3	1.10		
28		R14	152	272	29.0	1.5	0.14	271.4	0.38	3.36	89.5	35.4	2.53	9.8	81.9	1.09		
29		R15	152	272	29.9	4.2	0.43	267.4	1.15	3.60	149.6	107.2	1.39	17.0	140.2	1.07		
30		R16	152	272	31.6	4.2	0.43	267.4	1.15	3.60	149.6	107.2	1.39	16.6	143.8	1.04		
31		R17	152	272	12.8	1.5	0.21	276.2	0.58	3.36	70.0	54.1	1.29	17.8	67.3	1.04		
32		R18	152	272	31.3	1.5	0.21	276.2	0.58	3.36	84.5	54.1	1.56	11.8	103.9	0.81		
33		R19	152	272	30.3	1.5	0.43	267.4	1.15	3.36	119.8	107.2	1.12	16.9	141.0	0.85		
34		R20	152	272	42.5	1.5	0.21	276.2	0.58	3.36	89.9	54.1	1.66	10.3	118.6	0.76		
35		R21	152	272	48.1	4.2	0.43	267.4	1.15	3.60	160.0	107.2	1.49	13.9	172.8	0.93		
36		R22	152	272	29.5	1.5	0.21	276.2	0.58	4.50	79.6	54.1	1.47	12.1	101.2	0.79		
37		R24	152	272	30.9	4.2	0.21	276.2	0.58	5.05	98.6	54.1	1.82	11.8	103.4	0.95		
38		R25	152	272	30.8	4.2	0.21	276.2	0.58	3.60	111.9	54.1	2.07	11.8	103.2	1.08		
39		R28	152	272	31.6	4.2	0.84	267.9	2.25	3.60	191.9	192.5	1.00	23.6	192.5	1.00		
40		T1	152	272	27.9	1.3			0.58	3.36	109.9	53.7	2.05	12.3	98.4	1.12		

Test No.	Author [Source]	Beam name	b_w [mm]	d [mm]	f_{cm} [MPa]	ρ_l [%]	ρ_w [%]	f_{ywm} [MPa]	$\rho_w f_{ywm}$ [MPa]	a/d	$V_{experiment}$ [kN]	$V_{VSIM\text{-}Limit0}$ [kN]	$MF_{VSIM\text{-}Limit0}$	$\theta_{VSIM\text{-}Analytical}$ [°]	$V_{VSIM\text{-}Analytical}$ [kN]	$MF_{VSIM\text{-}Analytical}$	V_{R2k} [kN]	MF_{R2k}
41	3. Placas and Regan	T3	152	272	27.5	1.5			0.58	3.36	104.5	53.7	1.95	12.4	97.7	1.07		
42		T4	152	272	32.5	2.0			0.58	3.36	109.4	53.7	2.04	11.5	105.3	1.04		
43		T5	152	272	33.7	1.5			1.15	3.36	139.7	107.4	1.30	16.2	148.3	0.94		
44		T6	152	272	25.8	4.2			2.25	3.60	204.6	172.8	1.18	25.9	172.8	1.18		
45		T7	152	272	27.4	3.0			0.58	3.46	109.4	53.7	2.04	12.4	97.5	1.12		
46		T8	152	272	31.2	4.2			0.58	3.60	124.6	53.7	2.32	11.7	103.5	1.20		
47		T9	152	272	20.2	4.2			1.15	3.60	154.4	107.4	1.44	20.4	115.5	1.34		
48		T10	152	272	28.2	1.5			0.38	3.36	86.7	35.8	2.42	10.0	81.3	1.07		
49		T13	152	272	12.8	1.5			0.58	3.36	89.9	53.7	1.67	17.8	67.0	1.34		
50		T19	152	272	29.9	4.2			0.58	5.40	113.4	53.7	2.11	11.9	101.5	1.12		
51		T20	152	272	32.1	4.2			1.15	5.40	153.9	107.4	1.43	16.5	145.0	1.06		
52		T25	152	272	54.1	1.5			0.58	3.36	114.8	53.7	2.14	9.4	129.8	0.88		
53		T26	152	272	57.0	4.2			1.15	3.60	179.3	107.4	1.67	13.1	184.7	0.97		
54		T27	152	272	12.0	4.2			1.15	3.60	132.1	86.5	1.53	26.4	86.5	1.53		
55		T31	152	272	31.0	1.5			0.58	3.36	94.7	53.7	1.76	11.8	103.1	0.92		
56		T32	152	272	27.6	4.2			2.25	3.60	216.2	179.2	1.21	25.1	179.2	1.21		
57		T34	152	272	33.9	4.2			0.58	5.40	112.1	53.7	2.09	11.3	107.3	1.04		
58		T35	152	272	33.6	4.2			0.58	5.40	114.8	53.7	2.14	11.4	106.9	1.07		
59		T36	152	272	24.1	4.2			1.15	3.60	179.3	107.4	1.67	18.8	126.4	1.42		
60		T37	152	272	31.8	4.2			2.25	3.60	209.5	193.1	1.09	23.5	193.1	1.09		
61		T38	152	272	30.2	4.2			2.25	3.60	239.3	188.0	1.27	24.0	188.0	1.27		
62	4. Swamy and Andriopoulos	C3	76	95	29.4	2.0	0.31	270.274	0.85	3.00	15.6	13.8	1.13	14.7	21.1	0.74	17.4	0.90
63		R3	76	95	29.4	2.0	0.77	205.271	1.59	3.00	18.1	25.9	0.70	20.3	28.0	0.65	16.8	1.08
64		J3	76	95	29.4	2.0	0.85	253.182	2.14	3.00	20.5	31.8	0.65	23.7	31.8	0.65	17.1	1.20
65		O3	76	132	28.3	4.0	0.22	270.3	0.59	3.00	25.4	13.4	1.89	12.4	24.3	1.04	20.7	1.23
66		Z3	76	132	25.9	4.0	0.68	181.5	1.23	3.00	27.8	27.7	1.00	18.8	32.6	0.85	29	0.96
67		Y3	76	132	25.9	4.0	1.19	220.6	2.62	3.00	28.9	44.3	0.65	28.0	44.3	0.65	29.7	0.97
68		O4	76	132	28.3	4.0	0.22	270.3	0.59	4.00	20.0	13.4	1.49	12.4	24.3	0.82	20	1.00
69		Z4	76	132	25.9	4.0	0.68	181.5	1.23	4.00	25.6	27.7	0.92	18.8	32.6	0.79	23	1.11
70		O5	76	132	28.3	4.0	0.22	270.3	0.59	5.00	18.9	13.4	1.41	12.4	24.3	0.78	18.6	1.02
71	5. Mphonde and Frantz	B50-3-3	152	298	22.1	3.4	0.11	303.0	0.34	3.60	76.3	34.7	2.20	10.5	74.9	1.02	60.9	1.25
72		B50-7-3	152	298	39.9	3.4	0.11	303.0	0.34	3.60	93.9	34.7	2.71	8.1	97.3	0.96	73.8	1.27
73		B50-11-3	152	298	59.8	3.4	0.11	303.0	0.34	3.60	97.9	34.7	2.83	7.0	113.7	0.86	84.6	1.16
74		B50-15-3	152	298	83.0	3.4	0.11	303.0	0.34	3.60	111.4	34.7	3.21	6.3	125.6	0.89	92.1	1.21
75		B100-3-3	152	298	27.9	3.4	0.26	269.0	0.69	3.60	95.4	70.3	1.36	13.5	117.1	0.81	95.6	1.00
76		B100-7-3	152	298	47.1	3.4	0.26	269.0	0.69	3.60	120.5	70.3	1.71	10.8	146.8	0.82	114.8	1.05
77		B100-11-3	152	298	68.6	3.4	0.26	269.0	0.69	3.60	151.2	70.3	2.15	9.5	168.3	0.90	124.6	1.21
78		B100-15-3	152	298	82.0	3.4	0.26	269.0	0.69	3.60	115.8	70.3	1.65	9.0	177.3	0.65	130.8	0.89
79		B150-3-3	152	298	28.7	3.4	0.36	286.0	1.03	3.60	138.0	105.0	1.31	16.4	142.9	0.97	119.7	1.15
80		B150-7-3	152	298	46.6	3.4	0.36	286.0	1.03	3.60	133.4	105.0	1.27	13.3	177.0	0.75	141.3	0.94

Test No.	Author [Source]	Beam name	b_w [mm]	d [mm]	f_{cm} [MPa]	ρ_l [%]	ρ_w [%]	f_{ywm} [MPa]	$\rho_w f_{ywm}$ [MPa]	a/d	$V_{experiment}$ [kN]	$V_{VSIM\text{-}Limit\theta}$ [kN]	$MF_{VSIM\text{-}Limit\theta}$	$\theta_{VSIM\text{-}Analytical}$ [°]	$V_{VSIM\text{-}Analytical}$ [kN]	$MF_{VSIM\text{-}Analytical}$	V_{R2k} [kN]	MF_{R2k}
81	5. Mphonde and Frantz	B150-11-3	152	298	69.6	3.4	0.36	286.0	1.03	3.60	161.6	105.0	1.54	11.6	205.1	0.79	153.2	1.05
82		B150-15-3	152	298	82.8	3.4	0.36	286.0	1.03	3.60	150.0	105.0	1.43	11.0	215.8	0.70	156.2	0.96
83	6. Elzanaty, Nilson and Slate	G4	178	266	62.8	3.3	0.17	379.0	0.64	4.00	149.1	68.6	2.17	9.4	165.2	0.90	112.2	1.33
84		G5	178	266	40.0	2.5	0.17	379.0	0.64	4.00	111.3	68.6	1.62	11.2	138.9	0.80	99.7	1.12
85		G6	178	266	20.7	2.5	0.17	379.0	0.64	4.00	78.2	68.6	1.14	14.9	102.8	0.76	81.1	0.96
86	7. Johnson and Ramirez	1	305	539	36.4	2.5	0.14	479.2	0.67	3.10	338.8	247.9	1.37	11.9	471.8	0.72	394.9	0.86
87		2	305	539	36.4	2.5	0.07	479.2	0.34	3.10	222.1	123.9	1.79	8.4	337.3	0.66	261.8	0.85
88		4	305	539	72.4	2.5	0.07	479.2	0.34	3.10	316.0	123.9	2.55	6.5	435.6	0.73	323.7	0.98
89		5	305	539	55.8	2.5	0.14	479.2	0.67	3.10	382.9	247.9	1.54	10.0	560.4	0.68	446.9	0.86
90		7	305	539	51.3	2.5	0.07	479.2	0.34	3.10	280.9	123.9	2.27	7.3	387.1	0.73	290.8	0.97
91		8	305	539	51.3	2.5	0.07	479.2	0.34	3.10	258.3	123.9	2.08	7.3	387.1	0.67	290.8	0.89
92	8. Anserson and Ramirez	W1	406	344	29.2	2.3	0.39	548.7	2.14	2.65	460.1	611.5	0.75	23.8	611.5	0.75	388.7	1.18
93		W2	406	344	32.2	2.3	0.39	548.7	2.14	2.65	549.1	642.8	0.85	22.8	642.8	0.85		
94		W3	406	344	32.4	2.3	0.39	548.7	2.14	2.65	504.6	644.8	0.78	22.7	644.8	0.78	547	0.92
95	9. Roller and Russell	2	356	559	120.2	3.0	0.43	448.2	1.93	2.50	1097.4	862.9	1.27	14.2	1359.6	0.81	893.5	1.23
96		6	457	762	72.4	1.7	0.08	445.1	0.36	3.00	665.5	279.0	2.39	6.7	951.3	0.70	482.3	1.38
97		7	457	762	72.4	1.9	0.16	445.1	0.71	3.00	788.0	558.0	1.41	9.5	1336.0	0.59	650.3	1.21
98		9	457	762	125.4	2.4	0.16	445.1	0.71	3.00	749.6	558.0	1.34	8.6	1476.4	0.51	705.4	1.06
99		10	457	762	125.4	2.9	0.23	445.1	1.02	3.00	1172.4	802.1	1.46	10.3	1761.3	0.67	904.3	1.30
100	10. Sarsam and Al-Musawi	AL2-N	180	233	40.4	2.2	0.09	820.0	0.74	4.00	115.0	69.6	1.65	11.9	131.9	0.87	96.7	1.19
101		AL2-H	180	233	75.3	2.2	0.09	820.0	0.74	4.00	123.0	69.6	1.77	9.5	165.7	0.74	99.6	1.23
102		BL2-H	180	233	75.7	2.8	0.09	820.0	0.74	4.00	138.0	69.6	1.98	9.5	165.9	0.83	120.6	1.14
103		CL2-H	180	233	70.1	3.5	0.09	820.0	0.74	4.00	147.0	69.6	2.11	9.8	162.1	0.91	115.5	1.27
104		BS4-H	180	233	80.1	2.8	0.18	820.0	1.48	2.50	207.0	139.3	1.49	13.3	235.1	0.88	186.6	1.11
105		CS3-H	180	233	74.2	3.5	0.13	820.0	1.07	2.50	247.0	100.6	2.46	11.5	197.0	1.25	152.2	1.62
106		CS4-H	180	233	75.7	3.5	0.18	820.0	1.48	2.50	221.0	139.3	1.59	13.5	231.3	0.96	184.5	1.20
107	11. Xie et al.	NNW-3	127	203	40.7	3.2	0.49	324.0	1.59	3.00	87.1	92.1	0.95	17.6	116.2	0.75	110.6	0.79
108		NHW-3	127	198	98.3	4.5	0.51	324.0	1.65	3.00	102.4	93.5	1.10	13.5	156.0	0.66	132.7	0.77
109		NHW-3a	127	198	89.9	4.5	0.65	324.0	2.11	3.00	108.3	119.2	0.91	15.5	171.5	0.63	145.2	0.75
110		NHW-3b	127	198	103.2	4.5	0.78	324.0	2.53	3.00	122.6	143.0	0.86	16.6	191.7	0.64	147	0.83
111	12. McGormley, Creary and Ramirez.	BUS-1	203	419	42.2	3.0	0.34	426.5	1.45	3.27	271.5	277.5	0.98	16.5	373.8	0.73		
112		EUS-1	203	419	43.2	3.0	0.34	426.5	1.45	3.27	298.1	277.5	1.07	16.4	377.6	0.79		
113		BUH-1	203	419	45.5	3.0	0.34	426.5	1.45	3.27	275.9	277.5	0.99	16.0	386.0	0.71		
114		EUH-1	203	419	44.4	3.0	0.34	426.5	1.45	3.27	307.0	277.5	1.11	16.2	382.0	0.80		
115		BUIS-2	203	419	35.3	3.0	0.34	426.5	1.45	3.27	315.9	277.5	1.14	17.8	345.1	0.92		
116		EUIS-2	203	419	48.3	3.0	0.34	426.5	1.45	3.27	311.5	277.5	1.12	15.7	395.7	0.79		
117		BUIH-2	203	419	50.0	3.0	0.34	426.5	1.45	3.27	333.7	277.5	1.20	15.5	401.3	0.83		
118		EUIH-2	203	419	50.5	3.0	0.34	426.5	1.45	3.27	320.4	277.5	1.15	15.4	402.9	0.80		
119		BUH-3	203	419	53.4	3.0	0.34	426.5	1.45	3.27	289.2	277.5	1.04	15.1	411.9	0.70		
120		EUH-3	203	419	55.1	3.0	0.34	426.5	1.45	3.27	311.5	277.5	1.12	14.9	416.9	0.75		

Test No.	Author [Source]	Beam name	b_w [mm]	d [mm]	f_{cm} [MPa]	ρ_l [%]	ρ_w [%]	f_{ywm} [MPa]	$\rho_w f_{ywm}$ [MPa]	a/d	$V_{experiment}$ [kN]	$V_{VSIM\text{-}Limit0}$ [kN]	$MF_{VSIM\text{-}Limit0}$	$\theta_{VSIM\text{-}Analytical}$ [°]	$V_{VSIM\text{-}Analytical}$ [kN]	$MF_{VSIM\text{-}Analytical}$	V_{R2k} [kN]	MF_{R2k}
121	12. McGormley, Creary and Ramirez.	BUIS-3	203	419	56.7	3.0	0.34	426.5	1.45	3.27	267.0	277.5	0.96	14.8	421.5	0.63		
122		EUIS-3	203	419	56.1	3.0	0.34	426.5	1.45	3.27	267.0	277.5	0.96	14.8	419.8	0.64		
123	13. Yoon, Cook and Mitchell.	N1-N	375	655	36.0	2.8	0.08	430.0	0.34	3.28	457.0	190.1	2.40	8.5	508.3	0.90	338.8	1.35
124		N2-S	375	655	36.0	2.8	0.08	430.0	0.34	3.28	363.0	190.1	1.91	8.5	508.3	0.71	343	1.06
125		N2-N	375	655	36.0	2.8	0.12	430.0	0.52	3.28	483.0	285.2	1.69	10.4	619.1	0.78	382.8	1.26
126		M1-N	375	655	67.0	2.8	0.08	430.0	0.34	3.28	405.0	190.1	2.13	6.7	644.0	0.63	372.3	1.09
127		M2-S	375	655	67.0	2.8	0.12	430.0	0.52	3.28	552.0	285.2	1.94	8.3	785.9	0.70	428.8	1.29
128		M2-N	375	655	67.0	2.8	0.16	430.0	0.69	3.28	689.0	380.3	1.81	9.5	904.3	0.76	568.8	1.21
129		H1-N	375	655	87.0	2.8	0.08	430.0	0.34	3.28	483.0	190.1	2.54	6.3	693.2	0.70	368.8	1.31
130		H2-S	375	655	87.0	2.8	0.14	430.0	0.60	3.28	598.0	332.7	1.80	8.3	912.9	0.66	541.2	1.10
131		H2-N	375	655	87.0	2.8	0.23	430.0	0.99	3.28	721.0	546.6	1.32	10.7	1162.1	0.62	735.4	0.98
132	14. Kong and Rangan	S1-1	250	292	59.148	2.8	0.16	569.0	0.89	2.50	228.3	146.7	1.56	11.4	292.2	0.78	219.5	1.04
133		S1-2	250	292	59.148	2.8	0.16	569.0	0.89	2.50	208.3	146.7	1.42	11.4	292.2	0.71	219.5	0.95
134		S1-3	250	292	59.148	2.8	0.16	569.0	0.89	2.50	206.1	146.7	1.40	11.4	292.2	0.71	207.9	0.99
135		S1-4	250	292	59.148	2.8	0.16	569.0	0.89	2.50	277.9	146.7	1.89	11.4	292.2	0.95	207.9	1.34
136		S1-5	250	292	59.148	2.8	0.16	569.0	0.89	2.50	253.3	146.7	1.73	11.4	292.2	0.87	180.3	1.40
137		S1-6	250	292	59.148	2.8	0.16	569.0	0.89	2.50	224.1	146.7	1.53	11.4	292.2	0.77	180.3	1.24
138		S2-1	250	292	67.425	2.8	0.11	569.0	0.60	2.50	260.3	98.1	2.65	8.9	251.4	1.04	158.3	1.64
139		S2-2	250	292	67.425	2.8	0.13	569.0	0.72	2.50	232.5	117.8	1.97	9.7	274.8	0.85	185.6	1.25
140		S2-3	250	292	67.425	2.8	0.16	569.0	0.89	2.50	253.3	146.7	1.73	10.9	305.6	0.83	209.2	1.21
141		S2-4	250	292	67.425	2.8	0.16	569.0	0.89	2.50	219.4	146.7	1.50	10.9	305.6	0.72	209.2	1.05
142		S2-5	250	292	67.425	2.8	0.21	569.0	1.19	2.50	282.1	195.3	1.44	12.6	350.4	0.81	250.1	1.13
143		S3-1	250	297	62.682	1.7	0.10	632.0	0.64	2.49	209.2	106.6	1.96	9.4	257.8	0.81	172.7	1.21
144		S3-2	250	297	62.682	1.7	0.10	632.0	0.64	2.49	178.0	106.6	1.67	9.4	257.8	0.69	172.7	1.03
145		S3-3	250	293	62.682	2.8	0.10	632.0	0.64	2.49	228.6	105.2	2.17	9.4	254.3	0.90	163	1.40
146		S3-4	250	293	62.682	2.8	0.10	632.0	0.64	2.49	174.9	105.2	1.66	9.4	254.3	0.69	163	1.07
147		S4-4	250	292	81.189	2.8	0.16	569.0	0.89	2.50	258.1	146.7	1.76	10.3	323.1	0.80	230.3	1.12
148		S4-6	250	198	81.189	2.8	0.16	569.0	0.89	2.53	202.9	99.5	2.04	10.3	219.1	0.93	140.1	1.45
149		S5-1	250	292	83.142	2.8	0.16	569.0	0.89	3.01	241.7	146.7	1.65	10.2	325.1	0.74	228.9	1.06
150		S5-2	250	292	83.142	2.8	0.16	569.0	0.89	2.74	259.9	146.7	1.77	10.2	325.1	0.80	228.9	1.14
151		S5-3	250	292	83.142	2.8	0.16	569.0	0.89	2.50	243.8	146.7	1.66	10.2	325.1	0.75	228.9	1.07
152		S6-3	250	293	64.077	2.8	0.10	632.0	0.64	2.73	178.4	105.2	1.70	9.3	256.2	0.70		
153		S6-4	250	293	64.077	2.8	0.10	632.0	0.64	2.73	214.4	105.2	2.04	9.3	256.2	0.84		
154		S6-5	250	299	64.077	3.7	0.10	632.0	0.64	2.64	297.0	107.4	2.77	9.3	261.5	1.14		
155		S6-6	250	299	64.077	3.7	0.10	632.0	0.64	2.64	287.2	107.4	2.67	9.3	261.5	1.10		
156		S7-1	250	294	69.564	4.5	0.11	569.0	0.60	3.30	217.2	98.8	2.20	8.8	255.7	0.85	181.5	1.20
157		S7-2	250	294	69.564	4.5	0.13	569.0	0.72	3.30	205.4	118.6	1.73	9.6	279.4	0.74	197.8	1.04
158		S7-3	250	294	69.564	4.5	0.16	569.0	0.89	3.30	246.5	147.7	1.67	10.8	310.8	0.79	227.7	1.08
159		S7-4	250	294	69.564	4.5	0.20	569.0	1.12	3.30	273.6	184.4	1.48	12.0	345.7	0.79	271.1	1.01
160		S7-5	250	294	69.564	4.5	0.22	569.0	1.27	3.30	304.4	210.8	1.44	12.9	368.4	0.83	285.9	1.06

Test No.	Author [Source]	Beam name	b_w [mm]	d [mm]	f_{cm} [MPa]	ρ_l [%]	ρ_w [%]	f_{ywm} [MPa]	$\rho_w f_{ywm}$ [MPa]	a/d	$V_{experiment}$ [kN]	$V_{VSIM\text{-}Limit0}$ [kN]	$MF_{VSIM\text{-}Limit0}$	$\theta_{VSIM\text{-}Analytical}$ [°]	$V_{VSIM\text{-}Analytical}$ [kN]	$MF_{VSIM\text{-}Analytical}$	V_{R2k} [kN]	MF_{R2k}
161	14. Kong and Rangan	S7-6	250	294	69.564	4.5	0.26	569.0	1.49	3.30	310.6	246.6	1.26	14.0	396.6	0.78	317.3	0.98
162		S8-1	250	292	69.378	2.8	0.11	569.0	0.60	2.50	272.1	98.1	2.77	8.8	253.7	1.07	154.6	1.76
163		S8-2	250	292	69.378	2.8	0.13	569.0	0.72	2.50	250.9	117.8	2.13	9.6	277.3	0.90	178.2	1.41
164		S8-3	250	292	69.378	2.8	0.16	569.0	0.89	2.50	309.6	146.7	2.11	10.8	308.4	1.00	217.6	1.42
165		S8-4	250	292	69.378	2.8	0.16	569.0	0.89	2.50	265.8	146.7	1.81	10.8	308.4	0.86	217.6	1.22
166		S8-5	250	292	69.378	2.8	0.20	569.0	1.12	2.50	289.2	183.2	1.58	12.1	343.1	0.84	248.7	1.16
167		S8-6	250	292	69.378	2.8	0.22	569.0	1.27	2.50	283.9	209.4	1.36	12.9	365.6	0.78	240.3	1.18
168	15. Zararis and Papadakis	A033	140	235	22.4	1.4	0.09	266.7	0.24	3.60	40.2	17.8	2.26	8.7	46.2	0.87		
169		A050	140	235	23.9	1.4	0.14	264.3	0.37	3.60	49.7	27.4	1.81	10.6	58.8	0.85		
170		A066	140	235	22.5	1.4	0.19	263.2	0.50	3.60	59.2	37.0	1.60	12.6	66.0	0.90		
171		A1	140	235	23.0	1.4	0.27	270.4	0.73	3.60	63.5	54.0	1.18	15.2	79.7	0.80		
172		B050	140	235	23.9	1.4	0.09	255.6	0.23	3.60	43.7	17.0	2.57	8.3	46.7	0.94		
173		B066	140	235	20.8	1.4	0.12	258.3	0.31	3.60	44.7	22.9	1.95	10.3	50.6	0.88		
174		C5	140	235	21.6	0.7	0.27	270.4	0.73	3.60	56.2	54.0	1.04	15.6	77.3	0.73		
175		C6	140	235	21.3	0.7	0.17	270.6	0.46	3.60	47.2	34.1	1.39	12.4	61.8	0.76		
176	16. Karayiannis and Chalioris	A24	200	260	26.0	1.5	0.08	262.5	0.21	2.77	64.0	24.6	2.60	7.6	73.3	0.87		
177		A36	200	260	26.0	1.5	0.12	266.7	0.32	2.77	89.0	37.4	2.38	9.4	90.0	0.99		
178		A48	200	260	26.0	1.5	0.16	268.8	0.43	2.77	89.2	50.3	1.77	11.0	103.8	0.86		
179		A72	200	260	26.0	1.5	0.25	256.0	0.64	2.77	93.0	74.9	1.24	13.4	125.5	0.74		
180		B60	200	260	26.0	2.0	0.09	255.6	0.23	3.46	76.7	26.9	2.85	8.0	76.6	1.00		
181		B90	200	260	26.0	2.0	0.13	261.5	0.34	3.46	84.8	39.8	2.13	9.7	92.7	0.91		
182	17. Collins and Kuchma	SE100A-M-69	295	920	71.0	1.0	0.16	500.0	0.80	2.50	516.0	488.6	1.06	10.1	1095.1	0.47		
183		SE100B-M-69	295	920	75.0	1.4	0.16	500.0	0.80	2.50	583.0	488.6	1.19	10.0	1113.5	0.52		
184		SE50A-M-69	169	459	74.0	1.0	0.13	500.0	0.65	2.72	139.0	113.5	1.23	9.0	286.6	0.49		
185		SE50B-M-69	169	459	74.0	1.2	0.13	500.0	0.65	2.72	152.0	113.5	1.34	9.0	286.6	0.53		
186	18. Angelakos, Bentz and Collins.	DB0.530M	300	925	32.0	0.5	0.08	508.0	0.41	2.92	263.0	253.8	1.04	9.7	592.0	0.44	241.4	1.09
187		DB120M	300	925	21.0	1.0	0.08	508.0	0.41	2.92	282.0	253.8	1.11	11.7	488.2	0.58	337.9	0.83
188		DB140M	300	925	38.0	1.0	0.08	508.0	0.41	2.92	277.0	253.8	1.09	9.0	637.4	0.43	383.8	0.72
189		DB165M	300	925	65.0	1.0	0.08	508.0	0.41	2.92	452.0	253.8	1.78	7.4	782.0	0.58	415	1.09
190		DB180M	300	925	80.0	1.0	0.08	508.0	0.41	2.92	395.0	253.8	1.56	7.0	832.5	0.47	351.5	1.12
191		BM100	300	925	47.0	0.8	0.08	508.0	0.41	2.92	342.0	253.8	1.35	8.3	695.0	0.49	332.4	1.03
192	19. Adebar and Collins	ST4	290	278	49.0	2.0	0.11	430.0	0.47	2.88	158.0	85.8	1.84	8.8	221.0	0.71		
193		ST5	290	278	49.0	2.0	0.18	536.0	0.96	2.88	169.0	175.0	0.97	12.7	311.7	0.54		
194		ST6	290	278	49.0	2.0	0.28	430.0	1.20	2.88	230.0	218.4	1.05	14.2	346.0	0.66		
195		ST19	290	278	51.0	2.0	0.21	430.0	0.92	2.88	201.0	166.9	1.20	12.2	309.6	0.65		
196	20. Ozcebe et al.	TS36	150	310	75.0	2.6	0.24	255.0	0.61	3.00	156.0	63.8	2.45	8.7	167.1	0.93	125.4	1.24
197		TH39	150	310	73.0	3.1	0.17	255.0	0.43	3.00	143.0	45.4	3.15	7.4	140.3	1.02	121.7	1.18
198		ACI59	150	310	82.0	4.4	0.14	255.0	0.35	5.00	97.0	37.1	2.62	6.4	131.2	0.74	96.7	1.00
199		TH59	150	310	75.0	4.4	0.19	255.0	0.48	5.00	119.0	49.9	2.39	7.7	148.2	0.80	113.1	1.05
200		TS59	150	310	82.0	4.4	0.28	255.0	0.71	5.00	125.0	74.4	1.68	9.2	184.7	0.68	144.5	0.87

Test No.	Author [Source]	Beam name	b_w [mm]	d [mm]	f_{cm} [MPa]	ρ_l [%]	ρ_w [%]	f_{ywm} [MPa]	$\rho_w f_{ywm}$ [MPa]	a/d	$V_{experiment}$ [kN]	$V_{VSIM\text{-}Limit\theta}$ [kN]	$MF_{VSIM\text{-}Limit\theta}$	$\theta_{VSIM\text{-}Analytical}$ [°]	$V_{VSIM\text{-}Analytical}$ [kN]	$MF_{VSIM\text{-}Analytical}$	V_{R2k} [kN]	MF_{R2k}
201	21. Cladera and Mari	H50/2	200	353	49.9	2.3	0.11	530.0	0.58	3.06	178.0	91.8	1.94	9.7	214.9	0.83	125.6	1.42
202		H50/4	200	351	49.9	3.0	0.24	540.0	1.29	3.08	246.0	203.9	1.21	14.6	313.5	0.78	230.8	1.07
203		H60/2	200	353	60.8	2.3	0.14	530.0	0.75	3.06	180.0	118.7	1.52	10.3	261.8	0.69	169.1	1.06
204		H75/2	200	353	68.9	2.3	0.14	530.0	0.75	3.06	204.0	118.7	1.72	9.9	273.0	0.75	181.3	1.13
205		H75/4	200	351	68.9	3.0	0.24	530.0	1.27	3.08	255.0	200.1	1.27	12.9	349.7	0.73	247.4	1.03
206		H100/4	200	351	87.0	3.0	0.24	540.0	1.29	3.08	267.0	203.9	1.31	12.2	377.3	0.71	273.7	0.98
207	22. Etxeberria	HN-V3	200	303	42.0	3.0	0.17	530.0	0.88	3.30	177.0	120.0	1.48	12.8	210.6	0.84		
208		HN-V4	200	303	42.0	3.0	0.12	530.0	0.63	3.30	188.0	85.3	2.20	10.8	178.9	1.05		
209	23. Gonzalez-Fonteboa	V13HC	199	307	38.0	2.9	0.21	500.0	1.05	3.25	190.0	144.3	1.32	14.6	221.0	0.86		
210		V17HC	199	306	39.0	2.9	0.16	500.0	0.80	3.27	151.0	109.6	1.38	12.6	196.0	0.77		
211		V24HC	195	306	39.0	3.0	0.12	500.0	0.60	3.27	128.0	80.6	1.59	10.9	167.4	0.76		
212		V17HCS	200	312	45.0	2.9	0.16	500.0	0.80	3.21	200.0	112.3	1.78	11.9	213.2	0.94		
213		V24HCS	200	302	44.0	3.0	0.12	500.0	0.60	3.30	150.0	81.5	1.84	10.4	178.1	0.84		
214		V17HR	200	306	42.0	2.9	0.16	500.0	0.80	3.27	177.0	110.2	1.61	12.2	203.3	0.87		
215		V24HR	201	306	39.0	2.9	0.12	500.0	0.60	3.27	164.0	83.0	1.97	10.9	172.5	0.95		
216		V13HRS	199	305	41.0	2.9	0.21	500.0	1.05	3.28	202.0	143.4	1.41	14.2	226.9	0.89		
217		V17HRS	199	305	45.0	2.9	0.16	500.0	0.80	3.28	193.0	109.3	1.77	11.9	207.4	0.93		
218		V24HRS	199	307	43.0	2.9	0.12	500.0	0.60	3.25	147.0	82.5	1.78	10.5	178.5	0.82		
219	24. Tompos and Frosch	V36-2	457	851	42.7	1.0	0.08	482.6	0.41	3.00	755.7	354.9	2.13	8.6	937.0	0.81	467.9	1.62
220		V36-3	457	851	42.7	1.0	0.08	537.8	0.45	3.00	792.9	395.4	2.01	9.1	987.8	0.80	459.8	1.72
221		V18-2	229	425	35.9	1.0	0.15	482.6	0.72	3.00	266.8	157.4	1.70	12.4	286.9	0.93	169.5	1.57
222		V18-2c	229	425	35.9	1.0	0.33	482.6	1.61	3.00	237.2	352.8	0.67	18.7	416.6	0.57	169.6	1.40

	Model Factor (MF) Statistics for:				
	VSIM-Limitθ		**VSIM-Analytical**		**R2k**
Mean (μ_{MF})	1.65		0.84		1.14
Std. dev. (σ_{MF})	0.50		0.18		0.20